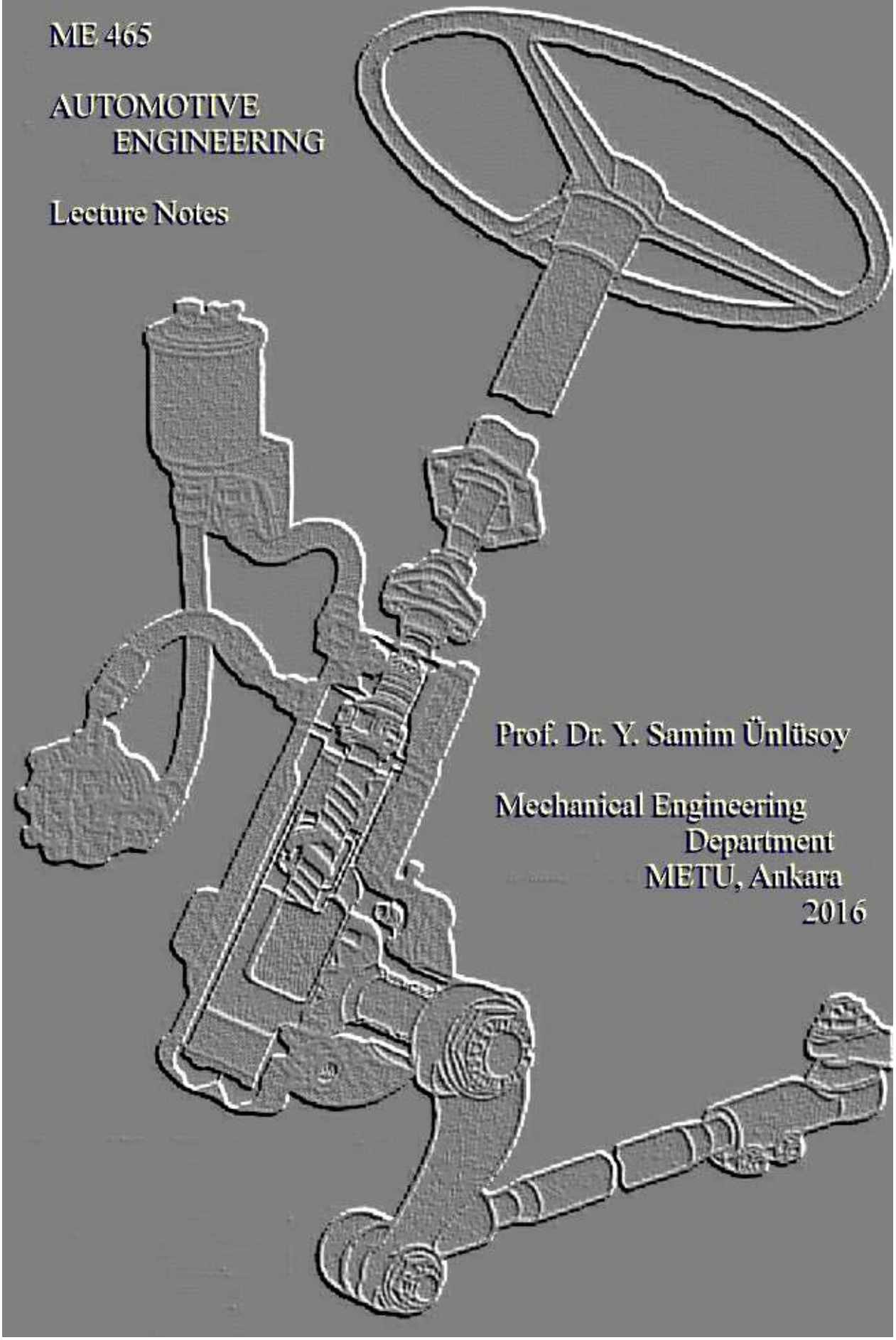
ME 465

AUTOMOTIVE ENGINEERING

Lecture Notes



Prof. Dr. Y. Samim Ünlüsoy

Mechanical Engineering Department
METU, Ankara

2016

PREFACE

Three courses related to Automotive Engineering are offered to senior students in the Mechanical Engineering Department of the Middle East Technical University. The undergraduate courses Automotive Engineering and Performance of Road Vehicles are designed to give basic information by providing an insight into the complex dynamic structure and behavior of motor vehicles. A balanced descriptive and analytical treatment of the subject is pursued to equip the graduating students not only with an understanding of the basic design principles but also with the basic engineering approach to the modeling and simulation for the prediction and optimization of performance. These two courses provide the background for the graduate course Vehicle Dynamics, in which the emerging technologies, as well as the basic issues in vehicle dynamics, are examined in more detail.

A considerable number of books are available on the subject of motor vehicles. With a few exceptions, these books are mostly related to the functioning, principles of construction, and maintenance and/or repair of motor vehicles. As such, they are intended mainly to provide information for the layman or the mechanic rather than engineers. These lecture notes are compiled from the material taught by the Author in the Automotive Engineering course with the primary goal of introducing the student to the functioning, analysis, and design of the subsystems that ultimately decide the dynamic behavior of motor vehicles.

The organization of the text and the selection of the topics represent the Author's view of the subject as course material and a primary reference for a senior undergraduate Mechanical Engineering class. It is sincerely hoped that the fundamental concepts provided here will equip the reader with a sound background in the subject of Automotive Engineering so that he/she can follow current literature on research and development or work towards the solution of a particular problem.

Y. Samim ÜNLÜSOY

Ankara

CONTENTS

			Page
PREFACE			ii
CONTENTS			iii
CHAPTER I	**PNEUMATIC TIRE**		
	I-1.	Introduction	I-1
	I-2.	Tyre Nomenclature	I-3
	I-3.	Types of Carcass Construction	I-4
	I-4.	Tyre Materials	I-8
	I-5.	Tread Pattern	I-11
	I-6.	Aspect Ratio	I-17
	I-7.	Ply Rating	I-16
	I-8.	Early Tire Designations	I-18
	I-9	New Tire Designations	I-21
	I-10	Tire Manufacture	I-25
		Exercises	I-28
CHAPTER II	**WHEELS**		
	II-1.	Introduction	II-1
	II-2.	Wheel Dimensions and Basic Designation	II-1
	II-3	Automobile Wheels	II-2
	II-4.	Commercial Vehicle Wheels	II-6
CHAPTER III	**STEERING SYSTEM**		
	III-1.	Introduction	III-1
	III-2.	Basic Types of Steering Systems	III-1
	III-3.	Geometrically Correct Steering	III-4
	III-4.	Determination of Steering Error	III-6
		III-4.1 Graphical Method	III-6
		III-4.2 Analytical Method	III-8
	III-5.	Multi-axle Steering	III-12
	III-6.	Ackerman Linkage	III-15
	III-7.	Steering System Arrangement	III-16
		III-7.1 Steering Gear Requirements	III-18
		III-7.2 Types of Steering Gear	III-19
	III-8.	Turning Radius	III-21
		Exercises	III-27

CHAPTER IV VEHICLE HANDLING

IV-1. Introduction IV-1
IV-2. Tire Cornering Force Characteristics IV-3
IV-3. Parameters Influencing Tire Cornering Force Characteristics IV-8
IV-3.1 Effects of Inflation Pressure IV-8
IV-3.2 Effects of Camber Angle IV-9
IV-3.3 Effects of Tractive Effort IV-11
IV-4. Self Aligning Torque IV-13
IV-5. Plane Motions of Vehicles IV-14
IV-5.1 Tire Slip Angles IV-17
IV-5.2 Bicycle Model IV-18
IV-5.3 Handling Behaviour IV-21
Exercises IV-26

CHAPTER V VEHICLE SUSPENSIONS

V-1. Basic Functions V-1
V-2. Basic Components V-2
V-3. Suspension Geometry V-8
V-4. Types of Vehicle Suspensions V-13
V-4.1 Rigid Axle Suspensions V-14
V-4.2 Independent Wheel Suspensions V-19
V-4.3 Interconnected Suspensions V-28
V-5. Anti-Roll Bar V-30
V-6. Roll Centre's and Roll Axis V-31
V-7. Kinematic Analysis of Suspension Systems V-35
Exercises V-47

CHAPTER VI VEHICLE RIDE

VI-1. Introduction VI-1
VI-2. Vibrational Characteristics of Vehicles VI-2
VI-3. Evaluation of Ride Quality for Motor Vehicles VI-3
VI-4 Body Bounce VI-5
VI-5 Wheel Hop VI-10
VI-6 Quarter Car Model VI-12
VI-7 Body Bounce and Pitch VI-20
Exercises VI-25

CHAPTER VII VEHICLE BODY CONSTRUCTION VII-1
VII-1. Introduction VII-1
VII-2. Functions VII-1
VII-3. Basic Types VII-3
VII-4. Vehicle Loads VII-6
VII-5. Conventional Design Process VII-7
VII-5.1 Styling and Clay Prototypes VII-7
VII-5.2 Full Size Clay Model VII-11
VII-5.3 Final Drawing VII-12
VII-5.4 Production VII-12
VII-6 Recent Developments VII-13

REFERENCES R-1

CHAPTER I

PNEUMATIC TIRE

I-1. Introduction

The transition from the early wooden and steel wheels first to solid rubber tires and then to pneumatic tires has probably had the most significant share in the level of sophistication reached by motor vehicles today. The development of the pneumatic tire has contributed significantly to the improved ride comfort, directional control, and stability, as well as to the safety and economy of the motor vehicle.

The first pneumatic tire was patented in 1845 by a Scottish engineer, R.W. Thomson, who sought to reduce the tractive effort to pull horse carriages and the noise they made when in motion. His tire consisted of a tube of rubberized canvas covered by a leather case which was bolted to a wooden rim, as shown in Fig. I-l. It was again the need to reduce the required tractive effort that led J.B. Dunlop, a Scottish veterinary surgeon, to re-invent the pneumatic tire in 1888 for his son's tricycle. His pneumatic tire was produced by nailing a natural rubber and cotton canvas to a wooden wheel.

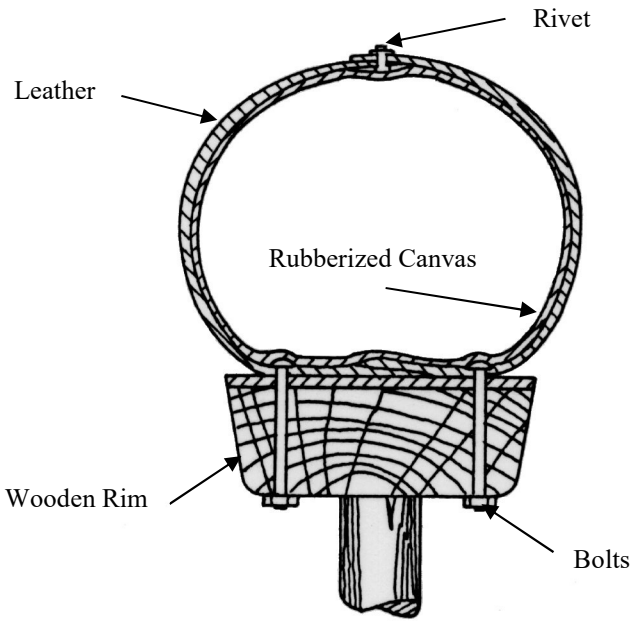


Figure I-1. Thomson's pneumatic tire

The advantages of the pneumatic tire soon became evident and enjoyed popularity in the cycle industry. Its application to motor vehicles, however, had to wait for the inventions patented by an Englishman C.K. Welsh and 36 days later by an American W. Bartlett in 1890, leading to detachable tires. The former invention incorporated steel wires and the latter internal air pressure to keep the tire on the rim, as shown in Fig. I-2. Finally, in 1895, a Frenchman, E. Michelin, produced the first practical pneumatic tire for use on motor vehicles.

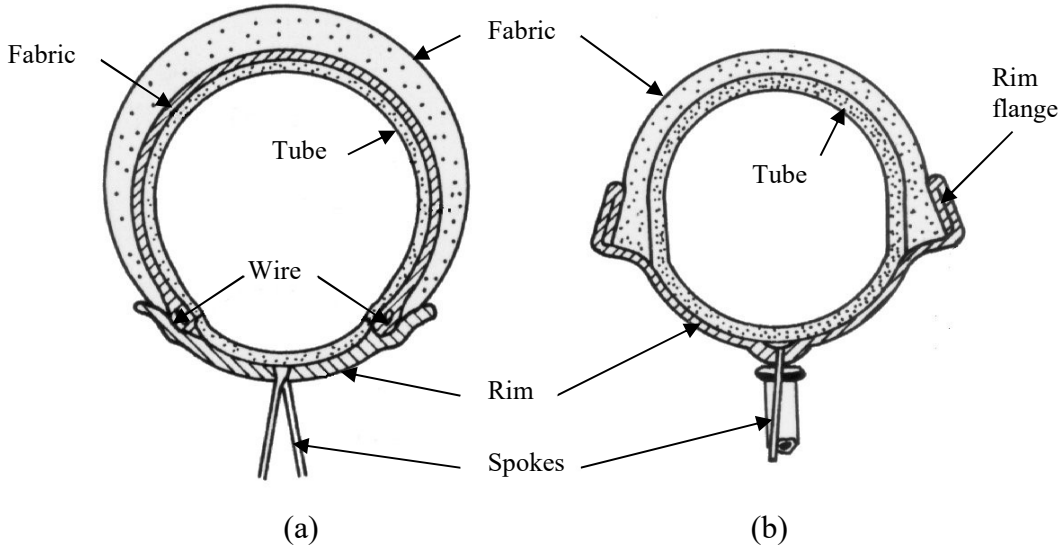


Figure I-2. Rim and bead designs of 1890, by a) C. K. Welsh, b) W. Bartlett

I-2. Tire Nomenclature

The load carried by the pneumatic tire cannot be related directly to the product of the inflation pressure and the contact area of the tire with the road surface. The common belief that it is the air inside the tire that carries the load, therefore, cannot be justified. It is evident that the outer rubber structure which forms the flesh of the tire cannot support the internal air pressure without a skeleton. This skeleton, which is called the carcass, is stressed by the air pressure and the other imposed loads on the tire and thus has a powerful influence on the determination of the final characteristics of the tire.

The pneumatic tire consists of three primary components. The carcass of a tire is composed of several layers of plies which are coated by a rubber compound on both sides. These layers maintain the internal air pressure of the tire in supporting the load. All plies are tied into bundles of steel wire which are called bead wires. The beads are the parts that fit the tire on the rim, preventing the tire from slipping out of the rim while the vehicle is in motion. Tread is the fleshy wearing surface of the tire and is molded to the carcass. It is manufactured from synthetic rubber compounds and provides resistance to abrasion and cutting, as well as a tread pattern to grip the road.

The standard nomenclature used for pneumatic tires of motor vehicles is shown in Fig. I-3.

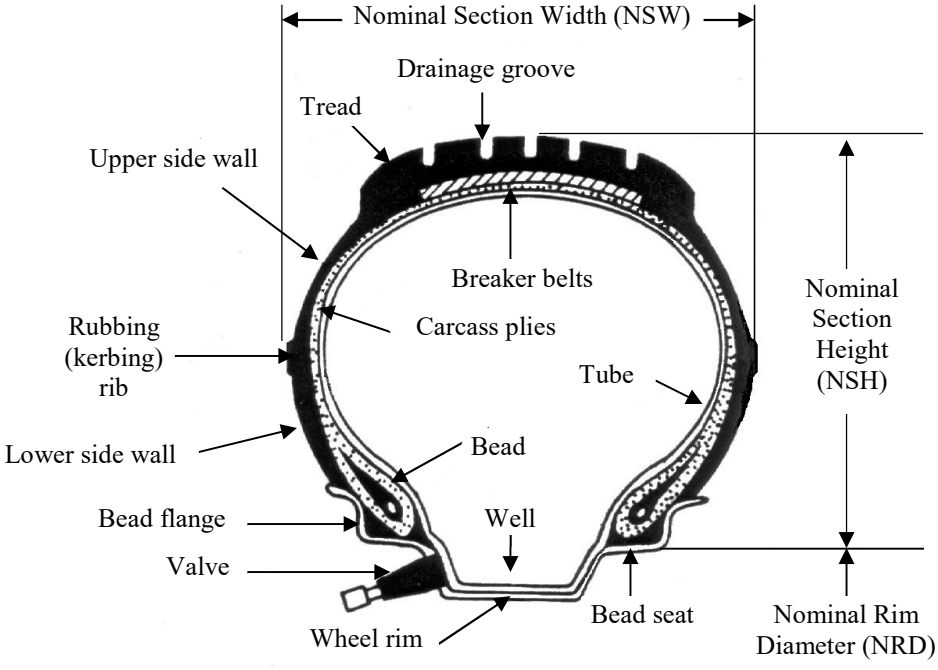


Figure I-3. Tire nomenclature

I-3. Types of Carcass Construction

There are two basic types of carcass construction:

i) Cross (bias or diagonal in the USA) ply,
ii) Radial ply.

These two basic constructions are illustrated in Fig. I-4.

A third type is produced by a combination of the two basic constructions and is named the belted bias tire. The belted bias carcass construction is illustrated in Fig. I-5.

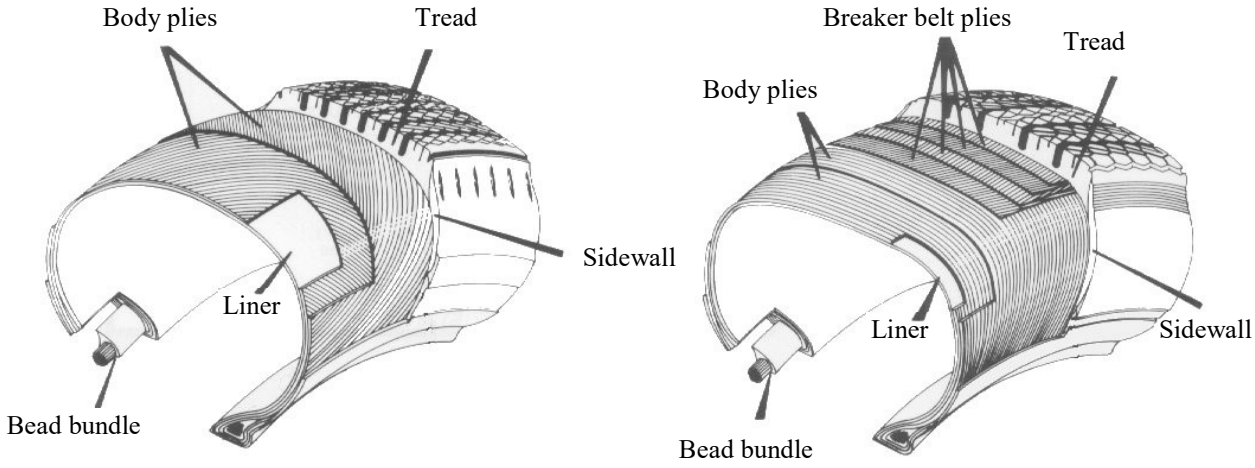


Figure I-4. Construction of cross and radial ply tires

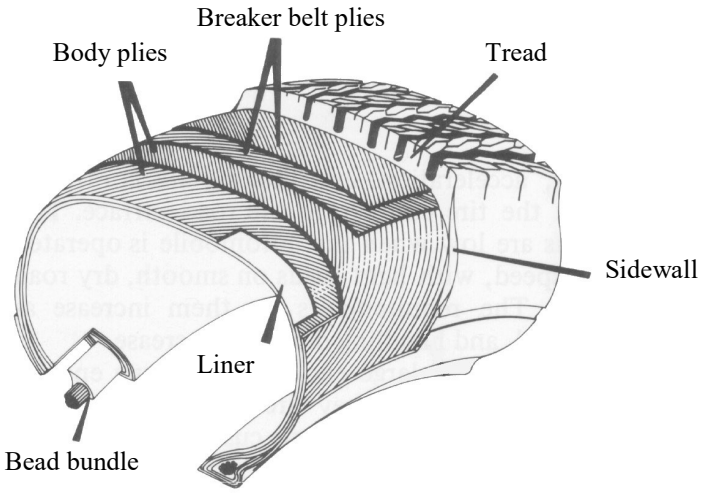


Figure I-5. Belted bias carcass construction

In the early versions of the pneumatic tire, the carcass consisted of rubberized cotton canvas consisting of woven cords embedded into a matrix of rubber, as illustrated in Fig. I-6. The chafing caused by the motion of the warp (longitudinal cords) and weft (lateral cords) during the deformation of the tire at the road contact patch together with the generation of heat in the natural rubber used resulted in a tire life of about 3-4000 km only.



Figure I-6 Rubberized canvas (woven fabric)

To overcome this deficiency, the first idea was to eliminate weft completely and use unwoven fabric consisting of layers of cords (threads) kept apart from each other by rubber.

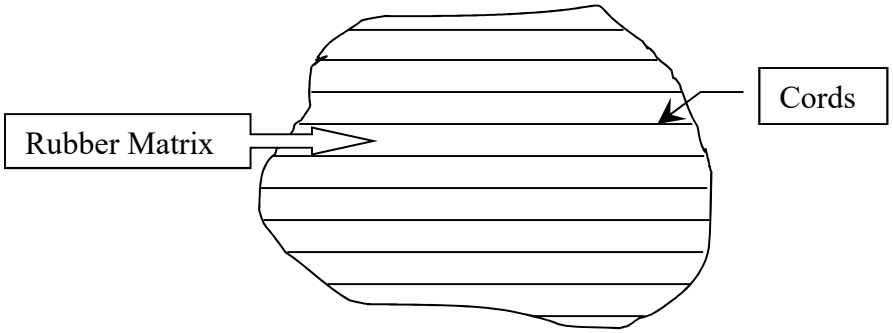


Figure I-7 Unwoven fabric

It soon became apparent, however, that the characteristics related to ride comfort and directional stability of the vehicle were mutually opposed and depended strongly on the direction of the cords in the fabric layers. ***When the direction of the cords approached the circumferential direction, directional stability improved, and the ride got harsher. If, on the other hand, the cords were placed at right angles to the circumference softest ride was obtained, but the directional stability was almost entirely lost.***

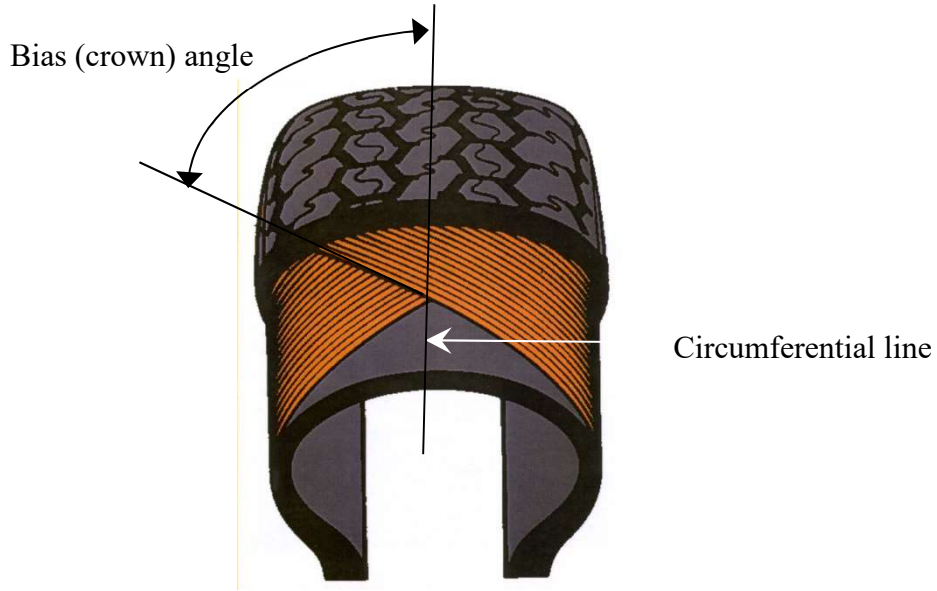


Figure I-8 Bias (or crown) angle

As a result of these experiments, ***cross-ply tires*** were introduced in the early 1920s with a tenfold increased tire life. In this type of construction, the carcass is made up of two or more plies (layers) of fabric that have all its cords running in one direction only. To obtain the apparent compromise between the two extremes, layers are placed such that the cords make an angle (***bias or crown angle***) of 45 degrees with the circumferential line of the tire, Fig. I-8. The adjacent layers are placed at opposite bias. The bias angle was later reduced to about 40 degrees. In racing car tires, bias angles down to 25 degrees are encountered.

The idea of dividing the tasks of providing a soft ride and reasonable directional control and stability between the two parts of the carcass led to the development of the ***radial-ply tire***. In this construction, the cords in the plies run from bead to bead across the circumferential line resulting in a very flexible sidewall. A very soft ride is thus assured. Directional stability and control are provided by a number (a minimum of two) of belts called breakers running round the circumference beneath the tread. The cords of the belts are slightly diagonal with bias angles of about 20 degrees. The zone beneath the tread is firmly restricted by the belts, and the lateral stiffness is increased. The overall result is reduced distortion as the tire passes through the contact area with the road surface. There is less friction between the cords of the plies, and less heat is generated.

The first example of the radial-ply tire as described above was the ***Michelin*** X introduced in 1948. Since then, the radial-ply tire has been accepted as the standard tire in the automobile industry. This is natural in view of the radial's many advantages. In addition to a longer life, it offers better cornering ability and directional stability together with lower rolling resistance to give improved fuel consumption and performance.

In the USA, in spite of its advantages, the adoption of radial-ply tires took some time because of the considerable expense involved in switching production from the cross to radial-ply tires. American tire manufacturers chose for a transition period to use their existing equipment to produce bias-belted tires. ***Bias-belted carcass construction*** consists basically of biased plies as in cross-ply tires and layers of belts beneath the tread as in radial tires and as such incorporates some features of both. Bias belted tires have not been accepted outside the USA to any extent.

I-4. Tire Materials

Natural rubber (NR), in its original state, is not a consistent engineering material. The means of imparting the desired properties of strength and elasticity to NR was accidentally discovered by C. **Goodyear** in 1839. This process involved heating NR mixed with sulfur and is called vulcanization. For many years after this discovery, tires were produced entirely of NR. It was shown in 1826 that the composition of NR could be expressed by the formula $(C_5H_8)n$, and in 1860 isoprene, C_5H_8, was isolated. Soon after, several synthetic rubber-like materials were produced from isoprene. Today, many synthetic rubber materials suitable for use in rubber compounds are available, and tires are manufactured almost entirely from various blends of synthetic rubbers.

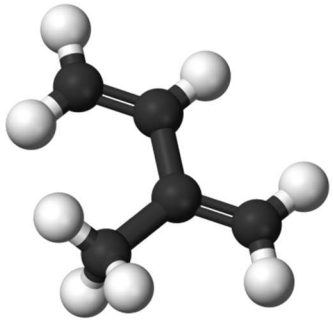


Figure I-9 Isoprene

I-4.1 Tread and Sidewall Materials

The rubber compound to be used in the tread must meet a number of requirements. It must provide a high frictional coefficient on the road surface. An adequate grip is expected on all kinds of road surfaces, cold, hot, wet, or covered with snow or ice. Tread rubber must have excellent abrasion resistance as well as resistance to tearing and cutting. It must provide acceptable behavior against cracking and oxygen and ozone attack. The ability to bond to carcass material effectively is still another requirement. Similar requirements are to be met by sidewall rubber, with the emphasis being on the cracking, abrasion, and bonding characteristics. It is evident that to meet such a diverse list of requirements, a compound of various synthetic rubbers together with other additives is necessary.

Styrene-butadiene rubber (SBR) is the most common synthetic material used in such compounds. It owes its popularity to the fact that it has excellent resistance to abrasion and a high degree of energy absorption (hysteresis), resulting in a less springy tire to provide a softer ride with good grip, particularly on wet road surfaces. Increasing the oil content of SBR results in oil extended SBR (OESBR), with even more improved wet grip. In addition, it is made from readily available materials and makes a firm bond with carcass materials. Its

weaknesses are few. Tear resistance and propagation of cuts and resistance to cracking in case of large deflections which are inferior with respect to NR are among these few.

Another very useful synthetic rubber is **polybutadiene** (BR or sometimes PB) which is very hard to wear and less sensitive to changes in temperature than other rubbers. Its resistance to cutting and tear propagation is also exceptionally high. However, too much of it will make tires scream on dry roads and slip on wet roads. It is usually added to SBR, to NR, or both in small quantities, causing a significant improvement in wear resistance with a slight decrease in wet grip because of its high resilience.

The synthetic, which is the nearest thing to natural rubber, is ***polyisoprene*** (PI). PI is mixed in small quantities with SBR or NR to provide better abrasion resistance due to its excellent wearing properties and extremely low sensitivity to heat. It is particularly suited for use in truck tires that run at relatively high temperatures.

I-4.2 Inner Lining Materials

The most crucial requirement in the case of inner tubes and the lining of tubeless tires is that of low permeability to gases. The synthetic rubber which meets this requirement best is the ***butyl rubber*** (IIR) which also has very high hysteresis and traction characteristics. It cannot be used as a tread material because it blends neither with NR and nor with SBR.

I-4.3 Carcass Materials

In carcass construction, the best material for impregnating and coating the fabrics is still natural rubber. In the early tires, cotton cords were used in the plies. The later use of plies made up of rayon, polyester, nylon, glass fiber, and more recently, aramids embedded in rubber has resulted in increased life as well as the load-carrying capacity of tires.

1-4.4 Breaker Cord Materials

The usual cord materials for the breaker belts of the radial-ply tires are rayon and fine steel wire. ***Steel belted radials*** (SBR) offer better cornering ability and directional control, lower rolling resistance improved fuel consumption and performance for the vehicle - and longer life at the expense of inferior ride comfort and quietness in addition to a 10 percent higher cost compared with ***textile belted radials*** (TBR). Recently nylon and glass fiber have been used for breaker cords. The former is stronger, more elastic, and more flexible than rayon and is preferred for applications involving high speeds and heavy loads. It tends, however, to lose its flexibility when cold. The latter is very strong and elastic but requires special techniques in production.

I-4.5 Additives

In addition to the main ingredients above, there are other additives used in rubber compounds. The most important of these are the following.

i/ ***Vulcanizing agents*** to impart strength and elasticity, basically sulfur.

ii/ ***Activators*** and accelerators to modify the chemical action before or during vulcanization.

iii/ ***Fillers*** to provide cheap bulk to save expensive rubber. Carbon black is the best filler that provides extra strength and resistance to wear and, as such, can be considered as a reinforcing agent as well. Carbon black gives the tires their characteristic black color. Recently, in the so-called "energy tires", some of the carbon black in the compound is replaced by silica. This reduces the rolling resistance and improves traction on wet or snowy road surfaces, while life and ride are unaffected.

iv/ ***Plastisizers*** (***extenders***) and softeners to reduce time and temperatures involved in processing. Oils of petroleum origin are used as extenders, and they provide the additional benefit of the better road holding at the expense of rapid tire wear.

v/ ***Antioxidants*** and ***antiozonants*** to preserve the consistency of rubber in time.

I-5. Tread Pattern

The primary function of the tread pattern is to improve the tire grip, particularly on road surfaces covered with water, snow, slush, mud, or ice. In performing its function, the tread pattern must meet the requirements on tread wear, noise generated, and other characteristics peculiar to the particular conditions and applications.

A completely smooth tire would give the greatest possible area of contact between the tire tread and the road surface, and consequently, the best possible grip, provided that the road surface is clean and dry. It will also have the longest working life because of reduced loading on the unit area of rubber. Such a tire would have hardly any grip, however, in the presence of even a slight amount of water on the road surface. The water forms, in this case, a lubricating film between the tire and the road surface, causing a loss of steering control and braking ability. If the amount of water is appreciable, it builds up in front of and beneath the tire forming a wedge as illustrated in Fig. I-9. The tire will then be lifted off the road and slide on the water with no directional control. This phenomenon is called ***aquaplaning*** (or ***hydroplaning***).

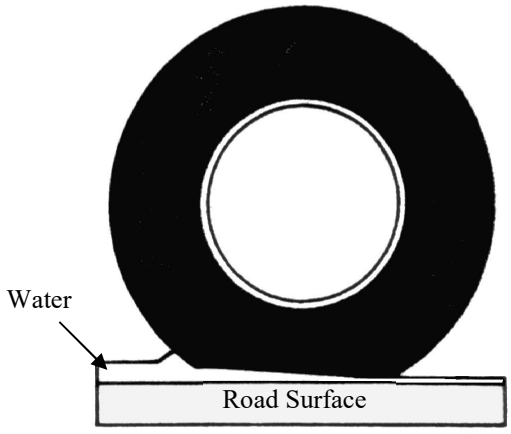


Figure I-9. Aqua(hydro)planing

To help the tire to grip the road surface in the presence of water, a tread pattern consisting of longitudinal primary and secondary ***drainage grooves*** (channels), lateral drainage grooves, and micro slits like knife cuts, which are called ***sipes***, must be provided. If there is only a thin film of water on the road, the tread pattern breaks through the film and grips the road surface. In the case of larger amounts of water on the road, the same function is performed in three stages.

i/ The tread pattern pushes the water aside and pumps it backward and sideways through the drainage grooves.

ii/ The remaining thin film of water is broken by the tread pattern, and the small amount of water left on the surface is absorbed by the sipes, which act like a sponge.

iii/ The tread pattern contacts the now dry road surface to develop the maximum possible grip.

It should be clear that as vehicle speed increases, there will be less time for the tread pattern to perform its function, and the grip provided will decrease. Aquaplaning is a possibility even with new tires of good tread design if there is plenty of water on the road and the vehicle speed is high enough.

In improving the grip of the tire, the mere frictional transmission of loads involved in acceleration, braking, and cornering is not sufficient, and some kind of mechanical grip must be provided. This requirement is met by a tread pattern having well-defined and sharp edges. When these biting edges are parallel to the circumference of the tire, good steering and cornering characteristics are obtained. Good traction and braking, on the other hand, are obtained with biting edges perpendicular to the circumference. Since traction, braking, and steering are all critical to most motor vehicles, the obvious compromise is to position these edges diagonally in a zig-zag pattern as illustrated in Fig. I-10.

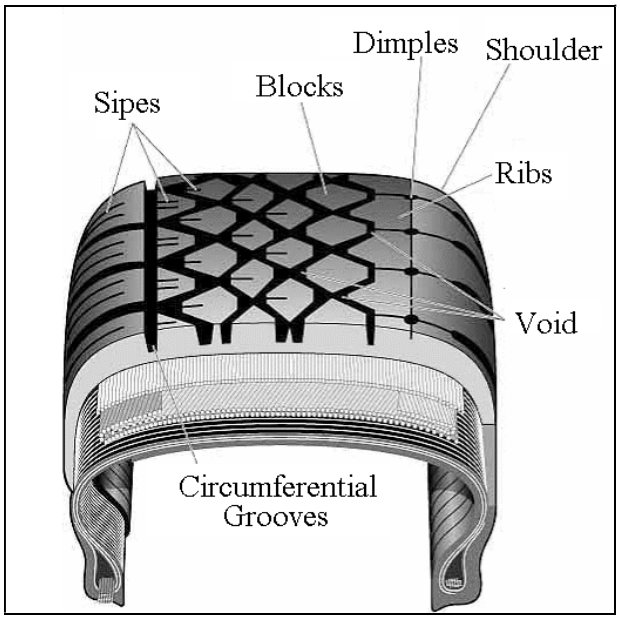
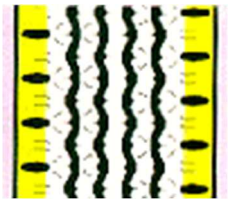
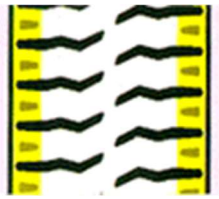


Figure I-10. Tread pattern

Basic types of tread patterns and their properties and applications are summarized below.



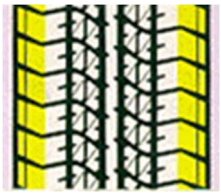
Rib Shape: This tread pattern is characterized by multiple circumferential grooves. Advantages include lower rolling resistance plus good directional stability, and steering control. Rib-type patterns are suitable for sustained high speeds because of their low levels of heat generation. They have, however, poor braking and acceleration grip on wet roads, and their use is confined to paved road surfaces and steered axles of trucks and buses.



Lug shape: These patterns are identified by their groove arrangements perpendicular to the circumference of the tire. The main advantage of lug patterns is their excellent braking and traction characteristics. Lug patterns are not suitable for high-speed driving due to their high rolling resistance and noise generation. They are mainly used for dirt roads, rear wheels of buses and agricultural tractors, industrial vehicles, and dump trucks.



Rib-Lug shape: This is a combination of rib and lug designs. The main features are a rib in the center providing directional control and shoulder lugs giving good braking and traction characteristics. They find applications in tires for both paved and dirt roads and are usually used in both front and rear wheels of trucks and buses.



Block-shape: These consist of independent blocks created by intersecting circumferential and lateral grooves. Block patterns provide good steering control and stability on snow-covered and wet roads as well as good water dispersal properties in the wet. However, because the tread blocks are smaller, tire wear tends to be fast. They are suitable for winter or all-season passenger car tires.



Asymmetric pattern: In this pattern, the design is different on either side of the tire. Asymmetric tires have been designed to optimize the opposing requirements of dry grip and water dispersal. They are suitable for high-speed cornering due to the greater contact area (low void ratio), which helps reduce tread wear on the outside of the tire. On the inside, the void ratio is higher to give a better wet grip. Asymmetric tires must be positioned the right way around as marked. They are implemented on high-performance vehicle tires.



Directional pattern: These are tread patterns characterized by lateral grooves on both sides of the tire which point in the same direction. The advantages of directional tread patterns are good driving force and braking performance. In particular directional patterns provide good water dispersal, meaning stability on wet roads. Directional tires must be mounted in the direction of the tread pattern. They are used on passenger car tires for high-speed use.

I-5.1 Void Ratio

The ratio of rubber-free (void) area to total area on the footprint of a tire is known as the void ratio.

Void area = Total footprint area – Rubber (touching road) area

The void ratio strongly affects the grip and wear characteristics of a tire. If the void ratio is large, then the wet grip is improved at the expense of tire wear and dry road grip and handling. The smaller the void ratio is, the better would be the tire wear and dry road grip, but now the wet grip will be degraded.

I-5.3 Seasonal Variations

Different tread patterns have been developed to suit various applications. For example, winter tires have wide and deep grooves on the tread to break away and clear loose upper surfaces of snow, slush, mud, and stones. This makes it possible for the tire to get a good grip on the firmer surface beneath. The tread pattern must then be able to clean itself; otherwise, its effectiveness will be reduced. The large rubber blocks of these tires, however, wear out rapidly through overheating if used on dry roads at high speeds. Several examples for various different applications are shown in Fig. I-11.

I-5.2 Noise Generation

There are three sources of tire noise generation. The first is related to friction between tread rubber and road surface and is influenced by the type of rubber compound used. The second is due to the distortion and vibration of the carcass as the tire rolls over irregular road surfaces. The periodic contact between the tread blocks and the road surface is the third source. If the tread pattern repeats itself accurately, this will result in noise with a dominant frequency and its harmonics, depending on vehicle speed. To avoid this very disturbing type of noise, it is usual to introduce intentional irregularities in tread patterns such as slightly varying block sizes or groove patterns.

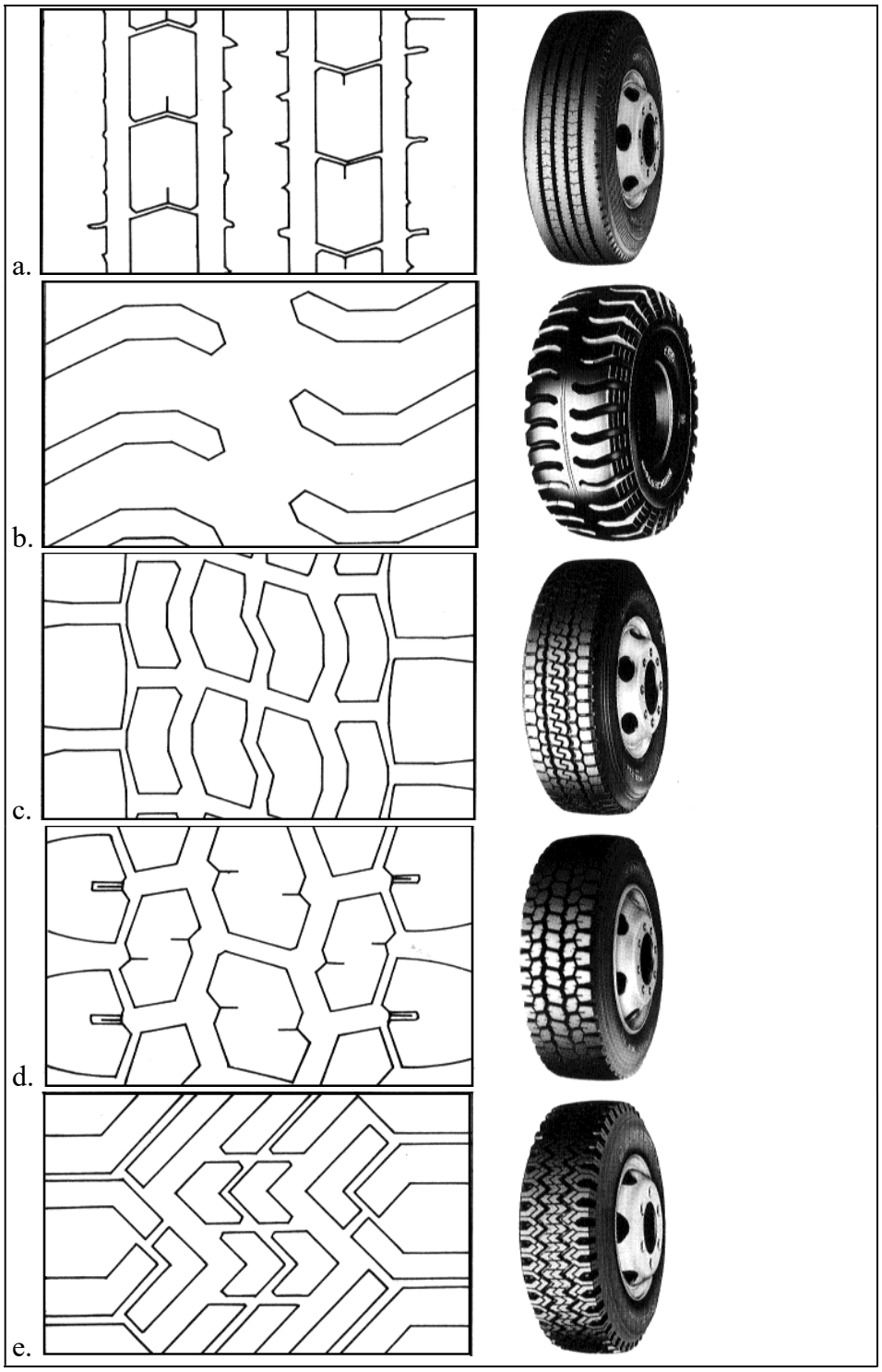


Figure I-11 Tires with various different tread pattern designs.

a. Rib type: Circumferential grooves for silent operation and better directional control,
b. Lug type: Tread for high traction performance, especially in off-road operation,
c. Block type: Circumferential grooves with teeth for handling and high traction performance,
d. Block type: For better traction and braking, especially on mud and snow,
e. Block type: Snow and mud tire.

I-6. Aspect Ratio

One of the most critical dimensions of a tire is the aspect ratio

$$\phi = \text{aspect ratio} = \frac{\text{section height}}{\text{section width}} \tag{I-1}$$

which is usually expressed as a percentage. The relevant terminology is given in Fig. I-12.

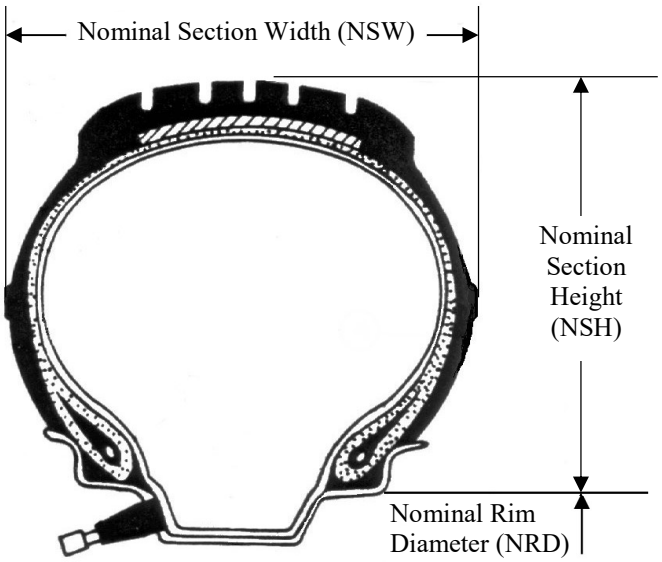


Figure I-12. Tire-rim terminology

Because the pneumatic tire evolved from a simple circular-section tube, the 100 percent ratio remained standard for several decades. It was found, however, that a tire behaved better when mounted on a wider rim - which increased the actual section width. A new European standard became established for the so-called low-pressure (super-balloon) tires with a ratio of about 95 percent. These tires were increasingly popular because the lower aspect ratio proved to give a better high-speed performance, better load carrying capacity, better wear, and higher cornering power.

The aspect ratio could not be reduced further because the shorter sidewalls and excellent vertical stiffness of the lower profile gave a harsher ride. Thus only as vehicle suspension systems became more sophisticated and vibration insulation more universal, further steps could be taken to lower the ratio without reducing the level of comfort below what was acceptable.

In time this was achieved with an 88 percent aspect ratio which became known as the medium-low profile and which was not superseded until the advent of the first fabric-breaker radial-ply tires. These needed a low aspect ratio if they were to exploit all their potential, and so a new European standard of 83 % was evolved, being referred to as low profile.

In the United States, the industry ignored radial-ply tires, and the 83 percent ratio never really caught on. Concentration there was on the development of bias-ply designs with an ultra-low profile with an aspect ratio of 78 percent.

Since 1966 the Americans pioneered a 70 percent profile for bias-ply tires and called them the Wide Ovals. In Europe, 70 percent aspect ratio was first applied to radial-ply tires, and the preferred term for these tires is 70 series.

More recently, profiles have come down even further. Tires down to 45 percent aspect ratio are quite common in the USA and Europe as radials. The trend towards decreasing aspect ratios is likely to continue in the future, and tires of 25 percent aspect ratio are being used in racing.

The reason for the trend to lower aspect ratios is that they offer the possibilities of improvement in most performance parameters except ride comfort, which is decreased. All these changes, whether improvements such as greater load-carrying capacity or otherwise (e.g., ride comfort), are derived from the generally greater vertical and lateral stiffness of the low profile of the tire.

There are other reasons for adopting low profile tires that bear no relationship to the performance of a tire at all:

- One of the most persuasive factors influencing the American car manufacturers was that it enabled them to fit larger diameter wheel rims to cars of the existing design, thus making room for larger or better-ventilated brakes.

- Further, stylists would insist on wide low-profile tires, and their views just cannot be ignored.

I-7. Ply rating

A tire's strength and load-carrying capacity were at one time indicated by the number of plies, a four-ply rating (marked 4PR), meaning that the tire carcass was made with four layers. Although ply rating is still used to indicate the load-carrying capacity, the stronger materials used today mean that fewer plies are needed. Thus, today, ply rating is an index of strength that does not necessarily represent the number of plies in the tire. A tire marked with a four-ply rating, for example, may only have two plies in the casing. Private cars are fitted with 4PR tires, light vans and estate cars that are usually used fully laden should be fitted with 6PR tires, and commercial vehicles are fitted with 10, 12, or 14 PR tires.

I-8. Early Tire Designations



Tire markings on the sidewall indicate the tire size and, in some cases, the maximum speed rating as well as the load capacity. These apply to a fitted, properly inflated tire carrying its rated load. There have been various tire markings in the history of pneumatic tires, as explained below. The relevant dimensions are as illustrated in Fig. I.9.

(i) International Tire Designation :

This designation is commonly used for cross-ply tires. A typical example is :

5.60 - 15

where 5.60 is the nominal section width in inches, and

15 is the nominal rim diameter in inches.

(ii) Millimeter-inch Designation:

This designation is now obsolete. A typical example is :

165 - 15

where 165 is the nominal section width in mm, and

15 is the nominal rim diameter in inches.

(iii) Early Radial Tire Designation

This designation is still used even though it has become outdated. A typical example is :

165 SR 13

where 165 is the nominal section width in mm,

S is the speed rating that indicates that this particular tire can be used up to 180 [kph]. Other alternative letters are H and V, which indicate allowable speeds up to 210 and above 210 [kph], respectively,

R indicates that the tire is a radial-ply tire, and

13 is the nominal rim diameter in inches.

(iv) P-Metric Designation (ISO):

This is a passenger tire designation system originated by the International Standards Organization (ISO) and had been considered, until recently, to become the international passenger car tire standard. A typical example is given in Figure I-13.

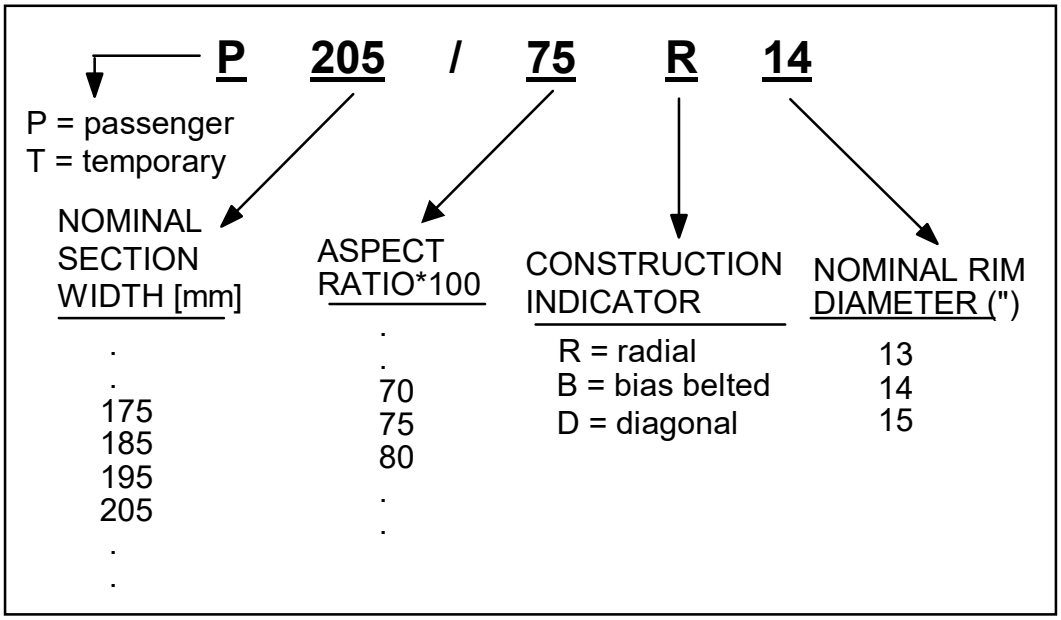


Figure I-13 P-metric size designation nomenclature

As illustrated in Figure I-13 :

- P is for the passenger (T is for temporary) - optional,
- 205 is the nominal section width in mm. Nominal section widths are permitted in 10 mm increments with endings in "5", e.g. ....., 175, 185, 195, 205 .....,
- 75 is the aspect ratio with endings in "0" or "5", e.g. ....., 70, 75, 80, ...,
- R is the construction indicator: R-radial, B-bias belted, D-diagonal, and
- 14 is the nominal rim diameter in inches (for the time being, due to the current worldwide availability of rims. New rim designs that are incompatible with current rims will have nominal rim diameters designated in millimeters).

I-9. New Tire Designations

I-9.1 Designation for Automobile Tires :

Recently, a new designation that is based on the earlier P-metric designation has been introduced. In this designation, a two-digit number varying from 50 to 110 and a capital letter indicating the load capacity and the speed rating, respectively, are added, as illustrated in Fig. I-14.

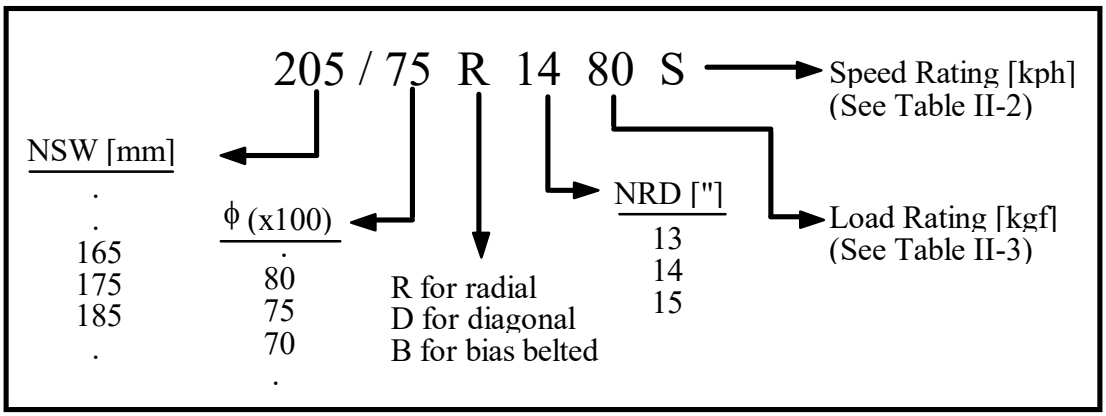


Figure I-14. New designation for automobile tires

The speed and load ratings indicated by the two-digit number and the capital letter added at the end of the designation are given in Table I-1 and I-2, respectively.

Table I-1. Speed ratings for automobile tires.

Letter	Speed rating [kph]
L	120
M	130
N	140
P	150
Q	160
R	170
S	180
T	190
U	200
H	210
V	240
W	270
Y	300
Z	>240

Table I-2. Load ratings for automobile tires.

Designation	**Load Rating [kgf]**	**Designation**	**Load Rating [kgf]**
50	190	80	450
51	195	81	462
52	200	82	475
.53	206	83	487
54	212	84	500
55	218	85	515
56	224	86	530
57	230	87	545
58	236	88	560
59	242	89	580
60	250	90	600
61	257	91	615
62	265	92	630
63	272	93	650
64	280	94	670
65	290	95	690
66	300	96	710
67	307	97	730
68.	315	98	750
69	325	99	775
70	335	100	800
71	345	101	825
72	355	102	850
73	365	103	875
74	375	104	900
75	387	105	925
76	400	106	950
77	412	107	975
78	425	108	1000
79	437	109	1030
		110	1060

I-9.2 Designation for Commercial Vehicle Tires :

Designation for commercial vehicle tires consists of the basic tire dimensions and construction indicator together with the load and speed ratings. A typical example is

11 R 22.5 145/142 L

where

11 is the nominal section width in inches,

R is the construction indicator - R for radial,

22.5 is the nominal rim diameter in inches,

145/142 is the load rating, the first number for a single wheel and the second number for a tandem wheel (the actual load capacities are given in Table I-4.),

L is the speed rating according to Table I-3.

Some new commercial vehicle tires may have a designation including the aspect ratio and/or nominal section width specified in [mm] just as in the case of automobile tires.

Table I-3. Speed ratings for commercial vehicle tires.

Letter	**Speed rating [kph]**
E	70
F	80
G	90
J	100
K	110
L	120
M	130
N	140

Table I-4. Load ratings for commercial vehicle tires.

Designation	Load Rating [kgf]	Designation	Load Rating [kgf]	Designation	Load Rating [kgf]
110	1060	142	2650	174	6700
111	1090	143	2725	175	6900
112	1120	144	2800	176	7100
113	1150	145	2900	177	7300
114	1180	146	3000	178	7500
115	1215	147	3075	179	7750
116	1250	148	3150	180	8000
117	1285	149	3250	181	8250
118	1320	150	3350	182	8500
119	1360	151	3450	183	8750
120	1400	152	3550	184	9000
121	1450	153	3660	185	9250
122	1500	154	3750	186	9500
123	1550	155	3875	187	9750
124	1600	156	4000	188	10000
125	1650	157	4125	189	10300
126	1700	158	4250	190	10600
127	1750	159	4375	191	10900
128	1800	160	4500	192	11200
129	1850	161	4625	193	11500
130	1900	162	4750	194	11800
131	1950	163	4875	195	12150
132	2000	164	5000	196	12500
133	2060	165	5150	197	12850
134	2120	166	5300	298	13200
135	2180	167	5450	299	13600
136	2240	168	5600	200	14000
137	2300	169	5800	201	14500
138	2360	170	6000	202	15000
139	2430	171	6150	203	15500
140	2500	172	6300	204	16000
141	2575	173	6500		

I-10. Tire Manufacture

The first process in the manufacture of tires is to masticate (to reduce to a pulp by crushing or kneading) and compound raw rubber (natural and/or synthetic), carbon black, and chemicals in a banbury (an internal mixer) to obtain a perfectly uniform compound. Sulfur and other chemicals are added to the compound and heated in another mixer. This blend is called the "masterbatch," and its make-up is carefully constructed according to the desired performance parameters of the tire. A continuous strip is then formed using dual mills which undergoes laboratory tests after cooling. The strips of the compound are used to:

i) coat textiles such as rayon, nylon, and polyester for the carcass plies and coat steel cords for the breaker plies on both sides,

ii) coat bead wires,

iii) construct tread and sidewalls.

In shaping the tread and sidewall, the tread extruder forces hot pliable rubber through a die which provides the correct shape, the compound is then cooled in a water tank, and the tread and sidewalls are cut into lengths for different tire sizes.

Meanwhile, specially woven nylon or rayon fabric is dipped into a bath of latex-based adhesive and then dried to remove excess moisture. It is then fed between rollers where a hot sticky rubber compound coats each cord.

After passing through the rollers, the fabric is tested and then cut into measured strips. Each strip is cut to the exact width and angle for the sizes and types of tires to be made. The bead wire - that's what grips the wheel rim to form an air-tight seal between wheel and tire - is made of strands of high tensile steel wires drawn together and coated with rubber. The wire is given its circular shape by a wheel that winds onto itself the exact amount of wire required.

Tire building is traditionally a two-stage process. Although modern tire factories now use a certain number of single-stage building machines, the two-stage building is still widely used, particularly for the more standard sizes. In the first stage, the inner liner, the body plies, and the sidewalls are placed on a building drum. The beads are then positioned, the ply edges are turned around the bead core and the sidewalls are simultaneously moved into position. In the second tire building stage, the tire is shaped by inflation with two belts, a cap ply and the tread being added. At the end of this stage, the tire is now known as a "green tire".

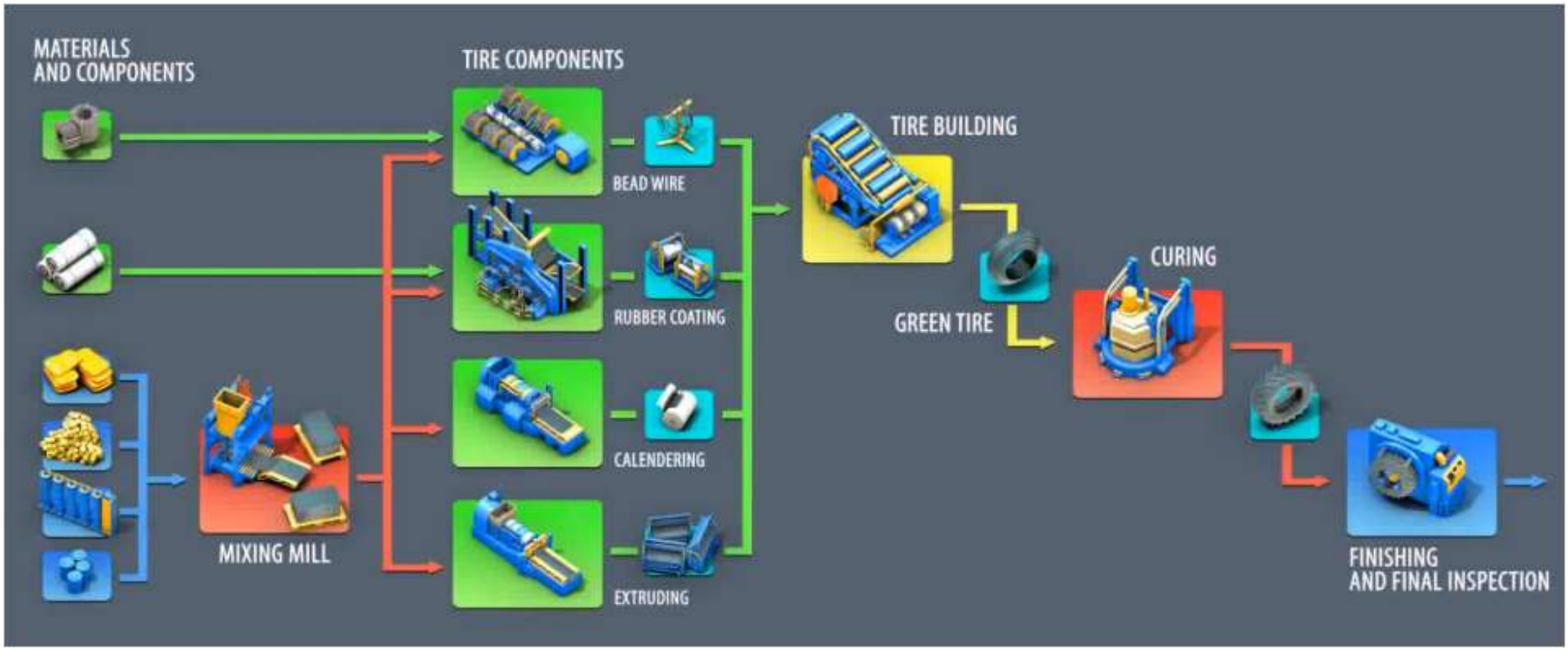


Figure I-15 Tire Manufacture

The final process is tire molding. Here two types of presses are used :

- the bag molding,

- the diaphragm molding.

In the *bag-molding method*, an airbag to form the inside of the tire is fitted into the built-up tire, which is then placed in the mold. Steam for heating the mold and hot water for inflating the airbag is then released and the tire is shaped to the pattern of the mold.

For the *diaphragm process*, an automatic mold that has a built-in diaphragm (the equivalent of the airbag) is used. A built-up tire is fitted over the diaphragm and is shaped during the press closing sequence. Each tire is then trimmed (excess rubber is removed from the cured tire). After visual inspection and tests, it is stamped "OK".

The process of tire manufacture is illustrated in Fig. I-15.

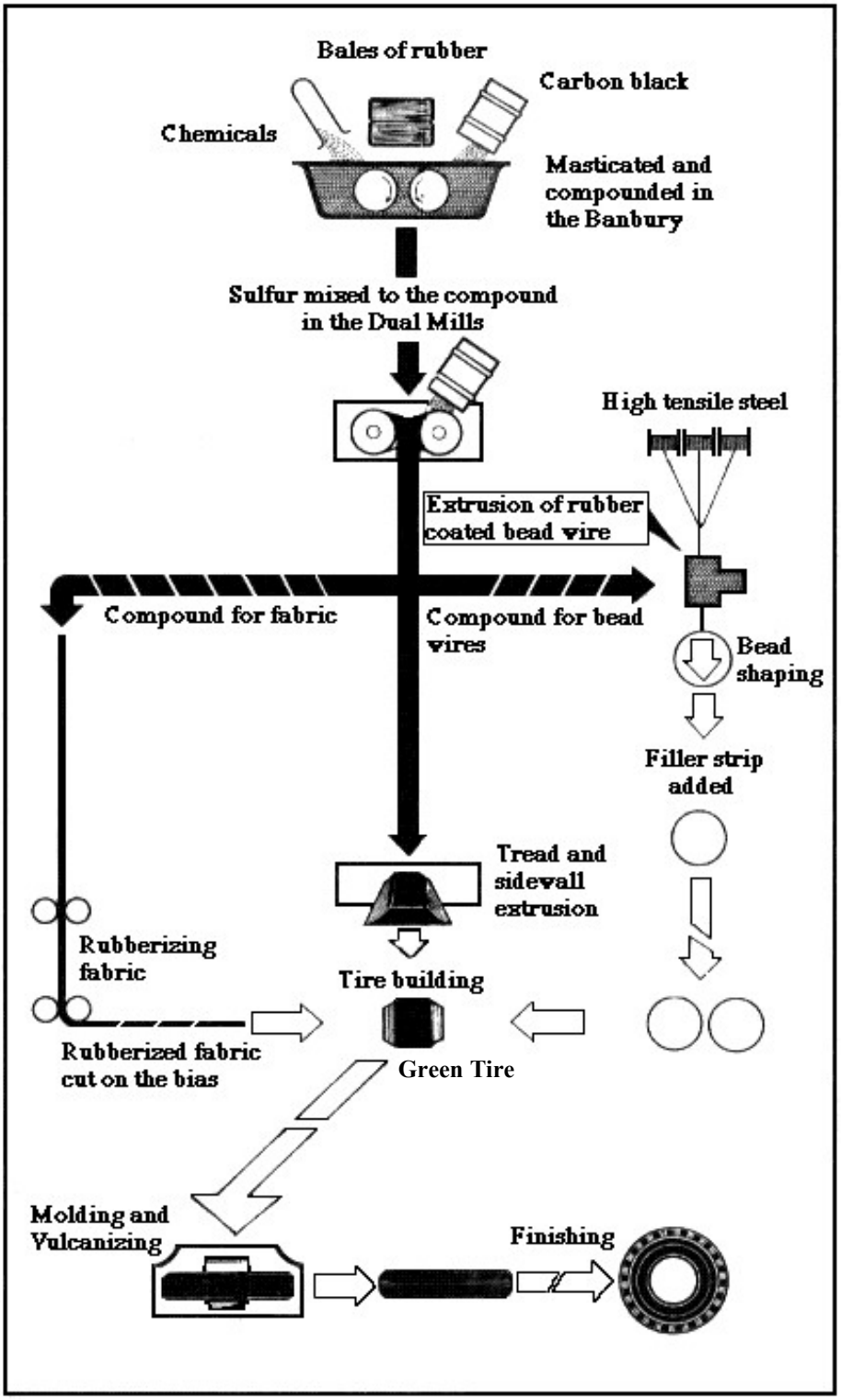


Figure I-15 Processes in the manufacture of tires.

Exercises

I-1) Sketch the tread patterns for two tires - provide all the designation written on the tires. Compare the two with respect to :

i/ shape, size, and height of blocks,

ii/ number, depth, and width of circumferential and side drainage grooves,

iii/ relative proportion of side to circumferential drainage grooves,

iv/ number and size of sipes,

v/ any other visible characteristics.

Try to assess the relative performances of the two tires.

I-2) Associate each group of functions with one of the components of a pneumatic tire.

Function Groups

a) Transmit torque
Connection to the rim
Air Sealing
Fix the casing

c) Carcass Protection
Bead Protection
Ageing Protection
Fatigue

e) Handle Pressure
Handle Torque
Fatigue
Impermeability
Suspension of wheel

b) Dimensional Stability
Handle Longitudinal Stress
Handle Cornering Forces
Tread Stabilization

d) Grip
Mileage
Carcass Protection
Low Noise
Aquaplaning

Components

1) TREAD
2) BEAD WIRES
3) SIDE WALLS
4) BREAKER BELTS
5) CARCASS

I-3) Associate each of the following specified characteristics with one of the tire types listed.

Characteristics

1. Designed for wet and dry weather driving but not for use on snow or ice as they do not provide the degree of traction offered by snow and all-season tires.

2. Provide maximum traction in snowy and icy conditions. The tread is designed for maximum grip in those conditions, and the tire is also constructed out of special material that remains pliable in cold weather. The tradeoff for this increased traction generally includes less handling ability on dry pavement, increased noise levels, and more rapid tread wear.

3. Provide a good balance for drivers looking for increased traction in rain or snow, as well as the handling, ride, and treadwear benefits offered by summer tires.

4. Offer a degree of handling, grip, and cornering ability superior to that of other tires. To provide a higher degree of performance, the tires must be able to withstand significantly higher temperatures. Consumers are typically willing to accommodate some tradeoffs in treadwear and ride comfort to attain this high degree of performance.

5. Developed over the past few years in order to provide the all-season capability for enthusiasts, which feature performance enhancement as well as good traction on snow and ice.

List of Tire Types

a. All-Season Tires
b. Snow Tires
c. All-Season Performance Tires
d. Summer Tires (also called Highway Tires)
e. Performance Tires

I-4) What may be the possible advantages of the tubeless tires over tubed ones ?

I-5) Consider the tread pattern design of the tire shown.

i) What can you say about the surface for which it is designed ? Check the best answer.

Hard ☐, rocky ☐, muddy ☐, icy ☐, sandy ☐, wet ☐.

ii) Check design priority.

Good directional control ☐, Good traction ☐,Good directional control and traction ☐



I-6) Consider the tires shown below. Looking at the tread pattern, compare the two with respect to directional control, traction and braking, and wet weather performance.



I-7) Tread patterns with rib designs (design elements principally oriented in the circumferential direction) have good lateral traction and uniform wear characteristics. They find almost exclusive use in tires designed for use on steering axles and on trailers where slow and uniform wear characteristics are even more appreciated.

On drive axles, traction is of primary importance, and fast wear is induced by slip due to traction. Then cross-lug design (design elements oriented in the lateral direction) offers the best performance. When even greater lateral and longitudinal traction requirements are required, tread pattern designs with tread elements in both lateral and circumferential directions have been designed.

In view of the information given above, associate each description with one of the 3 tires and explain your reasoning.

1) Tire designed for fitment to steering axles of trucks for specific winter use.
2) Tire designed for fitment to driven axles of high-powered vehicles. Improved water drainage and excellent grip
3) Tire designed for single fitment on towed axles of trailers and semitrailers. Provides excellent transversal grip and braking characteristics.



a)



b)

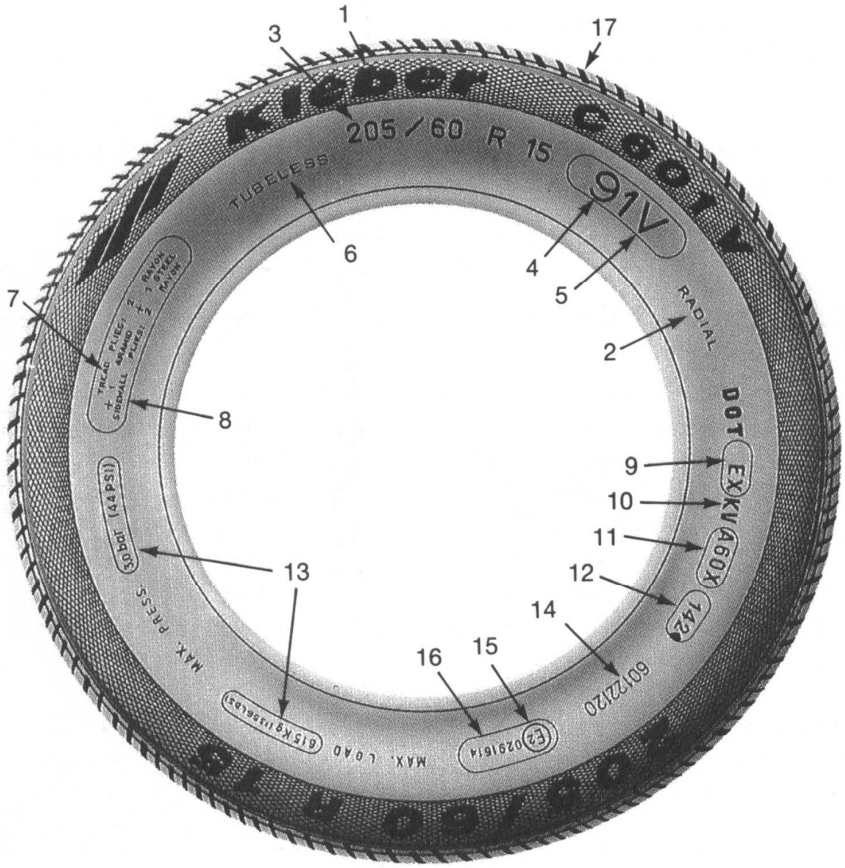


c)

I-8) Compare textile and steel-belted radials with respect to the characteristics listed below. Explain the source of superiority for each case. (For example, steel-belted radials are better w.r.t. directional stability, since steel corded breaker belts result in higher lateral stiffness and thus higher cornering power.)

a) Ride comfort
b) Cost
c) Performance
d) Noise
e) Life

I-9) Find out about the sidewall markings of automobile tires and identify the information marked and numbered on the tire below.


1
3
17
205 / 60 R 15
91V
TUBELESS
6
4
5
RADIAL
2
7
8
DOT
9
10
11
12
14
16
15
13
MAX. PRESS.
MAX. LOAD

CHAPTER II

WHEELS

II-1. Introduction

A wheel is that rotating part of a suspension system that supports the tire. It consists of two main elements :

i / The rim is the supporting frame for the tire.
ii / The disc provides the connection between the rim and the wheel hub.

These two elements may be integral or are joined together either permanently by welding or by bolts and nuts (i.e., detachable). Wheels can be classified according to the type of service as follows :

i / Automobile wheels.
ii / Wheels for commercial vehicles.
iii / Agricultural tractor wheels.
iv / Motorcycle, bicycle, and moto-scooter wheels.
v / Industrial and fork-lift truck wheels.
vi / Wheels for earth-moving machinery.

Only the first two types, i.e., the automobile wheels and wheels for commercial vehicles, will be examined here.

II-2. Wheel Dimensions / Basic Designation

A wheel is designated by two major dimensions; width and diameter of its rim, both given in inches. A typical designation is, therefore, may be of the form

5.50 x 13

The cross sign, x, separating the two dimensions, indicates that the rim has a single-piece construction as in automobile and agricultural tractor wheels. Commercial vehicle wheels, on the other hand, may have rims consisting of two or more detachable pieces for ease of tire mounting and removal. These wheels are identified by using a dash "-" instead of the cross in the designation, i.e.

5.50 - 16

II-3. Automobile Wheels

The automobile wheel has a single-piece rim spot welded to the disc. The nomenclature for a typical automobile wheel is given in Fig. II-1. The central part of the rim has a large peripheral depression which is called a "well" or "drop center" to facilitate mounting and removal of the tire. The flats on both sides of the drop center provide the bead seats and the two flanges retain the tire on the rim under the action of lateral tire forces.

The cross-section of the rim is usually asymmetrical, with the drop center displaced towards the outside of the wheel to allow more space for the brake assembly inside the wheel. The distance between the rim centerline and the mounting face of the disc is called the "offset". There are some symmetrical rims as well, however, and they are distinguished from asymmetrical rims by the addition of a suffix S at the end of the designation, i.e.

5.50 x 13 - S

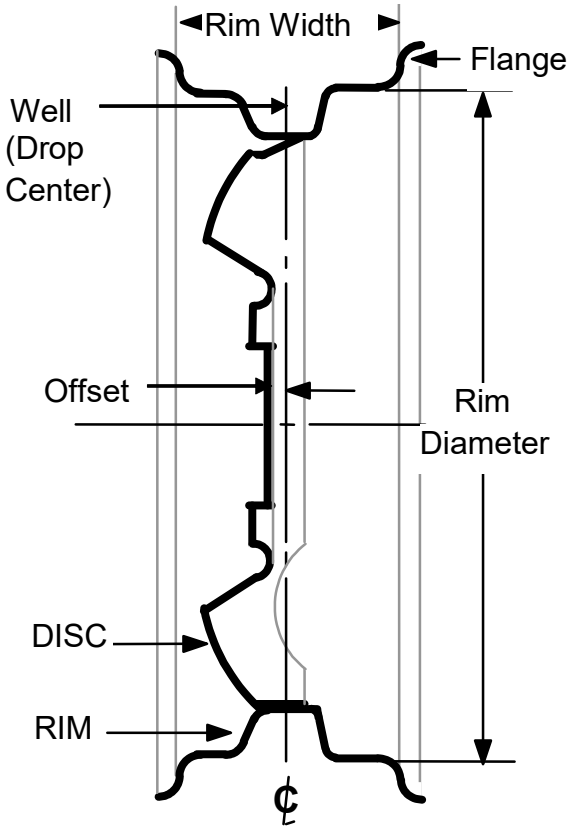


Figure II-1. A typical automobile wheel.

Sizes and tolerances of rims have been standardized, and inch units are used internationally. Rim widths vary from 4 inches to 9 inches in half-inch increments, the most commonly used sizes being in the range of 4.0 to 5.5 inches. Rim diameters vary from 12 to 19 inches, the most commonly used sizes being 13 to 15 inches.

There are several rim flange shapes with different heights, widths, and curvatures. They have been standardized into six basic shapes, designated by letters B, J, JJ, JK, K, and L, as illustrated in Fig. II-2 below.

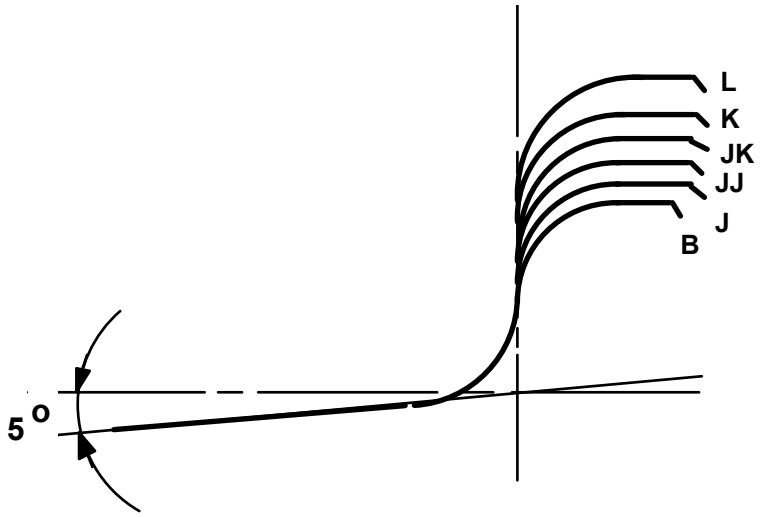


Figure II-2. Rim flange shapes.

The flange shape is indicated in the wheel designation by the shape symbol placed after the rim width.

5.50 JJ x 13

To improve the seating of the tire beads and ensure a tight fit, the surfaces on both sides of the well are slightly tapered. The standard slope towards the well is 5 degrees for automobile wheels. The seats may be flat or have a small obstruction called a "hump" at the well side. If the hump has a flat top, then it is called a "flat hump". These special bead seat contours keep the tire beads from being forced off the seats and fall into the well while cornering. Thus the accidental loss of air in tubeless tires is prevented. In addition, if the tire blows out, it won't leave the rim, improving safety and stability. If the seat is flat with no hump, then the bead seat is called "special ledge". The shapes of the hump, flat hump, and special ledge contours are given in Fig. II-3.

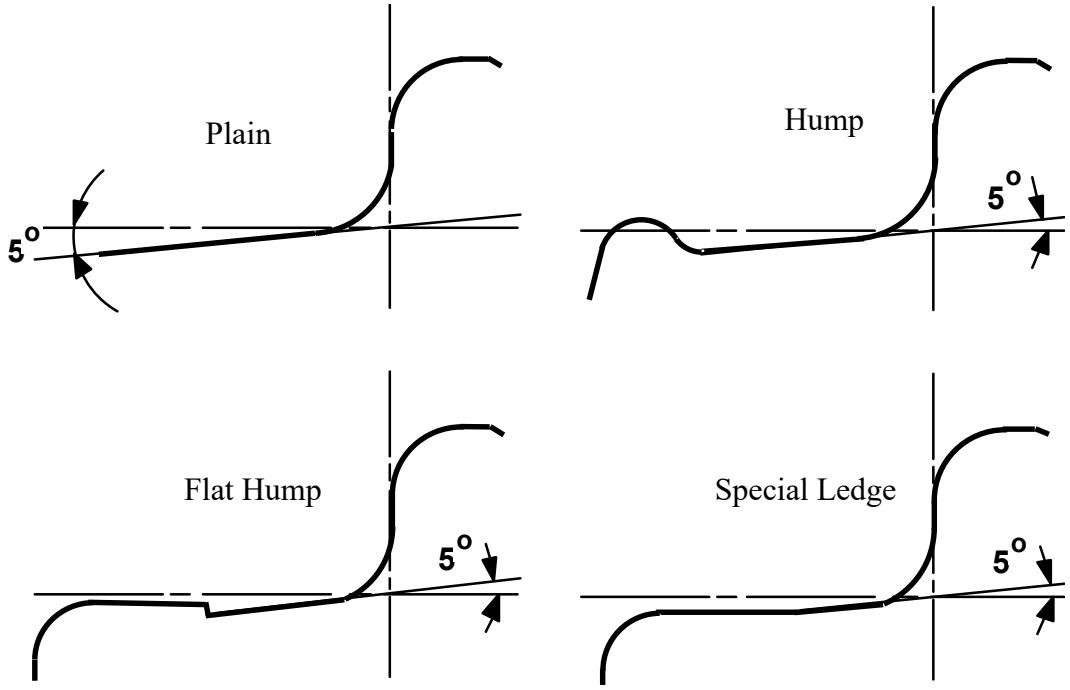


Figure II-3. Bead seat contours.

A rim may have any of these bead seat contours on any side of the well and is named according to the particular combination. Table II-2 gives a list of the combinations most commonly used and their corresponding symbols for use in wheel designations.

Table II-2. Bead seat contour combinations.

Designation	**Bead Seat Contour**		**Symbol**
	Outside	**Inside**	
Hump	Hump	Normal	H
Double hump	Hump	Hump	H2
Flat hump	Flat hump	Normal	FH
Double flat hump	Flat hump	Flat hump	FH2
Combination hump	Flat hump	Hump	CH
Special ledge	Special ledge	Normal	SL

Special bead seat contours are indicated by adding the appropriate symbol to the end of the basic rim designation, for example

5.50 JJ x 13 H2 - S

If there is no bead seat contour indication, then the bead seats are plain (5^o slope towards the well).

The disc shape has not been standardized to any extend and is determined according to:

i / the type (disc or drum) and the size of the brakes
ii / the shape of the hub
iii / the number of wheel studs
iv / the method of mounting the hub cap
v / the geometry of the steering system, etc.

Therefore the shape of the disc varies widely from one vehicle to another. Construction-wise, the wheels are either made from rolled sheet steel strips welded to pressed steel plate discs or cast from a light magnesium-aluminum alloy and machined. Wire wheels have also been used for a long time.



Cast Wheel Steel Wheel Wire Wheel

II-4. Wheels for Commercial Vehicles

Since commercial vehicle tires have a very rigid body construction, the rim drop center is either very shallow or non-existent. This is because the well cannot provide ease of mounting and removal for the tire, and the rim is made up of two or more pieces. A typical commercial vehicle wheel and the nomenclature used are given in Fig. II-4.

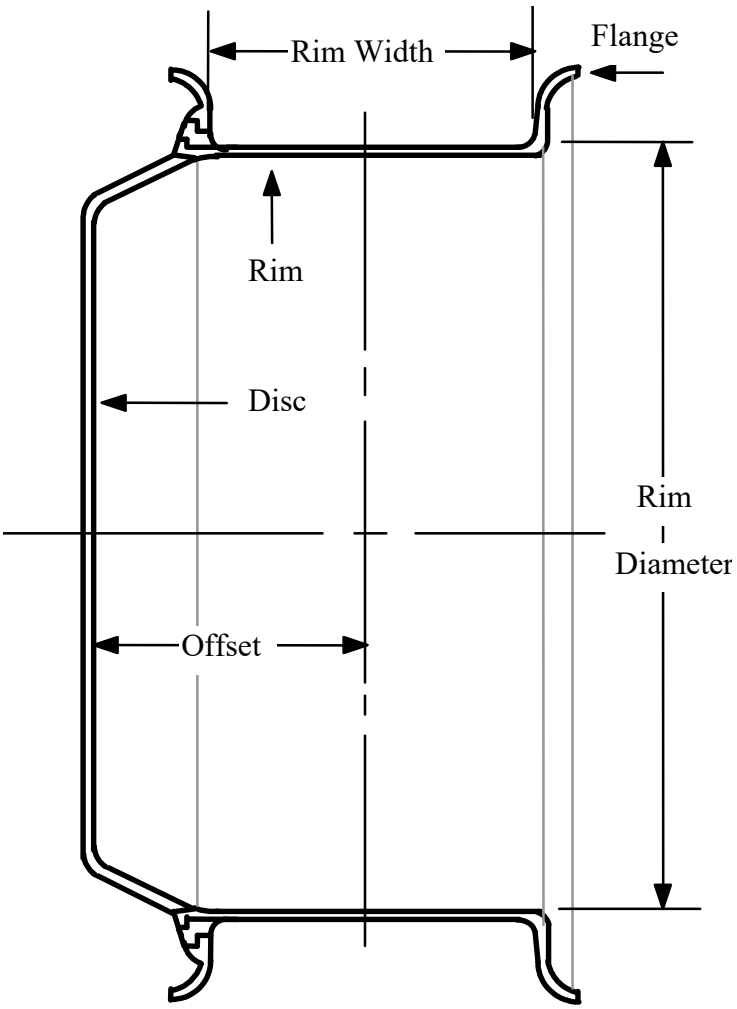


Figure II-4. A typical commercial vehicle wheel.

The principal commercial vehicle rim profiles are illustrated in Fig. II-5. The wide base 5º tapered rim is the most widely used type. The flat base rim, on the other hand, has minimal use. Semi-drop center rims are mainly used on light commercial vehicle wheels. The wide base 15º tapered rim has a single-piece construction and is suitable for use with tubeless tires. The highly tapered bead seats ensure maximum tightness and security. The drop center enables ease of mounting and removal of the tire as in automobile wheels.

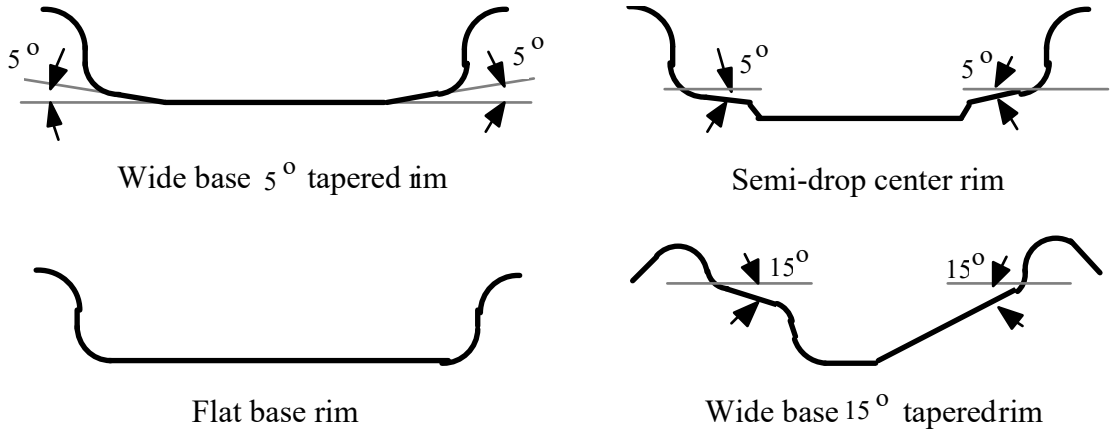


Figure II-5. Rim profiles for commercial vehicle wheels.

In wheels consisting of more than one piece, one of the rim flanges is removable, and it consists of one or two rings that are pushed in between the tire and the rim base. The pieces are held together by mechanical interlocking and tire pressure. In light commercial vehicles, a two-piece rim composed of a rim base and a combination ring is used. The combination ring is split to make fitting and removal possible functions as the bead seat as well as the flange. Three types of multi-piece rims are illustrated in Fig. II-6.

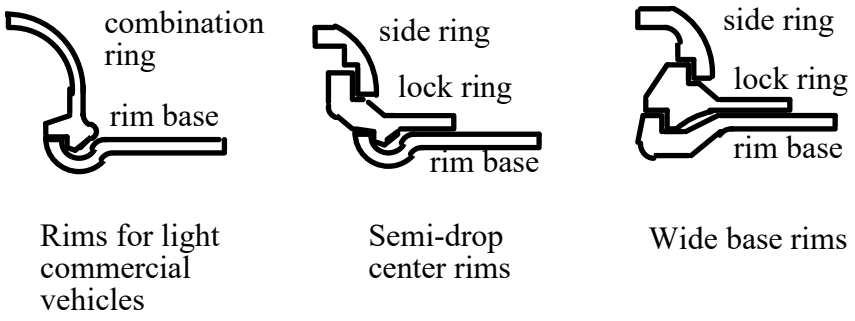


Figure II-6. Multi-piece rims.

The commonly used diameters for commercial vehicle wheels are 15, 17, 18, 20, 22, and 24 inches.

CHAPTER III

STEERING SYSTEM

III-1. Introduction

All vehicles operating on a non-fixed path require some kind of a steering system for directional control. Railway vehicles that operate on tracks have fixed paths and therefore do not require steering.

Directional control includes a change of direction as well as the maintenance of the required path under the influence of external forces.

III-2. Basic Types of Steering Systems

The following basic steering systems have been used for various vehicles depending on the requirements of the particular application:

1) *Differential (Skid) steering system*

The introduction of a velocity differential across the two sides of a vehicle results in a change of direction. The faster running side covers a greater distance in a given time, thus turning the vehicle toward the slower running track, Figure III-1. It is also possible to make a point turn. This system is mainly used in tracked (track laying) vehicles and on some particular purpose (such as small loaders and combat vehicles) tired vehicles.

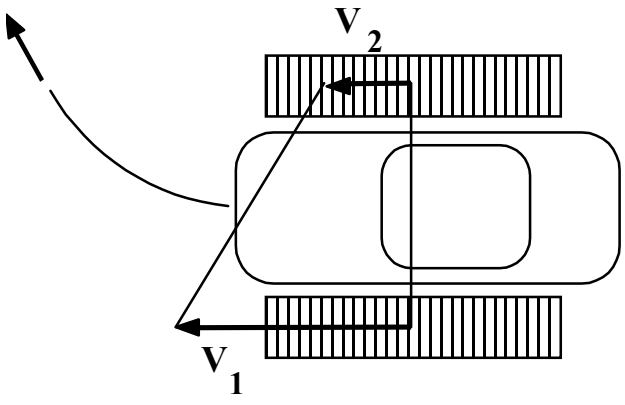


Figure III-1 Differential (skid) steering

2) *Articulated body steering*

For this type of steering, the vehicle body is articulated (hinged) at the mid-section about a vertical axis, Fig. III-2. The front half of the vehicle can thus be rotated with respect to the rear half. The wheels are fixed on the body. As a result of articulation, the direction of the front wheels changes with respect to the rear wheels, thus steering the vehicle.

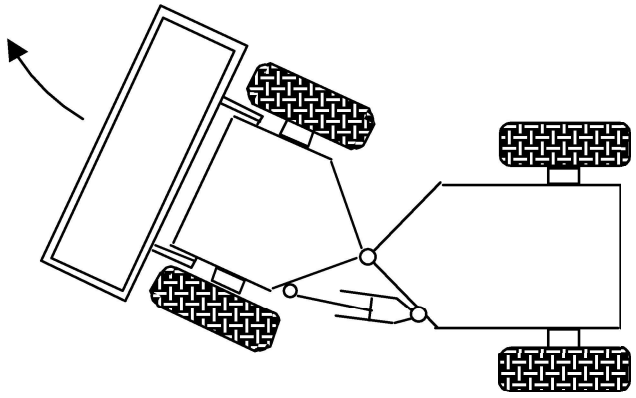


Figure III-2 Articulated body steering

This system is used in some type of wheeled off-the-road vehicles in which conventional pivoting of the steering wheels with respect to the body is not possible and/or desirable. For example, a loader with large diameter tires would require an extremely wide track at the front of the front wheels are to be pivoted with respect to the body.

3) *Fifth wheel steering*

This is the familiar system used in horse carriages. The front wheels are fixed on the solid front axle and are always perpendicular to it. The axle is pivoted on the vehicle body at its midpoint through a vertical axis. Thus, the axle is free to swivel in a horizontal plane, and hence the name "fifth wheel" is given, Fig. III-3.

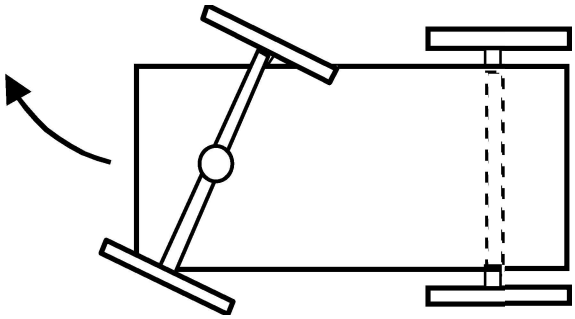


Figure III-3 Fifth wheel steering

This type of steering system requires a lot of space and a heavy axle and therefore is unsuitable for motor vehicles. It does, however, find applications in some trailer and semitrailer designs.

4) *Fixed pivot steering system*

In this system, the steering wheels are pivoted about a vertical axis which is fixed with respect to the body, as illustrated in Fig. III-4. The wheels are interconnected by the steering linkage which controls their relative motion. The steering wheels maintain a prescribed angular relationship with each other for the reasons explained in the following section.

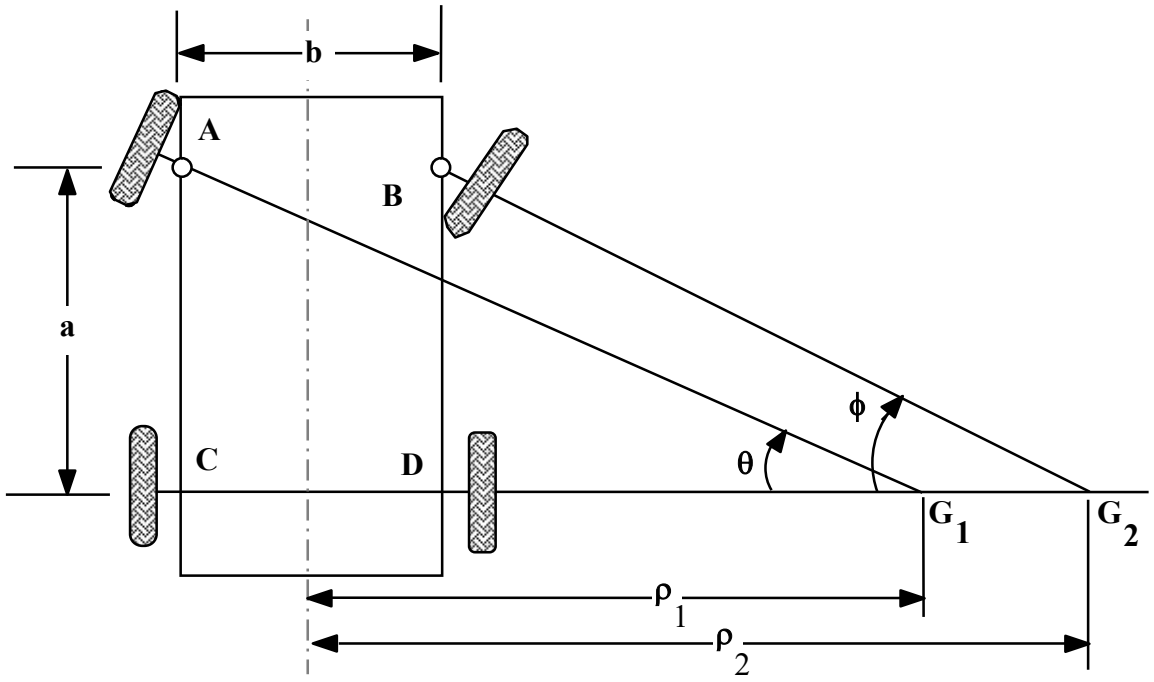


Figure III-4 Fixed pivot steering geometry.

It must be noted that the descriptions of the steering conditions described so far are applicable in low-speed applications. At high speeds, deformation of the tires results in slip angles which alter the position of the instantaneous center(s) of rotation.

III-3. Geometrically Correct Steering

It is desirable, during cornering, to have all the wheels going through a purely rotational motion without side-slipping, thus turning about a common instant center. This is called pure rolling. If this condition is not satisfied, the wheels will work against each other, producing increased wear on the tires, increased effort in the steering wheel, and additional drag which increases fuel consumption and decreases traction. Pure rolling can only be achieved by maintaining a particular angular relationship between the front wheels such that when the steering wheels are deflected from the straight-ahead position, the extensions of their axes of rotation intersect on the extension of the rear axle, Fig. III-5. Therefore, in Fig. III-4, the distance between the points G_1 and G_2 can be interpreted as a measure of the deviation from the pure rolling condition.

Geometrically correct steering implies that the condition for pure rolling is satisfied. From Fig. III-5, it is seen that in such a case, the inside wheel must be turned towards the center G through a greater angle than that of the outside wheel.

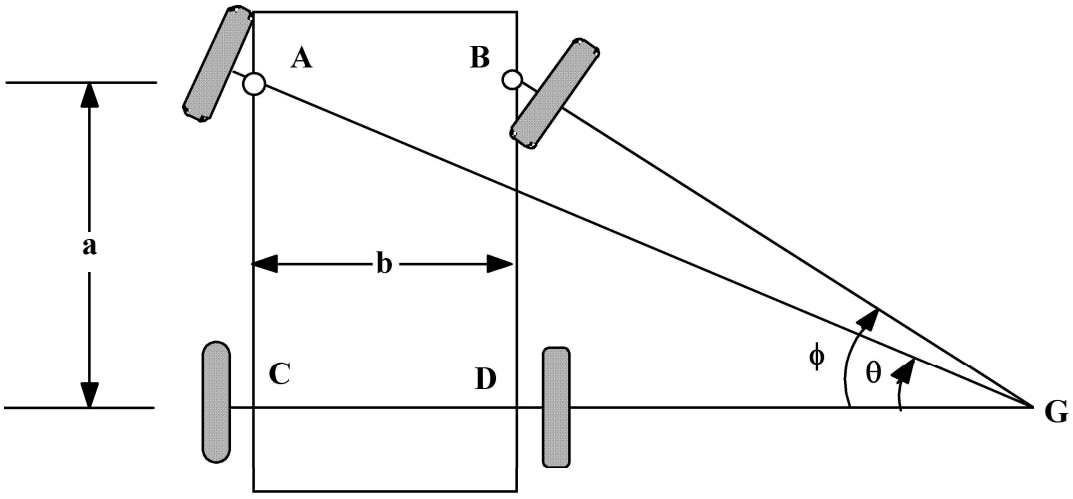


Figure III-5. Geometrically correct steering

The required angular relationship can be obtained as follows:

$$\cot\theta = \frac{CG}{AC} \qquad \text{(III-1)}$$

$$\cot\phi = \frac{DG}{BD} \qquad \text{(III-2)}$$

$$b = CG - DG$$

$$a = AC = BD$$

$$\cot\theta - \cot\phi = \frac{CG}{AC} - \frac{DG}{BD} = \frac{CG - DG}{a} = \frac{b}{a}$$

$$\frac{b}{a} = \cot\theta - \cot\phi \qquad \text{(III-3)}$$

Knowing the relation between the inner and outer wheel steering angles, in terms of the vehicle parameters, to obtain pure rolling, one can now define a steering error for a given steering linkage as :

$$\gamma = \left|\theta_{cor} - \theta_{act}\right| \qquad \text{(III-4)}$$

for a specified ϕ, where θ_{cor} is the angle obtained from eqn. (III-3) and θ_{act} is the actual angle provided by the linkage.

The requirement for pure rolling of the wheels is fully satisfied by the articulated body and the fifth wheel steering systems. For practical linkages of reasonable complexity and cost, this relation can only be approximately satisfied over a specific range of steering by the fixed pivot steering systems. However, practical limitations have made the fixed pivot steering universal on high-speed vehicles.

The steering wheels are usually the front wheels due to stability reasons. If rear wheels are used for steering, the vehicle will have better maneuverability at low-speed conditions but at high speeds, an unstable situation will arise. Therefore rear-wheel steering is used only on some low-speed vehicles operating within constrained area conditions such as fork-lift trucks and some earthmoving and agricultural machinery.

It is possible to achieve better low-speed maneuverability by four-wheel steering (4WS) while satisfying the geometrically correct steering condition, as illustrated in Figure III-6. By steering wheels at the rear in addition to those on the front, a smaller turning radius can be obtained, see Example III-2. Recent applications, however, have not been successful because of certain adverse effects on high-speed behavior.

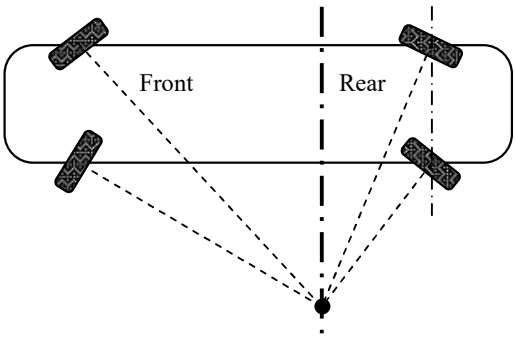


Figure III-6. Four-wheel steering

III-4. Determination of Steering Error

There is no general analytical solution for the determination of the optimum geometry for the Ackerman linkage, and both graphical and analytical solutions are commonly used.

III-4.1 Graphical Method

As Fig. III-5 implies, the graphical method looks inconvenient, particularly for small wheel deflections; the instant center of rotation lies at a point rather far away from the main part of the drawing. To overcome this difficulty, the following procedure is suggested. As shown in Fig. III-7:

i) From the steering pivots A and C, draw lines perpendicular to the rear axle, intersecting it at points E and F.

ii) Draw line GE from the midpoint of the front axle.

iii) Then, the lines drawn from the steering pivots A and C to any point on line GE will result in the steering angles θ and ϕ satisfying geometrically correct steering.

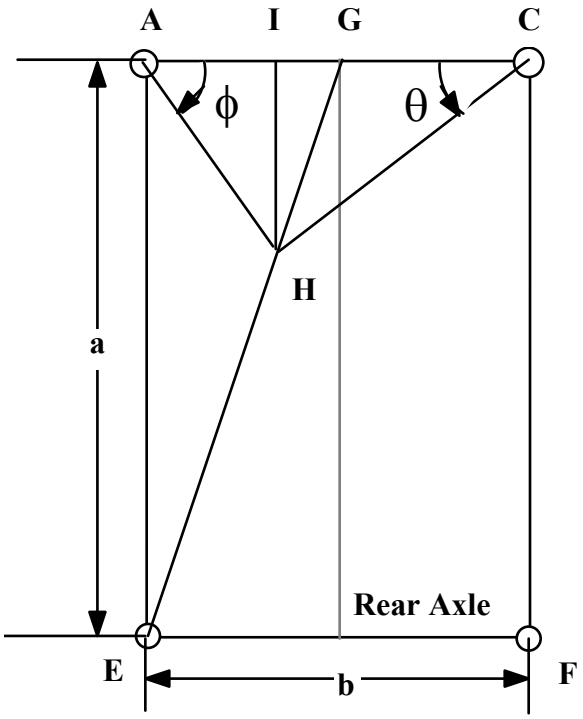


Figure III-7. Graphical Analysis.

The proof is as follows:

$$\cot \phi = \frac{AI}{IH} = \frac{AG\text{-}IG}{IH}$$

$$\cot \theta = \frac{CI}{IH} = \frac{CG+IG}{IH} = \frac{AG+IG}{IH}$$

and

$$\cot \theta - \cot \phi = \frac{2IG}{IH} = \frac{2AG}{AE} = \frac{b}{a}$$

In the design of a steering linkage, this graphical method can be utilized in the following manner.

A steering linkage geometry (dimensions and angles) is assumed, and the deflections of the outer wheel for several known angles of the inner wheel deflection are found graphically. These values are plotted as in Fig. III-8 and the points of intersection are determined. By connecting these points, one obtains the so-called "error curve". The deviation from the geometrically correct steering can, then, be seen as the deviation of the error curve from the true steering line.

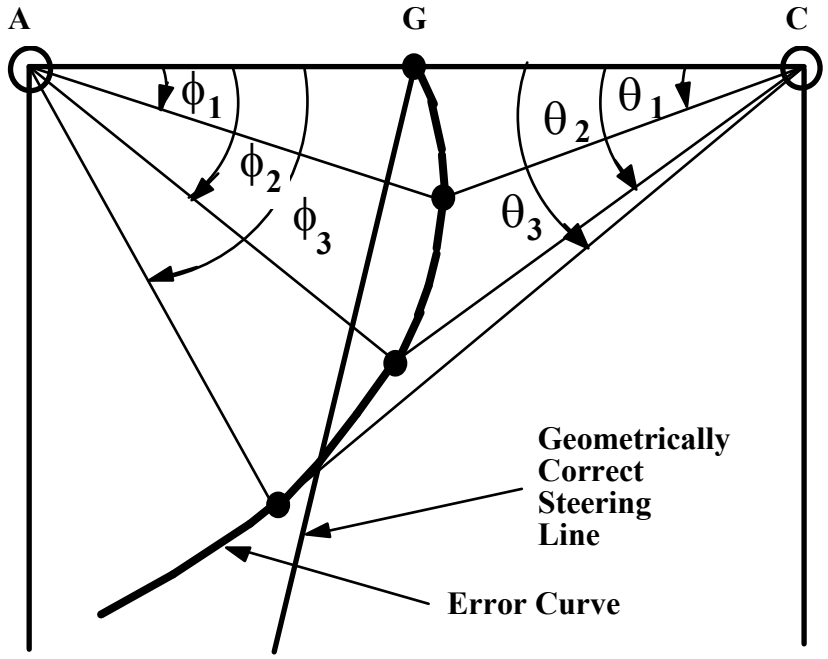


Figure III-8. Error curve.

Depending on the particular application, the maximum error can be adjusted by changing linkage geometry.

III-4.2 Analytical Method

An analytical method that allows the determination of the rotation angle of the outer wheel for a given inner wheel angle, provided that the steering linkage geometry is known, has also been developed.

Two different cases have to be considered:

i) Tie rod in front of the axle (leading-link),

ii) Tie rod behind the axle (trailing-link).

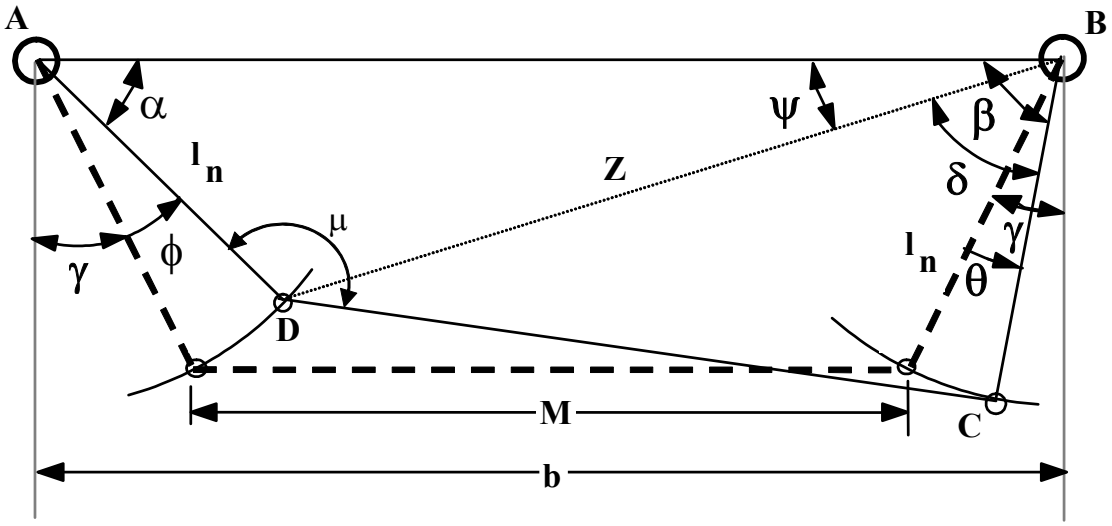


Figure III-9 Steering linkage geometry.

In Fig. III-9, the track arms are behind the axle, i.e., the second case is illustrated.

$$\alpha = \frac{\pi}{2} - \gamma - \phi$$

Using the cosine theorem for the triangle ABD, one can calculate Z.

$$Z = \sqrt{l_n^2 + b^2 - 2 l_n b \cos\alpha} \qquad \text{(III-5)}$$

Knowing Z and calculating the value of M from the relation

$$M = b - 2 l_n \sin\gamma$$

the angles ψ and δ can also be determined.

$$\psi = \cos^{-1}\left(\frac{b^2 + Z^2 - l_n^2}{2bZ}\right) \qquad \text{(III-6)}$$

$$\delta = \cos^{-1}\left(\frac{Z^2 + l_n^2 - M^2}{2Zl_n}\right) \qquad \text{(III-7)}$$

From Fig. III-9, the angle β can be expressed in terms of the known angles.

$$\beta = \psi + \delta$$

Thus, the output angle θ can be obtained in terms of the input angle ϕ.

$$\theta = \beta + \gamma - \frac{\pi}{2} \qquad \text{(III-8)}$$

Note that the force transmission angle

$$\mu = \frac{\pi}{2} + \gamma + \phi - \psi + \cos^{-1}\left(\frac{M^2 + Z^2 - l_n^2}{2MZ}\right) \qquad \text{(III-9)}$$

should be less than about 160^o for proper operation of the linkage for the whole range of ϕ values.

One can derive similar equations for the other case, i.e., where the tie rod is in front of the beam axle.

The general requirement from a steering linkage is that up to $\phi = 30^o$, the difference between the actual value of θ resulting from a proposed linkage and the geometrically correct value satisfying eqn. (III-3) is as small as possible. A practical limit is specified as:

$$| \theta_{act} - \theta_{corr} | \leq 0.5^o \qquad \text{(III-10)}$$

The above limiting value is kept quite tight since possible variations resulting from deflections of components, unaccounted clearances, wear, etc., may result in a larger steering error in operation. In some instances, the designer may relax the requirement such that the above relation is satisfied at least up to $\phi = 20^o$.

Example III-1

For the trailing Ackerman linkage specified by:

$\gamma = 20^o$
ln = 180 mm
b = 1080 mm
a = 2400 mm

Prepare a table including the actual and theoretically correct steering angles, the steering error, and the force transmission angle for input steering angles in the range from 10 to 30^o. Comment on the design.

Solution :

Let us determine first the θ value for geometrically correct steering from eqn. (III-3) for the input steering angle of 10^o at the wheel.

$$\theta_{cor} = \tan^{-1}\left(\frac{1}{\frac{b}{a}+\frac{1}{\tan\phi}}\right) = \tan^{-1}\left(\frac{1}{\frac{1080}{2400}+\frac{1}{\tan 10^o}}\right) \cong 9.28^o$$

$$\alpha = \frac{\pi}{2} - \gamma - \phi = 90 - 20 - 10 = 60^o$$

$$Z = \sqrt{l_n^2 + b^2 - 2l_n b\cos\alpha} = \sqrt{(180)^2 + (1080)^2 - 2(180)(1080)\cos(60)}$$
$$\cong 1002[\text{mm}]$$

$$\psi = \cos^{-1}\left(\frac{b^2 + Z^2 - l_n^2}{2bZ}\right) = \cos^{-1}\left(\frac{(1080)^2 + (1002)^2 - (180)^2}{2(1080)(1002)}\right) \cong 8.95^o$$

$$M = b - 2l_n \sin\gamma = 1080 - 2(180)\sin(20) \cong 956.87[\text{mm}]$$

$$\delta = \cos^{-1}\left(\frac{Z^2 + l_n^2 - M^2}{2Zl_n}\right) = \cos^{-1}\left(\frac{(1002)^2 + (180)^2 - (957)^2}{2(1002)(180)}\right) \cong 70.37^o$$

$$\beta = \psi + \delta = 8.95 + 70.37 = 79.32^o$$

$$\theta_{act} = \beta + \gamma - \frac{\pi}{2} = 79.32 + 20 - 90 = 9.32^o$$

Steering error = $\theta_{act} - \theta_{cor} = 9.32 - 9.28 = 0.04^o$

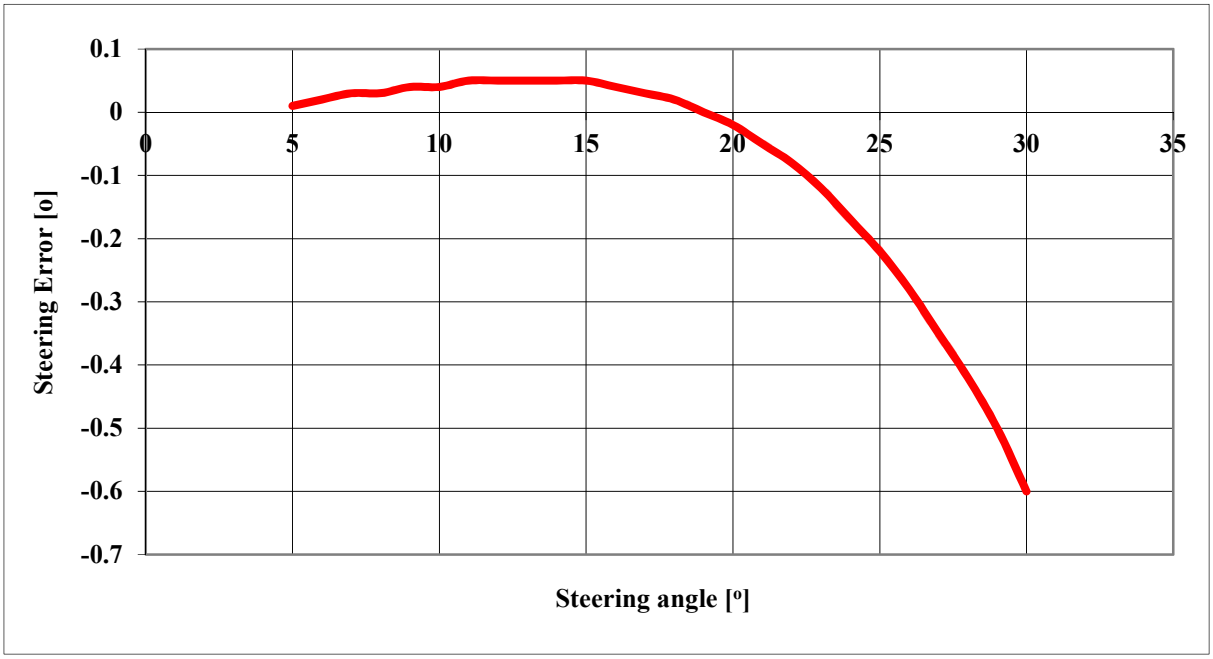
$$\mu = \frac{\pi}{2} + \gamma + \phi - \psi + \cos^{-1}\left(\frac{M^2 + Z^2 - l_n^2}{2MZ}\right)$$

$$= 90 + 20 + 10 - 8.95 + \cos^{-1}\left(\frac{(957)^2 + (1002)^2 - (180)^2}{2(957)(1002)}\right) \cong 121^o$$

The results of subsequent calculations are summarized in the table below. The variation of the steering error is plotted in the figure. Note that the force transmission angle should be less than about 160^o for proper operation of the linkage for the whole range of ϕ values.

According to the table and the plot, the proposed design cannot satisfy the requirement set in eqn. (III-10) even though it satisfies the condition related to the force transmission angle.

ϕ [^{o}]	α [^{o}]	Z [mm]	ψ [^{o}]	δ [^{o}]	β [^{o}]	θ_{act} [^{o}]	θ^i_{cor} [^{o}]	Error [^{o}]	Force Transmission Angle [^{o}]
10	60	1002	8.95	70.37	79.32	9.32	9.28	0.04	121
15	55	988	8.58	74.91	83.49	13.49	13.45	0.05	127
20	50	974.	8.14	79.21	87.34	17.34	17.37	-0.02	133
25	45	961	7.61	83.24	90.86	20.86	21.08	-0.22	138
30	40	949	7.00	87.02	94.02	24.02	24.62	**-0.60**	144



III-5. Multi-axle Steering

There are many vehicles that have more than two axles. Here the term "axle" may refer to a real beam axle or a set of independent suspensions. *As a general rule, for an "n-axle" vehicle, wheels on at least "n-1" axles should be steered to satisfy geometrically correct steering.* Steering all wheels on all the axles is usually preferred only if better maneuverability, i.e., a smaller turning radius, beyond that of steering wheels on "n-1" axles is required, as it involves more complexity at extra cost. An approximation to geometrically correct steering may be obtained by steering wheels on "n-2" axles, but whether this approximation is close enough to be acceptable requires a careful evaluation of the steering errors introduced.

For vehicles with three or more axles, common in heavy commercial vehicles such as trucks, it is possible to obtain a number of configurations that will provide geometrically correct steering. All-wheel steering (AWS) is usually reserved for vehicles where maneuverability requirements are strict, and thus, extra cost and complexity may be justified. Mining vehicles and heavy military vehicles are examples. An example of a six-wheeled AWS vehicle is given in Figure III-10.

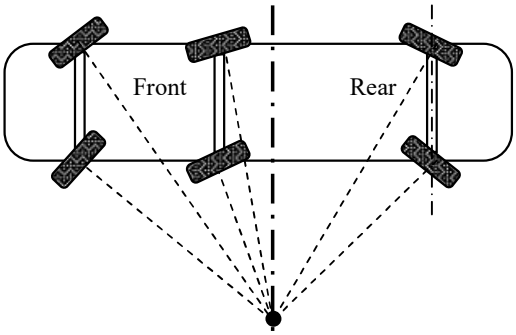
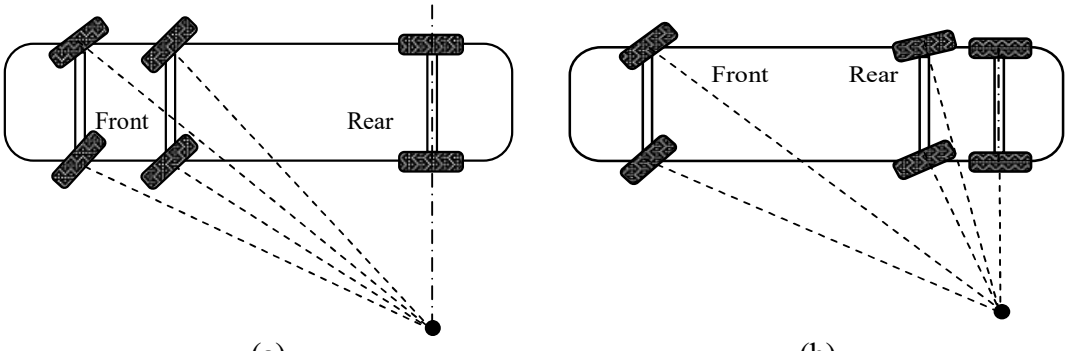


Figure III-10. All-wheel steering for a three-axle vehicle

Simpler solutions satisfying the condition of geometrically correct steering can be obtained by steering wheels on two axles only, as illustrated in Figures III-11 (a) and (b).



(a) (b)

Figure III-11. Simpler geometrically correct steering configurations

Note that if there is a fixed (non-steered) axle on a vehicle, the turning center is on the extension of this axle. If there is no fixed axle, then the turning center is located elsewhere, depending on the limiting steering angles of the steering axles.

In commercial vehicles such as conventional trucks, the design of the steering system is usually based on the closest possible approximation of the true rolling condition. In the case of double rear axle configuration common in heavy trucks, the usual (low cost) approach is to design the rear axles as close to each other as possible and then replace them with a single imaginary axle located at the midline between the two as illustrated in Figure III-12. It is evident that in this case, pure rolling cannot be satisfied; nevertheless, a close approximation can still be achieved. It is possible to evaluate the steering system for a four-axled vehicle in the same manner. Figure III-13 (a) and (b) illustrate two configurations; the first one has the potential to provide an acceptable approximation, while the second configuration will be unacceptable due to large steering errors involved.

A word of caution: The discussion so far assumes low speeds so that the slip angles of the tires are negligible.

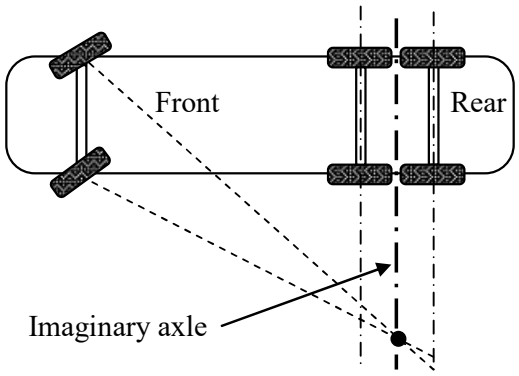


Figure III-12. Approximate configuration for three-axle vehicles

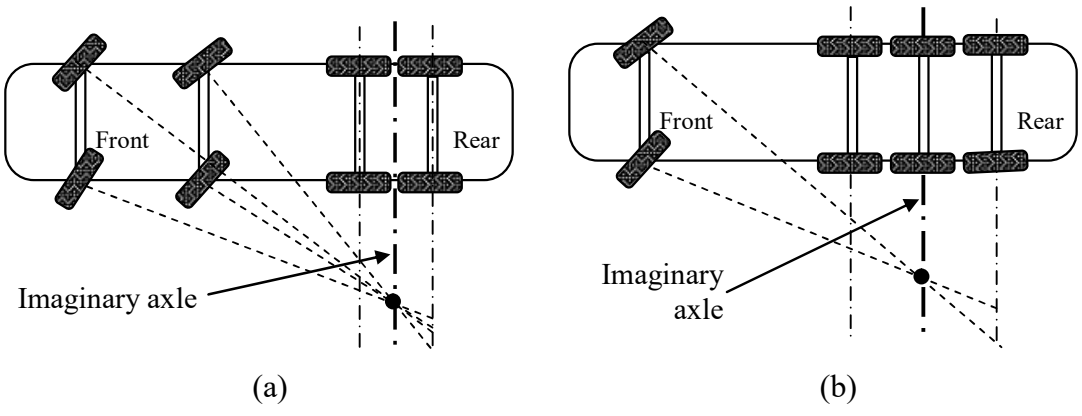
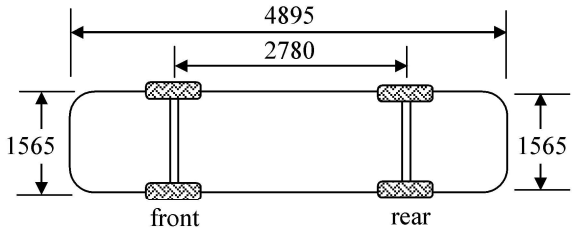


Figure III-13. Possibly (a) acceptable, (b) unacceptable designs for a four-axle vehicle

Example III-2

Consider the four-wheel steering (4WS) vehicle illustrated in the figure (all dimensions are in mm). Wheel locks for the inner wheels on the front and rear axles are limited to a maximum of 32^o and 6^o, respectively.



a) Estimate the minimum possible track turning radius. You can neglect scrub radii.

b) Estimate the track turning radius for the conventional front-wheel steering (FWS) with the same maximum front-wheel steering angle and comment on the results.

Solution:

a) $h = x_f \tan 58^o = x_r \tan 84^o$

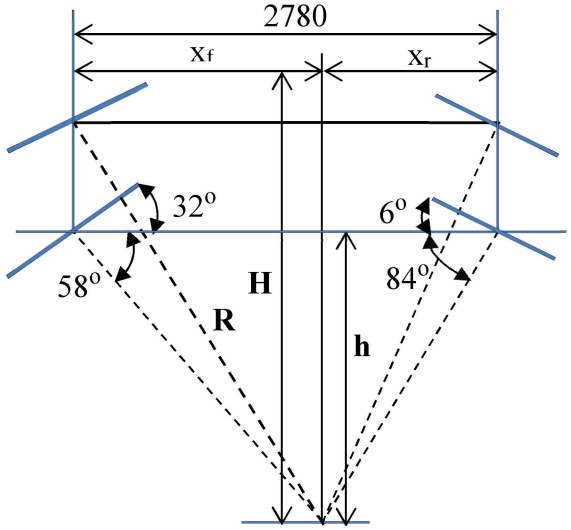
$$x_f + x_r = \left(1 + \frac{\tan 58}{\tan 84}\right) x_f = 2780$$

$$x_f = \frac{2780}{1 + \dfrac{\tan 58}{\tan 84}} = 2379.7[\text{mm}]$$

$$h = x_f \tan 58^o = 2379.7 \tan 58^o = 3808.3[\text{mm}]$$

$$H = h + 1565 = 3808.3 + 1565 = 5373.3[\text{mm}]$$

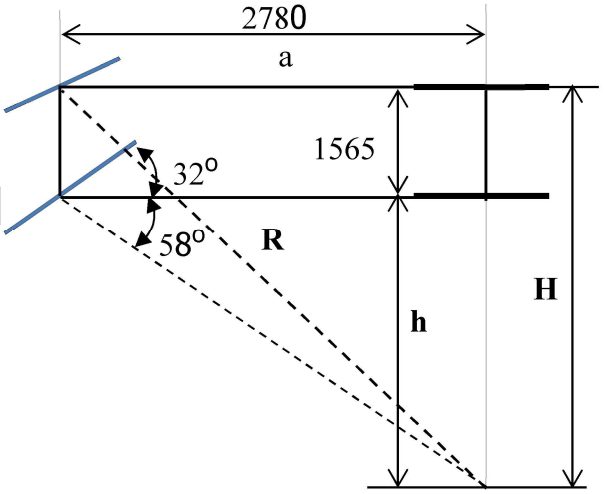
$$R^2 = x_f^2 + H^2 \quad \Rightarrow \quad R = \sqrt{2379.7^2 + 5373.3^2} = \mathbf{5877[mm]}$$



b) $h = a \tan\phi = 2780 \tan 58^o = 4449[\text{mm}]$

$$H = h + 1565 = 4449 + 1565 = 6014[\text{mm}]$$

$$R^2 = a^2 + H^2 \quad R = \sqrt{2780^2 + 6014^2} = \mathbf{6626[mm]}$$



It is observed that with the introduction of a steering angle of 6 degrees to the rear wheels, the track turning radius can be reduced by over 10%.

III-6. Ackerman Linkage

Long before the advent of the car, in 1818, the German inventor Rudolf Ackerman patented a device based on the principle of geometrically correct steering. It was, however, Lankensperberger, a carriage maker in Munich, who first devised it in 1817.

Ackerman Linkage is basically a four-bar linkage. As the track rod is shorter than the axle assembly, it moves the right wheel through a larger angle than the left in a right turn, and vice versa when the car is turning left, Fig. III-14.

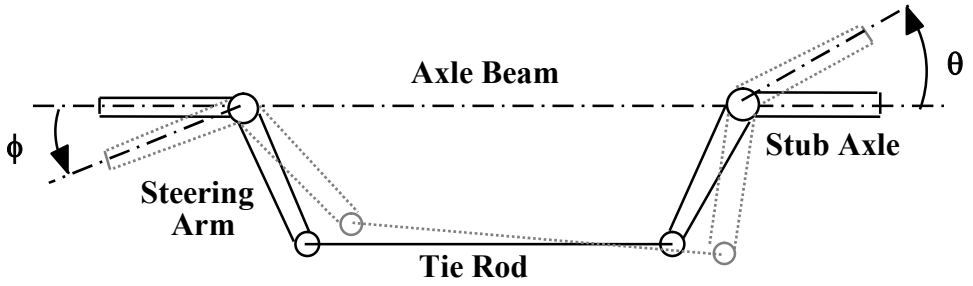


Figure III-14. Ackerman linkage

The tie rod can be placed behind or in front of the axle beam. Provided that track arms are suitably inclined to each other, a similar action in both cases can be obtained.

Ackerman linkage gives true rolling of the wheels in only three positions of the stub axles. One is when the wheels are parallel and the vehicle is traveling in a straight line, and the other positions are when the vehicle is turning either to the right or to the left, and the inner track arm has been turned through a certain angle depending on the design. In any other position, the axes of the front wheels do not intersect on the axis of the back wheels and a certain amount of lateral slip must occur between some of the wheels and the ground. Except when turning in a circle of a very small radius, the error is small.

In practice, the correct geometric relationship does not have to be satisfied precisely because pure rolling of the wheels during cornering can never be achieved. Tires must always run at a slip angle during cornering and their motion always include sliding along with rolling. As a result, modern car designers do not heave to follow geometrically correct steering strictly.

The Ackerman Linkage is almost universal even though there are several linkages that give perfect steering at all locks. This is because these systems are all somewhat complicated and they have not proved satisfactory in practice.

III-7. Steering System Arrangement

The basic steering system consists of the parts:

i) The *steering wheel* rests on top of the steering column. Steering input is fed into the system through the steering wheel.

ii) The *steering gear* multiplies the steering effort applied to the steering wheel by the driver. Also, the turning motion of the steering wheel is converted into a linear movement at one end of the *Pitman* arm.

iii) The *steering linkage* transmits motion from the steering gear to the wheels and at the same time adjusts the relative positions of the wheels.

Fig. III-15 illustrates the arrangement of the conventional steering system for a beam axle front suspension. The links are connected to each other by ball joints.

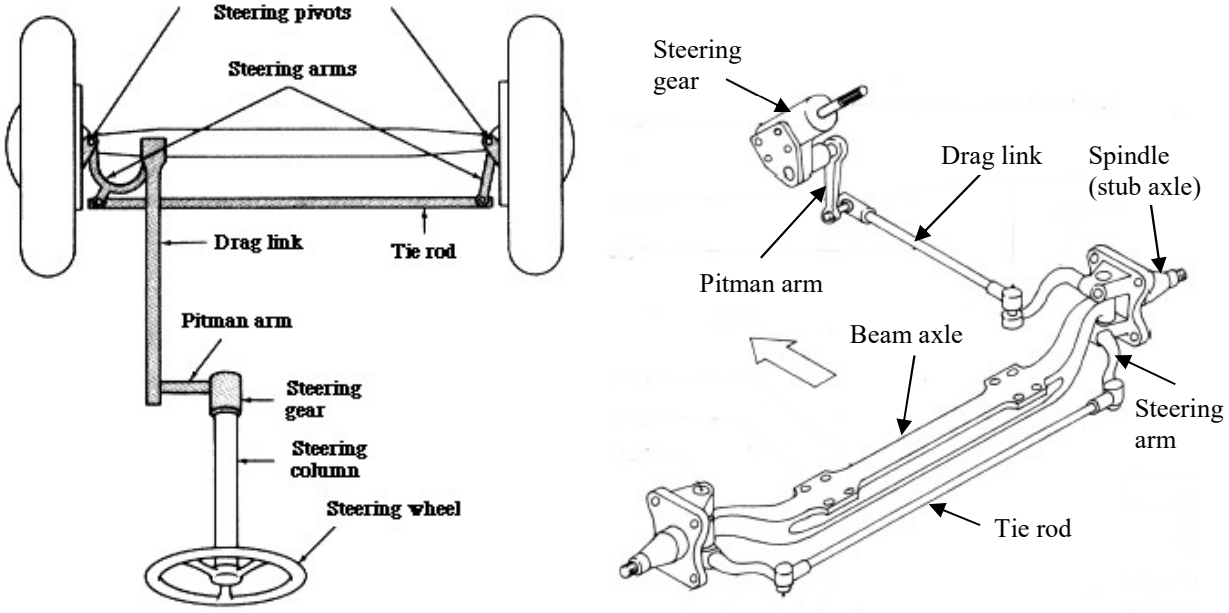


Figure III-15. The basic steering system for a rigid axle.

For vehicles with independent front suspension, this layout is not acceptable. Due to the independent motion of the wheels, their relative position and hence their distance varies during suspension motion. The fixed length of the tie rod would lead to excessive "*bump steer* - unwanted steering input created when one wheel travels up or down," and therefore, it is replaced by a multi-piece tie rod linkage, as shown in Fig. III-16.

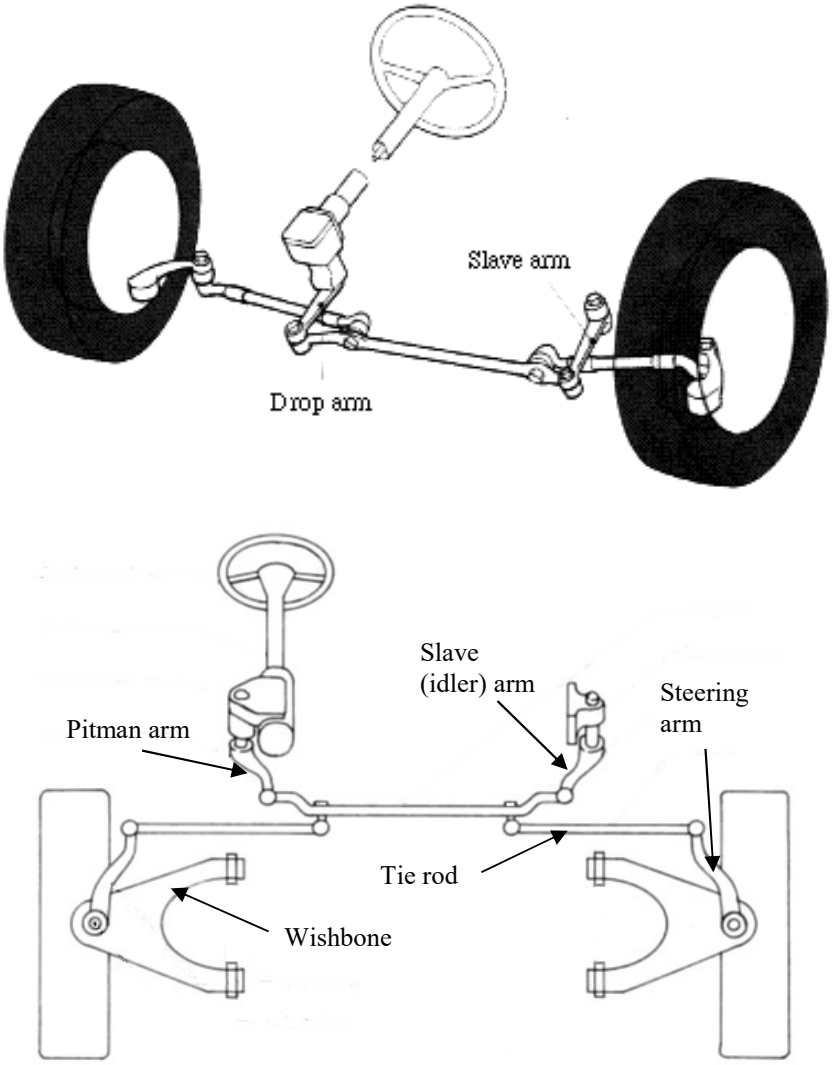


Figure III-16. Multi-piece tie rod linkages.

III-7.1 Steering Gear Requirements

The main objective of the steering gear is to multiply the steering effort impressed on the steering wheel by the driver. It is desirable that driving take a minimum of physical effort. The gear should also be irreversible to a certain extent such that the inputs through the road wheels will not be transmitted to the driver completely. A small amount of reversibility is desired in order to provide a sensory indication - road feel - of the behavior of the vehicle. This is necessary so that the right amount of correction can be applied to the steering wheel before the external disturbances deflect the vehicle from its course. This requirement can be met by mechanisms that are more efficient in one direction of motion transmission than in the other.

Requirements as to the steering gear ratio are also conflicting. For high-speed driving, a low reduction ratio is preferred for a quick response from the road wheels. For city driving and parking, when steering feels much stiffer, a high ratio is desirable.

As can be seen, the steering gear requirements are quite contradictory, and a good steering gear ratio represents a balanced combination of compromises depending on the particular application. For passenger cars, the steering gear ratio varies between a low value of 14 for sporty or high-performance vehicles and a high value of 20 for smaller vehicles. The corresponding range of gear ratios for commercial vehicles is 20-36. Consequently, the research is focused on finding a steering system with variable steering gear. Such a steering gear would provide a high gear ratio at low speeds for easy parking and a low gear ratio for quick response at high speeds.

III-7.2 Types of Steering Gear

There are two basic types of steering gear in use in recent motor vehicles:

1) *Rack and pinion*

With this design, a toothed rack is moved by a small pinion at the lower end of the steering shaft. When the steering wheel is turned, the rack moves from side to side and causes the stub axles - the two short shafts on which the front wheels are mounted - to swivel.

Rack and pinion steering gear is the simpler of the two types and also provides the most positive road feel. Because of these characteristics, it is widely employed in passenger cars and racing cars.

Rack and pinion steering gear illustrated in Fig. III-17 can only provide a constant steering gear ratio.

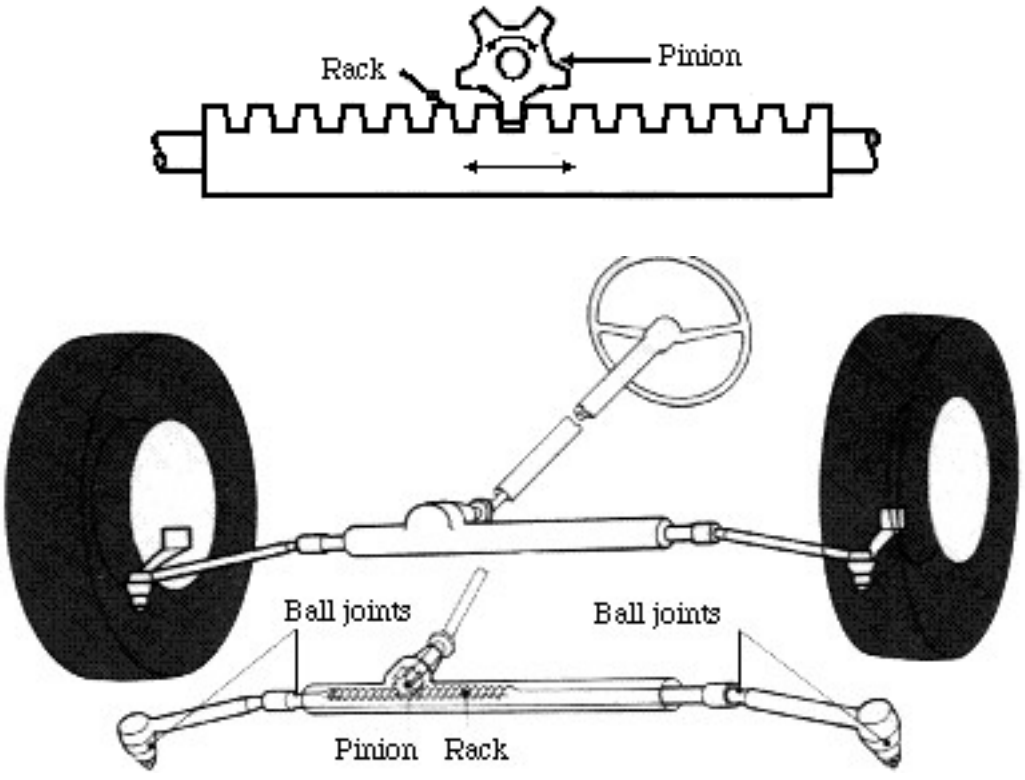
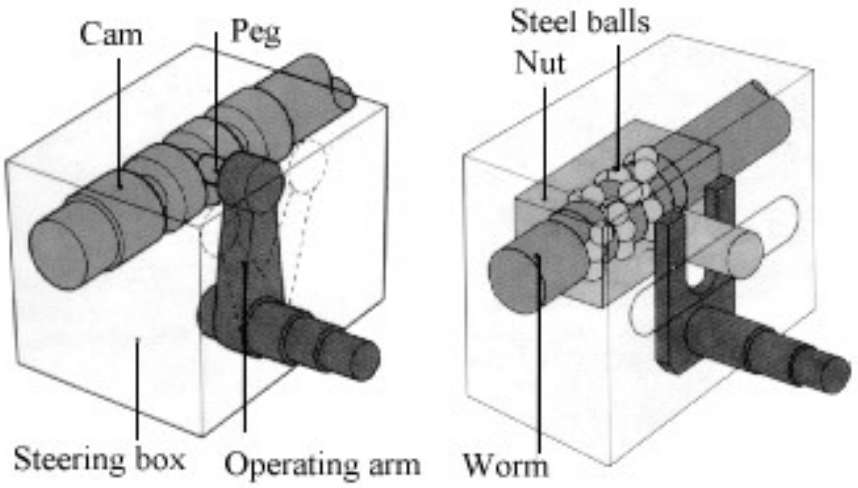


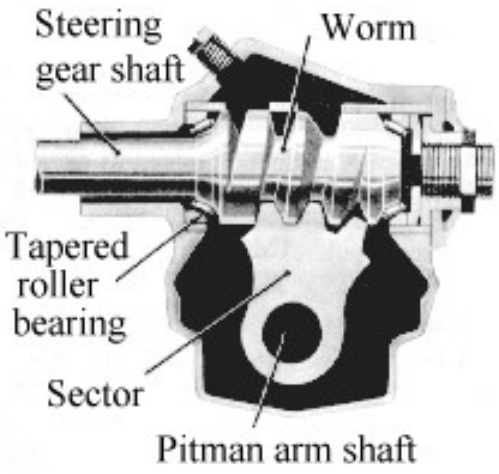
Figure III-17. Rack and pinion steering gear

2) *Cam or Worm and Peg, Nut, or Sector*

Variations of this kind of steering gear are commonly used in commercial vehicles. Cam and peg, worm and nut, and worm and sector designs are illustrated in Fig. III-18.



a) Cam and Peg b) Worm and Nut



c) Worm and Sector

Figure III-18. Various steering gears for commercial vehicles.

III-8 Turning Radius

The formal definition of track turning radius is as follows:

"The turning radius of an automotive vehicle is the radius of the arc described by the center of the track made by the outside front wheel of the vehicle when making its shortest turn".

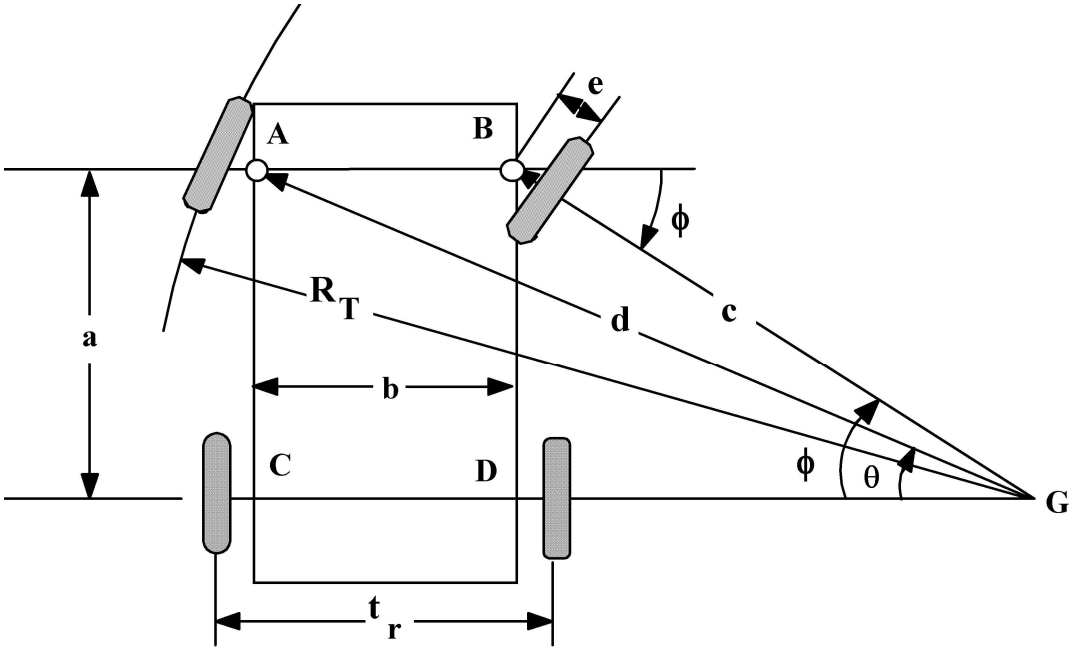


Figure III-19. Turning radius.

This radius depends on the wheelbase a, the distance b between the steering pivot axes, the maximum angle ϕ through which the inside front wheel can be turned from the straight-ahead position, and the *scrub radius*, e. In Fig. III.19, ϕ and θ are the inside and outside wheel locks, respectively. The front and rear tracks are denoted by t_f and t_r. Noting that

$$t_f = b + 2e \qquad \text{(III-11)}$$

one can write

$$d = \left[b^2 + c^2 - 2bc\cos(180 - \phi) \right]^{1/2}$$

$$\cos(180 - \phi) = -\cos\phi$$

$$d = \left[b^2 + c^2 + 2bc\cos\phi \right]^{1/2}$$

Substituting the value of c (c = a / sin ϕ), one obtains:

$$d = \left[b^2 + \left(\frac{a}{\sin\phi} \right)^2 + \frac{2ab}{\tan\phi} \right]^{1/2}$$

By definition the turning radius is equal to:

$R_T = d + e$

$$d = \left[b^2 + \left(\frac{a}{\sin\phi} \right)^2 + \frac{2ab}{\tan\phi} \right]^{1/2} + e \qquad \text{(III-12)}$$

The above equation shows that a smaller turning radius can be obtained if

i) a is smaller, or
ii) ϕ is larger.

In practice, however, ϕ is limited by constructional requirements. At full lock and bump, the inside wheel must well clear the body, and of course, there must be sufficient foot room. In front-wheel drive vehicles, there must be additional space for snow chains. Further, aerodynamic drag increases. Therefore, the inner wheel lock is limited.

The outer wheel lock, which is smaller, is usually not subject to such severe limitations. Therefore it is possible to increase θ, thereby decreasing the turning radius at the expense of increasing steering error. In this case, the cornering force capacity of the outer tire will be higher. One can express track turning radius in terms of the outer wheel lock corresponding to geometrically correct steering, i.e., θ_{corr}.

$$R_T = \frac{a}{\sin \theta_{corr}} + e \qquad \text{(III-13)}$$

All the relations derived so far assume geometrically correct steering. In real applications, it is not possible to achieve pure rolling and hence a correction must be included. Empirically, a 1° increase in steering error γ reduces track turning radius by 0.05 [m]. The Therefore, modifying eq. (III-13):

$$R_T \cong \frac{a}{\sin \theta_{corr}} + e - 0.05\,(\gamma) \qquad \text{(III-14)}$$

It should be noted that correct units should be used for the parameters in eqn. (III-14).

From drivers' point of view, turning diameter between curbs is more important and can be expressed as, Fig. III-20:

$$D_K = 2R_T + SW \qquad \text{(III-15)}$$

where SW is the tire section width.

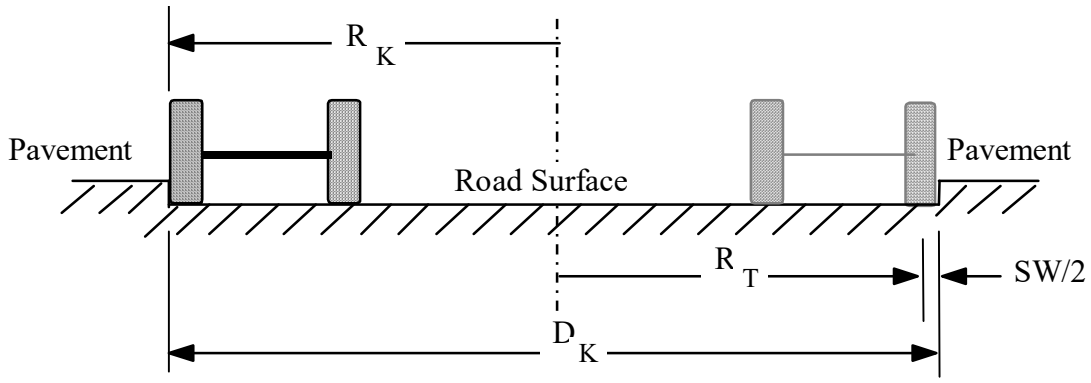


Figure III-20. Turning diameter between curbs

Turning diameter, D_w, wall to wall is even more important. It is defined as the diameter of the circle that the outermost point of the vehicle describes in turning, Fig. III-21.

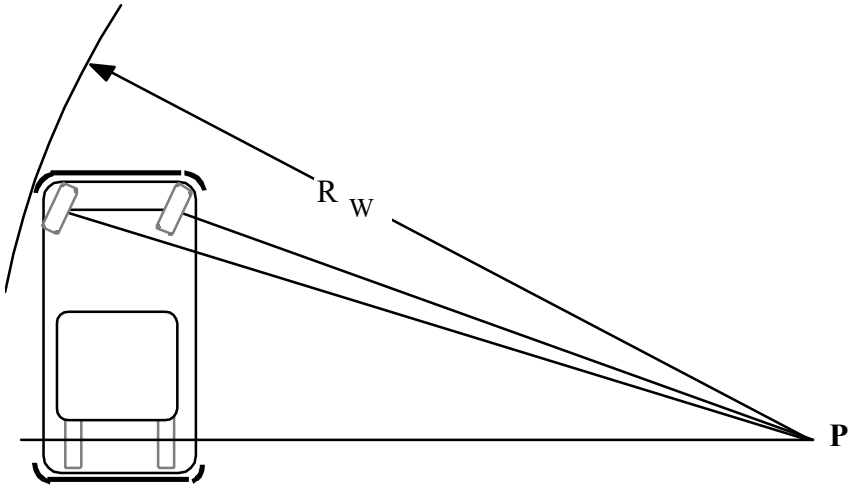


Figure III-21 Turning diameter between walls

Table III-1 lists the turning circle diameter and the inner and outer wheel lock values for some vehicle models.

Table III-1 Turning circle diameters for some automobiles

		Turning circle diameter [m]
Vehicle	Model	Left lock/Right lock
Alfa Romeo 159 2.4 20V	2006	11.8/11.8
Audi S6 i A4 2.0 TFSI	2004	11.1/11.3
Audi S6	2006	12.0/12.1
BMW 320D	2005	11.2/11.1
BMW 730D	2005	12.52/12.56
BMW X3	2006	11.9/11.8
BMW ZM Coupe	2006	10.5/10.4
Chrysler 300S AWD	2005	11.9/12.3
Citroen C3 Pluriel 1.4	2003	11.5/11.5
Daihatsu Terios	2006	9.8/9.8
Dacia Logan	2006	11.0/11.2
Fiat Croma 2.2 16V	2005	10.9/11.0
Fiat Panda 1.2 8V	2003	9.9/9.8
Ford Focus CC 2.0 TDCi	2006	11.1/11.5
Ford Mondeo 1.8 Sci	2003	11.4/11.3
Hyundai Santa Fe GLS 2.4 16V 4WD	2001	12.20/11.98
Jaguar XKR	2006	11.1/11.2
Kia Sportage 2.0 CRDi	2006	11.8/11.4
Lamborghini Gallardo Spyder	2006	13.5/13.4
Mazda 3 Sport 1.6	2003	11.0/10.9
Mazda 5 1.8 MZR	2005	11.3/11.3
Mercedes-Benz B150	2006	12.1/12.0
Mercedes-Benz ML350	2005	12.0/11.8
Nissan Micra C+C 1.6	2006	10.8/10.8
Opel Corsa	2006	10.6/10.5
Opel Astra Twintop 1.8 Ecotec	2006	11.2/11.3
Peugeot 407 Coupe Sport V6 210	2005	12.4/12.2
Porsche 911 Carrera Cabriolet	2005	11.0/11.00
Renault Clio 1.5 DCI	2005	11.4/11.4
Rolls-Royce Phantom	2006	13.8/13.5
Suzuki Swift 1.3	2005	10.5/10.3
Toyota Avensis 2.2 D-Cat	2005	11.2/11.9
Volkswagen New Beetle Cabriolet 2.0	2003	11.03/11.43
Volkswagen Touareg R5 TDI	2003	12.10/12.0

Table III-2 Turning circle diameter data for some light and heavy commercial vehicles

Vehicle		Turning circle diameter [m] Left Lock	Right Lock
Renault Trafic 1.9dCi 80	R_K	11.4	
Iveco Daily 35S12		11.2	
IvecoTurbocity 100 double deck		15.6	15.8
Mercedes 811RD Coach		15.49	12.47
Mitsubishi Canter	R_K	14.2	
Mitsubishi L200 4x4 pickup	R_K	13.25	13.85
	R_W	13.45	14.05
Citroen C25D 4x4 Van	R_K	11.94	12.59
	R_W	11.73	12.38
Fiat Ducato 1.4 ton Van	R_K	12.04	12.70
	R_W	11.62	12.28

Table III-3 Turning circle diameters and inner and outer wheel locks for some older models

Vehicle	Turning circle diameter [m] R_W	R_K	Inner wheel lock [°]	Outer wheel lock [°]
BMW 2002	10.4	9.6	42	34
VW 1300	11.0	10.5	34	28
VW 1600	11.1	10.3	30	27
Porsche 917	11.8		29	25
Rolls-Royce Silver Shadow	11.6		41	33.5
Ford Cortina 1300	9.14		41.9	37.9
Renault 4L	11.6		39	31.8
Ford Capri	9.75		41.6	39.1
Range Rover			33	29
Audi 100LS	10.5		39	34.16
Mercedes 250	10.85	10.0	43	35

Example III-3

Determine the turning circle diameter for the vehicle with the specifications given below.

Wheelbase = 2.527 [m]
Track (front) = 1.321 [m]
e = 0.015 [m]
$\phi = 38^o$, $\theta_{act} = 36^o\ 20'$

Solution :

$$t = b + 2e$$

$$b = t - 2e$$

$$= 1.321 - 2(0.015)$$

$$= 1.291 \text{ [m]}$$

$$R_T = \left[1.291^2 + \left(\frac{2.527}{\sin 38} \right)^2 + \frac{2(2.527)(1.291)}{\tan 38} \right]^{1/2} + 0.015$$

$R_T = 5.2$ [m], $D_T = 10.4$ [m]

Note that this result is valid only for geometrically correct steering. Thus one must check if geometrically correct steering is satisfied.

$$\cot\theta = \frac{b}{a} + \cot\phi = \frac{1.291}{2.527} + \cot 38^o = 1.791$$

$$\theta \cong 29.2^o$$

It is clear that a nonzero steering error exists. Thus the previous results must be modified according to the existing steering error.

$$\gamma = 36^o\ 20' - 29^o\ 12' = 7^o\ 08'$$

$$R_T = \frac{2.527}{\sin 29.2} + 0.015 - 0.05\ (7.13) = 4.84 \text{ [m]}$$

$$D_T = 2R_T = 2x4.84 = 9.7 \text{ [m]}$$

Exercises

III-1) The front wheels of an average passenger car have a total rotation (lock to lock) of about 70º. For unassisted steering, the number of turns of the steering wheel from lock to lock varies from 3 to 4 turns. What is the range of steering gear ratios for the average passenger car?

III-2) Illustrate by a sketch and clearly indicate

a) Front and rear tracks, and

b) Wheelbase

for

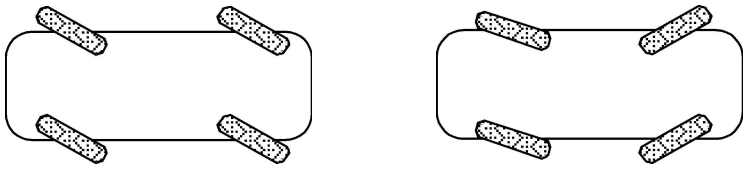
i) Passenger cars,

ii) Trucks with one front and two rear axles,

- single wheels on all axles, and

- tandem wheels on rear axles.

III-3) Show by an illustration that the true rolling condition (geometrically correct steering) can be obtained for a four-wheel steered passenger car in the two special configurations (exaggerated) illustrated below.



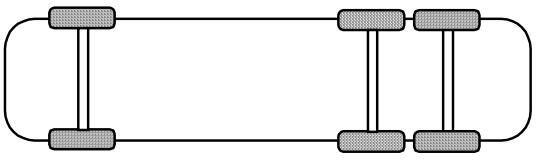
III-4) Illustrate and explain, for the three-axle vehicle in the figure, whether the true rolling condition (geometrically correct steering) can be obtained for the cases :

a) Front-wheel steering only, for the case of the single front axle and double rear axles.

b) Steering with the wheels on the first two front axles, for the case of two axles in front and a single rear axle.

c) Steering with the wheels on the first and last axles,

d) All-wheel steering.

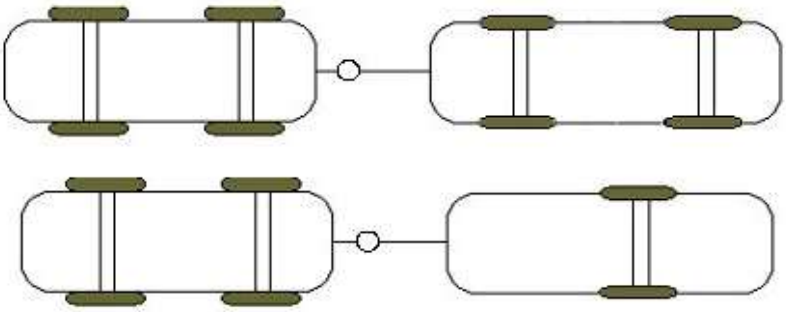


III-5) Consider the cases of

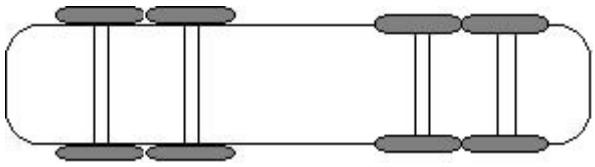
a) Truck (2 axles) and trailer(2 axles), and (first figure below)
b) Tractor (2 axles) and semitrailer (single axle) (second figure below)

and illustrate geometrically

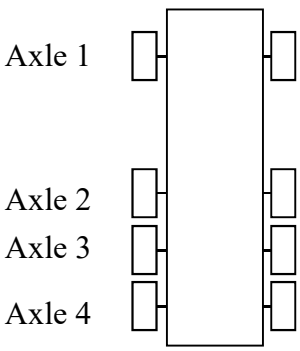
a) the steering error for front wheel steering of the truck and tractor, and
b) how one can obtain pure rolling (show all possible steering configurations to obtain pure rolling).



III-6) Use your engineering sense and make your choice of steered axles for the 8 wheel vehicle in the figure. Explain your reasoning and illustrate the resulting steering error (if there is any).



III-7) Indicate the best possible steering configurations for the vehicle with four axles, as illustrated in the figure. Order the possible configurations in the order of closeness to geometrically correct steering and in each possible configuration mark the axles as ST: Steered, NS: Non-Steered. Also, indicate (check) if the configuration satisfies geometrically correct steering (GCS) exactly.

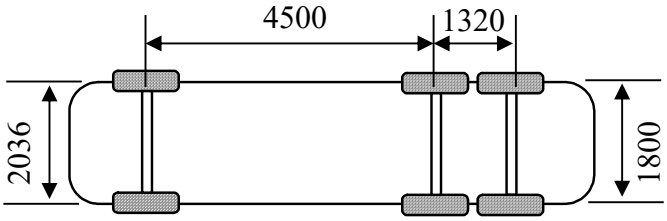


	Configuration					
Axle	**1**	**2**	**3**	**4**	**5**	**6**
1	…	…	…	…	…	…
2	…	…	…	…	…	…
3	…	…	…	…	…	…
4	…	…	…	…	…	…
GCS?	☐	☐	☐	☐	☐	☐

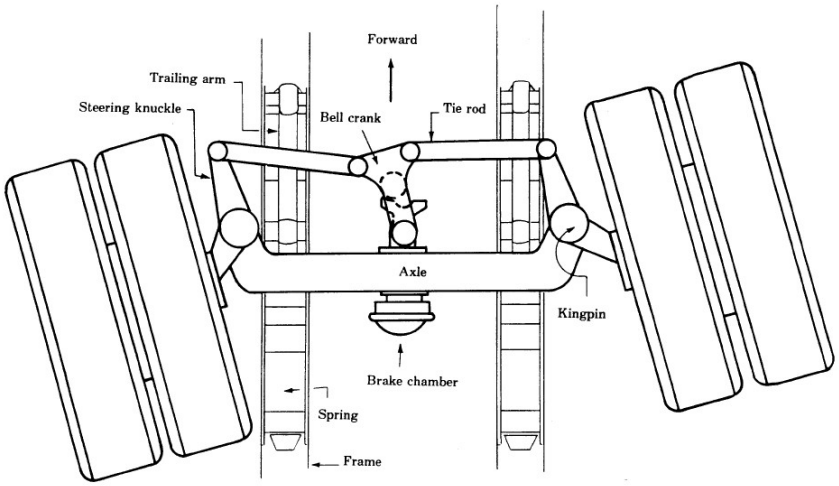
III-8) Illustrate, graphically, the practical (approximate) solution with respect to geometrically correct steering for a vehicle having three axles. Then calculate the outer wheel angle

corresponding to an inner wheel angle of 20º for this case. You can neglect the scrub radius for a first approximation. All dimensions are in [mm].

Ans.: 17.6º

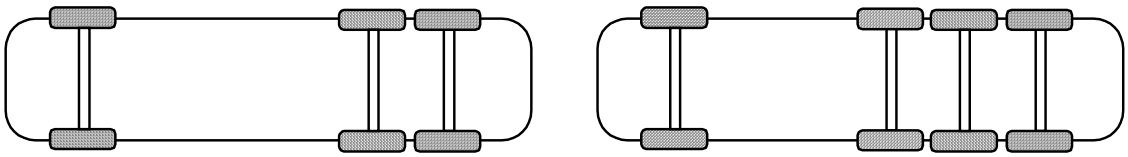


III-9) In a self-steering axle, the wheels are steered by the action of the lateral tire forces. The wheels are restrained by springs and dampers which may be preloaded. A self-steering axle is usually used on the rear axles of heavy trucks. A typical example is shown in the figure.



In order to achieve 32-ton load carrying capacity without exceeding the load limit per axle on roads, you are going to modify a truck by adding a third rear axle to the existing two, as illustrated. Comment on (with illustrations) the steering strategy for the third (additional) axle. Clearly indicate your choice, stating the advantages and disadvantages involved in each choice.

i) Steer it ? Draw the sketch showing the possible design strategy !
ii) Let it freely determine the wheel steering angles (self-steering).
iii) Fix it rigidly so that it is not steered at all!



III-10) For the trailing Ackerman linkage specified by:

$$\gamma = 25^o \qquad \frac{l_n}{b} = 0.0797 \qquad \frac{b}{a} = 0.5$$

a) Plot the actual and theoretically correct steering angle curves.

b) Plot steering error versus input steering angle variation.

c) Plot force transmission angle versus input steering angle variation.

Is this design acceptable ? Explain.

III-11) For the trailing Ackerman linkage specified by:

$\gamma = 21^o$ $\quad a = 2500$ mm $\quad b = 1600$ mm $\quad l_n = 200$ mm

vary the input steering angle, ϕ, in the range 0 to 35^o degrees by 1^o increments.

a) Plot

i) the actual and theoretically correct steering angle curves,

ii) Plot steering error, and

iii) Plot force transmission angle

versus input steering angle variation. Is this design acceptable ? Explain.

b) If the vehicle is modified by increasing the wheelbase by 10 %, what would be the effect on the steering ? Show by calculation.

III-12) Determine the sensitivities of the track turning diameter to changes in the parameters a, b, e, ϕ, θ , and γ.

III-13) For the vehicle specified below,

a) What should be the outside wheel lock to obtain geometrically correct steering ?

b) Calculate the track turning diameter for geometrically correct steering.

c) Calculate the outside wheel lock to reduce the turning diameter by 120 [mm].

Wheelbase [mm]	2480	Inside wheel lock [^{o}]	36^o
Overall length/width [mm]	4042/1625	Scrub radius [mm]	50
Track (f/r) [mm]	1330/1300		

III-14) For the vehicle specified below, calculate the

i) outer wheel lock, and
ii) track turning circle radius

for geometrically correct steering (i.e., pure rolling).

Wheelbase	:	3600 mm
Front track	:	1600 mm
Scrub radius	:	70 mm
Inner wheel lock	:	39º

Ans. : 6980 [mm]

III-15) For the vehicle specified below, the turning circle radius is found to be 4.46 m. Estimate the steering error.

Wheelbase	:	2450 mm
Front track	:	1240 mm
Scrub radius	:	52 mm
Inner wheel lock	:	42º

Ans. : 3.3º

III-16) Does the vehicle specified below satisfy the condition for geometrically correct steering (i.e., pure rolling) ?

Wheelbase	:	2370 mm
Track (f/r)	:	1273/1278 mm
Scrub radius	:	51 mm
Inner wheel lock	:	39º18’
Outer wheel lock	:	33º

Ans. : No !

III-17) Calculate the turning circle radius for the vehicle specified below.

Wheelbase	:	2440 mm
Front track	:	1318 mm
Scrub radius	:	48 mm
Inner wheel lock	:	37º
Outer wheel lock	:	32º

Ans. : 4964 [mm]

III-18) Calculate the turning circle diameter for two passenger cars with the specifications given below.

	Car A	Car B
Wheelbase [mm]	2420	2490
Track (front) [mm]	1330	1372
Track (rear) [mm]	1300	1315
Overall length [mm]	4042	4264
Overall width [mm]	1625	1642
Inside wheel lock [^{o}]	$35^o\ 50' \pm 1^o\ 30'$	$35^o \pm 1^o\ 30'$
Outside wheel lock [^{o}]	$28^o\ 30'$	31^o
Scrub radius [mm]	55	56
Tires	195/60 R 15	205/65 R 15

CHAPTER IV

VEHICLE HANDLING

IV.1. Introduction

Vehicle handling is that area of vehicle dynamics that is related to the motion of a vehicle under the action of directional commands and/or environmental inputs.

As can be seen in Fig. IV-1, a vehicle system consists of two main parts; the driver and the vehicle. From the point of view of the driver, handling quality is his/her subjective impression of the response of the vehicle to directional commands or inputs.

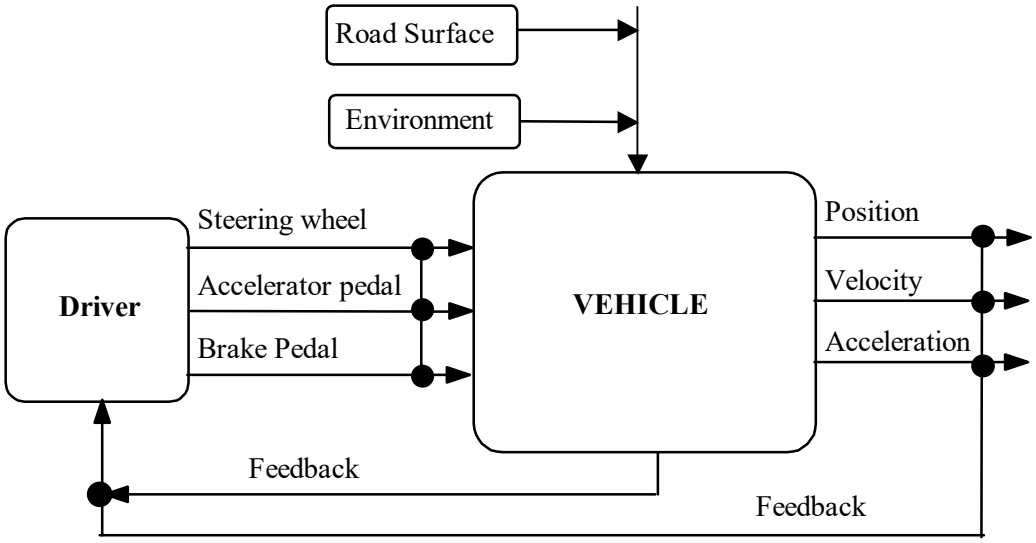


Figure IV-1. Block diagram for the man-vehicle system

The driver is the more complex part of the system. The available mathematical models of the driver can only represent specific idealized response behavior patterns. It has not yet been possible to incorporate in a mathematical model such subjective phenomena as experience or physical and emotional condition of the driver. Considering the effects of age, sex, alcohol, and drugs, more research in the psychology and response patterns of drivers is necessary to be able to simulate the driver adequately.

It is possible, on the other hand, to model the vehicle mathematically and study its behavior to simulated inputs. The input variables for such a mathematical model will be the steering and throttle positions and the brake force, which are the driver outputs, the vehicle load distribution, and the environmental inputs including the road disturbances and aerodynamic forces such as cross-winds. The vehicle response is then predicted from the model in terms of variables such as slip angles, forward velocity, yaw velocity, lateral acceleration, etc.

In the following sections, the driver part of the vehicle system, as well as the road disturbances, will be left out to simplify the analysis. The part of the system that will be taken into consideration reduces, therefore, to that shown in Fig. IV-2.

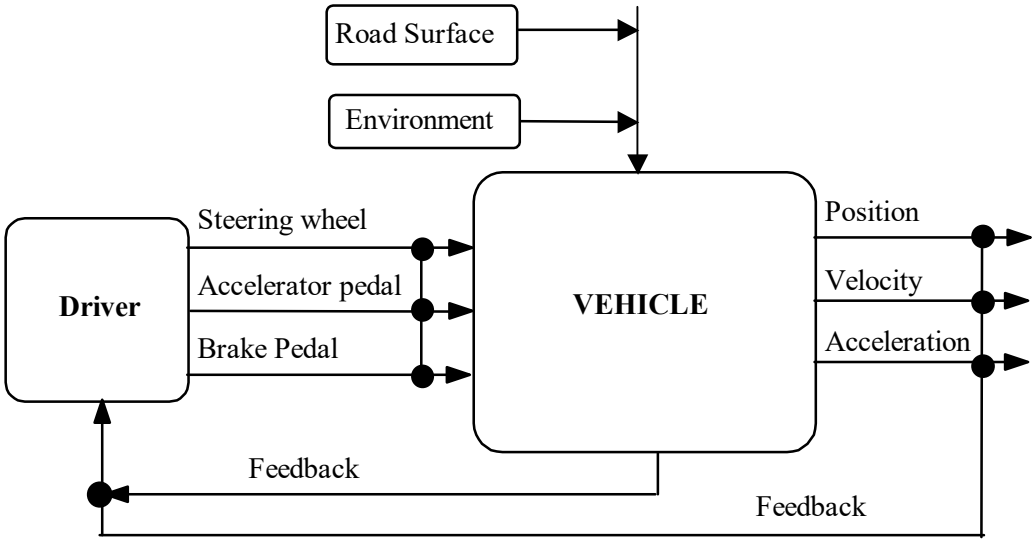


Figure IV-2. Block diagram for the vehicle system

IV.2. Tire Cornering Force Characteristics

The motion of a vehicle under the driver control and aerodynamic inputs depends mainly on the forces applied through the tire-road contact. The study of vehicle handling, therefore, requires a thorough understanding of the force and moment characteristics of rolling tires.

The dynamic behavior of the tire, however, is so complex and nonlinear that no adequate mathematical model has so far been obtained. Experimental methods have been, therefore, used extensively in the study of tire behavior.

If a moving vehicle is steered away from the straight-ahead position because of its inertia, it will still tend to go straight on. The steered wheels, on the other hand, will try to move in a direction dictated by the steering angle. Therefore, there will always be a difference between the direction of motion of the vehicle and the direction to which the wheels are turned.

In such a case, the tread in the contact patch, which is the part of the tire in contact with the road surface, is forced by friction to move in the direction of motion of the vehicle. The other parts of the tire, however, will move in the plane of the wheel. The tread in the contact patch will, therefore, deflect laterally, and this deflection will gradually increase from front to rear of the contact patch. A force at right angles to the plane of the tire is thus produced. This force which is called the cornering force (or lateral force), is proportional to the lateral deflection of the tread in the contact patch and therefore will increase toward the back of the contact patch where it reaches the value of the friction force and the tread breaks loose gradually resuming its initial undisturbed position, Fig. IV-3.

The angle between the direction of motion and the plane of the wheel is called the slip angle. As previously explained, the tread distortion and, therefore, the lateral force increases gradually from front to rear of the contact patch and then drops sharply to zero. The line of action of the lateral force is thus behind the center of the tire contact patch (or the intersection of the wheel plane and the projection on the road plane of the wheel axis of rotation). The distance between the line of action of the lateral force and the projection of the wheel axis of rotation on the road is called the pneumatic trail. The lateral force thus exerts a moment about the center point of the contact patch tending to reduce the slip angle and thus turn the wheel towards the straight-ahead position, Fig. IV-4. This moment is called the self-aligning torque. It will be felt at the steering wheel providing feedback.

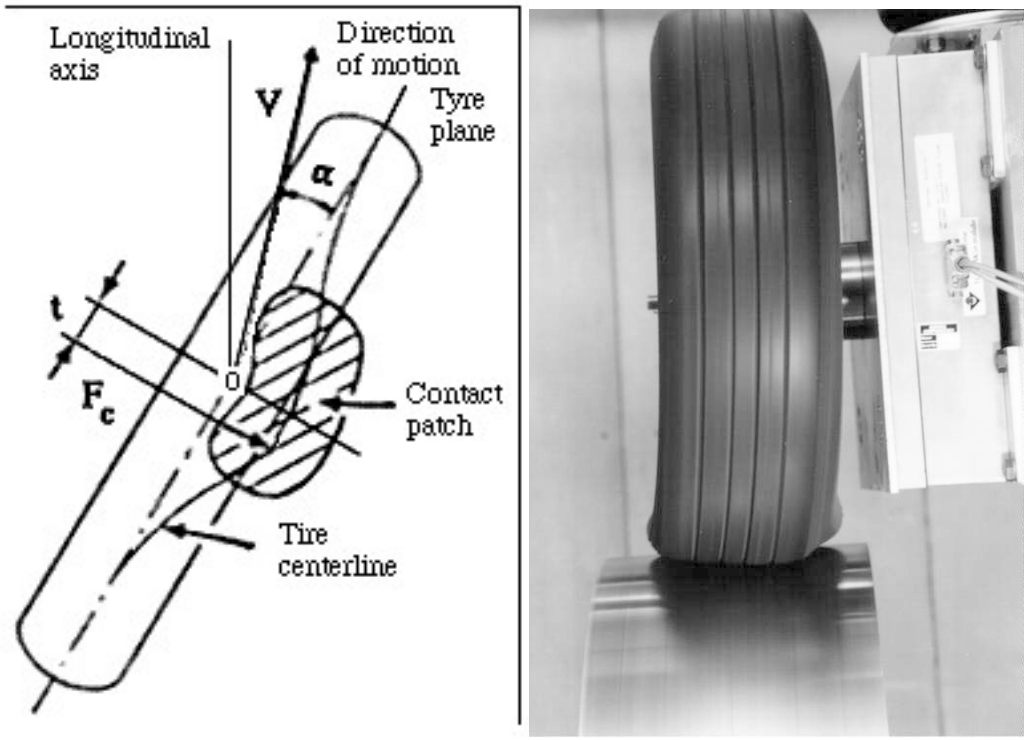


Figure IV-3. Tire/road interaction

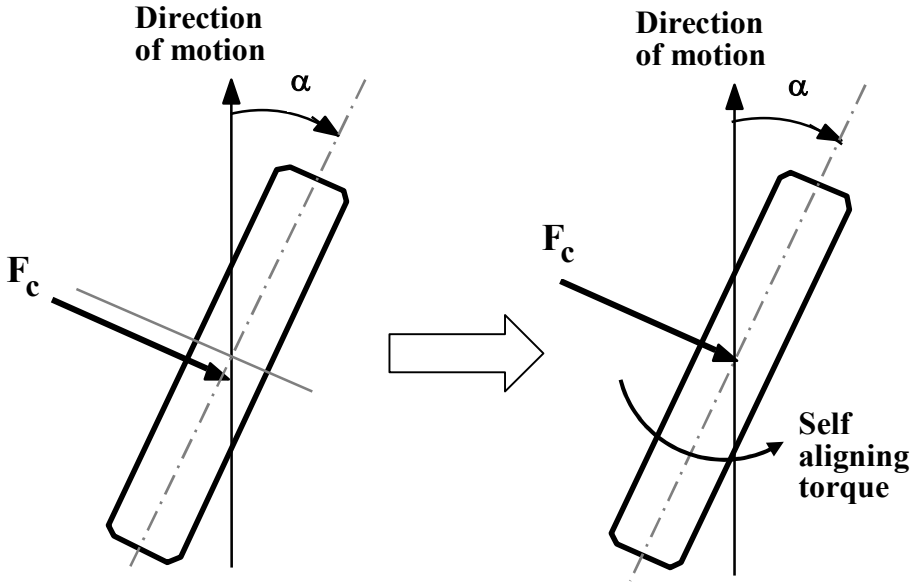


Figure IV-4. Self-aligning torque

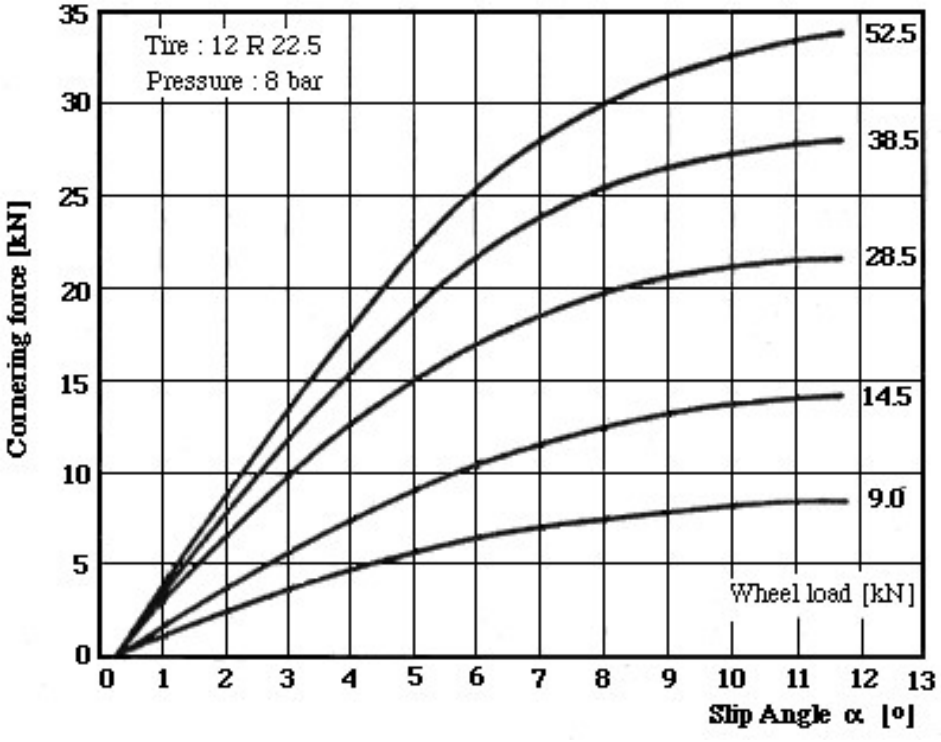
The cornering behavior of a tire depends on many factors. The three main parameters, however, are the magnitude of the cornering force and of the vertical tire load, and the slip angle. There are three ways of displaying the cornering characteristics of a tire in common use:

i) Cornering force as a function of slip angle vertical tire loading appearing as a parameter.

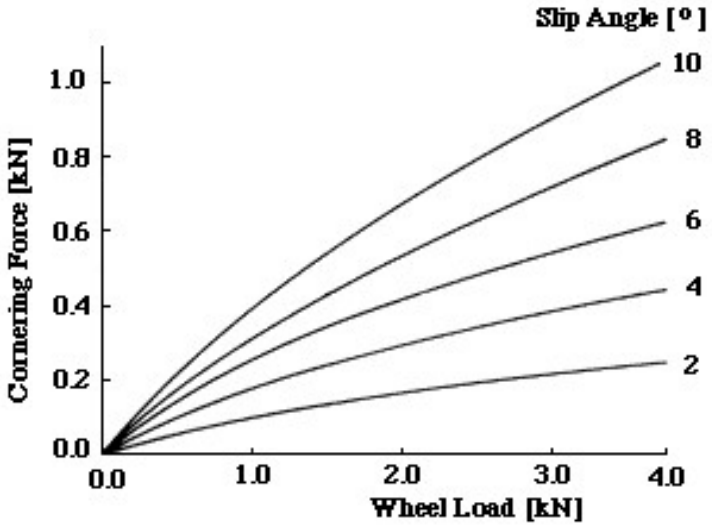
ii) Cornering force as a function of vertical tire load slip angle appearing as a parameter.

iii) Carpet plot.

The second case is now obsolete and very rarely used. Fig. IV-5 (a) and (b) illustrate the first and second cases. Fig. IV-6, on the other hand, provides the same information on a carpet plot.



(a)



(b)

Figure IV-5. Cornering force characteristics

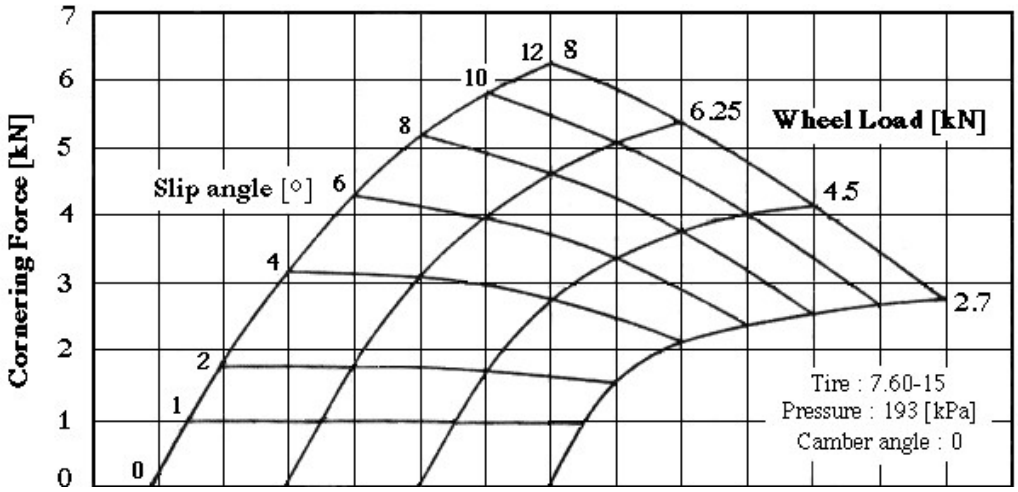


Figure IV-6. Carpet plot of tire cornering force characteristics

It is observed that at small slip angles (below about 4°), the cornering force is approximately a linear function of the slip angle. This linear relationship can be described by a constant of proportionality relating cornering force to slip angle. This constant is defined as the derivative of the cornering force with respect to slip angle evaluated at zero slip angle and is called the cornering stiffness.

$$C_s = \frac{\partial F_c}{\partial \alpha}\Big|_{\alpha=0} \cong \frac{\Delta F_c}{\Delta \alpha} \qquad \text{(IV-1)}$$

$$F_c = C_s \,.\, \alpha \qquad \text{(IV-2)}$$

Eqn. (IV-2) represents the **linear tire model** and is commonly used in vehicle dynamics studies. Fig. IV-7 illustrates the geometrical interpretation of cornering stiffness.

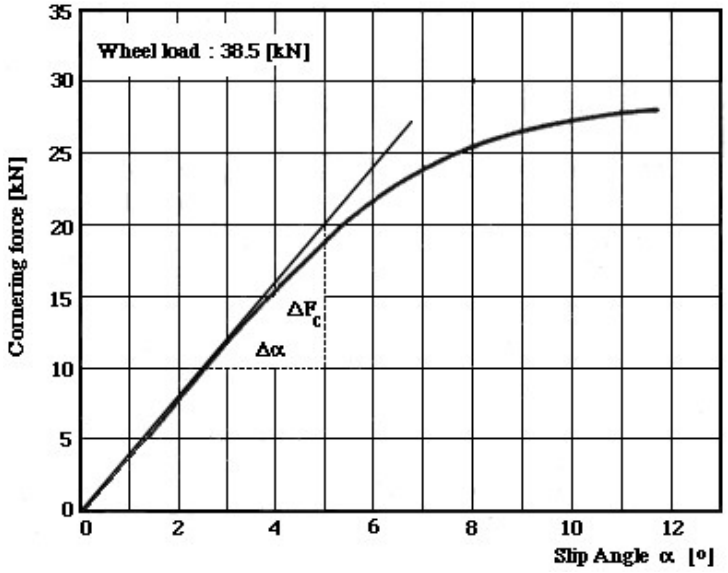


Figure IV-7. Cornering stiffness

It is possible to define cornering stiffness at a certain slip angle. A tangent to the cornering force curve for a specified wheel load at a slip angle is drawn, and the slope of this line is then used as the cornering stiffness to be used around this particular operating point.

A convenient sign convention for the slip angles for a steady-state right-hand turn requires the use of

- a negative slip angle, if the plane of the wheel is reached by a clockwise rotation from the direction of motion, and

- a positive slip angle if the plane of the wheel is reached by a counterclockwise rotation from the direction of motion as illustrated in Fig. IV-8.

For a steady-state right-hand turn, the cornering force will be directed towards the center of curvature. Therefore the cornering force will have the signs shown in Fig. IV-8. The sign conventions for the slip angle and the cornering force indicate that a negative slip angle is associated with a positive cornering force and vice versa. Thus, from eqn. IV-2, one can conclude that the cornering stiffness is by definition a negative quantity. Thus even if a positive value is specified, it should be used with a minus sign in the equations to be introduced in the following sections.

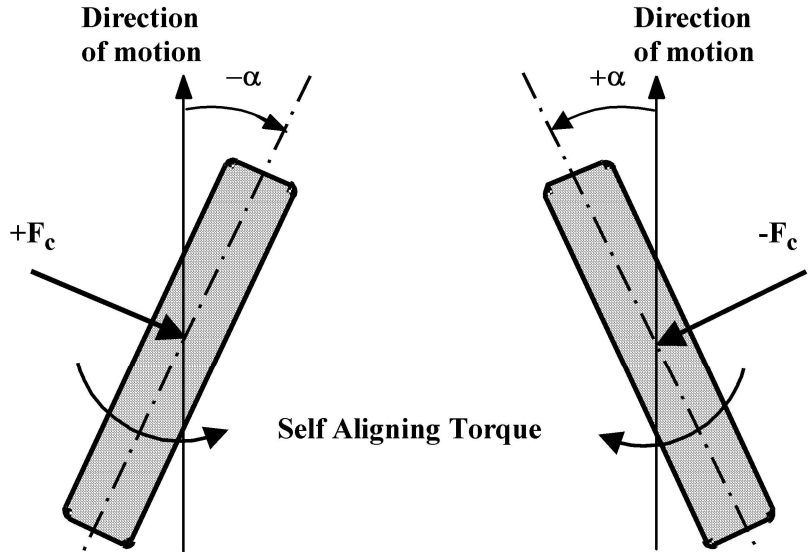


Figure IV-8. Sign convention for a steady-state right-hand turn

IV.3. Parameters Influencing Tire Cornering Characteristics

The cornering behavior of tires is influenced by various parameters and the cornering characteristics in Figs. IV.5 and 6 must be modified to take their effects into consideration. Here, the variation of basic tire cornering characteristics with varying tire inflation pressure, camber angle, and with the application of tractive or braking forces will be examined.

IV.3.1. Effects of Inflation Pressure

In the usual working range of tire pressures, increasing pressure improves the cornering force by increasing the lateral stiffness of the tire. This improvement, however, diminishes at higher pressures because of the reduction in the size of the contact patch, Fig. IV-9.

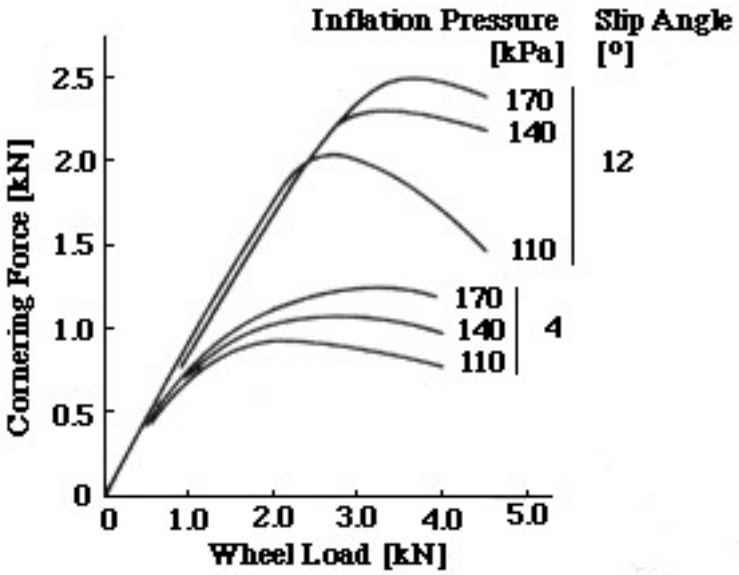


Figure IV-9. Effect of inflation pressure on cornering force characteristics

In Fig. IV-9, it is clear that the effect of the increasing inflation pressure in increasing the cornering force is more emphasized at high slip angles. For example, at a slip angle of 12°, there is a substantial improvement in cornering force at all-wheel loads when the inflation pressure is increased from 110 kPa to 140 kPa. When the tire inflation pressure is increased from 140 to 170 kPa, however, the resulting improvement in cornering force is somewhat smaller. On the other hand, the corresponding improvements in cornering force are smaller for a slip angle of 4°, and it seems that the improvement is not affected by the increasing levels of inflation pressure.

IV.3.2. Effects of Camber Angle

The deviation of the central plane of a tire from the vertical plane is known as camber, and the angle between the two planes is called the camber angle. The angle is positive when the tire leans away from the vehicle body and negative when it leans towards the vehicle body at the top, Fig. IV-10.

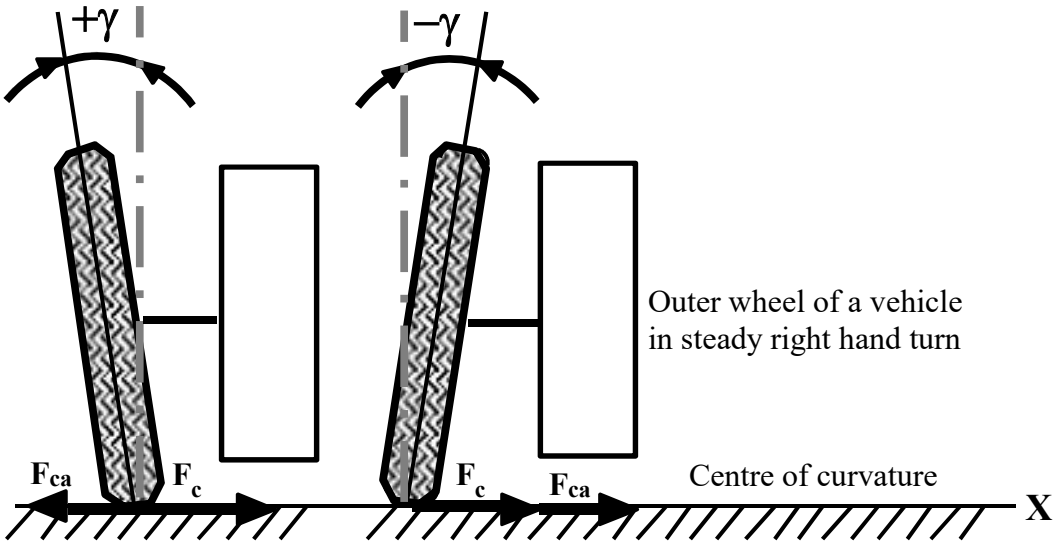


Figure IV-10. Camber angle

In Sect. IV-2., the plane of the wheel was assumed to be always vertical; hence the tire cornering characteristics presented in this section are valid for zero camber. In practice, however, vehicles frequently have their wheel planes at some angle to the vertical.

The camber angle given to the wheels during assembly is called static camber. Dynamic camber, on the other hand, may result from the roll motion of the body during cornering or from wheel movement.

When the camber angle is positive, cornering force is reduced compared to that of a vertical tire, whereas a negative camber angle results in increased cornering force, in general. The camber force (or thrust) can be explained by the fact that a cambered wheel tends to move like a rolling cone and thus tries to pull the vehicle to one side, as illustrated in Fig IV-11. It should be noted that the effect of camber is different for the inner and outer wheels while the vehicle is going around a curve. The overall effect on the cornering forces acting on the front or rear wheels, however, will be towards reduction of the total cornering force because of the nonlinear tire cornering force versus tire load characteristics.

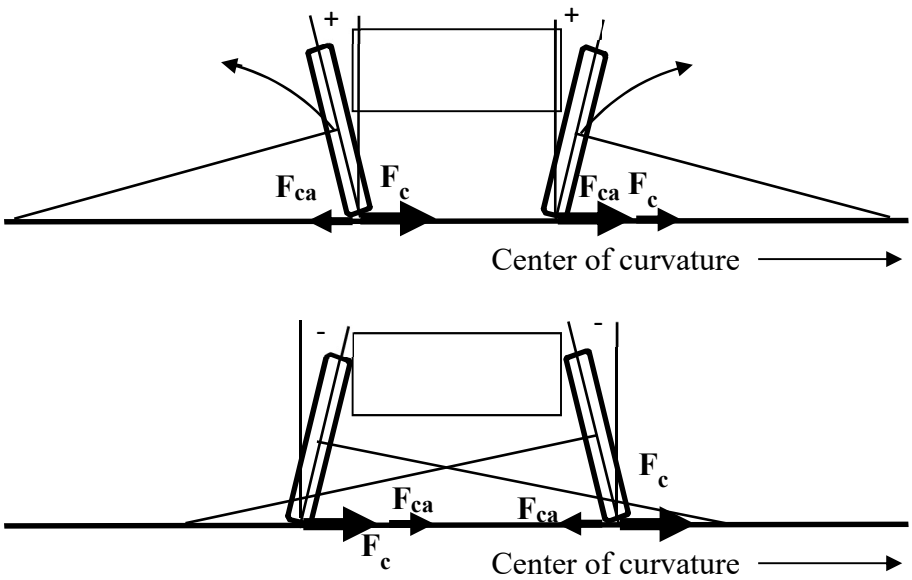


Figure IV-11a. Cornering force and camber thrust

The maximum cornering force is not significantly altered by the presence of camber, Fig. IV-11b.

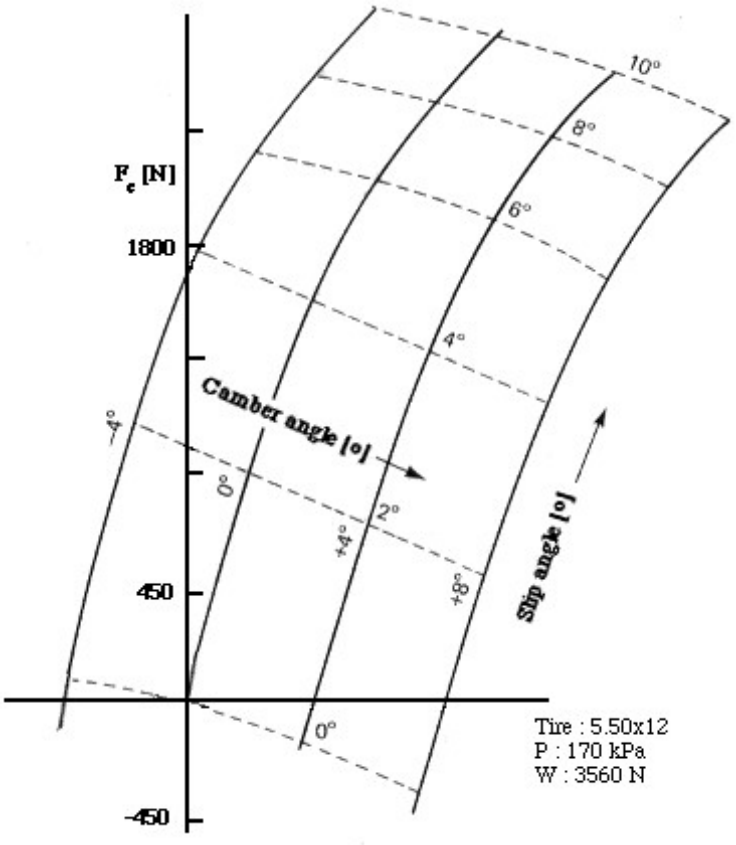


Figure IV-11b. Effects of camber angle on tire cornering force characteristics

IV.3.3. Effects of Tractive Effort

The cornering force developed at any fixed slip angle is reduced by the application of tractive or braking force. This basically follows from:

$$\sqrt{F_T^2 + F_C^2} \leq \mu W \qquad \text{(IV-3)}$$

where

F_T = tractive or braking force,
F_C = cornering force,
μ = available coefficient of adhesion,
W = vertical tire load.

Therefore tractive effort reduces the local friction available in the lateral direction. The same argument applies to the case of braking. Fig. IV-12 illustrates the reduction in tire cornering force with increasing brake force.

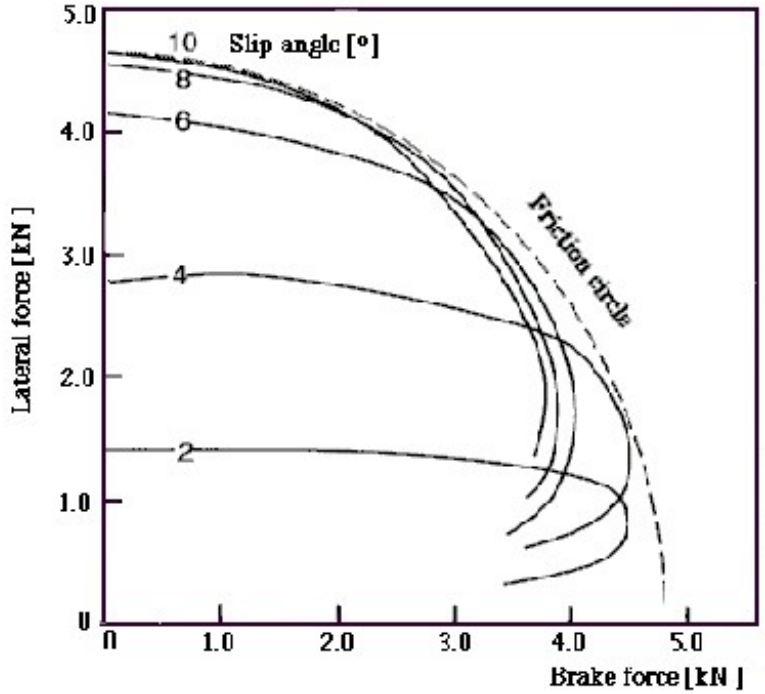


Figure IV-12. Effects of tractive effort on tire cornering force characteristics

An approximate method of determining the lateral force available during the presence of tractive and braking effort is possible if it is assumed that the tire may reach its limiting force condition in any direction, but that the maximum force may not exceed a given value in either the lateral or fore and aft direction as shown in Fig. IV-13(a). The so-called friction circle concept is based on the condition that the limiting force is the same for cornering and braking forces. In the development of some tires, however, traction or braking effort is

emphasized. Thus, the force limit is different for traction and braking. In this case, the friction ellipse takes the place of the friction circle, Fig. IV-13(b).

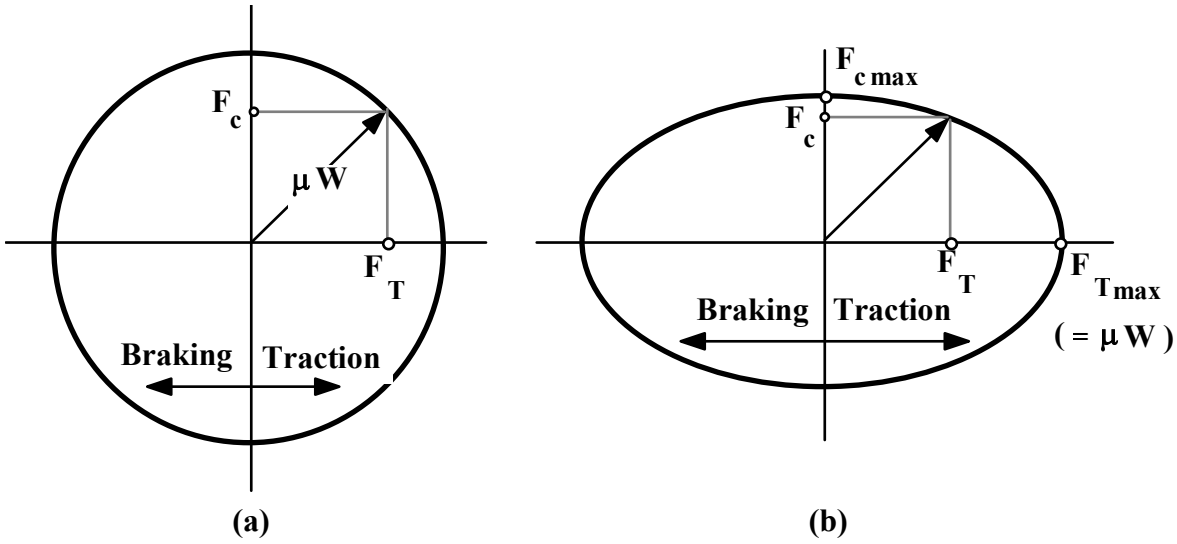


Figure IV-13. Friction circle and friction ellipse.

IV.4. Self-Aligning Torque(SAT)

The variation of self-aligning torque, which gives the feel of steering, may be given as a function of slip angle. It is, however, more meaningful to plot SAT against cornering force. This is because slip angle is merely something that the driver can deduce but cannot sense, whereas the cornering force is determined by the radius of the turn (which is beyond the driver's control) and the speed of the vehicle which is what the driver controls. Fig. IV-14, therefore, gives a much truer measure of the difference in steering produced by various tires.

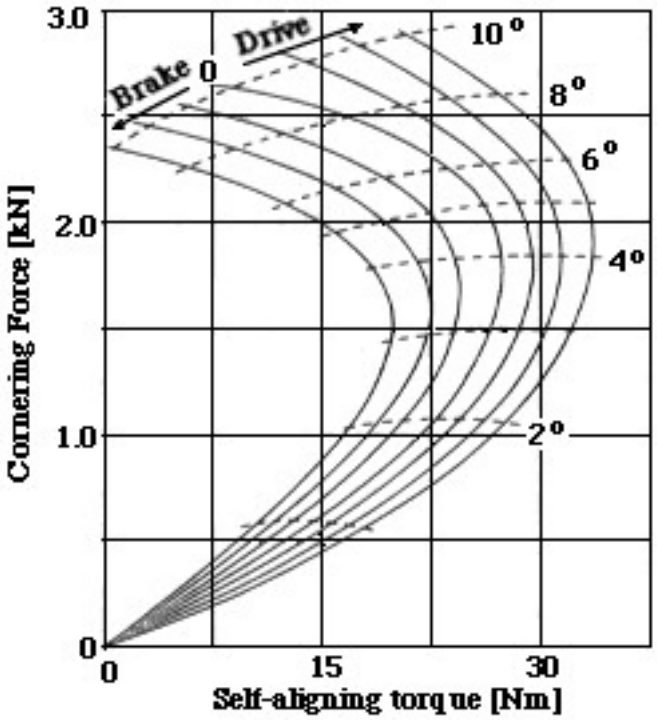


Figure IV-14. Variation of self-aligning torque

The application of tractive effort increases SAT, whereas the application of a braking force on the tire has the reverse effect. SAT increases initially with increasing slip angle, but after a certain slip angle, it starts decreasing with increasing slip angles. In the extreme cases of slip angles around 15º, SAT may even become negative.

There are other factors that affect SAT. One of these is the load on the tire; the greater the load, the greater is the deflection of the tire, and correspondingly the length of the contact patch is greater. From this, it follows that the amount of pneumatic trail will be increased, and hence the SAT will also rise. The converse is also true; increasing the inflation pressure for a given load will reduce the pneumatic trail by the same means and thus diminish the self-aligning torque.

IV.5. Plane Motions of Vehicles

The full range of lateral acceleration, a_L, to which a vehicle is subjected under various conditions, can be divided into two phases.

i) In the first phase, the vehicle is subjected up to 0.3 g lateral acceleration[1] during everyday straight-ahead driving; the side loading being caused by crosswinds, incorrectly banked road, variations of road surface, and fast curves.

In this range of lateral accelerations, vehicle roll is usually not significant, and hence the flexibility of suspension can be neglected. A simplified vehicle model, taking into account of plane motion of the vehicle only, is then sufficient to describe basic handling behavior in terms of main vehicle parameters such as weight distribution, tire specification, tire pressures, and tire camber angles. With a given vehicle design, changes to ground stability during the first phase can only be made by alterations to these main parameters. In the earlier design stages of a new model, when suspension data are not yet available, such information will be extremely valuable.

ii) The second phase, from 0.3 g upwards, involves average to hard cornering and maneuvers usually producing visible roll. In this phase, changes to spring rates, roll axis, and the addition of auxiliary roll stiffening devices affecting the distribution of roll stiffness are effective.

The handling of the vehicle must, therefore, be checked using a three degree of freedom (yaw, side slip, and roll) model as soon as the suspension data are available. Such an analysis normally requires a mathematical model of the vehicle including the suspension system and the solution can be performed on a computer.

A simple four-wheel vehicle model moving on a smooth level road surface is shown in Fig. IV-15. OXYZ is the inertial reference frame fixed to the road. The moving reference frame $C\xi\eta\zeta$ is attached to the center of gravity of the vehicle. The use of the body-fixed reference frame at the center of gravity with the axes corresponding to the principal axes of inertia allows the use of

- Fixed rotational inertia properties, and
- Zero products of inertia

together with

[1] * International standard ISO-TR 8726, *Road vehicles - Transient open-loop response test method with pseudo-random steering input.* 1988

- No inertial coupling between translational and rotational coordinates

resulting in the simplest set of governing equations.

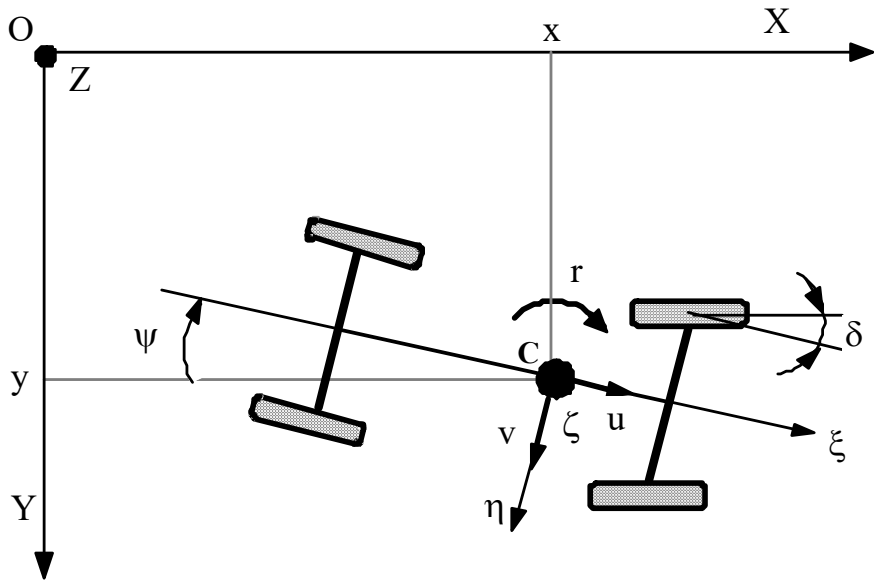


Figure IV-15. Plane motions of the vehicle

The variables describing the motion of the vehicle may be restricted to the three variables u, v, and r representing the longitudinal, lateral, and yaw motions of the vehicle. It is evident that the trajectory of the vehicle can be plotted if the location of the center of gravity and the direction of the vehicle's longitudinal axis, i.e., x, y, and ψ, are known at any instant.

$$\dot{\psi} = r \qquad \dot{y} = v\cos\psi + u\sin\psi \qquad \dot{x} = u\cos\psi - v\sin\psi \qquad \text{(IV-4)}$$

The vehicle has a mass m and a moment of inertia J about the vertical axis through its center of gravity. A number of assumptions are made in obtaining a four-wheel vehicle model illustrated in Fig. IV-16.

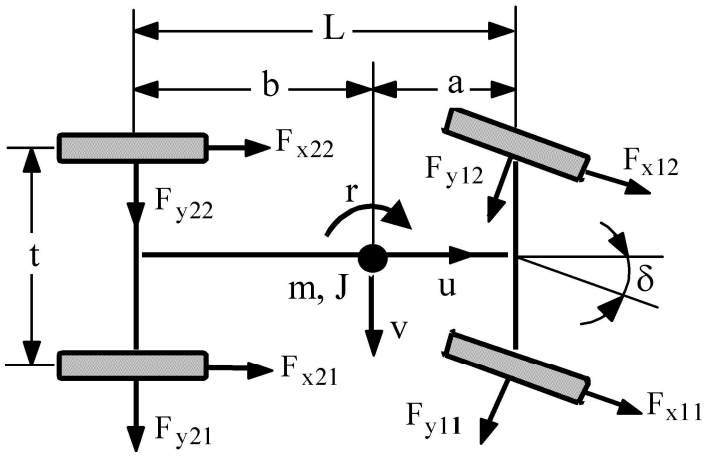


Figure IV-16. Four wheel vehicle model

1) External forces are assumed to act from the ground to the four tires in their contact centers, disregarding the self-aligning torques.

2) Fixed steering control with equal steering angles δ of the left and right front wheels is assumed.

3) Wheels are supposed to remain in a vertical position, i.e., no camber.

4) Suspension is assumed to be very stiff so that roll and pitch motions are disregarded.

5) The effects of tractive force on tire side force characteristics are neglected.

6) Moreover, if the height of the center of gravity is assumed to be small with respect to the track of the vehicle, one can assume that load transfer from inside wheels to outside wheels during cornering, and the corresponding change in tire side force characteristics are negligible.

IV.5.1. Tire Slip Angles

The individual tire slip angles for the four-wheel vehicle model are illustrated in Fig.IV-17. The steering angle is not included for clarity. The expressions for each individual tire are as follows.

$$\tan\alpha_{11} = \frac{v + ar}{u - r\frac{t_f}{2}} \qquad \tan\alpha_{12} = \frac{v + ar}{u + r\frac{t_f}{2}}$$

$$\tan\alpha_{21} = \frac{v - br}{u - r\frac{t_r}{2}} \qquad \tan\alpha_{22} = \frac{v - br}{u + r\frac{t_r}{2}} \tag{IV-5}$$

For small slip angles, tan α may be replaced by α. Since the magnitude of r is much smaller than that of u, the second term in the denominator of each expression can be neglected. Thus, the slip angles on the right and left-hand tires become identical. It is then sufficient to specify a single slip angle each for the front and rear tires.

$$\alpha_f \cong \frac{v + ar}{u} \qquad \alpha_r \cong \frac{v - br}{u} \tag{IV-6}$$

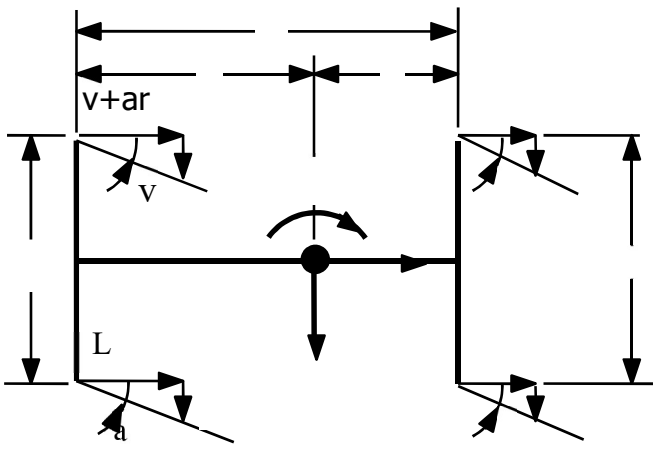


Figure IV-17 Slip angles

IV.5.2. Bicycle Model

The representation of a slip angle for the front and rear axles, α_f and α_r, allows the combination of tire side forces for each axle, i.e.,

$2F_{y11} = 2F_{y12} = F_{yf}$ front axle side force
$2F_{y21} = 2F_{y22} = F_{yr}$ rear axle side force

The vehicle model considered may now be reduced to a two-wheel model illustrated in Fig.IV-18. It should be obvious that the direction of motion can be taken arbitrarily as long as the sign convention for the slip angles is correctly applied.

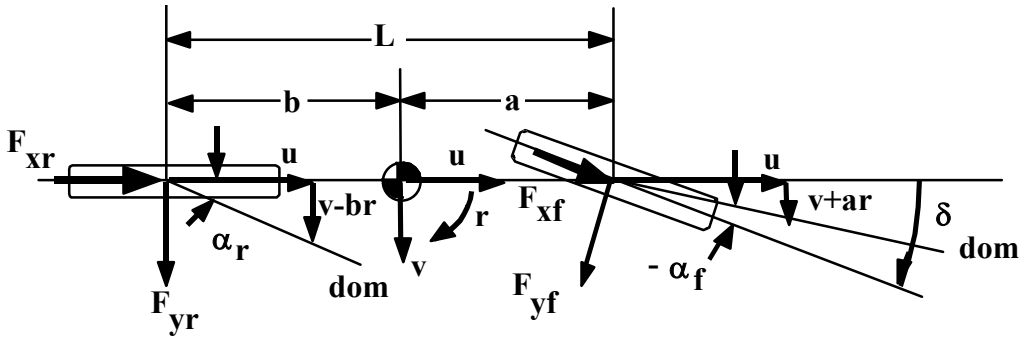


Figure IV-18 Bicycle model

The equations of motion can be written as :

$$\begin{aligned} m(\dot{u} - vr) &= F_{xf}\cos\delta + F_{xr} - F_{yf}\sin\delta \\ m(\dot{v} + ur) &= F_{yf}\cos\delta + F_{yr} + F_{xf}\sin\delta \\ J\dot{r} &= aF_{yf}\cos\delta - bF_{yr} + aF_{xf}\sin\delta \end{aligned} \qquad \text{(IV-7)}$$

These equations, for small steer angles δ, of the steered wheels, will simplify to:

$$\begin{aligned} m(\dot{u} - vr) &= F_{xf} + F_{xr} \\ m(\dot{v} + ur) &= F_{yf} + F_{yr} \\ J\dot{r} &= aF_{yf} - bF_{yr} \end{aligned} \qquad \text{(IV-8)}$$

In the first equation, the term vr on the left-hand side is a product of two variables of small magnitude and hence can be neglected. Then this equation is uncoupled from the other two equations and can be used to study the acceleration performance of the vehicle in straight motion along the longitudinal axis of the vehicle. The remaining two equations involve the yawing and side slip motions of the vehicle and will be examined in detail. The forward speed

of the vehicle will be kept as a constant parameter, U, and the degrees of freedom of the vehicle model is now two.

The maximum side force of tires running on dry roads may be attained at slip angles of 10 to 12 degrees, whereas for normal driving, slip angles do not exceed, say, 4 degrees. Therefore, a restriction of vehicle motions to small slip angles is justified.

If C_f and C_r are the cornering stiffnesses for the front and rear axles, respectively, for small slip angles

$$F_{yf} = C_f \alpha_f$$
$$F_{yr} = C_r \alpha_r$$

and the two equations of motion related to vehicle handling can be written in the form:

$$m(\dot{v} + Ur) = C_f\alpha_f + C_r\alpha_r$$

$$J\dot{r} = aC_f\alpha_f - bC_r\alpha_r$$

It should be noted that cornering stiffness is by definition negative, i.e., $C_f < 0$ and $C_r < 0$.

The slip angles α_f and α_r can be written from Fig. IV-18. as

$$\alpha_f = \frac{v + ar}{U} - \delta$$
$$\alpha_r = \frac{v - br}{U} \qquad \text{(IV-9)}$$

Inserting the above values into the equations of motion:

$$m(\dot{v} + Ur) = (C_f + C_r)\frac{v}{U} + (aC_f - bC_r)\frac{r}{U} - C_f\delta \qquad \text{(IV-10)}$$

$$J\dot{r} = (aC_f - bC_r)\frac{v}{U} + (a^2C_f - b^2C_r)\frac{r}{U} - aC_f\delta \qquad \text{(IV-11)}$$

The above equations can be put into the general matrix state equation form

$$\{\dot{x}(t)\} = [A]\{x(t)\} + [B]\{u(t)\}$$

as follows :

$$\begin{Bmatrix} \dot{v} \\ \dot{r} \end{Bmatrix} = \begin{bmatrix} \frac{C_f + C_r}{mU} & \frac{aC_f - bC_r}{mU} - U \\ \frac{aC_f - bC_r}{JU} & \frac{a^2C_f + b^2C_r}{JU} \end{bmatrix} \begin{Bmatrix} v \\ r \end{Bmatrix} + \begin{Bmatrix} -\frac{C_f}{m} \\ -\frac{aC_f}{J} \end{Bmatrix} \delta \qquad \text{(IV-12)}$$

Here we will assume that a steady angle of steer, δ, is applied and held. In a steady-state turn, the yawing and slip accelerations become zero and the yawing velocity is the rate of turning, i.e.,

$$\dot{r} = \dot{v} = 0$$

So the steady-state equations become

$$\frac{1}{U} \begin{bmatrix} C_f + C_r & (aC_f - bC_r) - mU^2 \\ aC_f - bC_r & a^2C_f + b^2C_r \end{bmatrix} \begin{Bmatrix} v \\ r \end{Bmatrix} = C_f \begin{Bmatrix} 1 \\ a \end{Bmatrix} \delta \qquad \text{(IV-13)}$$

Further, denoting steering wheel angle by $\delta_{sw} = G\delta$, and eliminating v from the two equations, one can obtain the yaw velocity gain

$$\frac{r}{\delta_{sw}}\Big|_{ss} = \frac{1}{G}\left[\frac{ULC_fC_r}{(aC_f - bC_r)\, mU^2 + L^2C_fC_r}\right] \qquad \text{(IV-14)}$$

where G is the steering gear ratio.

Multiplying eqn. (IV.14) by U, lateral acceleration gain is obtained.

$$\frac{U^2/R}{\delta_{sw}}\Big|_{ss} = \frac{1}{G}\left[\frac{U^2LC_fC_r}{(aC_f - bC_r)\, mU^2 + L^2C_fC_r}\right] \qquad \text{(IV-15)}$$

If the yaw velocity and lateral acceleration gains are referred to as wheel steering angle δ, then G is taken to be unity.

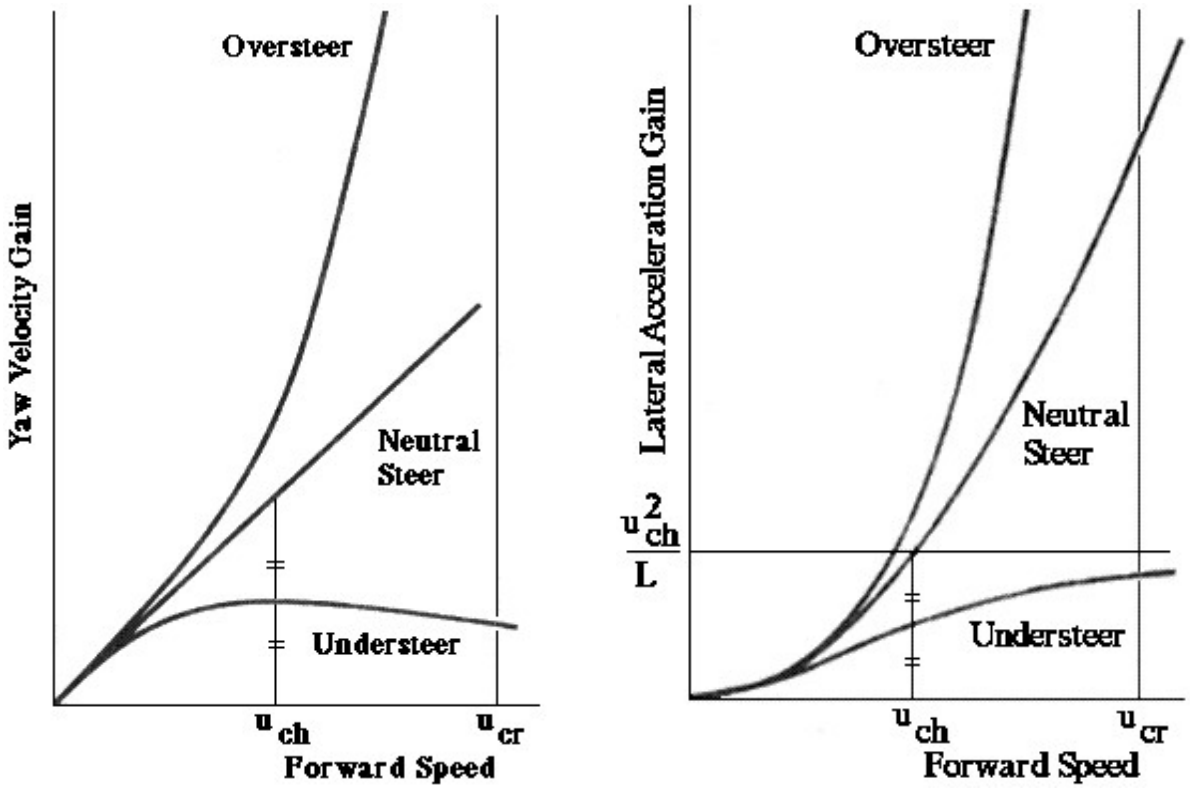
It is sometimes convenient to write the yaw velocity gain expression in a compact form.

$$\frac{r}{\delta}\Big|_{ss} = \frac{U}{A + BU^2}$$

The expressions for A and B in terms of vehicle and tire parameters can be deduced by comparison to eqn. (IV-14).

IV.5.3. Handling Behavior

A plot of yaw velocity gain versus vehicle speed for three classes of vehicles is shown in Fig. IV-19 (a). The neutral steer vehicle has yaw velocity gain in direct proportion to its speed. The oversteer vehicle has yaw velocity gain greater than in proportion to the speed and reaches an infinite value, indicating fixed control instability at the particular speed called the critical speed. The understeer vehicle reaches a maximum gain at the characteristic speed, and this value is one-half that of the neutral steer vehicle.



(a) (b)

Figure IV-19. Vehicle handling behavior

A similar plot is shown in Fig. IV-19 (b) for the lateral acceleration gain. It is interesting to note that the understeer vehicle tends toward a constant control sensitivity at speeds well above the characteristic speed. In other words, the vehicle would respond to a particular input of steer angle with nearly the same steady-state lateral acceleration regardless of vehicle speed as long as it is sufficiently high. The relation for lateral acceleration can be rewritten in the form

For a neutral steer vehicle

$$aC_f = bC_r \qquad \text{(IV-16)}$$

hence

$$\frac{r}{\delta_w}\Big|_{ss}^{\text{neutral steer}} = \frac{U}{L} \qquad \text{(IV-17)}$$

and

$$(U^2/R) / \delta_{sw}\Big|_{ss}^{\text{neutral steer}} = \frac{U^2}{L} \qquad \text{(IV-18)}$$

A critical speed is defined for an oversteer vehicle as that forward speed at which the yaw velocity and lateral acceleration gains both go to infinity, i.e., the vehicle is stable at speeds of forward motion less than the critical speed and is unstable at speeds higher than the critical speed.

To find an expression for the critical speed, one can equate the denominator of eqn. (IV.15) to zero to obtain

$$U_{cr}^2 (aC_f - bC_r)\, m + L^2 C_f C_r = 0$$

$$U_{cr}^2 = \frac{-L^2 C_f C_r}{(aC_f - bC_r)\, m} \qquad \text{(IV-19)}$$

For U_{cr} to be real, one must have (note that cornering stiffness values are by definition negative, i.e. $C_f < 0$ and $C_r < 0$)

$$(aC_f - bC_r) < 0$$

or

$$|aC_f| > |bC_r| \qquad \text{(IV-20)}$$

Thus the elementary vehicle with a fixed steering angle will be stable under all conditions of forward speed, provided that

$$|bC_r| > |aC_f| \qquad \text{(IV-21)}$$

which, in effect, suggests that the practical vehicle with the same tires on all wheels should have the center of gravity located forward of the wheelbase midpoint - for identical inflation pressure and camber characteristics.

Ineq. (IV-21) can be satisfied by choosing tires so that C_r is sufficiently greater than C_f. Since the values of C_r and C_f depend on vertical tire loads, increasing with the increase of load, the effect of reducing b and increasing a will also give the required increase

of C_r and reduction of C_f. The final adjustment would have to be made by adjusting the inflation pressures of the front and rear tires or by using different types of tires.

A characteristic speed can be defined for an understeer vehicle as that forward speed at which the yaw velocity and lateral acceleration gains are one-half the corresponding gains of a neutral steer vehicle. Alternatively, characteristic speed corresponds to the maximum yaw velocity response of an understeer vehicle.

To find an expression for the characteristic speed, one can equate the right-hand side of eqn. (IV-15) to half the yaw velocity gain for a neutral steer vehicle as given by eqn. (IV-18).

$$\frac{U_{ch}\, L\, C_f C_r}{U_{ch}^2 m\,(aC_f - bC_r) + L^2\, C_f C_r} = \frac{U_{ch}}{2L}$$

$$U_{ch}^2 = \frac{L^2\, C_f C_r}{(aC_f - bC_r)\, m} \qquad \text{(IV-22)}$$

The similarity of the expressions for U_{cr}^2 and U_{ch}^2 is obvious. It should be pointed out that whereas eqn. (IV-19) is used when $|aC_f| > |bC_r|$, eqn. (IV-22) is useful only for the case of an understeer vehicle, i.e., one with $|bC_r| > |aC_f|$.

The handling behavior of a vehicle can also be interpreted in terms of the relative magnitudes of the front and rear axle slip angles. This is shown in Figure IV-20, where the effects of a side force on a vehicle with zero steering input are illustrated.

It is observed that for an understeer vehicle, the resulting front slip angle is larger than the actual slip angle, and thus, the generated centrifugal force tends to cancel the effect of the side force. For an oversteer vehicle on the other hand, the centrifugal force tends to add to the side force as now the rear slip angle is larger than the front slip angle. Thus

$\alpha_f - \alpha_r > 0 \rightarrow$ understeering vehicle

$\alpha_f - \alpha_r = 0 \rightarrow$ neutral steer vehicle

$\alpha_f - \alpha_r < 0 \rightarrow$ oversteering vehicle

The effect of any changes in the vehicle specifications on the handling behavior can be judged by examining the changes induced in the front and rear slip angles. Any change increasing the front slip angle will thus introduce some understeering tendency to the original handling behavior, whereas increasing the rear slip angle will add an oversteering tendency.

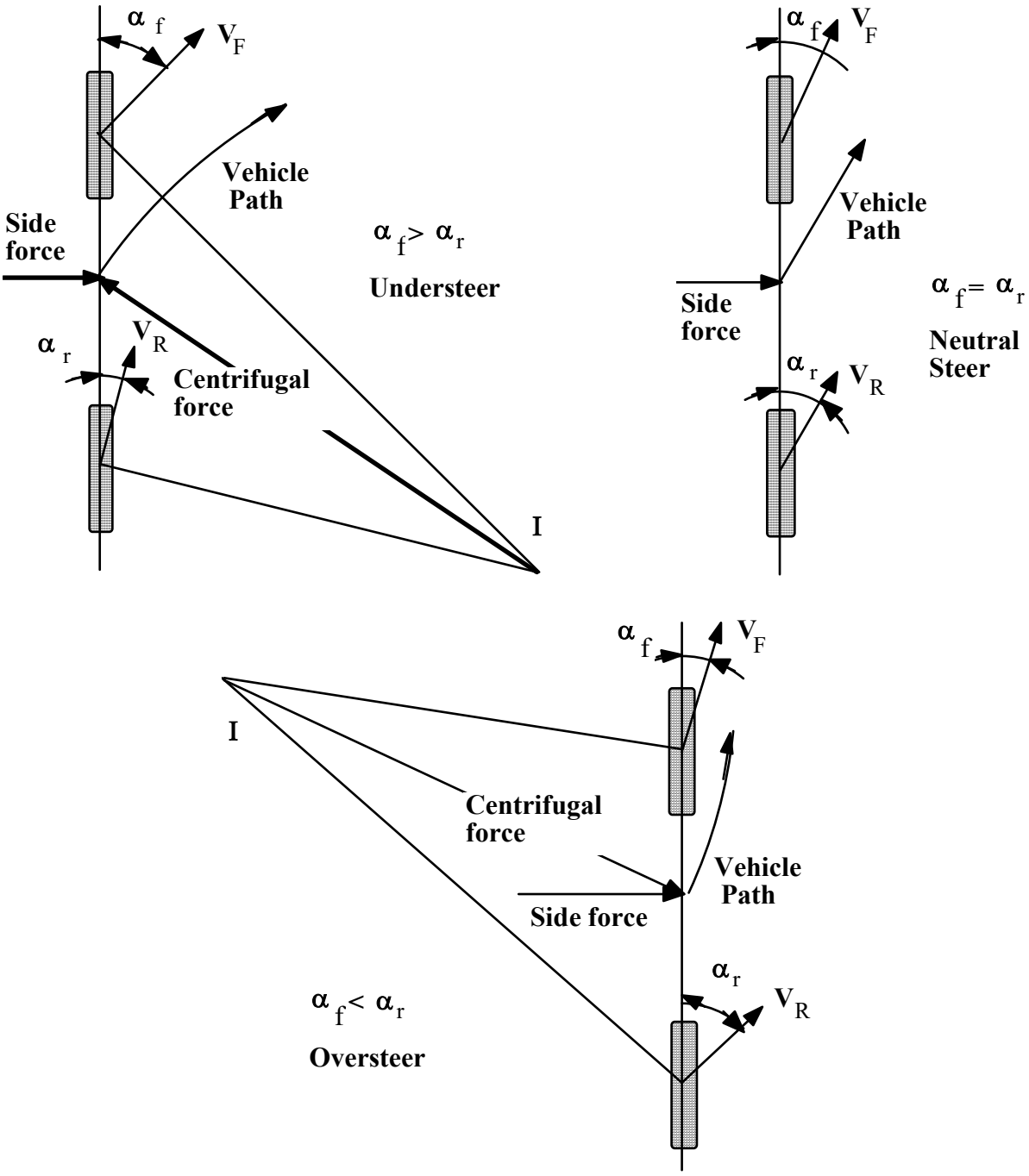
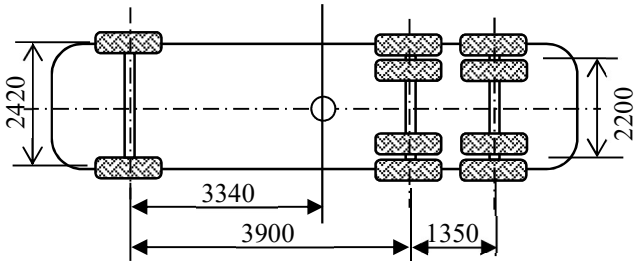


Figure IV-20. Vehicle handling behavior

Example IV-1

Consider a 22-ton truck with three axles as illustrated in the figure (all dimensions are in [mm]). There is a single set of tires on the front axle. Tandem wheels are used on the intermediate and rear axles. The cornering stiffnesses of tires are given below.

Front : $C_{sf} = 2.00$ [kN/°/tire]
Intermediate : $C_{si} = 1.25$ [kN/°/tire]
Rear : $C_{sr} = 1.50$ [kN/°/tire]



Use a suitable model to estimate the handling behavior of the truck at the low lateral acceleration range and calculate the corresponding critical or characteristic speed.

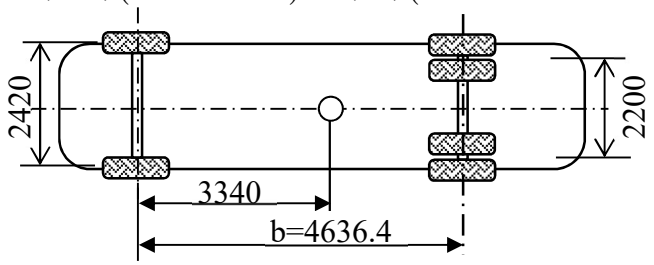
Let us combine the intermediate and rear axles into a single equivalent axle with total cornering stiffnesses $\sum C_{sf}$ and use a simple bicycle model with total cornering stiffnesses $\sum C_{sf}$ and $\sum C_{sr}$ at the front and rear axles.

$$\sum C_{sf} = 2(2000) = 4000\left[\frac{N}{o}\right]\left(\frac{180^o}{\pi rad}\right) = 229183\left[\frac{N}{rad}\right]$$

$$\sum C_{sr} = 4[1250+1500] = 11000\left[\frac{N}{o}\right]\left(\frac{180^o}{\pi rad}\right) = 630254\left[\frac{N}{rad}\right]$$

Since the cornering stiffnesses of the tires on the actual intermediate and rear axles are different, the location "b" of the equivalent axle will be different from the midpoint between these two axles. One approximation would be:

$$[4(1.25)+4(1.5)]b = 4(1.25)(3900-3340)+4(1.5)(3900-3340+1350) \Rightarrow b = 1296.4[mm]$$



Note that negative values for cornering stiffnesses must be used in the calculations.

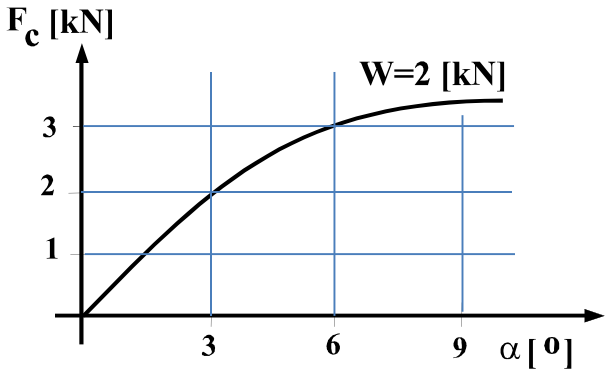
$$a\sum C_{sf} - b\sum C_{sr} = 3.340(-229183) - (1.2964)(-630254) = 51590[Nm]$$

Obviously, the truck will be understeering. The characteristic speed is:

$$U_{ch} = \sqrt{\frac{L^2\sum C_{sf}\sum C_{sr}}{(a\sum C_{sf} - b\sum C_{sr})m}} = \sqrt{\frac{(3.34+1.296)^2(229183)(630254)}{51590(22000)}} = 52.3\left[\frac{m}{s}\right] \cong 188[kph]$$

Exercises

IV-1) Estimate the cornering stiffness for the tire with a cornering force characteristic as given in the figure. Then calculate the cornering force at a slip angle of 2.7°.



IV-2) Using the cornering force characteristics shown in Fig. IV-5 and tabulated below, estimate the cornering stiffnesses in [N/deg] of a truck tire at wheel loads of 0.0, 14.5, 28.5, 38.5, and 52.5 [kN].

α [°]	Wheel load [kN]				
	9.0	14.5	28.5	38.5	52.5
	F_c [kN]				
0	0	0	0	0	0
1	1.0	1.8	3.1	3.8	4.0
2	2.1	3.5	6.5	7.6	9.0
3	3.5	5.4	10.0	11.6	13.5
4	4.5	7.2	12.4	15.5	17.6
5	5.3	8.8	15.0	18.6	21.9
6	6.2	10.3	16.8	21.4	25.2
7	6.8	11.2	18.1	23.6	27.5
8	7.0	12.0	19.5	25.2	30.0
9	7.4	12.7	20.4	26.1	31.2
10	7.7	13.1	21.0	26.9	32.1

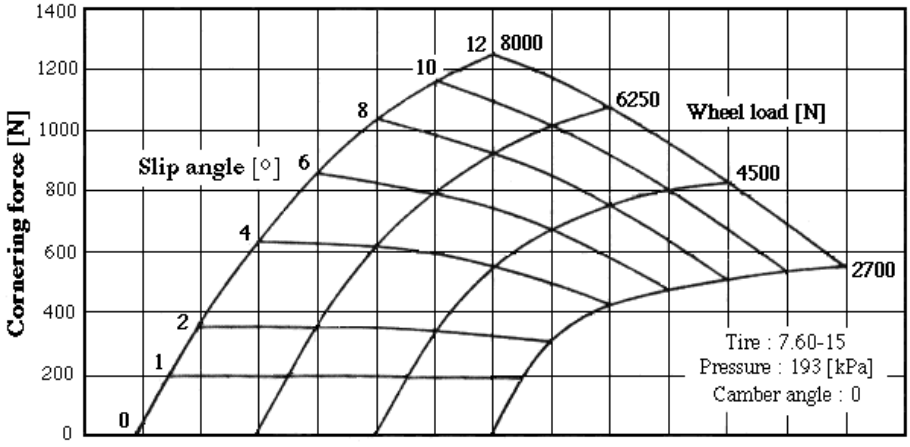
IV-3) Estimate the cornering stiffness of the truck tire around a slip angle of 8° at wheel loads of 52.5, 38.5, 28.5, 14.5, 9.0 [kN] using the cornering force characteristics given in exercise IV-2. Plot cornering stiffness versus wheel load curve for the specified slip angle.

IV-4) Estimate the cornering stiffness of the truck tire around slip angles of 1 - 8° at a wheel load of 38.5 [kN] using the cornering force characteristics given in exercise IV-2. Plot cornering stiffness versus slip angle curve for the specified wheel load.

IV-5) Using the tire characteristics given below, estimate

a) the cornering force at a wheel load of 5.3 kN and a slip angle of 4°.

b) the slip angle to generate a cornering force of 1.1 kN at a wheel load of 7.2 kN.



IV-6) The equations of motion of the bicycle model of the plane motions of a motor vehicle were obtained in terms of the velocities u, v, and r of the reference frame $C\varepsilon\eta\zeta$, attached to the center of gravity of the vehicle. Determine the expressions to specify the position and direction of the vehicle with respect to a fixed set of axes OXYZ, i.e., x(u, v, r), y(u, v, r), and ϕ(u, v, r).

IV-7) Consider the simple bicycle model of a vehicle. The longitudinal, lateral (side slip), and angular velocities at the vehicle center of gravity are specified as u, v, and r. Write down an expression for the vehicle sideslip angle, **β,** which is defined as the angle between the longitudinal axis of the vehicle and the direction of motion at the center of gravity.

IV-8) The motion of a vehicle is described by the forward velocity, u = 60 kph, the side slip velocity, v = 0.8 m/s, of its center of gravity, and the yaw velocity, r = 0.18 rad/s, about the center of gravity. The position of the center of gravity is denoted by the distances from the front and rear axles, a = 1.18 m and b = 1.05 m, respectively. The vehicle has equal front and rear tracks, t = 1.32 m. Calculate the slip angles of the right and left front tires if the front wheels are given a steering angle of δ=1.5°.

Ans.: α_{fr}=2.0°, α_{fl}=1.95°

IV-9) Obtain the expression for the sideslip velocity gain $\frac{v}{\delta}\Big|_{ss}$ for the plane motion vehicle model and plot versus forward speed, in the range from 0 to 150 kph with 5 kph increments, using the vehicle specified in Exercise IV-10.

IV-10) For the vehicle specified below, estimate the forward speeds at which the vehicle will

a) tip over the outer wheels,
b) slide out of the curve under the action of the centrifugal force
c) start an uncontrollable rotation about the center of gravity for even an infinitesimally small steering action

while going around a circular path of 120 m radius. The coefficient of adhesion between the tires and the road is specified as 0.86.

Vehicle Specifications:

Mass	:	1280 kg
Load distribution (f/r)	:	52/48 %
Wheelbase	:	2510 mm
Track	:	1224 mm
Height of center of gravity	:	512 mm
Cornering stiffness (f/r)	:	84.2/61.4 kN/rad

Ans.: a) 135 kph, b) 115 kph. c) 124 kph

IV-11) Consider a passenger vehicle with a mass of 1320 [kg]. The height of the center of gravity of the vehicle is 550 [mm], and the front and rear tracks are both 1400 [mm].The distance between the center of gravity and the front axle is 0.45 times the wheelbase. Tire cornering force characteristics at zero camber are identical and are tabulated below. Calculate the steady-state front and rear wheel slip angles at a lateral acceleration of 0.25 [g]. Neglect the effects of traction, camber, etc., and interpolate or extrapolate if and when necessary.

	Slip Angle [º]			
Tyre Load [N]	**1**	**2**	**3**	**4**
1000	430	670	810	900
2000	525	1000	1400	1650
3000	675	1275	1775	2250
4000	750	1500	2050	2670
5000	780	1625	2325	3000
6000	800	1650	2425	3100
7000	790	1640	2450	3120

IV-12) Using the bicycle model,

a) Show analytically that the peak of the yaw velocity gain for an understeer vehicle is obtained at characteristic speed and obtain the expression for the peak value.

b) Derive the limiting value of the lateral acceleration response of an understeer vehicle as the forward speed approaches infinity.

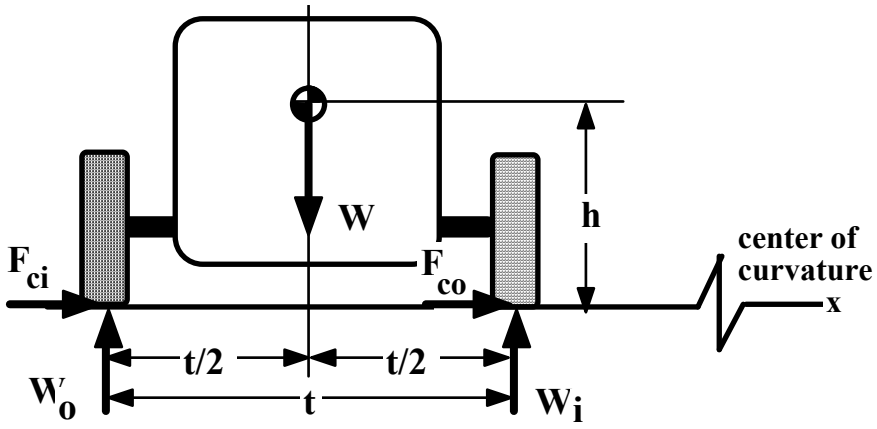
IV-13) For the vehicle illustrated in the figure,

a) Derive expressions for the loads on the inner and outer tires. The vehicle is going around a curve with a forward speed **u**, and the radius of curvature is **R**. Find the expression for the load transfer from inner to outer tires in terms of the lateral acceleration.

b) Plot load transfer from inner to outer tires for lateral accelerations, from 0 to 0.3 [g] with 0.025 [g] increments, using vehicle parameters :

m = 1120 [kg], h = 0.48 [m], t = 1.56 [m], a = 1.20 [m], b=1.30 [m].

c) Calculate the total cornering forces developed by the inner and outer tires at a lateral acceleration of 0.25 [g]. All the tires are identical with cornering force characteristics as given in the table below, and the center of gravity of the vehicle is at the midpoint between the front and rear axles. Assume a constant steering angle of 3º, and a forward velocity of 60 kph, a lateral (side slip) velocity of 1 m/s, and a yaw velocity of 0.37 rad/s.



W_V [N]	α [º]	1	2	3	4	5	6	7	8	9
2000	F_c [N]	380	800	1120	1360	1500	1570	1580	1590	1600
3000		450	860	1280	1560	1710	1860	2040	2200	2300
4000		480	910	1300	1640	1920	2190	2420	2610	2800

IV-14) Calculate the radius of curvature of the trajectory of a vehicle with a forward speed of 120 kph and a steady-state yaw velocity of 0.27 rad/s.

Ans.: 123 [m]

IV-15) For the vehicle below, plot the variations of

a) yaw velocity gain [rad/s/rad], and
b) lateral acceleration gain [g/rad]

with respect to steering wheel angle versus forward speed in the range of 0 to 150 kph.

Mass: 20105 kN.
Wheelbase: 3.2 m
Load distribution (f/r): % 53.5/46.5
Cornering stiffness of each front tire: 39.0 kN/rad
Cornering stiffness of each rear tire: 38.0 kN/rad

IV-16) A large saloon car has a mass of 2040 kg. The wheelbase is 2.95 m, and the front axle carries 54.0 % of the static load. Determine the steady-state handling behavior (whether understeer, oversteer, or neutral steer; characteristic or critical speed as appropriate) of the vehicles equipped with tires specified below.

a) All cross-ply tires with
Cornering stiffness of each front tire : 38.9 kN/rad
Cornering stiffness of each rear tire : 38.2 kN/rad

b) Front tires replaced with radial ply tires, each having a cornering stiffness of 47.8 kN/rad.

Ans. : a) Understeer, 143 [kph], b) Oversteer, 361 [kph]

IV-17) Consider the truck in Example IV-1.

a) Check the handling behavior if the equivalent rear axle is assumed to be at the midpoint between the intermediate and rear axles.

b) Calculate the relevant characteristic or critical speed in this case.

c) Comment on the handling behavior of the truck? Do you think it is satisfactory?

IV-18) The yaw velocity gain expression for a bicycle model of a car is given below. Obtain the steady-state yaw velocity and lateral acceleration gains for a neutral steer vehicle.

$$\left.\frac{r}{\delta_{sw}}\right|_{ss} = \frac{1}{G}\left[\frac{uL\,C_f C_r}{(aC_f - bC_r)\,mu^2 + L^2\,C_f C_r}\right]$$

IV-19) The yaw velocity gain expression (with respect to the steering angle δ in [rad] of the front wheels) of a car is given as a function of forward speed U in [m/s], below.

$$\frac{r}{\delta} = \frac{U}{2.48 + 0.00124\,U^2}$$

a) What can you say about the handling behavior of the vehicle? Determine the critical or characteristic speed, whichever is appropriate, of the car.

b) Calculate the maximum yaw velocity gain of the car.

c) Calculate the lateral acceleration of the car at a forward speed of 60 kph for a steering angle of 3° of the front wheels.

Ans. : a) Understeer, 161 [kph], b) 9.0 [rad/rad/s], c) 5.15 [m/s^2]

IV-20) Consider a car with specifications as follows :

Mass : 1400 kg, L=2.45 m,
C_f = 75000 N/rad, C_r = 100000 N/rad, G=17.

(a) Calculate the lateral acceleration gain for a forward speed of 60 kph if the load distribution (f/r) is specified as 42/58 %

(b) Calculate the load distribution (front and rear axle loads in %) to result in a neutral steer vehicle.

IV-21) The yaw velocity gain expression (with respect to the steering angle δ in [rad] of the front wheels) of a car is given as a function of forward speed U in [m/s], in terms of constant parameters A and B, below.

$$\frac{r}{\delta} = \frac{U}{A + BU^2}$$

a) Write down the conditions on the values of A and B for the vehicle to have oversteer, understeer, and neutral steer characteristics.

b) Write down the expression, in terms of A and B, for the critical and characteristic speeds of the vehicle.

c) If A = 2.42 and B = - 0.0019 for r in [(i.e., m, s, rad,…), calculate the lateral acceleration gain of the car in [(m/s2)/^{o}] at a forward speed of 60 kph and determine the critical or characteristic speed of the car in [kph].

IV-22) Consider a vehicle with a mass of 1280 kg and front and rear axle cornering stiffnesses of 75000 and 96000 N/rad. Assume two different cases, where the mass of the vehicle is distributed such that the position of the center of gravity is specified as :

Case 1 : a = 1.12 m, b = 1.43 m
Case 2 : a = 1.43 m, b = 1.12 m.

Calculate the steady-state radius of curvature of the trajectory and the lateral acceleration of the vehicle at a forward speed of 90 kph, for a steering angle of 1.2^{o} of the front tires, under the two cases specified. Explain the differences between the two cases.

IV-23) Explain the effects on the handling characteristics of an automobile, with zero camber angles at the front and at the rear and all tires identical at the rated inflation pressures, of

a) increasing front tire inflation pressure,
b) giving positive camber angles to rear tires,
c) applying braking effort in a greater proportion to front tires than the rear tires,
d) including the effects of load transfer from inside to outside tires,

IV-24) The characteristic speeds of the two cars are determined to be 125 and 189 kph, respectively. Which has heavier understeering ? Explain or illustrate.

CHAPTER V

VEHICLE SUSPENSIONS

V-1. Basic Functions

The suspension system basically consists of all the elements that provide the connection between the wheels and the vehicle body and is designed to meet the following main requirements:

i) Ride comfort: Insulates the vehicle and its occupants from road shocks and against transmission of vibration from the road surface, which results in road noise within the passenger compartment, and thus provides a comfortable ride.

ii) Road Holding: Keeps the wheels in contact with the road surface at all times for better traction, braking, and directional control and stability.

iii) Handling: Provides suitable handling characteristics by locating the wheels, regulating their motions, and allowing easy steering of the wheels.

It is evident that a suspension system must be able to withstand the loads acting on it. These forces may be in the longitudinal direction such as acceleration and braking forces, in the lateral direction such as cornering forces, and in the vertical direction. Further, driving and braking torques should also be considered.

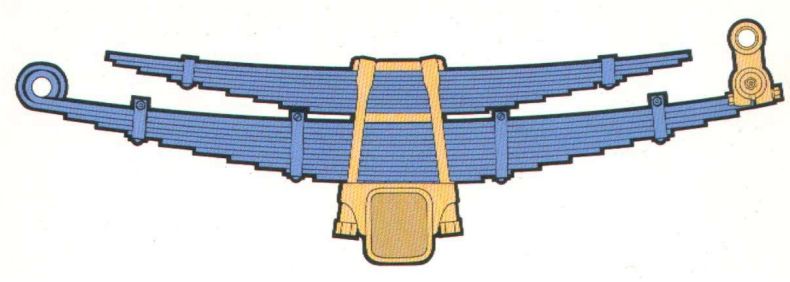
A well-designed suspension system is expected to give a balanced compromise solution for the above-mentioned aspects of performance which require conflicting specifications. Thus, different designers and manufacturers place emphasis on one or another aspect, which usually reflects the particular road conditions and driving habits applicable in the target country. For example, in the case of generally straight but rough road surfaces good ride is always the first in the list of preferences. The case of mountainous areas requires an emphasis on handling quality, and finally, on straight roads with good surfaces accent is on straight-line stability.

V-2. Basic Components

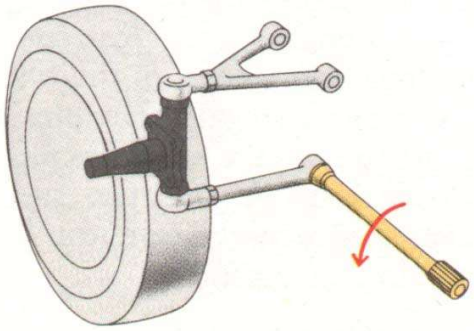
V-2.1 Spring

The first requirement from the suspension system requires an elastic resistance to absorb the road shocks. This primary function is fulfilled by the suspension springs. Various different types of springs have been used in vehicle suspensions. Among these are :

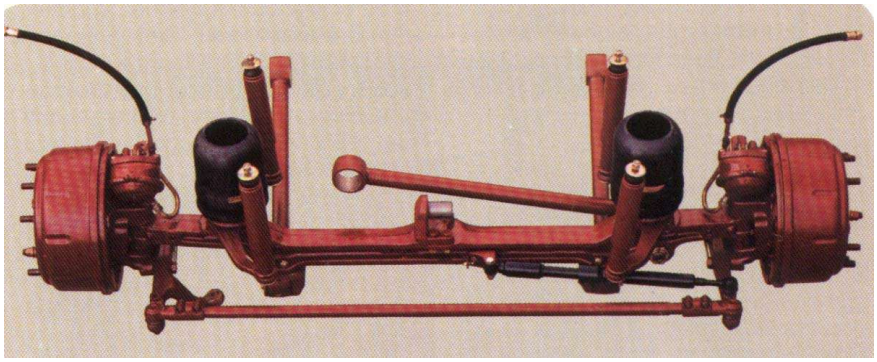
i) Leaf springs,
ii) Helical coil springs,
iii) Torsion bar springs,
iv) Air springs, and
v) Rubber springs.



(a) Leaf spring



(b) Torsion bar spring



(c) Air spring

Figure V-1. Automotive suspension springs

V-2.2 Damper[1]

If the energy absorbed by the suspension springs is not dissipated, the vehicle will continue to oscillate up and down. A damper, which converts mechanical energy into heat energy, is thus necessary. It should be noted that in spite of the commonly used name "shock absorber", dampers do not absorb shocks.

The structure of single and double cylinder dampers commonly used in road vehicles is illustrated in Figure V-2.

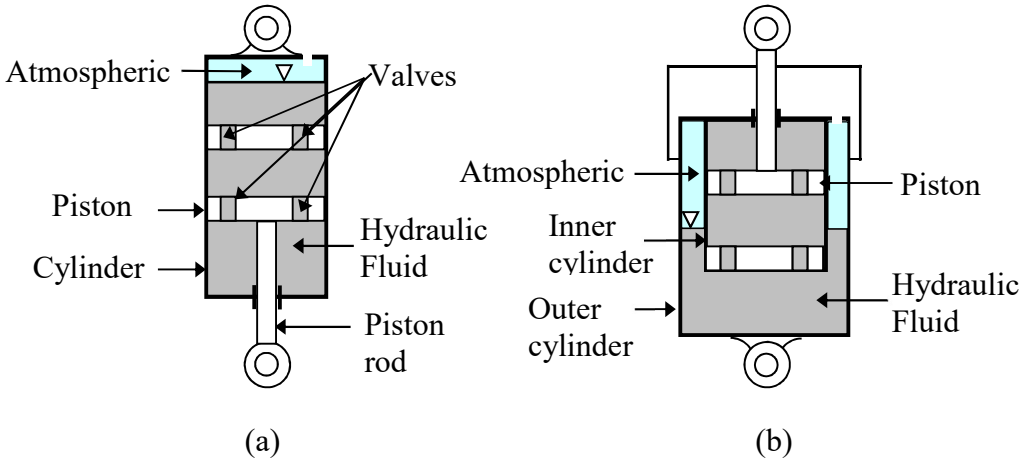


Figure V-2. Damper design, (a) single-cylinder, (b) double-cylinder

The essential data used in the application of dampers is the force-piston speed characteristic, usually approximated by straight lines, from which an estimation for a linear damping coefficient can be obtained. In vehicle suspension applications, the speed of the wheel in the upward direction (as in going over a bump) is roughly twice that in the case of downward direction (rebound). To equalize the force applied on the vehicle body, the suspension dampers are designed to produce asymmetric characteristics illustrated in Figure V-3.[2]

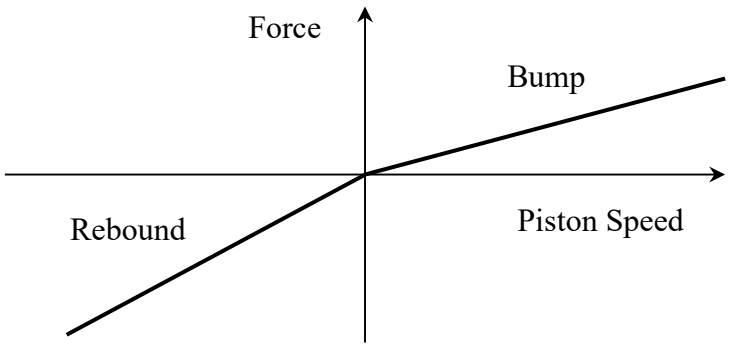


Figure V-3. Damper force-piston speed characteristic

[1] Balkan, T., Ünlüsoy, Y. S., "Servohidrolik Amortisör Dinamometresinin Dinamik Modeli ve Simülasyonu", II. Hidrolik ve Pnömatik Kongresi ve Sergisi Bildiriler Kitabı, s. 442-451, İzmir, Kasım 2001.
[2] Milliken, W. F. ve Milliken, D. L., "Race Car Vehicle Dynamics", SAE International, 1995.

The Force-piston speed characteristic of a damper is obtained experimentally. In these tests, one end of the damper is fixed on a rigid frame through a force transducer. An actuator is then used to excite the other end at a fixed stroke and a series of speeds. During tests, force and piston displacement data are collected.

Testing machines for measuring damper characteristics are classified into three groups: mechanical, servo-hydraulic, and electromagnetic. Mechanical setups are commonly used because of their simplicity. They can not, however, provide the flexibility and performance of the more complex and expensive servo-hydraulic and electromagnetic counterparts.

In mechanical testing machines, a Scotch Yoke mechanism is used to give the free end of the damper a fixed amplitude, variable frequency sinusoidal displacement, as illustrated in Figure V-4 (a). The amplitude and/or the frequency can be changed by adjusting the mechanism and/or the speed of the drive motor using a variable frequency drive. Tests performed at various motor speeds will result in the families of closed force-piston displacement curves. Piston speed corresponding to each motor speed can be calculated and associated with the particular force-piston displacement curve obtained at that speed.

A typical servo-hydraulic test machine is illustrated in Figure V-4 (b).

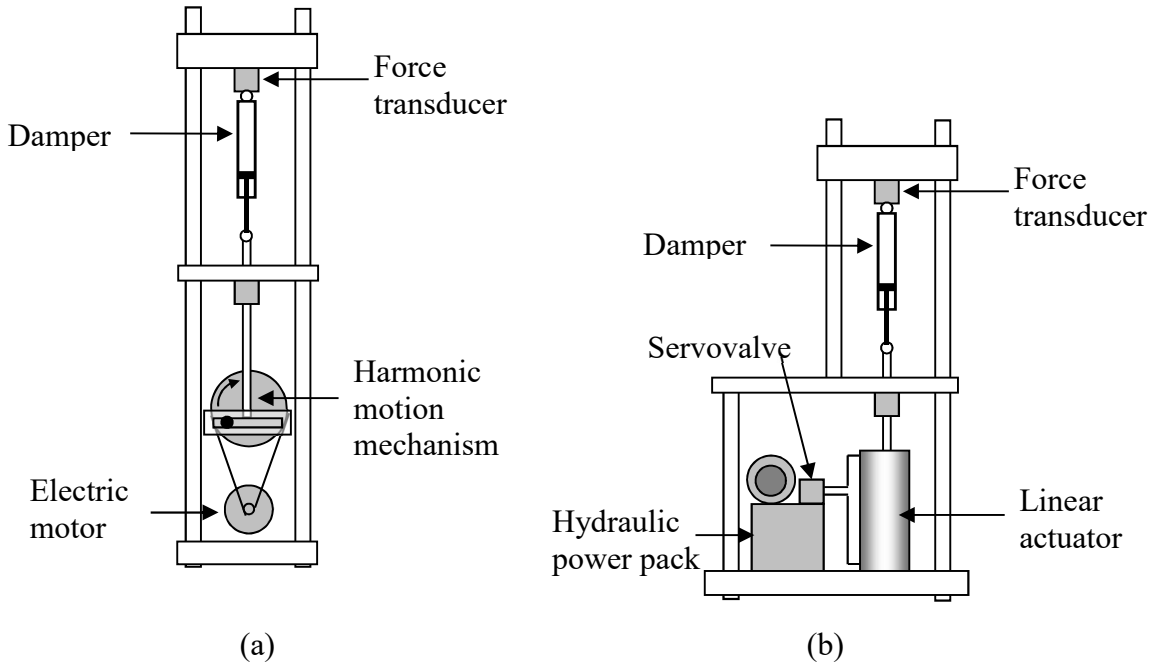
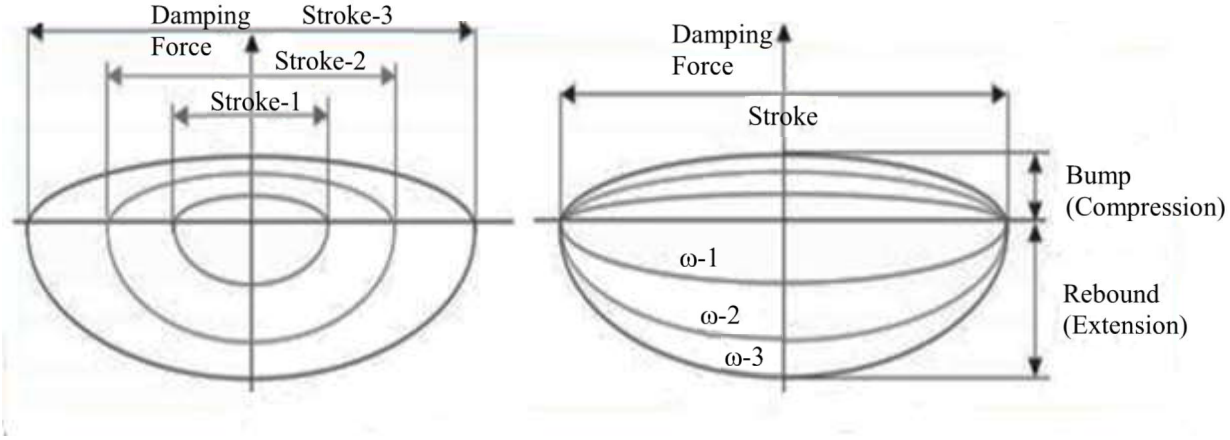


Figure V-4. Damper testing machines, (a) Mechanical, (b) Servohydraulic

Typical damper characteristic curves obtained through tests for fixed piston speed at varying strokes and fixed piston stroke at varying piston speeds are illustrated in Figure V-5 (a) and (b).

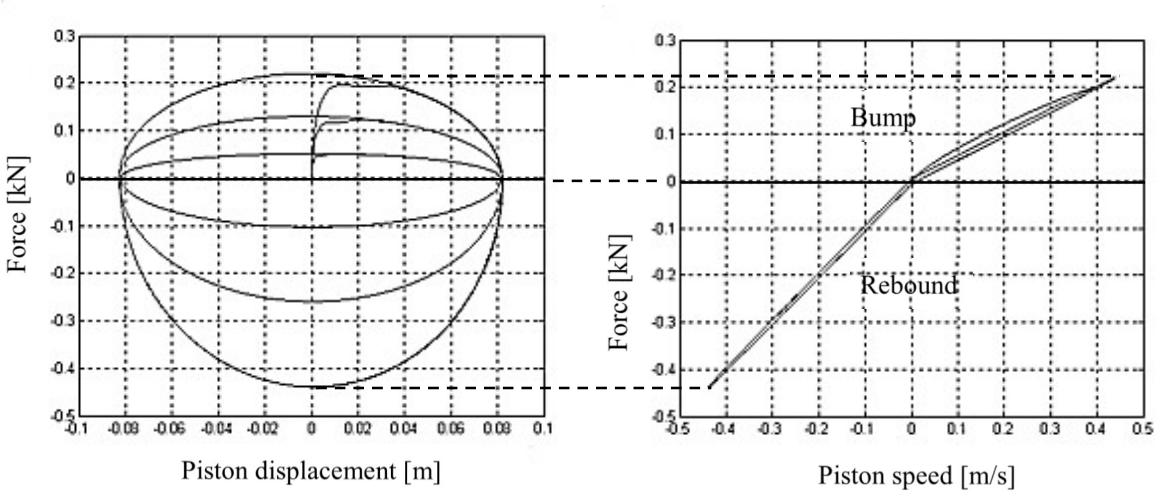


(a) (b)

Figure V-5. Damper characteristics; (a) force-piston displacement, (b) force-piston speed

Example V-1

Consider a damper test using a mechanical damper testing machine. Estimate the damping coefficients of the test damper in bump and in rebound, considering the experimental damping force versus piston displacement characteristics given in the figure on the left below. The rotational speed of the drive motor during the test is 51 [rpm], corresponding to the outermost characteristic in the figure.



Solution:

It is evident from the figure that the stroke of the hydraulic actuator of the test system, S_0, is 0.08 [m]. Since the position of the piston is given by $S = S_0\sin(\omega t)$, the speed of the piston is given by $V = \omega S_0\cos(\omega t)$, where t is time. Thus the maximum piston speed is obtained as:

$$V_{max} = \omega S_0 = 51\left[\frac{\text{rev}}{\text{min}}\right]\left(\frac{2\pi\text{rad}}{\text{rev}}\right)\left(\frac{\text{min}}{60\text{s}}\right)0.08[\text{m}] = 0.427\left[\frac{\text{m}}{\text{s}}\right]$$

The maximum damper forces corresponding to the maximum piston speeds can be read from the experimental characteristics approximately as 0.22 [N] for bump and 0.43 [N] for rebound. Thus the linear damping coefficients in bump and rebound can be estimated as 515 and 1007 [N/m/s] from the slopes of the damping force versus piston speed lines.

V-2.3 Other Components

To reduce vibrations and the resulting road-noise, rubber mounts and bushes are used at all points of connection between the suspension and the vehicle body, Fig. V-6. Further mechanical members (arms and rods) which will locate the road wheels and stabilizing members (such as anti-roll bars) to modify suspension behavior are other components of a suspension system.

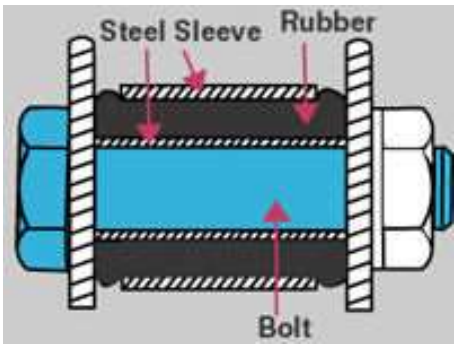


Figure V-6. Rubber bushing

Some vehicles have their suspension systems indirectly connected to the body through sub-frame assemblies which enable simplified line assembly, adjustment, and repair work and which provide better vibration isolation resulting in less road noise, Figure V-7.

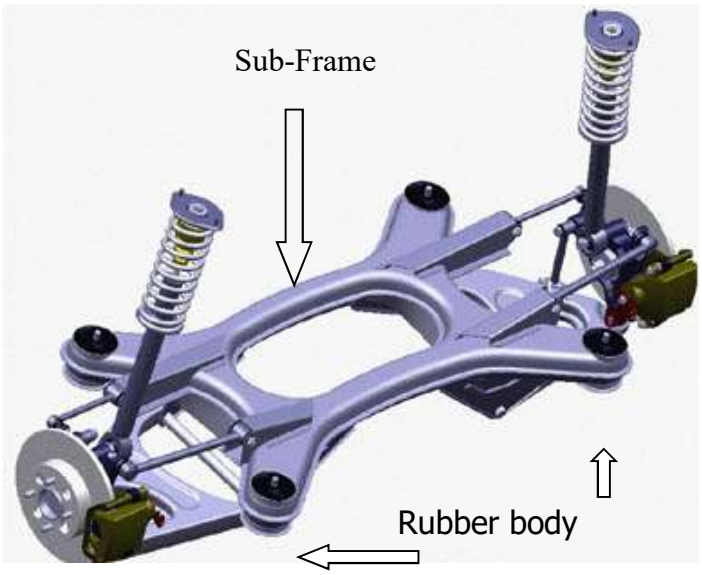


Figure V-7. Subframe

V-3. Suspension Geometry

For good steering control and for minimum tire and parts wear, the front wheels must be aligned. The factors that define suspension geometry include camber, caster, steering axis inclination, scrub radius, toe-in, and toe-out.

Camber Angle

Camber is the angle between the central plane of symmetry of the wheel and the vertical plane at the center of the contact patch, as illustrated in Figure V-8.

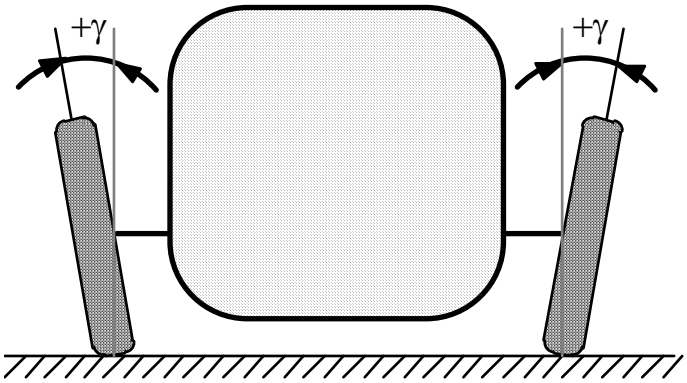


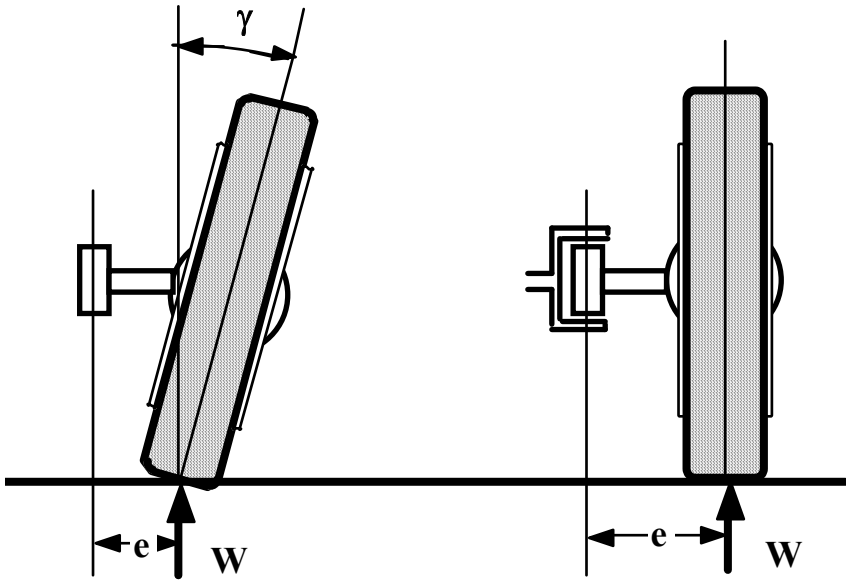
Figure V-8. Camber angle

Camber angle is said to be positive when the wheels are further apart at the top than at the bottom.

The purpose of the camber angle is to align the wheel load with the point of contact of the tire on the road surface. In heavy trucks, a slight amount of positive camber is machined into the axles to compensate for the deflection of the axle beam under load.

The effort to steer a vehicle with the camber arrangement shown in Figure V-9(a) would be less than that necessary with the arrangement shown in Figure V-9(b). Another important reason for camber is that a greater portion of the load is supported closer to the inner end of the wheel spindle; consequently, the arrangement in Figure V-9(a) results in a smaller bending moment in the wheel spindle than the case of Figure V-9(b).

It should be noted that camber is a tire wearing angle, i.e., incorrect camber will result in premature tire wear. Excessive camber creates a diameter variation across the tire contact patch. The smallest diameter slips and slides to equal speed of the largest diameter, resulting in undue wear on one side of the tire. Excessive camber causes damages to the kingpin and its bushes as well as wheel bearings.



(a) (b)

Figure V-9. Effect of camber angle

In the past, considerable positive camber was used to decrease cornering power at the front axle to reduce oversteer tendency (or impart understeer tendency). In modern passenger cars, the camber angles have been reduced to below 1º (Typically 0º to 0.25º for independent suspensions and 0.75º to 1.25º for beam axles). It must be noted that when a wheel is steered, its camber angle will change, and this change will be controlled by front suspension geometry. It is possible, therefore, to design the desired camber change characteristics by a proper choice of front suspension geometric parameters. Negative front wheel camber, for example, is used in some recent sports cars to improve cornering ability.

Caster Angle

The caster angle is the angle between the pivot pin (in a solid axle) or the spindle support (in an independent suspension) and the vertical to the road surface in side view, as illustrated in Figure V-10 for the case of positive caster. Positive caster results in a caster offset in front of the contact patch center. Note that caster is not a tire-wearing angle.

The purpose of caster is to keep the front wheels of an automobile in a straight-ahead position. Caster will also assist in returning the wheels to a straight-ahead position. This effect is obtained through an additional torque around the center of the tire contact patch when the wheel is steered, as illustrated in Figure V-11.

Negative caster results in poor directional control unless the accompanying steering axis inclination is adequately chosen. Note, however, that a negative caster is usually used for the rear wheel steered vehicles.

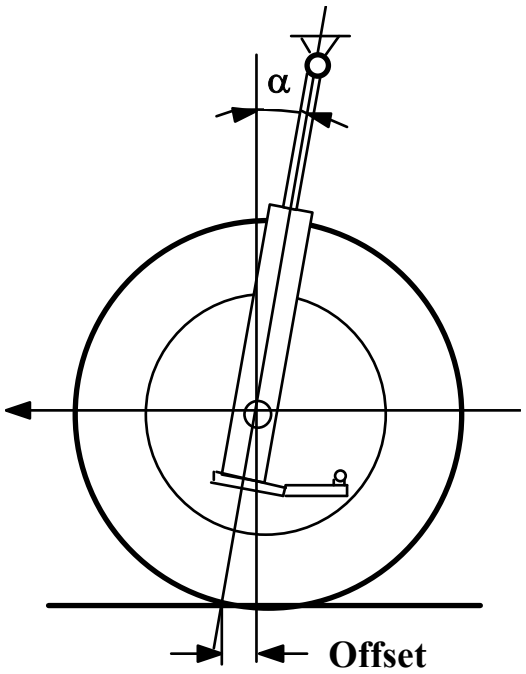


Figure V-10. Caster angle

The amount of caster, depending on the weight of the vehicle, varies between 3 to 6 degrees. For easier steering, a slight caster angle is required.

Caster results in negative camber of the outside wheel during cornering and thus increases cornering force and oversteer tendency.

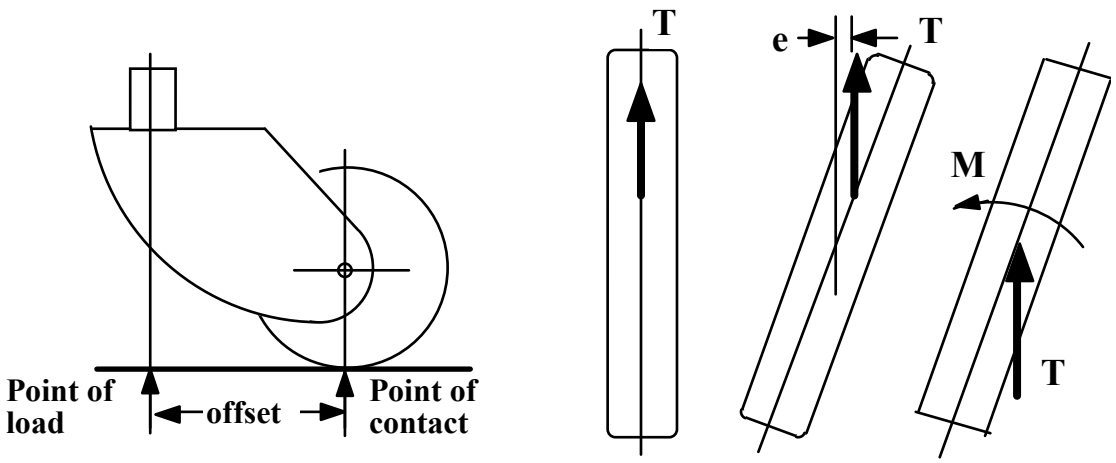


Figure V-11. Caster action

Steering axis inclination

Steering axis inclination is the angle in degrees that the axis of the steering knuckles is tilted towards the vehicle from the vertical, as viewed from the front of the vehicle, shown in Figure V-12. It is fixed during the assembly of the suspension system and is non-adjustable. In some vehicles, a negative offset is used to improve stability during tire blowout on one wheel.

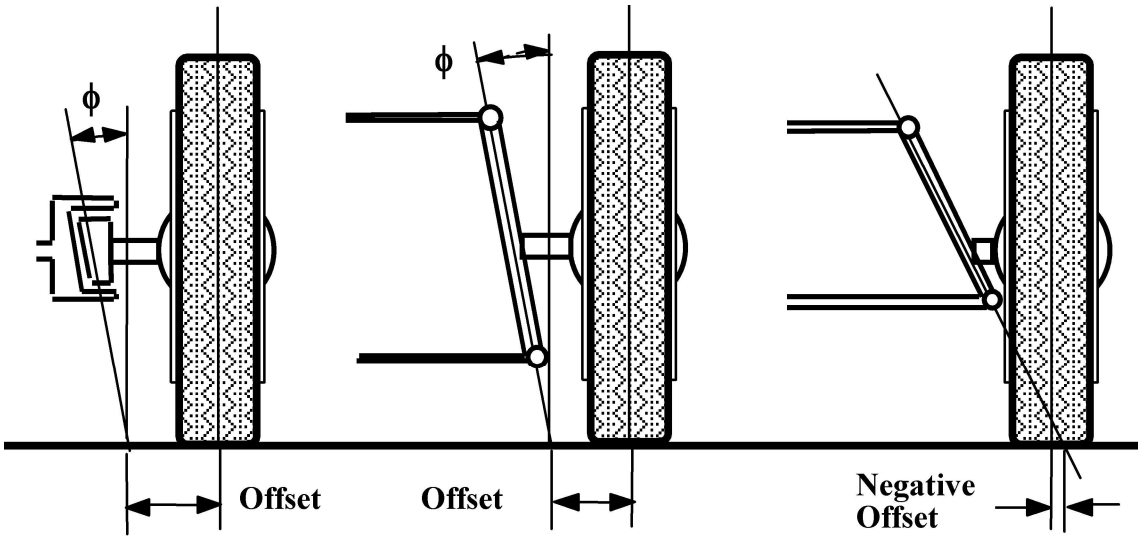


Figure V-12. Steering axis inclination

The purpose of the steering axis inclination is the same as that of the camber. In addition, it causes the front end of the vehicle to rise as the wheel is turned. Therefore, a self-aligning torque is produced resulting in better directional stability.

Another effect of the steering axis inclination is to produce positive camber at the outside wheel during cornering. This property can be used for increasing understeer characteristics.

Steering axis inclination is usually about 3 to 7 degrees for passenger cars, the higher values being used for lighter vehicles. For trucks, it is reduced down to zero degrees.

Toe-in and Toe-out

When the distance between the wheels on the same axle is smaller (as measured at axle height) at the front, the difference is called toe-in. Similarly, if the distance between the wheels on the same axle is smaller at the rear, the difference is called toe-out.

Toe-out is usually produced during straight-ahead driving due to the elasticity and clearances of the steering linkage, worn parts, etc. and during cornering - the inner and outer wheels are steered at different angles. Further, because of the presence of camber angle, the

axis of the wheel, when extended, will intersect the road at some point. The wheel tends to rotate like a cone about this point. Hence, there is a natural tendency for the tires on the same axle to slip away from each other, Figure V-13. Toe-out will cause tire wear and, in addition, may cause the vehicle to wander as the tires hit road bumps.

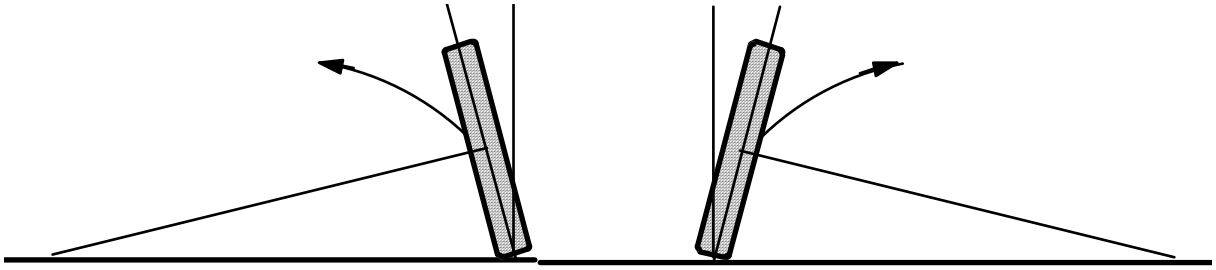


Figure V-13. Toe-out due to camber

The toe-in is, therefore, given to the wheels to cancel the effects of toe-out. Toe-in creates a natural slip angle, i.e., an angle between the wheel plane and the direction of motion. Thus it provides a lateral force to resist side loads from the road surface. Further, it is useful in eliminating the flutter of the steering wheel known as "shimmy". Too much of toe-in, however, results in excessive tire wear and high rolling resistance.

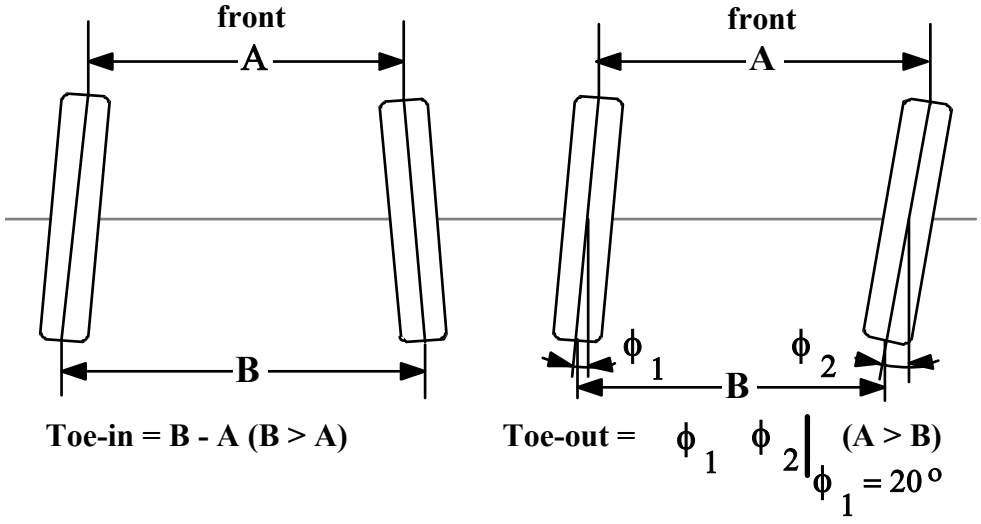


Figure V-14. Toe-in and toe-out

It should be noted that toe-in is specified by the distance between the wheels on the same axle (as measured at axle height) at the front and at the back. Toe-out, on the other hand, is specified by the angle difference between the right and left wheels as illustrated in Figure V-14.

V-4. Types of Vehicle Suspensions

Vehicle suspensions may be classified into two broad groups:

i) Rigid axle suspensions,
ii) Independent wheel suspensions.

Each group may further be classified as front or rear suspensions.

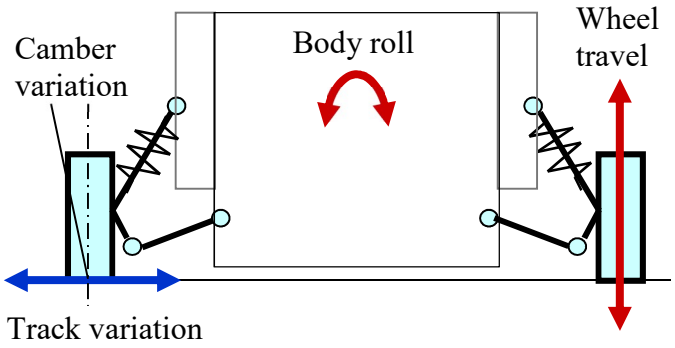
In assessing the design of an existing or proposed suspension, it would be good practice to examine carefully the components providing the location of the wheel by restraining its motion in the three directions, namely the vertical, lateral, and longitudinal directions.

In evaluating the quality of a suspension system and its suitability for a particular vehicle, it is customary to examine

a) camber angle, and
b) track variation

with

a) wheel travel, and
b) body roll



in detail, together with a number of other factors. Variation of camber angle will affect the handling behavior of the vehicle and thus should be in accordance with the handling requirements. Track variation, on the other hand, is undesirable as it will degrade both directional control and stability and ride comfort.

Further considerations with respect to ride comfort require the minimization of unsprung mass. In vehicle dynamics terminology, the mass of the vehicle, which is supported by the suspension springs, is called the sprung mass, and the part below the suspension springs is called the unsprung mass, Figure V-15.

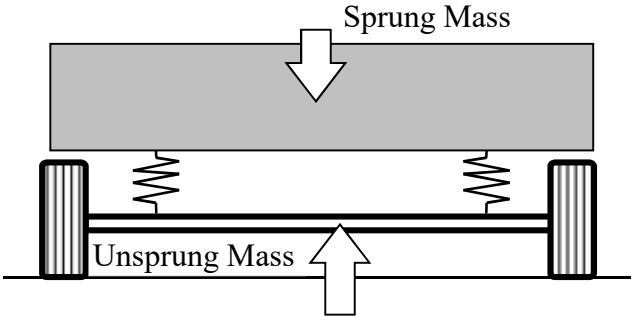


Figure V-15. Camber and track variation with body roll and wheel travel

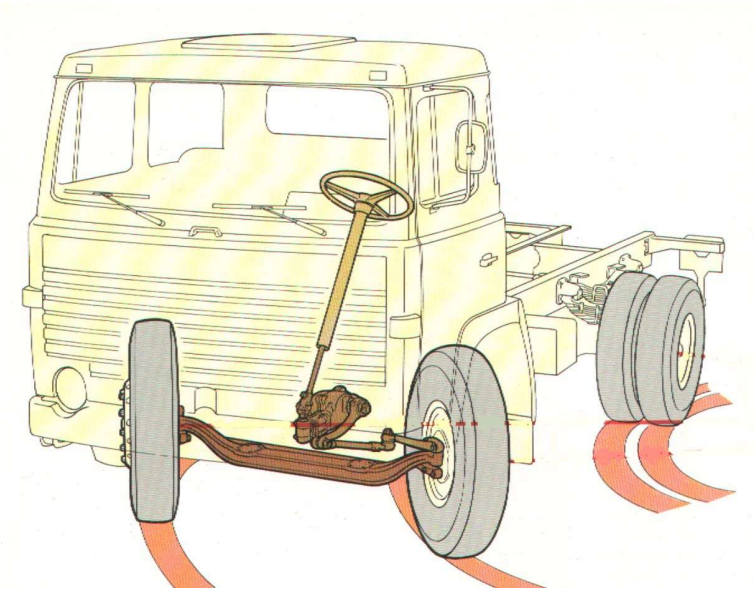
V-4.1 Rigid (Beam) Axle Suspensions

In the rigid axle arrangement, the left and right wheels are connected by a rigid axle such that the movement of one wheel will affect the other.

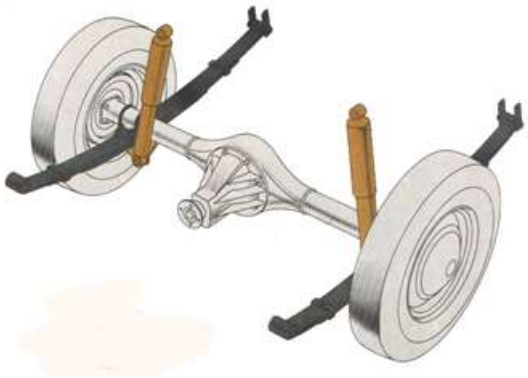
There are two basic types of rigid axles:

i) *Dead axle* : consists of a solid rigid beam and is used for the front suspension of RWD or the rear suspension of FWD vehicles, Figure V-16 (a). Therefore, the wheels on dead axles are not driven. Practically all heavy commercial vehicles are equipped with dead beam axles at the front.

ii) *Live axle* : is used for the driven wheels, and therefore carries the differential, in the basic design, Figure V-16 (b). Hence, it is mainly used for the rear suspensions in RWD vehicles. It should be noted that 4WD vehicles are equipped with live axles both at the front and rear.



(a)



(b)

Figure V-16. (a) Dead axle, (b) Live axle

In both types of rigid axles, the rise of one wheel, i.e. suspension travel, causes both wheels to have a camber change. Further, a change in the track will accompany camber change as illustrated in Figure V-17. The camber change due to body roll, on the other hand, is zero with rigid axles.

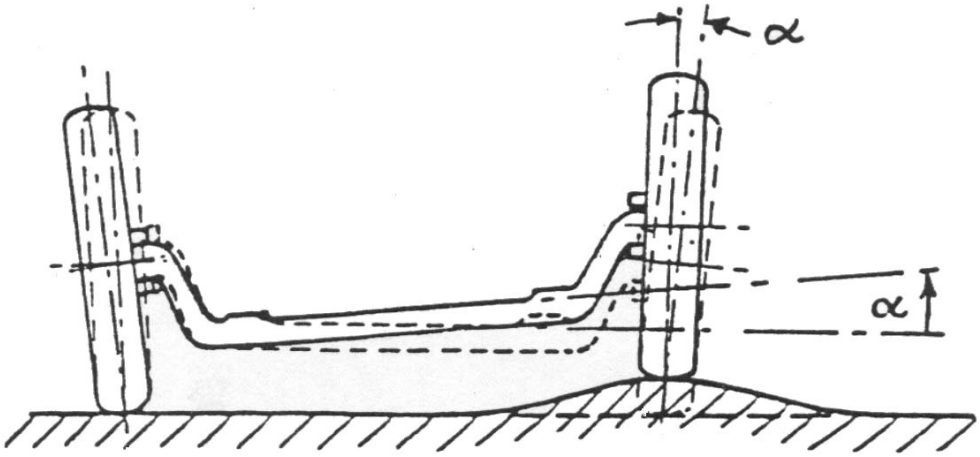


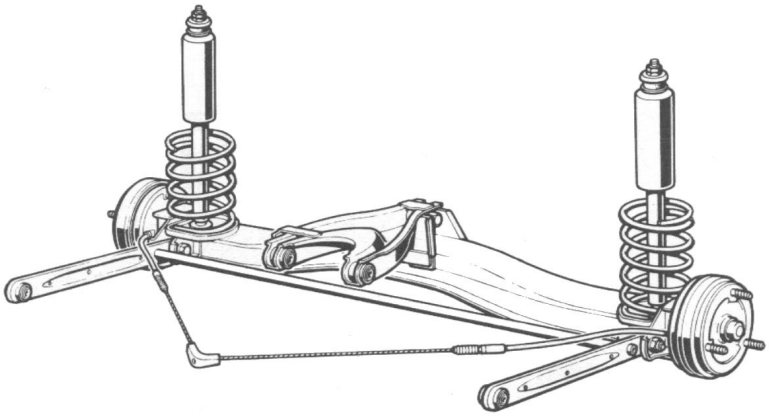
Figure V-17 Rigid axle - camber variation with suspension travel

Dead Axle Suspensions

This type of suspension is basically used at the front of commercial vehicles. The simplest type consists of a rigid beam axle and leaf springs which locate the axle vertically, longitudinally, and laterally similar to those of the live axle shown in Figure V-16 (b).

In its basic form, dead axle suspension is also used as the rear suspension for FWD cars. However, since the leaf springs have to locate the axle in three directions, the location is not precise. Particularly, when coil springs are used instead of leaf springs, the axle has to be located in the longitudinal and lateral direction by other means. Most common configurations use longitudinal arms and either an A-bracket, lateral arms, or a Panhard rod for the lateral location as illustrated in Figure V-18(a), (b), and (c). Panhard rod may be arranged either transversely or diagonally, and for proper operation must be as long as possible.

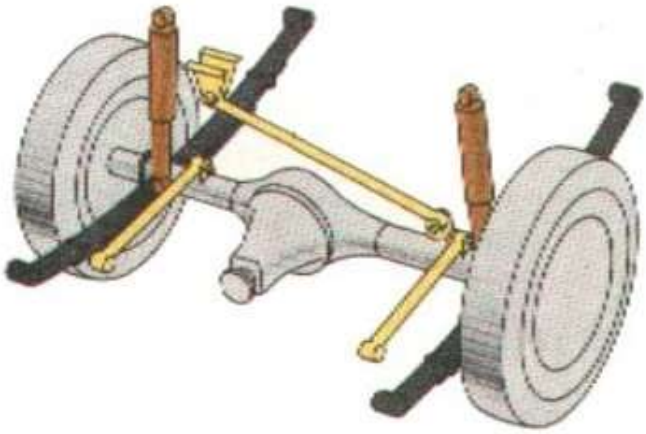
a) Longitudinal arms and A-bracket

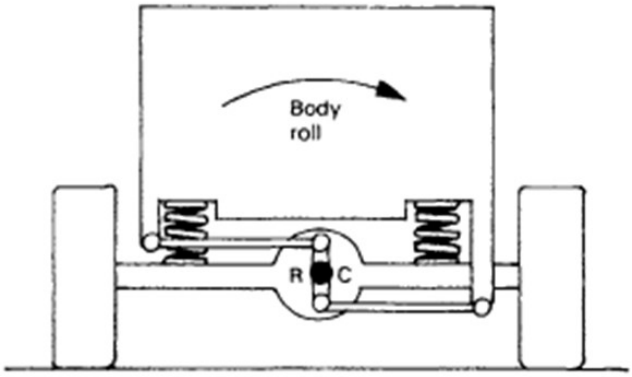


b) Longitudinal and diagonal arms



c) Longitudinal arms and Panhard rod





d) Watt's linkage

Figure V-18. Longitudinal and lateral location of the rigid axle

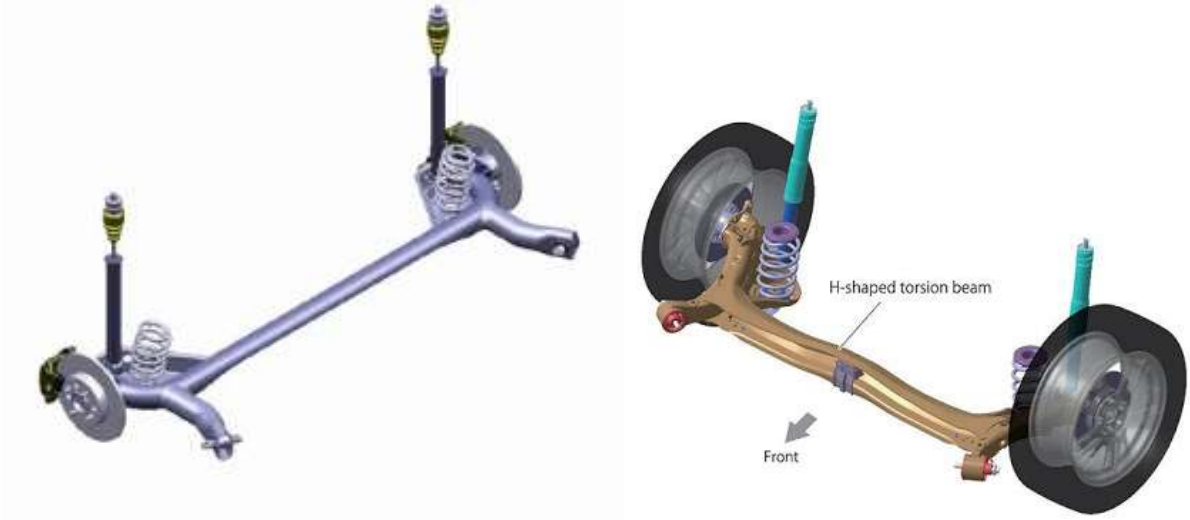


Figure V-19. Twist (torsion) beam rear suspensions

Another dead axle configuration, illustrated in Figure V-19, has recently become popular and consists of longitudinal arms rigidly connected to the axle. Unequal deflections of the wheels are obtained by the torsion of the axle. At one extreme, if the axle is between the wheels, a rigid axle suspension will be obtained. At the other extreme, if the axle is closer to the body, an almost independent suspension will result, Figure V-20. In most designs, the axle is placed at some intermediate position between the wheels and the body. For the lateral location, a Panhard rod is usually added to the system. This system represents an intermediate step between dependent and independent suspensions.

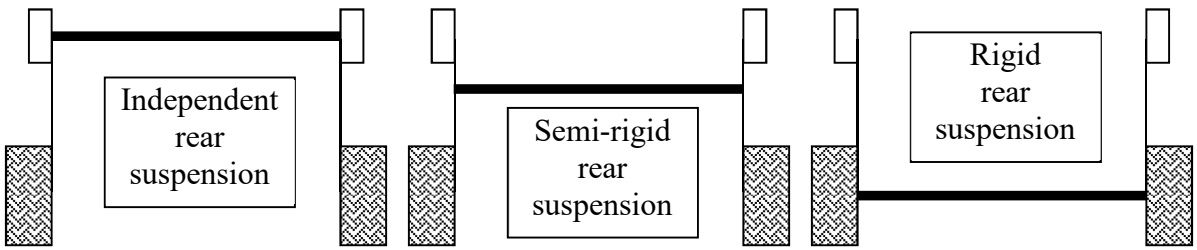


Figure V-20. Twist (torsion) beam rear suspension – rigid to independent

Live Rear Axles

The wheels on a live axle are driven. Thus it houses shafts that drive the wheels, while the wheels on the dead axles rotate freely.

The connections between a live axle and the body must be capable of dealing with four separate actions, namely:

i) weight of the body,
ii) torque reaction,
iii) driving or braking forces,
iv) lateral forces.

The torque reaction and the driving forces are the extra loads introduced in the case of live axles and which do not act on the dead axles.

A live axle carrying the differential and the drive shafts results in an excessively large unsprung mass and, therefore, is common in commercial vehicles. In cars, they are used only when low cost is the top priority. One way of using a dead axle for the driven wheels to reduce unsprung mass is to use the de Dion axle. Here, the differential is mounted on the chassis and not on the axle, as illustrated in Figure V-21.

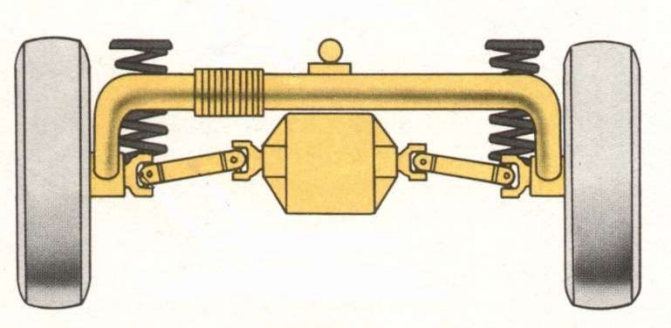


Figure V-21. De Dion axle

V-4.2 Independent Wheel Suspensions

In independent suspensions, the configuration is such that the movement of one wheel has no direct effect on the other wheels. The types of independent suspensions for front and rear wheels will be examined separately.

Front Wheel Suspensions

Today two types of independent suspension systems have superseded all other types, namely the MacPherson strut and the double-wishbone type of front suspension systems.

The MacPherson strut, shown and illustrated in Figures V-22 and 23, is very popular because it is mechanically simple, requires very little lateral space, its unsprung mass is small, and its up-and-down motion causes very little camber change. The location of the wheel is controlled in the vertical direction by the strut, which consists of a damper and a coil spring mounted coaxially. The strut is either integral with or rigidly connected to the wheel hub. The lateral motion of the wheel is restrained by the track control arm which is connected to the wheel hub by a spherical joint at one end and pivoted to the body at the other end. The longitudinal location of the wheel can be controlled by a number of different configurations. One alternative is to have a wishbone-shaped track control arm connecting to the body at two points. Another choice is the use of an independent bar positioned at an angle to the track control arm. Recent designs employ the anti-roll bar for the same purpose as can be seen in Fig. V-23.

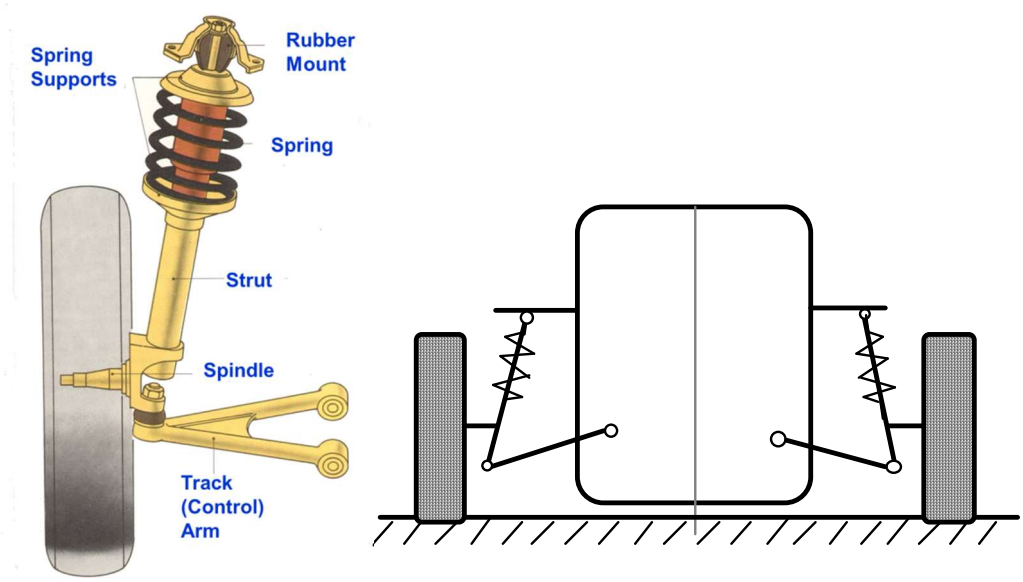


Figure V-22 MacPherson strut suspension – illustration

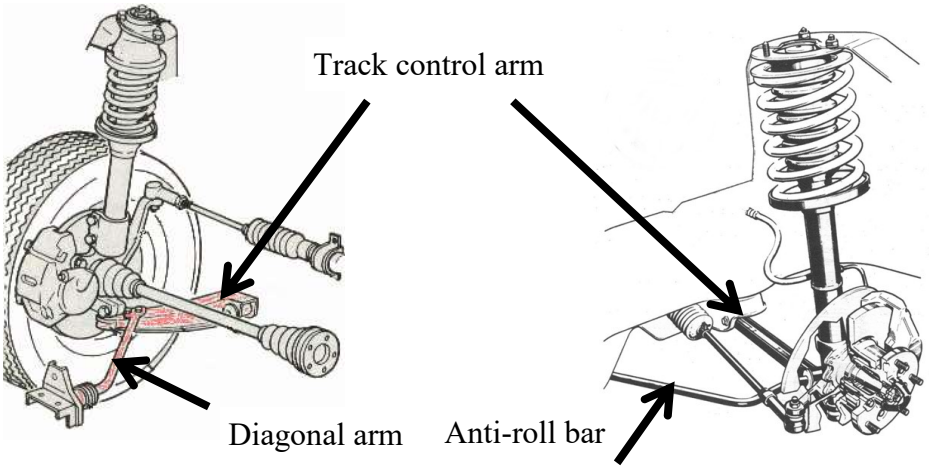


Figure V-23. MacPherson strut suspension-variations

MacPherson strut type of suspension has some disadvantages. It requires considerable space in the vertical direction which conflicts with the trend of lower vehicle lines. Further, lateral loads on the strut increase damper friction resulting in reduced ride comfort, as illustrated in Fig. V-24. The second disadvantage can be overcome by

a) adjusting the geometry of the strut, wheel, and the track arm, Fig. V-24, or

b) inclining the spring axis relative to the damper axis, V-25 (a).

As illustrated in Figure V-24, the inclination of the strut should be such that its axis, the effective axis of the track control arm, and the line of action of the wheel load intersect at a single point. This eliminates the bending moment on the strut, reducing the sliding friction between the piston and the cylinder of the damper. This requirement, however, introduces severe limits on the design possibilities for better performance.

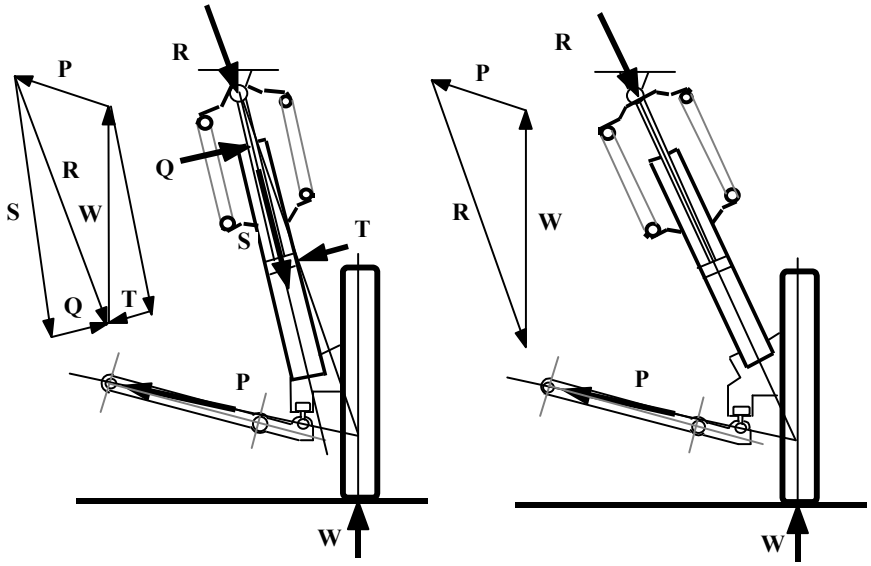


Figure V-24 Force diagrams for MacPherson strut suspension designs

The most recent application is the use of the so-called side force spring. A side force spring creates a side force when deformed due to its curved centerline (S-shaped median line in unloaded condition), or varying diameter and/or pitch, Figure V-25. This side force acts to cancel the lateral force on the damper.

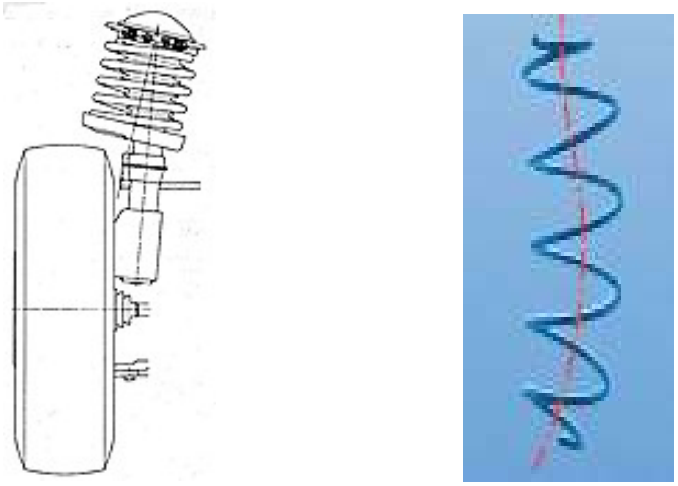
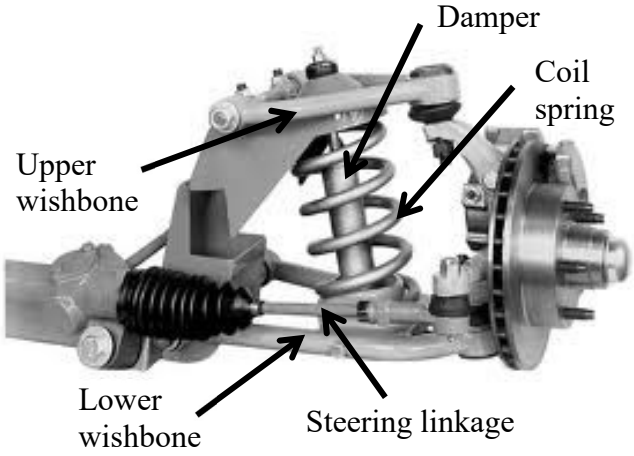
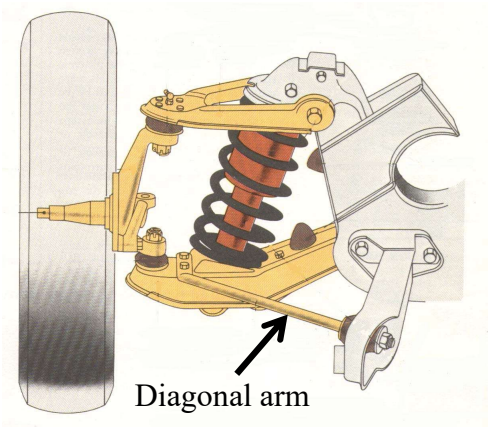
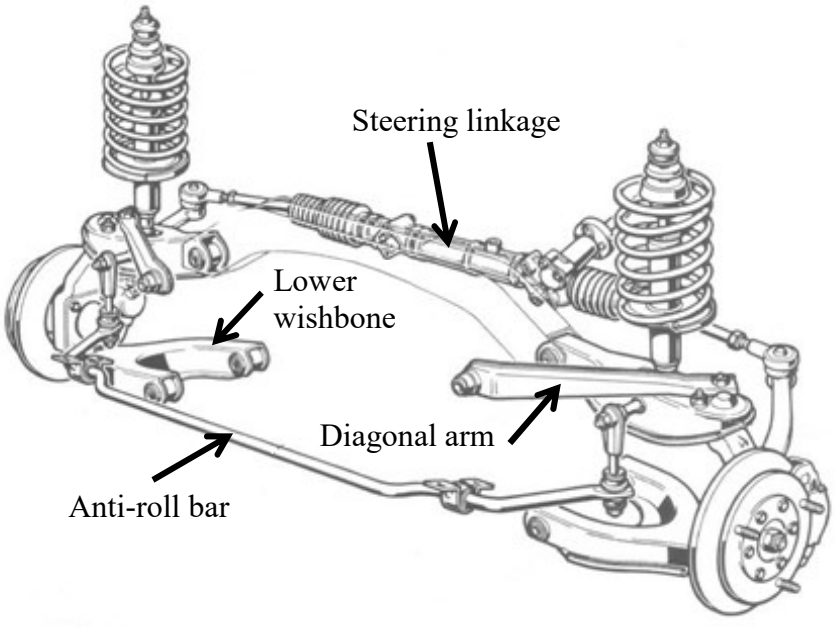


Figure V-25 Inclined and side force spring

The double wishbone suspension, shown and illustrated in Figure V-26, can have specific variations. The coil spring and the damper need not be coaxial and they may be placed on either the lower or upper wishbone. Further, the wishbones may or may not be equal or parallel.







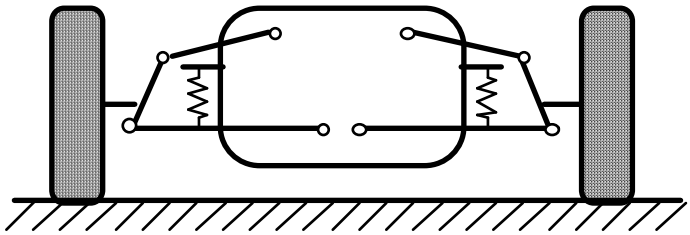
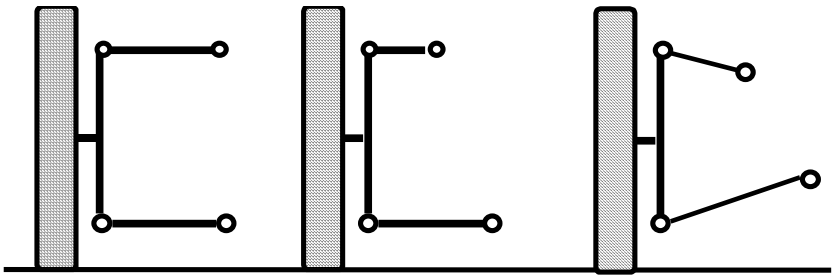


Figure V-26. Double wishbone suspensions - illustration

If the wishbones are *parallel and equal* in length, Figure V-27 (a), the camber change will equal the body roll angle. Thus the outer wheel assumes positive camber during cornering, which reduces the cornering power, i.e., built-in understeer tendency. The wheel also moves over bumps without any camber change, but the track will change affecting linear stability by introducing lateral forces and impairing ride comfort as well. Because of these disadvantages, the equal-parallel wishbone suspension is not used in modern vehicles.

The double wishbone suspension can be improved by shortening the upper wishbone, in which case constant track can be obtained introducing, however, a camber change, Figure V-27 (b). In addition, camber change due to body roll during cornering is reduced.

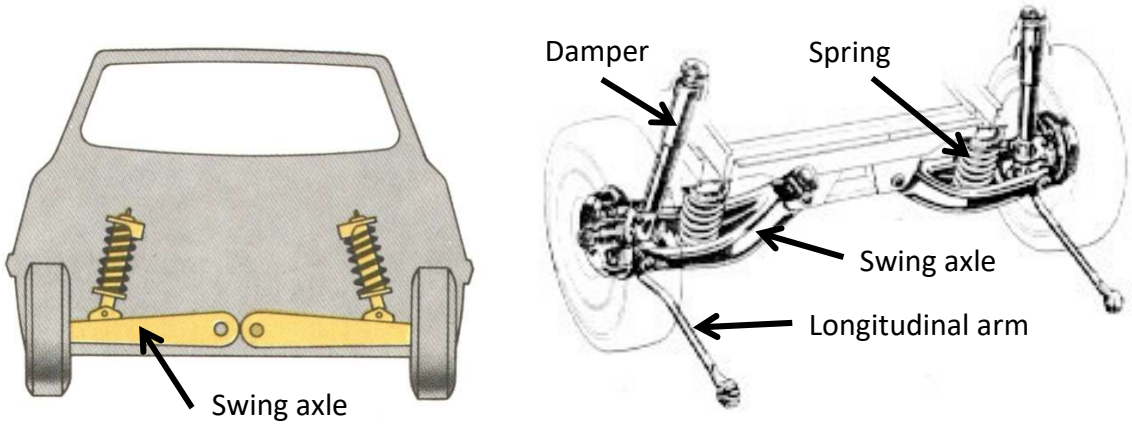
A further refinement is the non-parallel, unequal-length wishbone suspension system illustrated in Figure V-27 (c). It is then possible, by proper design, to keep the outside wheel virtually upright irrespective of the body roll and a relatively constant track can be maintained at least for a limited range of suspension motion.



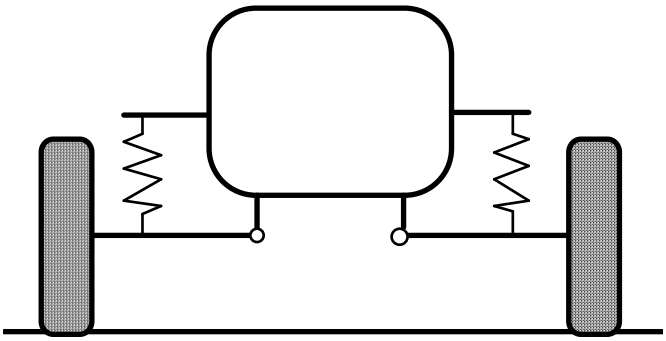
a) Parallel and equal, b) Parallel and unequal, c) Nonparallel and unequal

Figure V-27. Double wishbone suspension designs

The third type of independent suspension, sometimes used in small commercial vehicles, shown in Figure V-28 (a) and illustrated in Figure V-28 (b), is called the swing axle suspension. The wheel and its half-axle form a rigid assembly pivoted near the middle of the car.



(a)



(b)

Figure V-28. Swing axle suspension - illustration

It is clear that with this kind of suspension, wheel travel results in considerable camber change due to a relatively short swing radius. Track variation during suspension travel and body roll is also excessive.

In addition, upon hard cornering, the swing axle tends to lift the vehicle such that the outer wheel which is generating the higher cornering force is "tuck under" the body. Thus the vehicle body is “jacked up”, and the rollover resistance of the vehicle is reduced. When coupled with the effects of excessive camber change, inconsistent cornering performance results. Therefore, the swing axle is used in low-cost, low-performance vehicles. The so-called "jacking" effect is illustrated in Figure V-29.

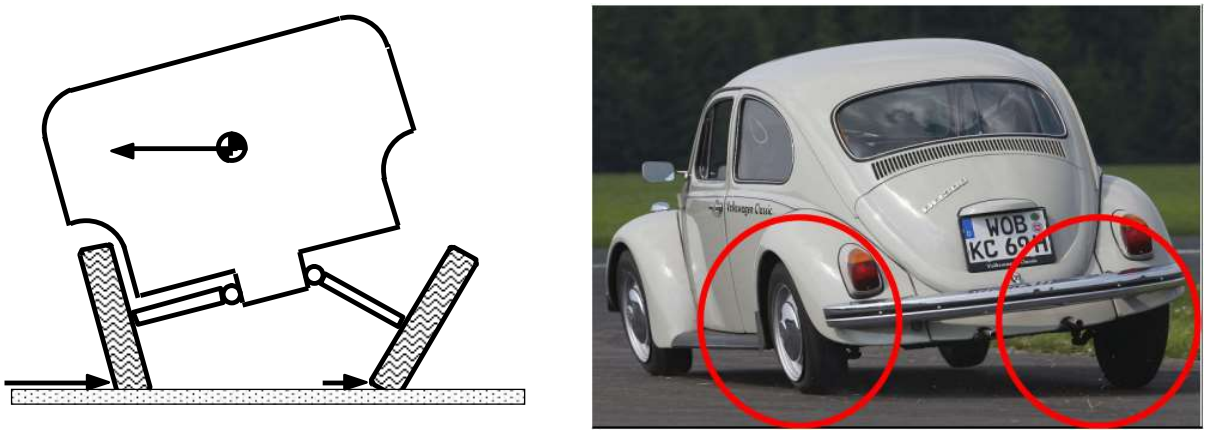


Figure V-29. Jacking effect

Recently, multi-link suspensions are used on high-performance vehicles. They closely resemble the double wishbone suspension. On the double wishbone design, the upper and lower wishbones are attached to the wheel hub by spherical joints on the steering (kingpin) axis. The five-link suspension, for example, has four separate links corresponding to the two wishbones and the tie rod becomes the fifth link, Figure V-30. It does not have a physically defined steering axis; the steering axis is a virtual, instantaneous, and movable one.

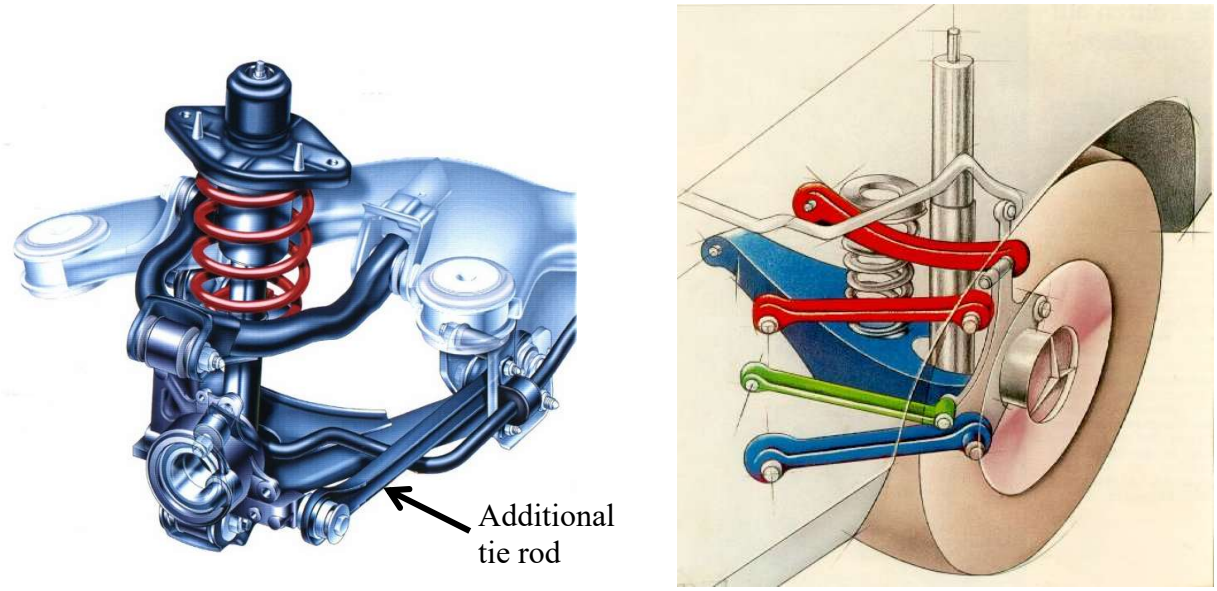


Figure V-30. Five-link suspensions

Rear Wheel Suspensions

Most common independent rear wheel suspensions are:

i) Trailing arm,
ii) Semi-trailing arm,
iii) Double wishbone or MacPherson strut suspensions.

In *trailing arm suspension*, illustrated in Figure V-31, each wheel is connected to an arm pivoted at two points to the vehicle body. The spring and damper are mounted between the arm and the body. The arm pivots are at right angles to the longitudinal axis of the vehicle, resulting in an axis of rotation parallel to the lateral axis of the vehicle. Thus the wheel can go over bumps without any camber or toe change due to suspension travel. The differential is mounted on the body. Compared with the rigid beam axle, the unsprung mass is much less in trailing arm suspensions.

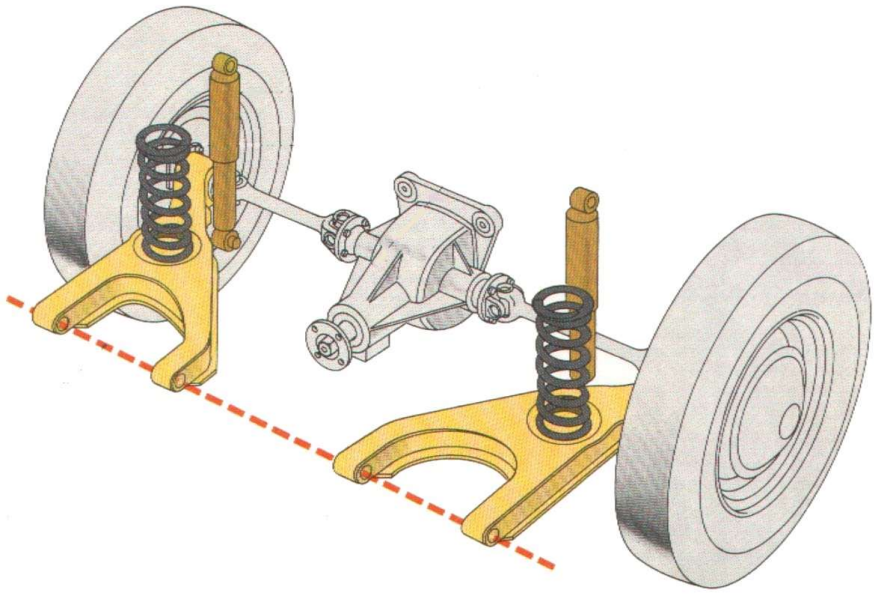


Figure V-31. Trailing arm suspension

The trailing arm suspension is excellent with respect to directional stability and comfort because of smaller toe and camber variation. It is less favorable, however, if cornering behavior and the limits of cornering are considered. The reason for this is the high compliance to lateral force resulting in sharply increasing toe at high lateral forces.

Semi-trailing arm suspension differs from trailing arm design in that the axes of rotation of the left and right arms do not coincide as they are not perpendicular to the longitudinal vehicle axis, Figure V-32. With the semi-trailing suspension, the compliance to lateral force is reduced, improving the cornering behavior. The camber angle and toe changes introduced by the intersecting axes of rotation can be used to further control cornering behavior. Examples of semi-trailing arm suspensions are given in Figure V-33.

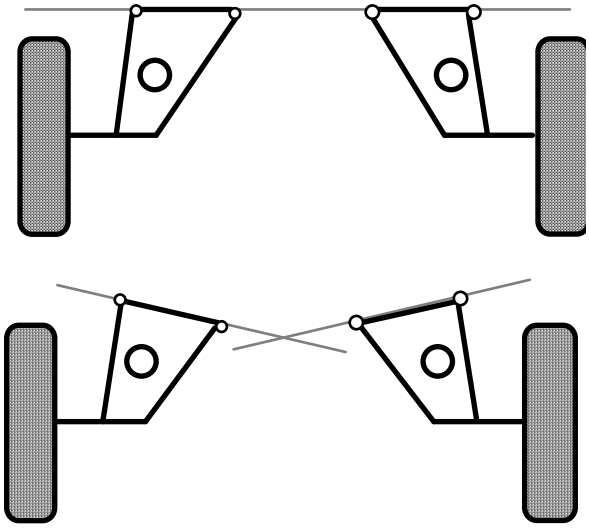


Figure V-32. Trailing arm and semi-trailing arm suspension systems

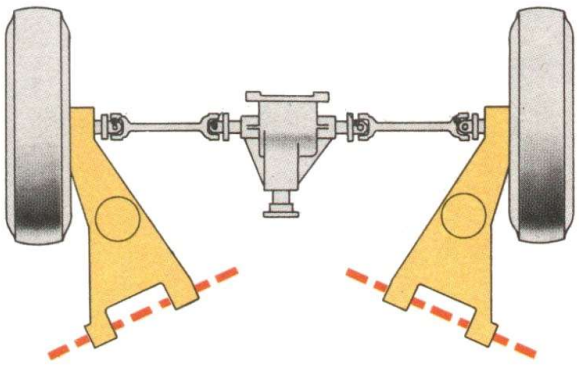


Figure V-33. The semi-trailing arm suspension system

V-4.3 Interconnected Suspensions

As a car is driven along a road, the body can move in a number of ways on its suspension:

i) on corners, it rolls,
ii) if all the wheels strike bumps simultaneously, it bounces,
iii) if the front wheels strike a bump first and the rear wheels hit that bump later, it will pitch - first, the front, and then the rear of the body will rise.

In addition, one wheel alone can hit a bump, in which case, one side of the car pitches, and the vehicle will bounce, pitch and roll. The suspension system must be designed to keep the vehicle under control under all these conditions to provide the passenger with a comfortable ride.

With a conventional system, it has been found that to minimize car pitching, the rear suspension frequency must be slightly higher than the front suspension frequency.

Hydropneumatic suspensions, illustrated in Figure V-34, may be used to reduce pitching oscillations by providing simultaneous front and rear wheel deflections. This is achieved by connecting front and rear suspension units, as shown in Figure V-35. Thus when the front or rear wheels go over a bump, the other end of the vehicle is raised preventing pitching of the body as illustrated in Figure V-36. It is evident that a similar connection between the right and left wheels can be used to control the roll motion of the vehicle.

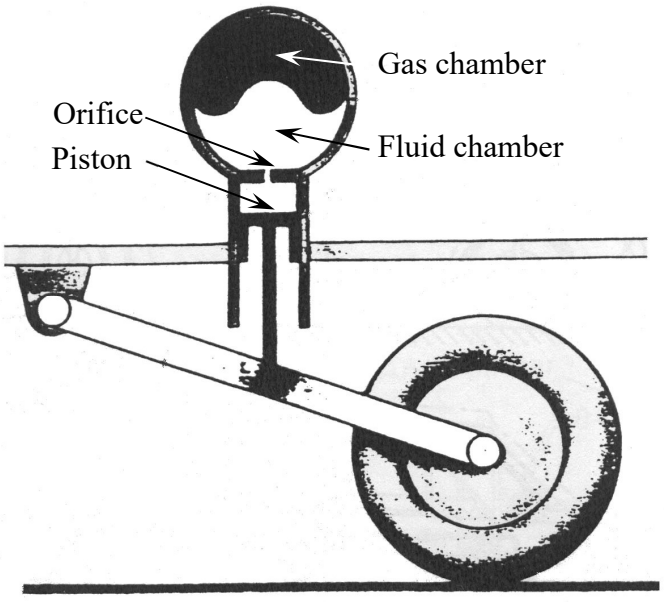


Figure V-34. Hydropneumatic suspension

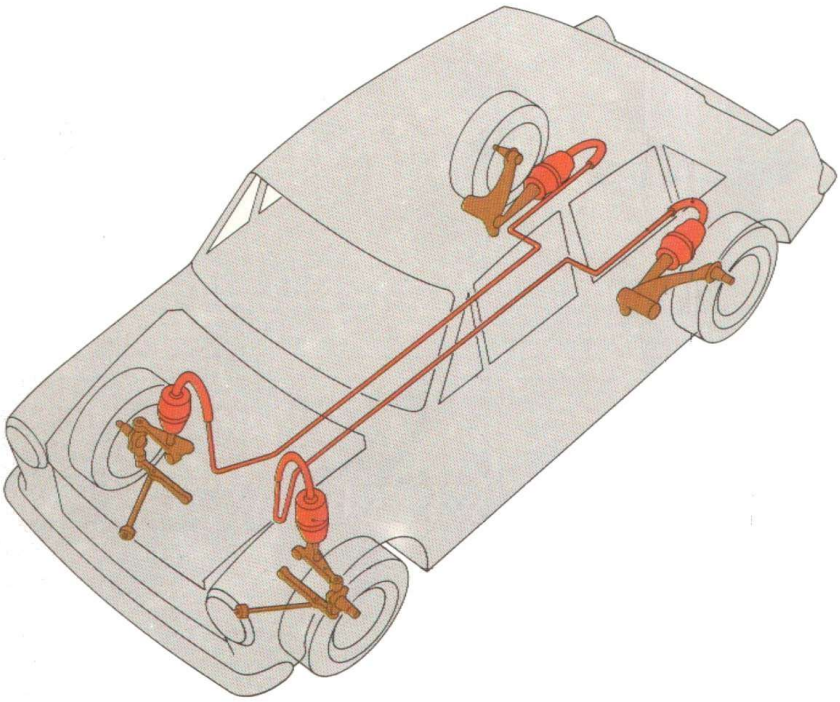


Figure V-35. Interconnected suspension

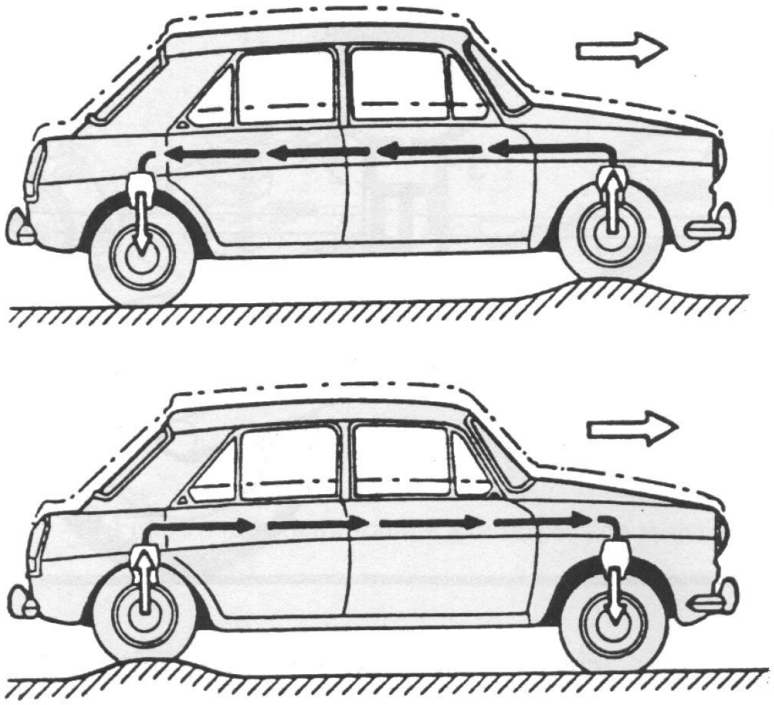


Figure V-36. Interconnected suspension going over bumps

V-5. Anti-Roll Bar

The anti-roll bar connects one side of a suspension with the other and acts in torsion. It is mounted across the vehicle with ends attached to the unsprung mass on each side. It is attached to the body such that it can rotate in rubber bushings, Figure V-37. An anti-roll bar can be fitted to the front suspension, rear suspension, or both. The suspension may be a rigid axle or independent type.

The function of the anti-roll bar is to reduce the roll motion of the vehicle body. During equal vertical wheel travel, the anti-roll bar simply rotates about the bushings at the body attachment points without twisting. Thus the anti-roll bar has no effect on the body bounce motion, front end lift during acceleration or dive during deceleration. If a wheel encounters a bump or hole on one side only, then the bar is subjected to torsion, and resistance to body roll is obtained. If the anti-roll bar is too stiff, then it may act like a beam axle reducing ride comfort.

During cornering, the vehicle body leans outwards under the action of centrifugal force. Thus the inner suspension spring extends while the outer suspension spring is compressed. The bar will be subjected to torsion and it will reduce the body roll, at the same time minimizing the camber changes of the tires due to body roll. Therefore the main effect of the anti-roll bar is the increased roll stiffness. The distribution of this increase in roll stiffness between the front and rear suspensions, in turn, will modify the handling behavior of the vehicle, i.e., the understeer, oversteer, or neutral steer tendency.

The addition of an anti-roll bar to a front or rear suspension originally without one or replacement of the existing one with a stiffer one will increase the slip angle of the tires through redistribution of the load transfer from inside to outside wheels in favor of the front wheels. Thus, an additional anti-roll bar at the front will introduce an understeering tendency, and if added at the back, an oversteering tendency will be obtained.

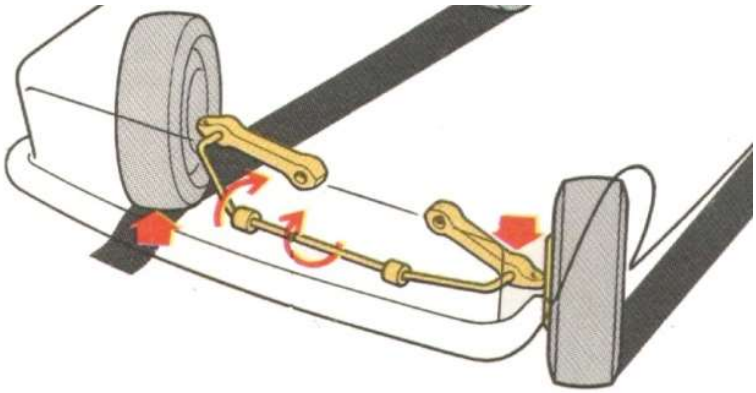


Figure V-37. Anti-roll bar

V-6. Roll Centers and Roll Axis

The roll center is defined as the point in the lateral plane of the front or rear suspension about which the sprung mass of the vehicle rolls under the action of a side force, for example, the centrifugal force during cornering. For a vehicle, there are two roll centers, one for the front suspension and one for the rear suspension. These two roll centers define a roll axis which is then the axis of rotation of the sprung mass under the action of a side force, as illustrated in Figure V-38.

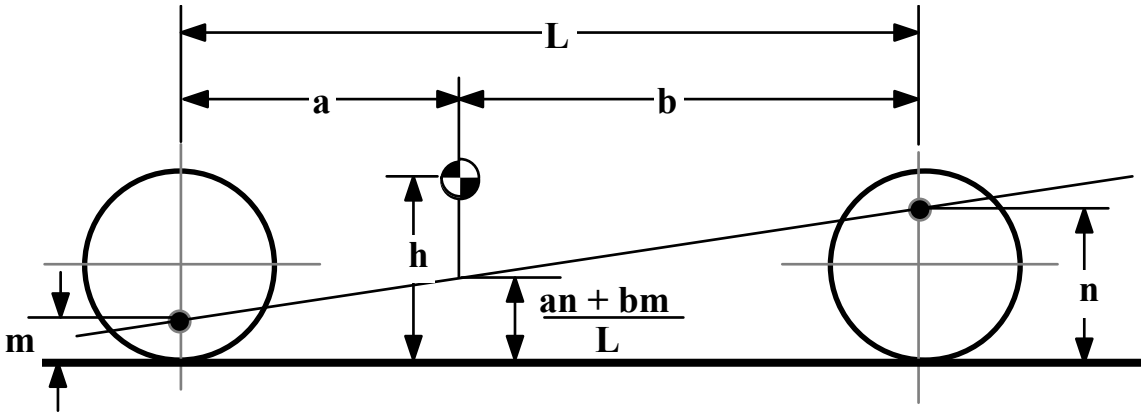


Figure V-38. Roll centers and the roll axis

The roll moment, which causes the vehicle to roll about the roll axis, is given by the product of the centrifugal force and the distance of the center of gravity to the roll axis. Therefore, it is theoretically possible to eliminate roll by locating the center of gravity on the roll axis which requires the roll centers to be high. Usually, the roll angle and the load transfer during cornering will be reduced with high roll centers. An additional benefit of eliminating roll is that the associated camber change of the wheels is also eliminated.

High roll centers have certain disadvantages as well. They result in considerable lateral wheel displacements during bump and rebound with track variations during operation. Low roll centers, on the other hand, reduce lateral wheel displacements at the cost of higher roll angles and larger load transfers during cornering.

The actual heights of the roll centers are, therefore, decided to give the best compromise between the roll angle and lateral wheel deflections. In practice, a certain amount of roll is desirable as it gives the driver an indication of how hard he/she is cornering. In practice, the rear roll center is designed to be slightly higher than the front. This introduces a larger load transfer at the front resulting in an understeering tendency.

For racing cars, the maximum permissible roll angles are specified as 3 to 4º at a lateral acceleration of 0.75 g. For passenger cars, permissible roll angles are of the same magnitude but attained at lower values of lateral acceleration. For example, in the development of Austin Allegro, the primary overriding design parameter was that the roll angle at a lateral acceleration of 0.5 g should be no more than 3 1/2 º. The current trend in passenger car suspension engineering is to use fairly low roll centers together with anti-roll bars to reduce roll.

The roll centers are determined by the relative positions of the suspension linkages. It must be kept in mind that, as a result of suspension deflection during the roll, the positions of the roll centers are also variable. The basic assumption in the roll axis approach is that the roll center locations do not change. In spite of this rather severe assumption, the approach still gives an insight into the dynamic behavior of vehicles.

The graphical determination of the roll center for some commonly used independent suspensions is illustrated in Figures V-39 to V-42. In each case, the vehicle is assumed to be symmetrical with respect to the longitudinal plane and thus, the roll center is always on the vehicle centerline of a lateral section.

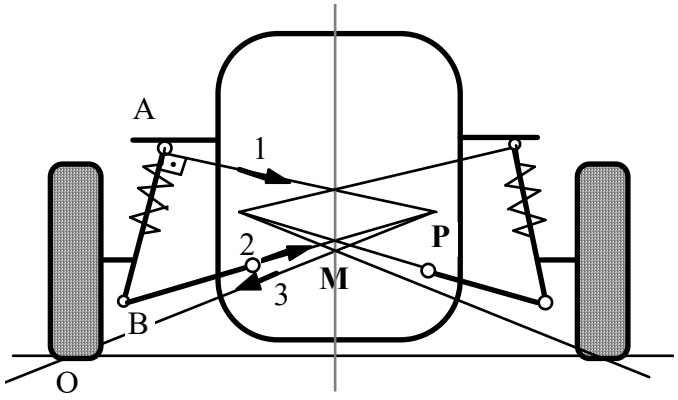


Figure V-39. Determination of roll center for MacPherson strut suspension

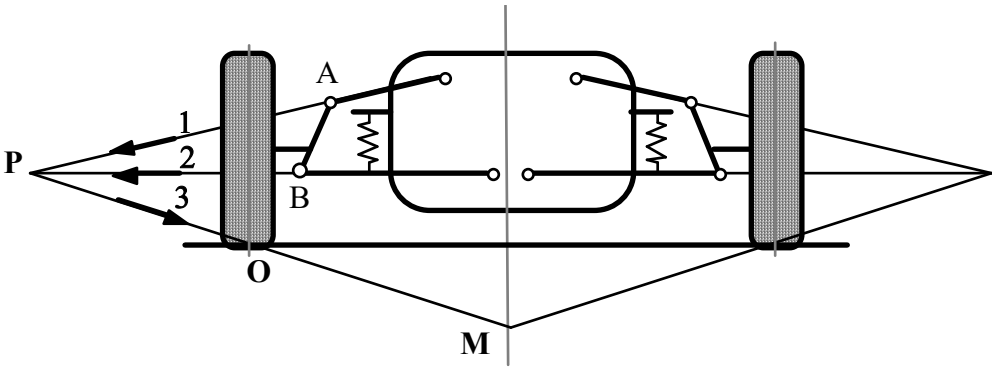


Figure V-40. Determination of roll center for double wishbone suspension

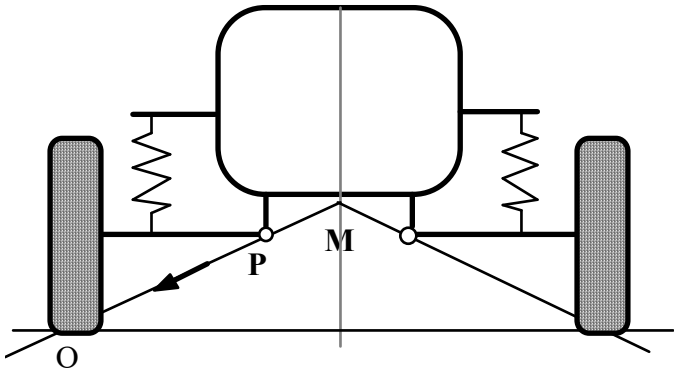


Figure V-41. Determination of roll center for swing axle suspension

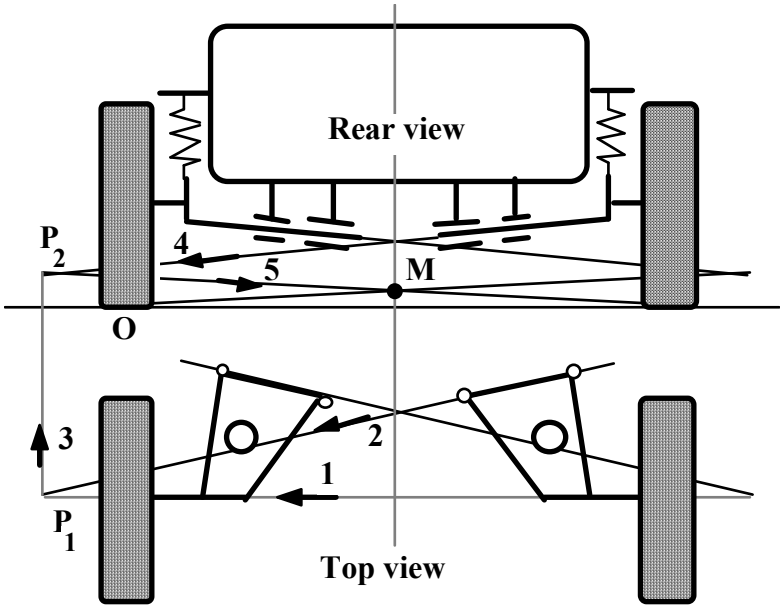


Figure V-42. Determination of roll center for semi-trailing arm suspension

V-7. Kinematic Analysis of Suspension Systems

Vehicle suspension systems are, in general, three-dimensional mechanisms. In the design of suspensions, 5 of the 6 degrees of freedom of a non steering wheel must be constrained. The wheel should have the freedom to move up and down relative to the vehicle's body. A steered wheel will have a second degree of freedom for steering. Thus, using a kinematical model, linear and nonlinear position analyses may be used to obtain critical geometrical factors such as camber, caster, kingpin inclination, track, and toe changes which can be examined for a given configuration of suspension deflection or body roll. It is evident that such a model would be invaluable in the design and comparison of various alternatives.

Commonly used suspension components and the number of degrees of freedom constrained by each link are illustrated in Figure V-43[3].

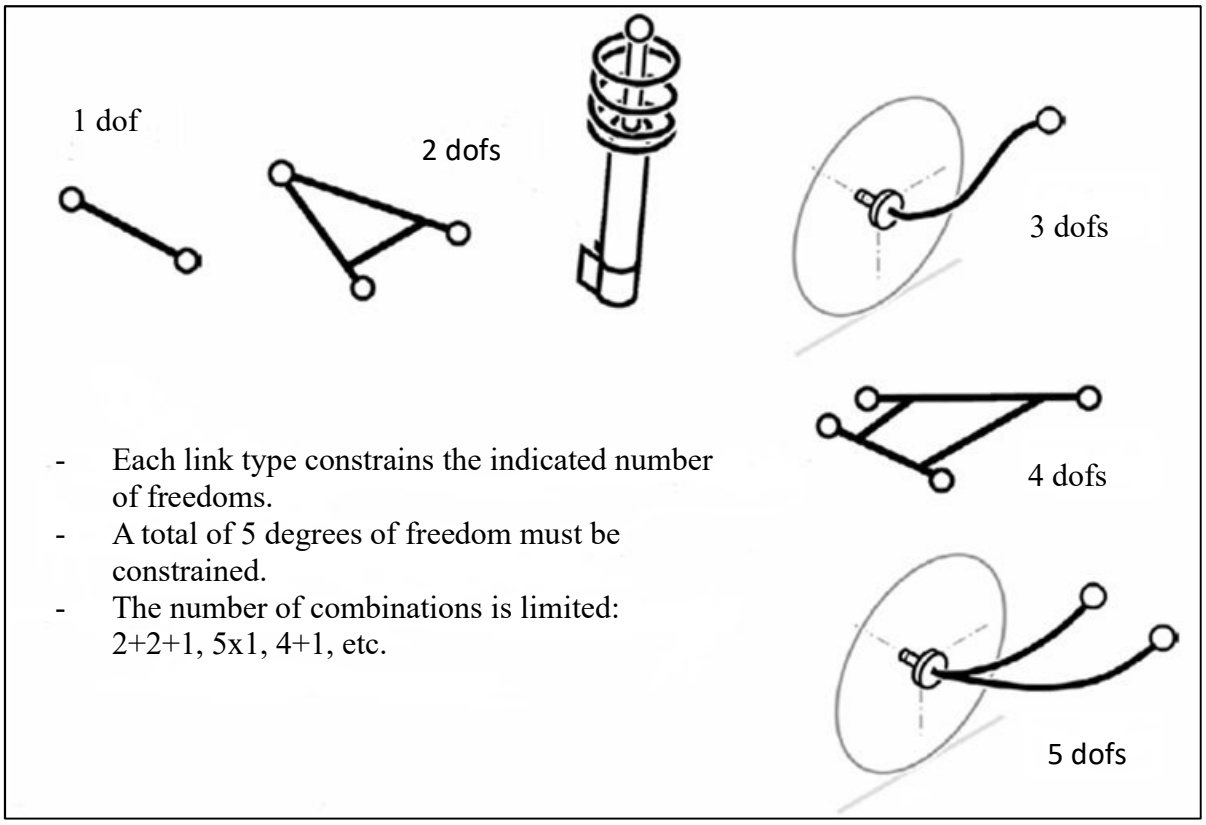


Figure V-43. Commonly used links and the corresponding number of constrained dofs

Construction of the commonly used independent suspensions as combinations of various components is illustrated in Figs. V-44-46.

[3] Gerrard, B., "A New Suspension Architecture For Small Cars". Presented at Open Technology Forum, Vehicle Dynamics Expo, 2005.

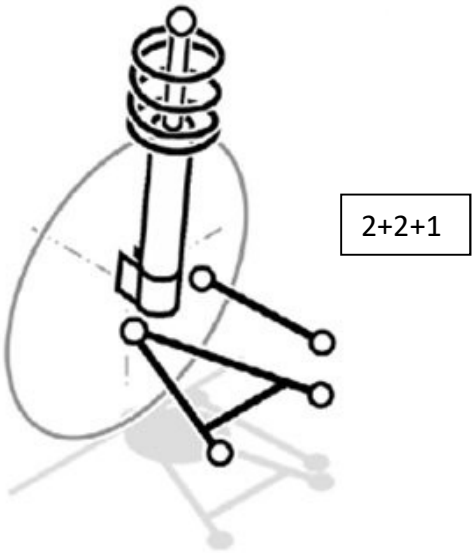


Figure V-44. McPherson strut suspension

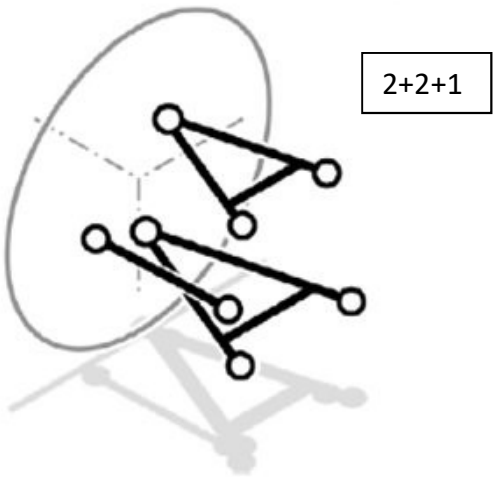


Figure V-45. Double Wishbone suspension

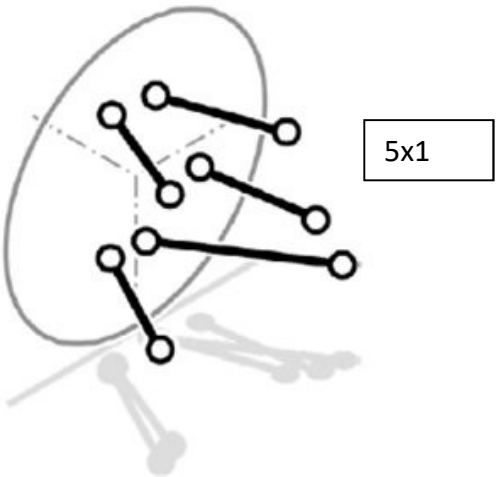


Figure V-46. Multilink suspension

A typical example for a MacPherson strut suspension is given in Figure V-47[4]. In the model, the links identified as 2, 3, 4, and 5 are the track control arm, strut, tie rod, and rack, respectively. Links 2, 4, 5 and the upper and lower portions of the strut are treated as rigid. Joints at B, C, D, and E are spherical. Joints at O_2 and A are revolute. The rack and its case and the upper and lower parts of the strut are sliding pairs.

The model has two degrees of freedom :

1) Wheel displacement involving the relative motion of the upper and lower parts of the strut and the rotation of the track control arm about the axis O_2A.

2) Steering involving the motion of the rack relative to its case, the accompanying motion of the tie rod, and the rotation of the strut about the axis BC.

It is also noted that the tie rod can rotate about the axis DE, but this degree of freedom does not affect the global motion and thus is considered redundant.

Using the data in Table V-1, the camber, caster, kingpin inclination, track, and toe changes with the vertical deflection of the spindle, i.e., point G, have been calculated using both linear and nonlinear position analyses. The results are given in Figs. V-48-50.

Table V-1 Suspension system dimensions

Point	x[mm]	y[mm]	z[mm]
O_2	0	0	0
A	540	-10	-20
B	450	-330	-40
C	460	-180	470
D	560	-300	60
E	570	60	90
G	452	-410	20
H	452	-320	20

[4] Cronin, D. L., "MacPherson Strut Kinematics", Mechanism and Machine Theory, v16 (1981), n6, pp.631-644.

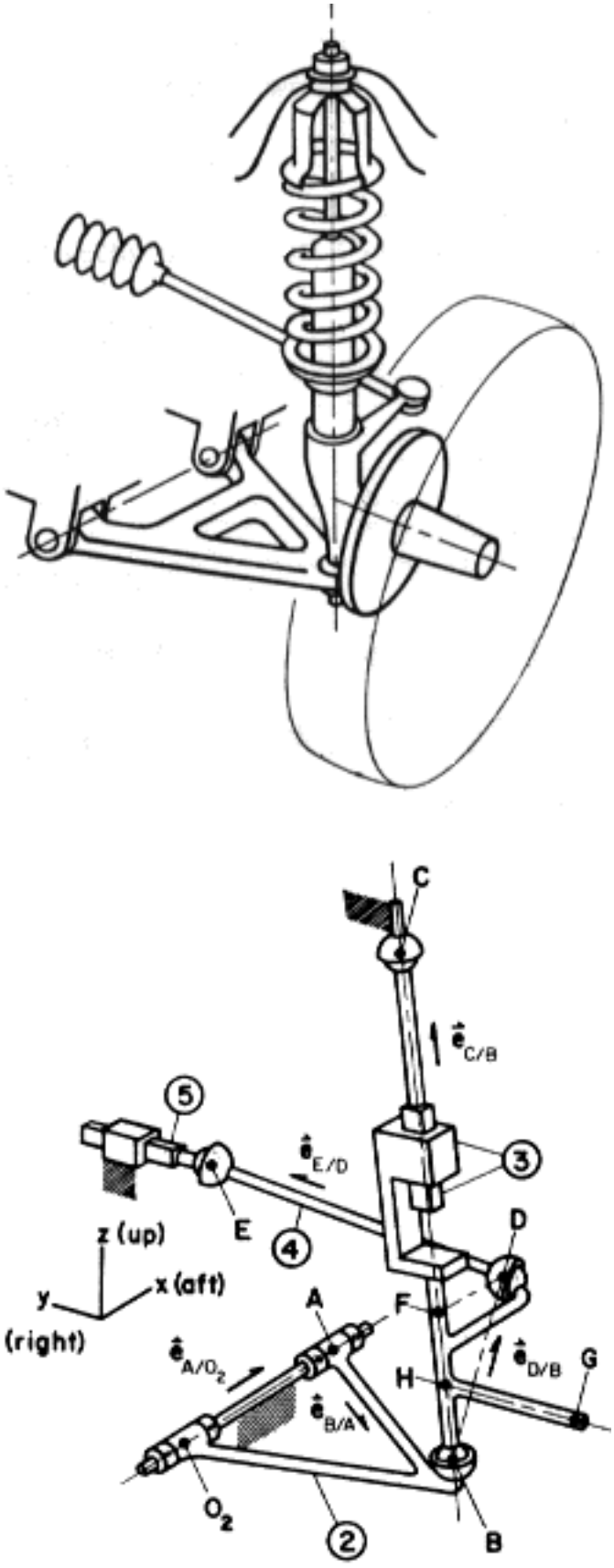


Figure V-47. McPherson strut suspension and its 3-dimensional model

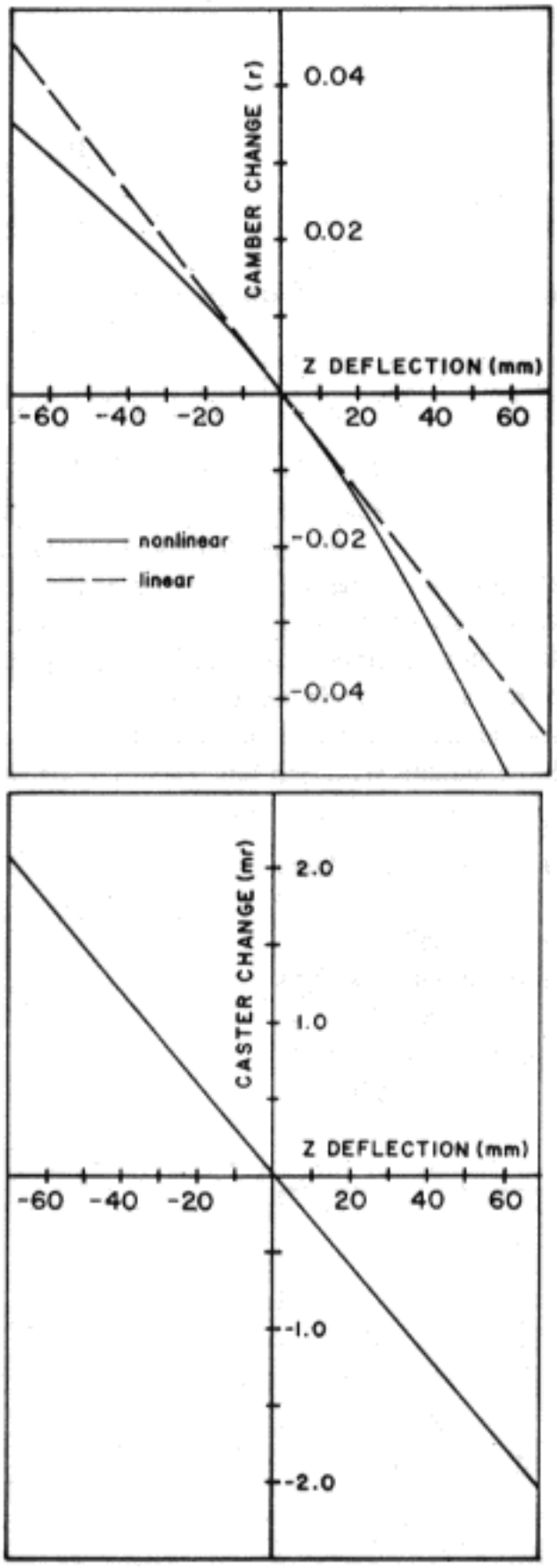


Figure V-48. Camber and caster angle change with wheel travel

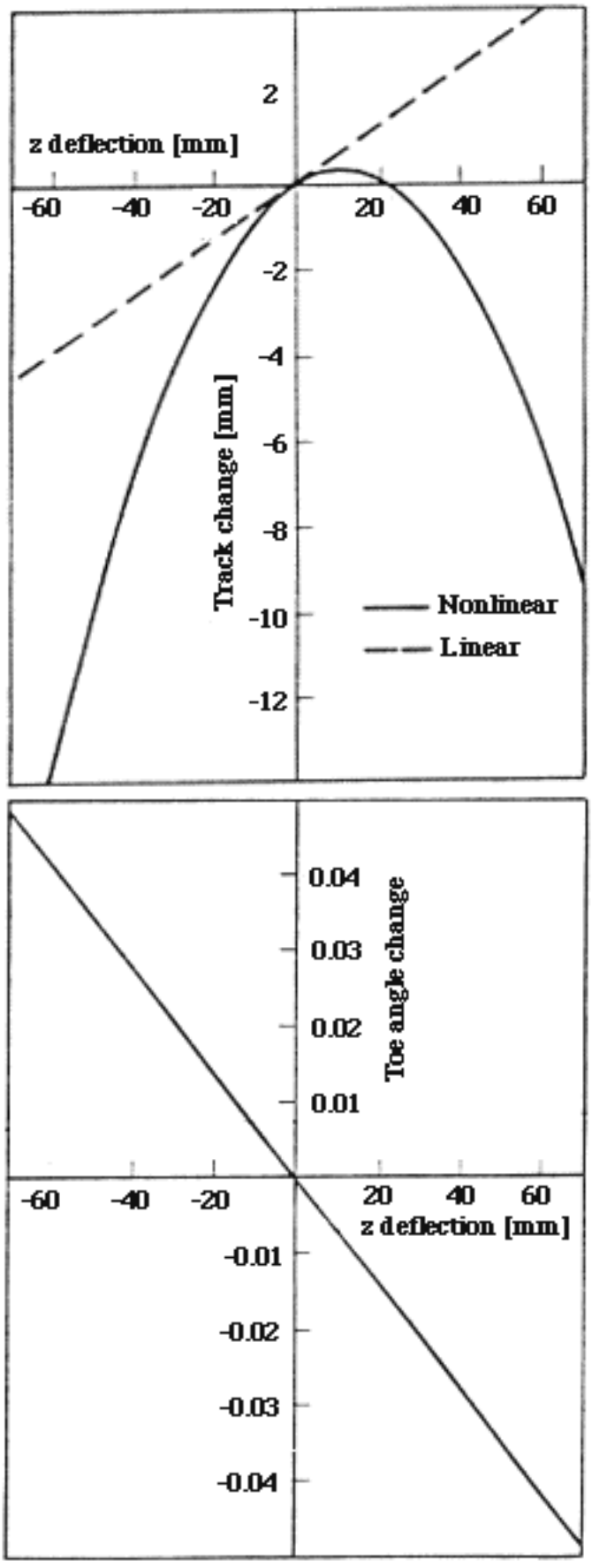


Figure V-49 Track and toe change with wheel travel

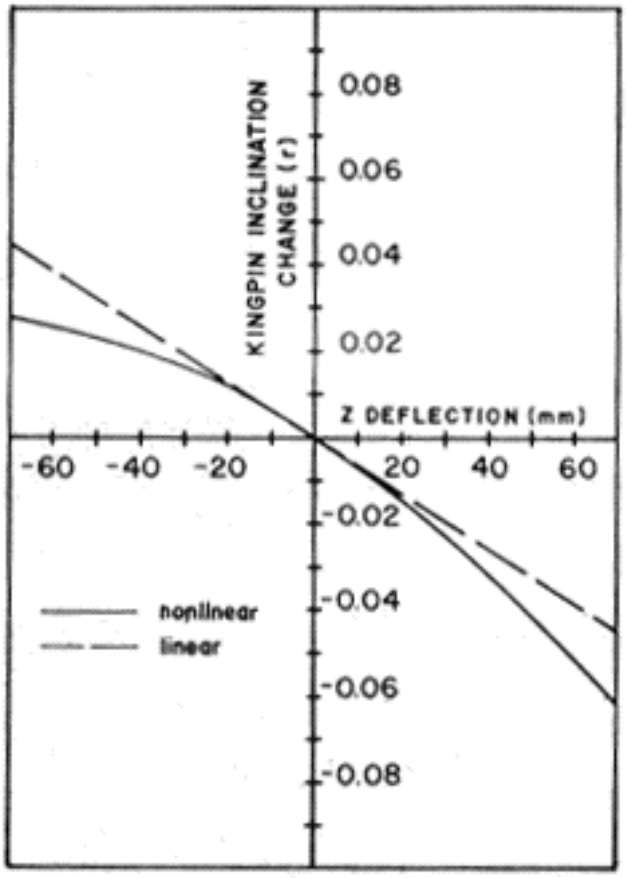


Figure V-50. Kingpin angle change with wheel travel

The three-dimensional model is somewhat difficult to analyze and in some cases, a two-dimensional model may be sufficient to give the required characteristics. Two-dimensional models for the MacPherson strut, double wishbone, and swing axle type of suspensions are shown in Figure. V-43.

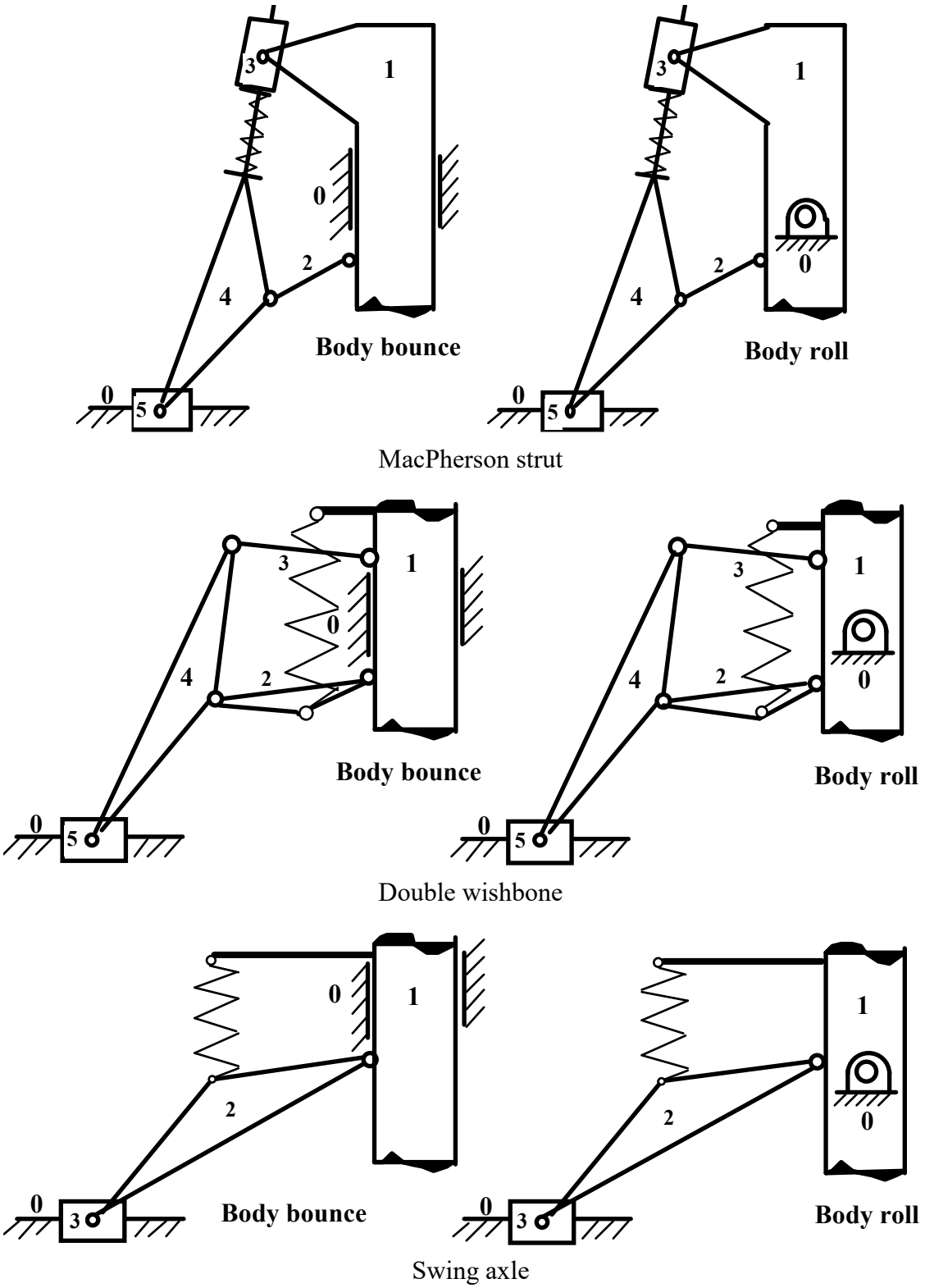
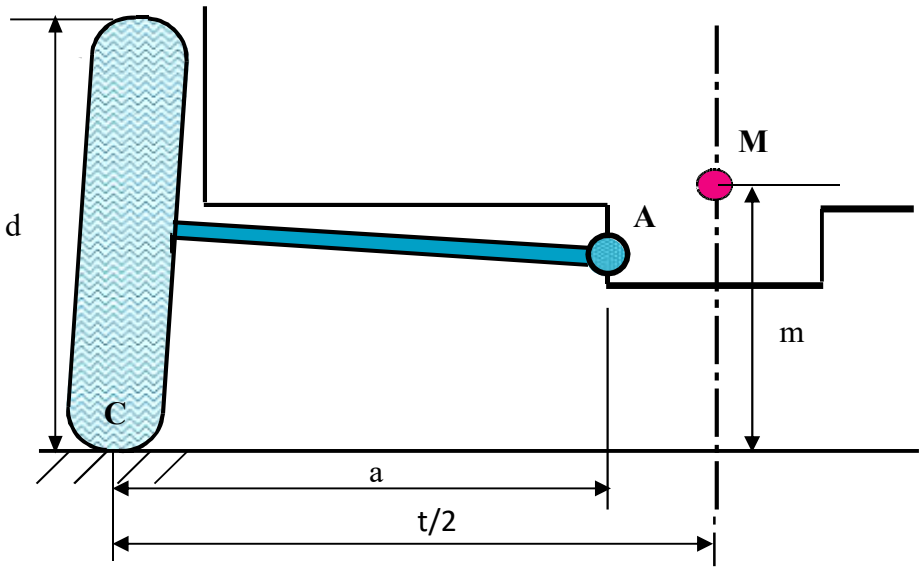


Figure V-51. Two-dimensional models

Example V-2

Draw a kinematic model, providing roll freedom to the vehicle body, of the swing axle suspension illustrated in the figure. Determine the degree of freedom of the linkage, the number of independent loops, and the number of variables involved. Then write the loop closure equation(s), clearly indicating the input and output variables. Plot the relation of the input and output variables to body roll angle, wheel camber, and track changes.



Solution

A possible linkage for the swing axle suspension is given in the figure. It is clear that the variation of camber angle is given by

$$\Delta\gamma = -\Delta\theta_{13}$$

and track change corresponds to

$$\Delta t = S_4 - \frac{t}{2}$$

where t is the initial track.

The degree of freedom of the linkage can be calculated from the fundamental criterion (Kutzbach Criterion)

$$F = b(n-1) - \sum_{i=1}^{j}(b - f_i)$$

where F = degrees of freedom of the linkage

b = number of maximum degree of freedom of a link

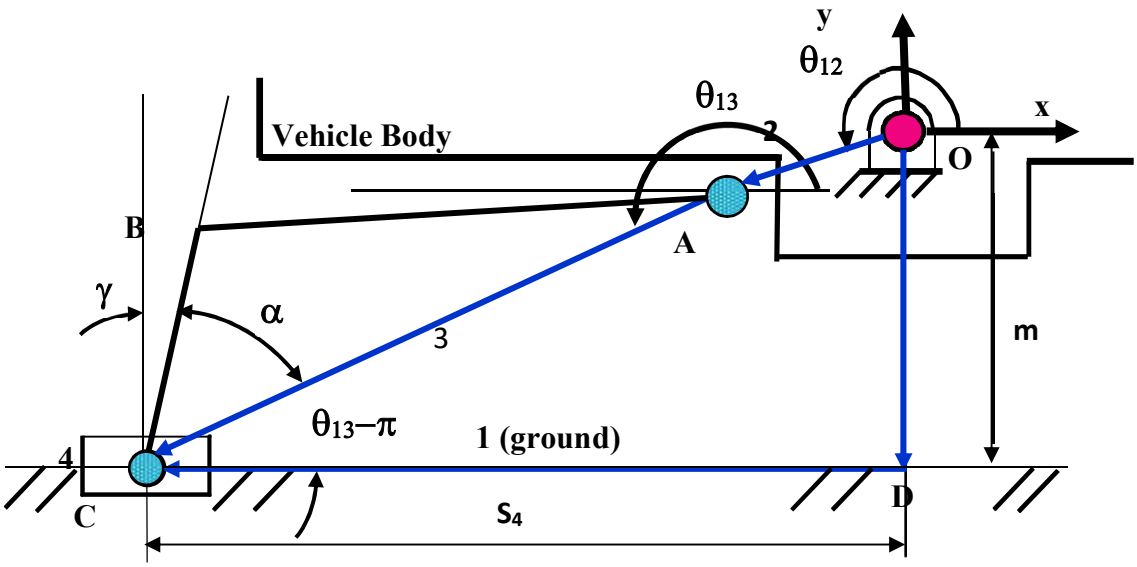
b = 6 for a 3-D linkage

b = 3 for a 2-D linkage

n = number of links

f_i = number of degree of freedom of jth joint

j = number of joints in the linkage.



For the problem in hand, b = 3, n = 4, j = 4 (3 revolute, 1 sliding)

$$F = 3(4 - 1) - 4(3 - 1) = 1$$

The number of independent loops, L, and the number of variables, p, are calculated as

$$L = j - n + 1 = 4 - 4 + 1 = 1$$

$$p = 2L + F = 2(1) + 1 = 3$$

The input is taken as the roll angle of the body, θ_{12}, and the output variables will be the angular displacement of link3, θ_{13}, related to wheel camber angle and the linear position of slider 4, S_4, related to track change.

The loop closure equation can be written as

$$\vec{OA} + \vec{AC} = \vec{OD} + \vec{DC}$$

or

$$\overline{OA}e^{j\theta_{12}} + \overline{AC}e^{j\theta_{13}} = -jm - S_4$$

and using the relation

$$e^{j\theta} = \cos\theta + j\sin\theta$$

one gets

$$\overline{OA}\cos\theta_{12} + j\overline{OA}\sin\theta_{12} + \overline{AC}\cos\theta_{13} + j\overline{AC}\sin\theta_{13} = -jm - S_4$$

This vector equation can be written as two scalar equations

$$\overline{OA}\sin\theta_{12} + \overline{AC}\sin\theta_{13} = -m$$
$$\overline{OA}\cos\theta_{12} + \overline{AC}\cos\theta_{13} = -S_4$$

in the two unknowns S_4 and θ_{13},

It should be noted that an exact analytical solution to these two simultaneous nonlinear equations can be obtained. From the first equation

$$\sin\theta_{13} = \frac{-m - \overline{OA}\sin\theta_{12}}{\overline{AC}}$$

and from the second equation :

$$S_4 = -\overline{OA}\cos\theta_{12} - \overline{AC}\cos\theta_{13}$$

Repeating the solution for a range of values of θ_{12}, plots of camber angle and track change versus body roll angle can be drawn.

For the following set of data, in [mm], the variation of track and camber angle are plotted for a body roll angle range from –20 to +20º.

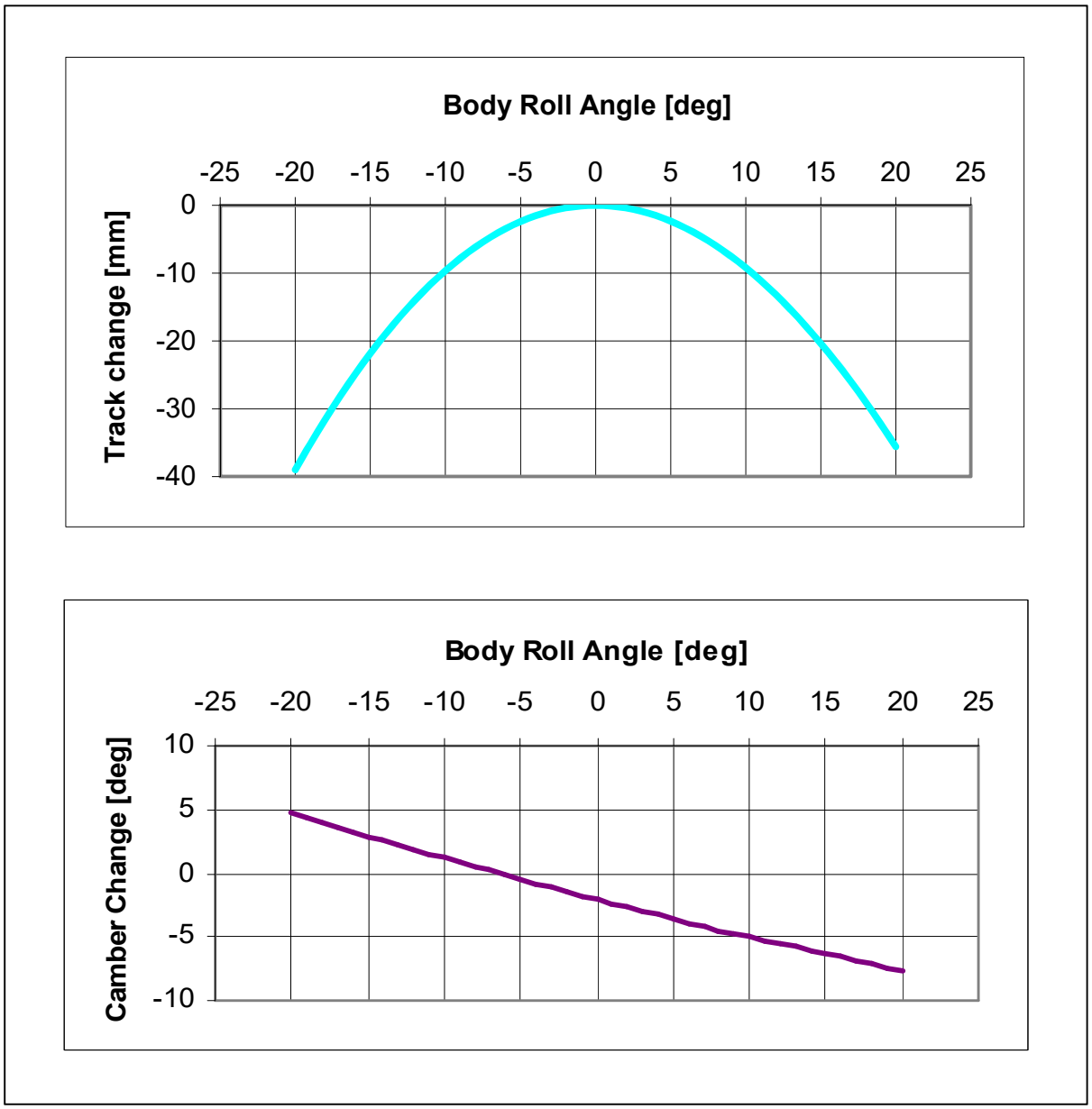
O = [0, 0]

A = [-200, -85]

B = [-850, -80]

C = [-840, -357]

D = [0, -357]


Body Roll Angle [deg]
-25 -20 -15 -10 -5 0 5 10 15 20 25
Track change [mm]
0 -10 -20 -30 -40
Body Roll Angle [deg]
-25 -20 -15 -10 -5 0 5 10 15 20 25
Camber Change [deg]
10 5 0 -5 -10

Exercises

V-1) Find an example of each of the suspension types listed below. On a print, photocopy, or drawing of each type of suspension, indicate the components providing for the location of the wheel in the vertical, lateral, and longitudinal directions.

i) An independent front wheel suspension,

ii) An independent rear wheel suspension other than Macpherson strut and double wishbone types,

iii) A beam axle (live or dead, front or rear).

The reference(s) from which the examples are taken should be fully specified.

V-2) Illustrate the graphical determination of the roll centers for

a) Parallel and equal double wishbones,

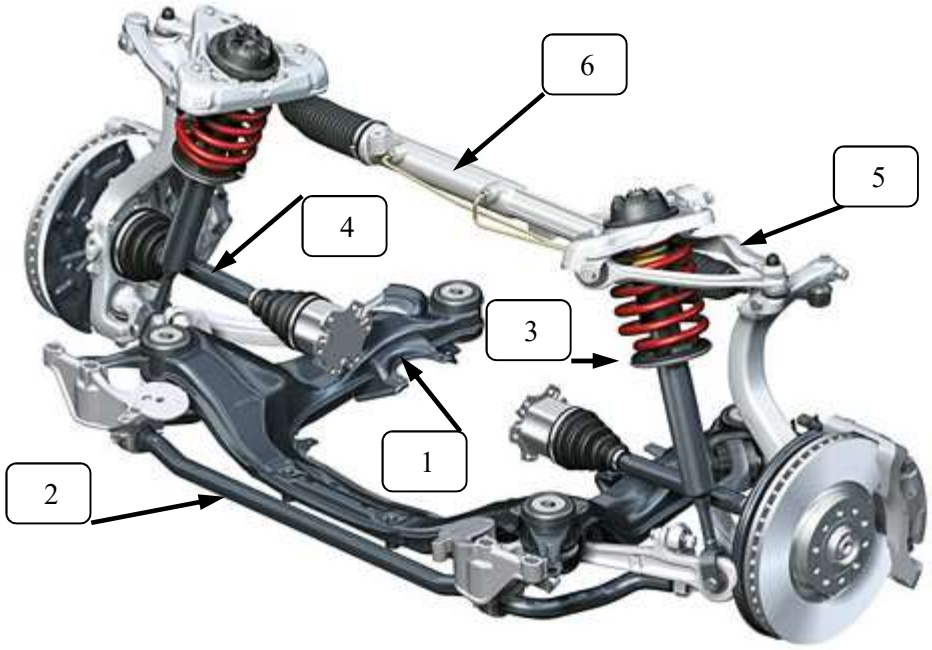
b) Parallel and unequal double wishbones.

V-3) Consider the suspension system shown in the figure.

a) Identify the type of the suspension system.

b) Write the names of all the major components indicated on the figure.

c) Which components provide vertical, lateral, and longitudinal locations of the wheels ?

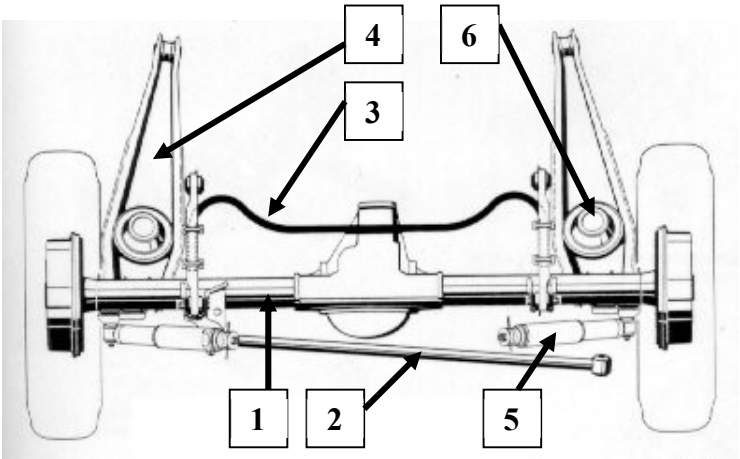


V-4) Consider the knuckle-strut suspension system designed for a medium-size FEFWD saloon car, shown in the figure.

a) Is this an independent suspension system ? Explain shortly.
b) Is this suspension system designed for use in front or rear ? Explain shortly.
c) Why is the axis of the spring tilted with respect to the strut axis ?



V-5) Examine the suspension system given in the figure. Identify the type of the suspension system. Name all the major components indicated on the figure and mark the components that provide the vertical, lateral, and longitudinal locations of the wheels.



V-6) For the double wishbone suspension illustrated in the figure. Draw the force polygons, including

a) the wheel load W, upper wishbone load F_A (two force member), and lower wishbone load F_B (three force member) in the force balance, and

b) the cornering force F_c, upper wishbone load F_A (two force member), and lower wishbone load F_B (three force member).

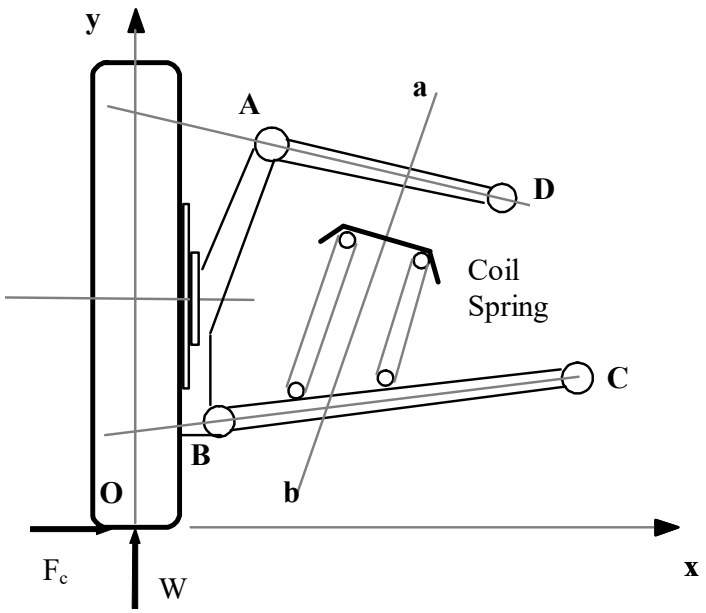
Calculate the magnitude of the spring force, F_s, and the wishbone loads in each case separately.

c) Calculate the magnitude of the spring force, F_s, and the wishbone loads by superimposing the forces found in the two cases above.

Hint : For static equilibrium:

i) The wheel load acting at point O and the wishbone loads acting at points A and B should intersect at a single point.

ii) The spring load and the lower wishbone loads acting at points B and C should intersect at a single point.

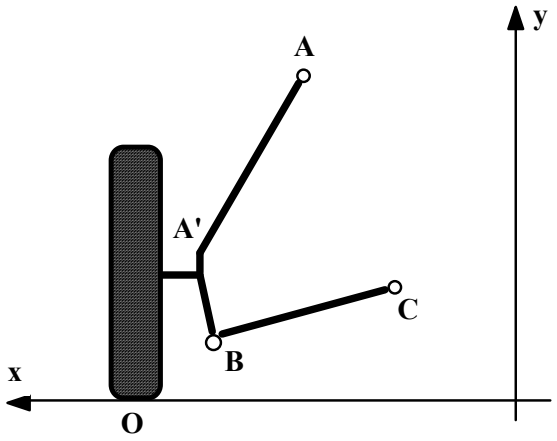


All dimensions are in [mm]

A [97, 436]
B [95, 213]
C [495, 258]
D [351, 418]
a [285, 455]
b [278, 108]
F_c = 2600 N
W = 4000 N

Ans.: a) F_s=2804 [N], F_A=1610 [N], F_B=4205 [N]

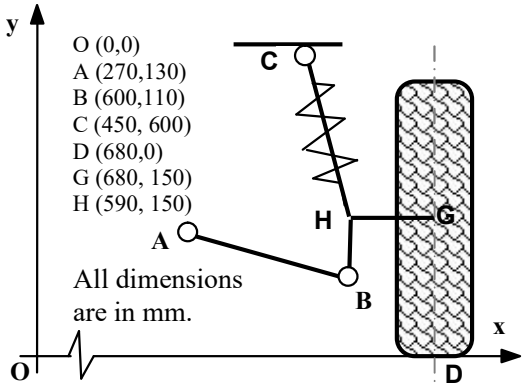
V-7) Calculate the roll center height for the McPherson strut suspension given in the figure.



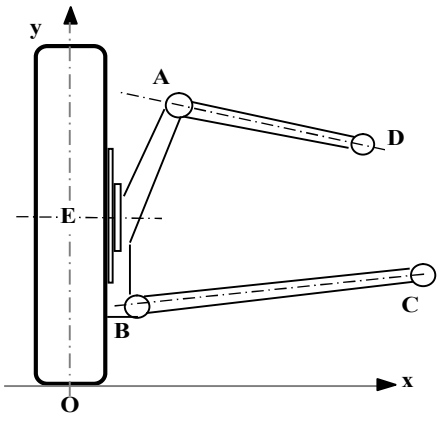
A (0.40, 0.75), A' (0.47, 0.40), B (0.45, 0.20), C (0.15, 0.25), O (0.65, 0.00)

Ans. : 0.171 [m]

V-8) Calculate the roll center height for the McPherson strut suspension given in the figure.



V-9) Calculate the roll center height for the double wishbone suspension given in the figure.



A [97, 436]
B [95, 213]
C [495, 258]
D [351, 418]
E [0, 290]
O [0,0]
t = 1280

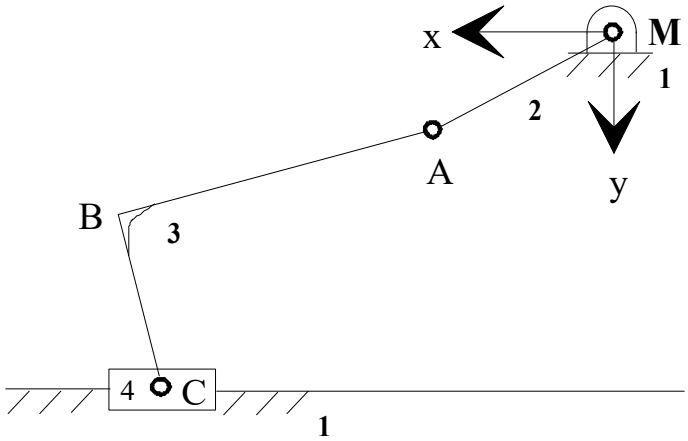
All
dimensions
are in [mm]

V-10) Consider the kinematic model for a swing axle suspension, illustrated in the figure.

a) Calculate the degree of freedom and the number of independent loops.

b) List all the variables and specified parameters and write down the loop closure equation(s).

c) Plot the camber angle and track variation versus body roll for a range of body roll angles from -15º to +15º with 1º increments.



M(0,0),
A(200, 88),
B(839, 90),
C(825, 363).

All dimensions are in mm.

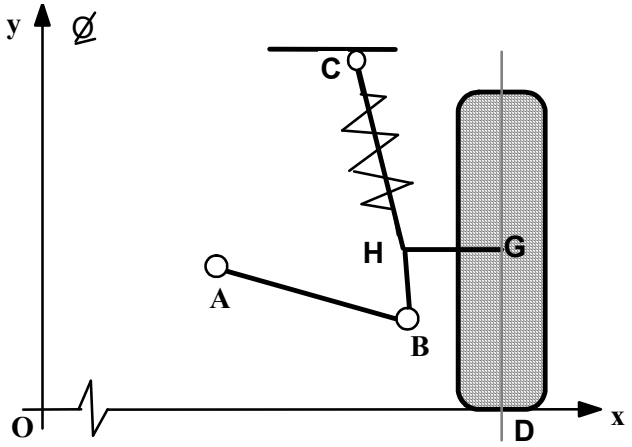
V-11) For the suspension system specified in the figure,

a) Suggest a two-dimensional kinematic model considering body roll only. Show all the relevant dimensions.

b) Determine the degree of freedom, the number of variables, and the number of independent loops. List all variables and identify the input and output variables.

c) Write down (do not solve) the loop closure equation(s).

d) Plot the changes of camber and track for the suspension specified in the figure for a range of body roll angles between -20º to +20º with 1º increments.



O(0,0),
A(270, 130),
B(600, 10),
C(450, 600),
D(680, 0),
G(680, 150),
H(590, 150).

All dimensions are in mm.

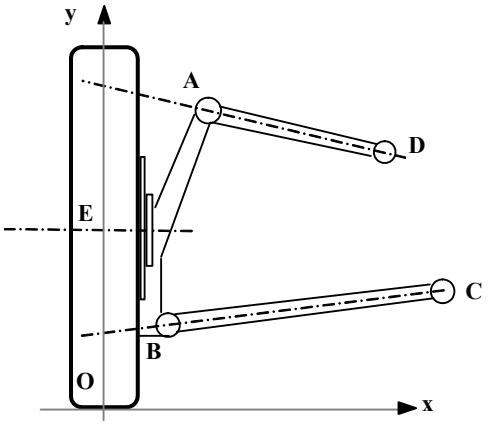
V-12) For the suspension system specified in the figure,

a) Suggest a two-dimensional kinematic model considering body roll only. Show all the relevant dimensions.

b) Determine the degree of freedom, the number of variables, and the number of independent loops. List all variables and identify the input and output variables.

c) Write down (do not solve) the loop closure equation(s).

d) Plot the changes of camber and track for the suspension specified in the figure for a range of body roll angles between -20º to +20º with 1º increments.



A(97, 436),
B(95, 213),
C(495, 258),
D(351, 418),
E(0, 290),
O(0, 0).
Track=1356

All dimensions are in mm.

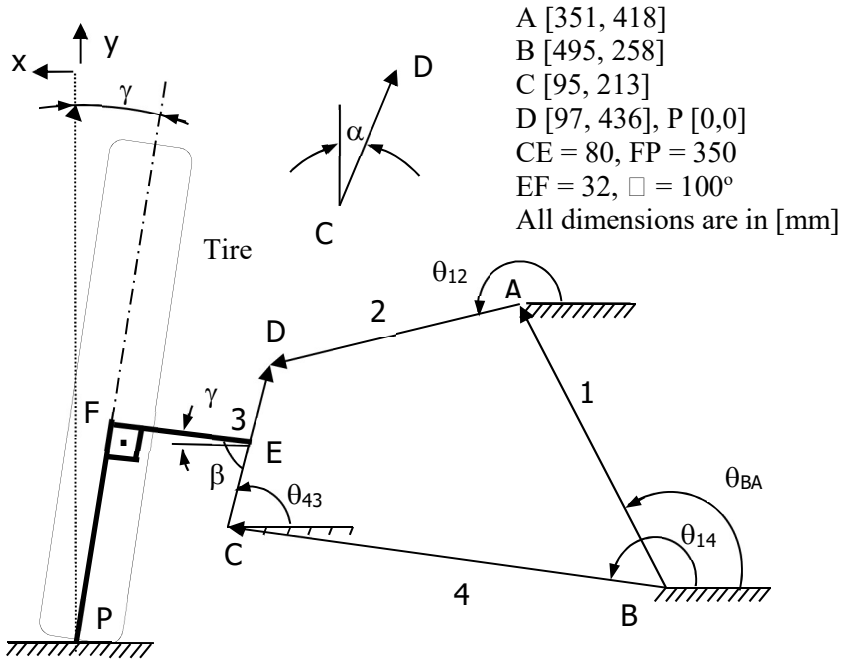
V-13) Consider the kinematic model for a double wishbone suspension shown in the figure in its original position. The suspension mechanism is basically a four-bar linkage with the spindle and the tire assumed to be rigid extensions.

a) Determine the degree of freedom, the number of variables, and the number of independent loops. List all variables and identify the input and output variables.

b) Write down the loop closure equation(s).

c) Given the position of the lower control arm (LCA), $\theta_{14} = 180^o$, solve the equations for θ_{12} and θ_{43}.

d) Calculate the camber angle γ and the x and y positions of the tire contact patch center P.



Hint : Assume that you have two nonlinear algebraic equations of the form

$$A\cos\alpha + B\cos\beta = C\cos\phi + D\cos\theta$$

$$A\sin\alpha + B\sin\beta = C\sin\phi + D\sin\theta$$

where ϕ is known, α is specified, and β and θ are to be solved. You can then leave the terms involving one of the unknown on the left, square both sides of the equations, and sum the two equations side by side.

$$B\cos\beta = C\cos\phi + D\cos\theta - A\cos\alpha$$

$$B\sin\beta = C\sin\phi + D\sin\theta - A\sin\alpha$$

$$B^2\cos^2\beta = \left[C\cos\phi + D\cos\theta - A\cos\alpha\right]^2$$

$$B^2\sin^2\beta = \left[C\sin\phi + D\sin\theta - A\sin\alpha\right]^2$$

$$B^2\left(\cos^2\beta+\sin^2\beta\right)=\left[C\cos\phi+D\cos\theta-A\cos\alpha\right]^2+\left[G\sin\phi+H\sin\theta-E\sin\alpha\right]^2$$

Thus one of the unknowns, β, is eliminated. Now you can define

$$u=\tan\left(\frac{\theta}{2}\right),\qquad \cos\theta=\frac{1-u^2}{1+u^2},\qquad \sin\theta=\frac{2u}{1+u^2}$$

Insert in the equations, and you get a fourth-order equation in terms of u.

$$au^4+bu^3+cu^2+du+e=0$$

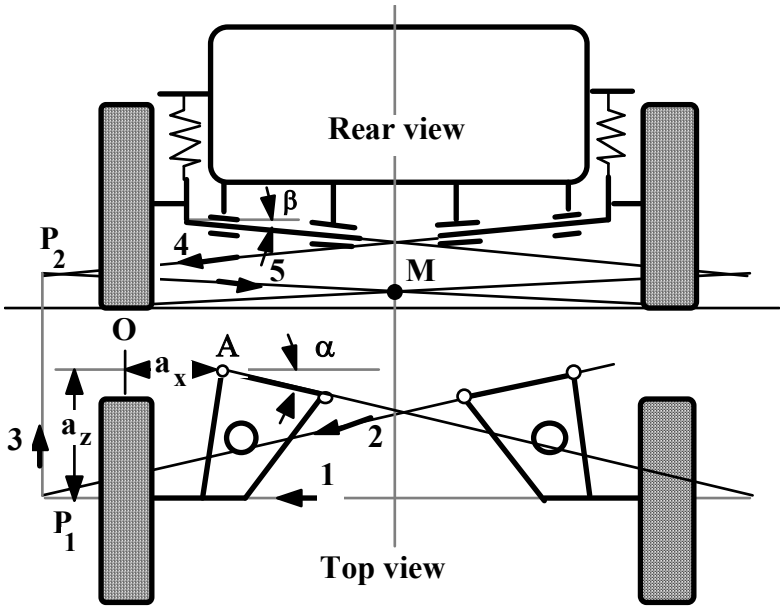
Solve the quadratic for u and then obtain the unknown angle from

$$\theta=2\tan^{-1}\left(u^+\right)=2\tan^{-1}\left(u^-\right)$$

V-14) Determine the roll center height for the semi-trailing arm suspension with relevant dimensions listed below.

a_x = 160 mm
a_y = 384 mm
a_z = 400 mm
t_r = 1310 mm
α = 12º
β = 3º

Ans.: 93 [mm]



CHAPTER VI

VEHICLE RIDE

VI-1. Introduction

Vehicle ride refers to the vibrations of a vehicle that adversely affect the passengers and/or the load. The vibrational activity of a vehicle may be excited by a variety of sources. Excitation may arise from the unbalance of the engine, torsional fluctuations in the engine output, tires, etc. Irregular road surface profile, however, is almost exclusively considered to be the primary excitation in ride comfort studies.

In general, the vehicle has six degrees of freedom, three linear motions, and three rotations in space if considered as a rigid body. The nomenclature used in automotive engineering literature for these degrees of freedom is illustrated in Fig. VI-1. The relative emphasis on each degree of freedom in various subsections of vehicle dynamics is given in Table VI-1.

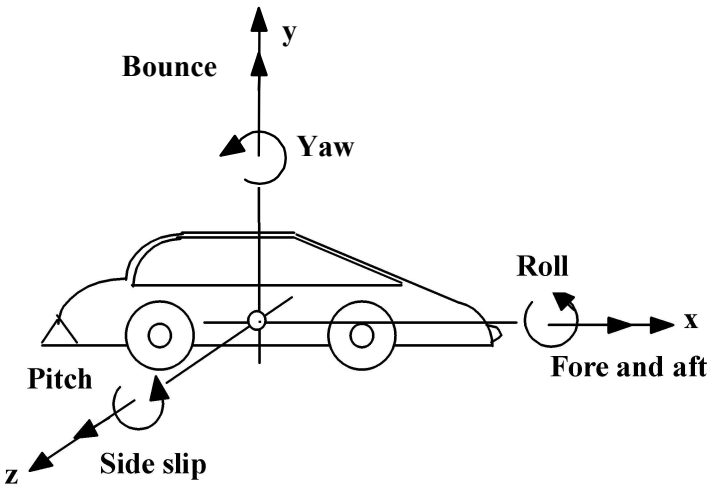


Figure VI-1. Vehicle as a rigid body and the associated nomenclature.

Table VI-1. Emphasis on freedoms in vehicle dynamics subjects

Freedom	Subject
Bounce	Ride
Side slip	Handling
Fore and aft	Performance
Yaw	Handling
Pitch	Ride
Roll	Handling, Ride

In reality, the motor vehicle is a system of bodies and thus can have a large number of degrees of freedom. For this reason, analysis of vehicle ride can be very complex, and simplifying assumptions must be made to be able to obtain results.

It is usually convenient to separate the ride movements from the handling responses and performance estimates. The justification for this separation is simply that road irregularities mainly cause the car body to pitch, bounce, and roll, and although it can be seen from the more precise suspension analyses that these body displacements give rise to steering inputs, these are usually second-order effects such as roll steer. On the other hand, the steering inputs do not cause large pitch and bounce motions.

VI-2. Vibrational Characteristics of Vehicle Systems

Most of the ride studies consider the frequency range from 0.5 to 25 [Hz], even though in some studies, the frequency range may be extended to about 50 [Hz]. Major resonant frequencies of common motor vehicles, i.e., passenger vehicles, light and heavy commercial vehicles, in this range are given in Table VI-2.

Table VI-2. Resonant frequencies in the ride range for motor vehicles.

Frequency Range [Hz]			Source
0.5	to	2.5	Motion of the sprung mass on suspension system approximated by pitching and bouncing modes.
2		4	Man on seat
3		5	Motion of sprung and unsprung masses, suspension locked by friction, on the tires. Pitch and bounce frequencies are increased by about twice-called "Boulevarde jerk".
7		16	Motion of the unsprung mass on the combined tire and spring elasticity. Called "wheel hop". Also includes "tramp" of beam axles where wheels on each side move out of phase.
7		18	Motion of engine mass on rubber engine mounts.
13		40	Body beam and torsion modes.

VI-3. Evaluation of Ride Quality for Motor Vehicles

Although a large number of criteria to evaluate ride quality for vehicles traveling on roads have been proposed, the use of ISO 2631 "Guide for the Evaluation of Human Exposure to Whole-Body Vibration" by the International Standards Organization has been commonly accepted. It is based mainly on existing data regarding human exposure to sinusoidal vibrations and thus is directed towards the evaluation of sinusoidal and periodic vibrations. ISO 2631 specifies comfort boundaries for acceleration described by the rms values calculated in specified 1/3 octave bands for a number of central frequency values. The vibrations in motor vehicles are random, however, and thus the standard has also been converted to a form usable for data presented in the form of power spectral density of the random vehicle vibrations.

The so-called reduced comfort boundaries are given for 1, 16, and 25 minutes as well as 1, 2.5, 4, and 8 hours exposure and represent the limiting values of acceleration in the frequency range from 1 to 80 Hz. These reduced comfort boundaries are plotted in Fig. VI-2 (a) and (b) for vertical and lateral vibrations, respectively. The values at corner frequencies for 1 and 8-hour exposures are listed in Table VI-3.

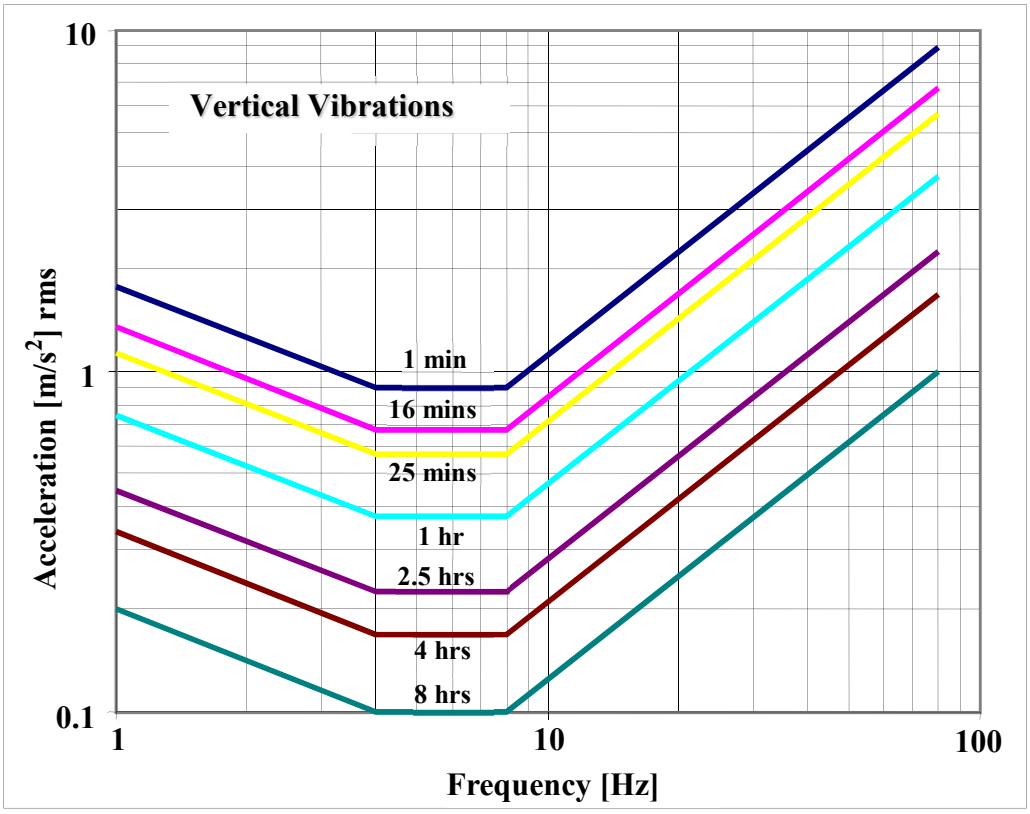


Figure VI-2 (a) ISO reduced comfort boundaries for vertical vibrations

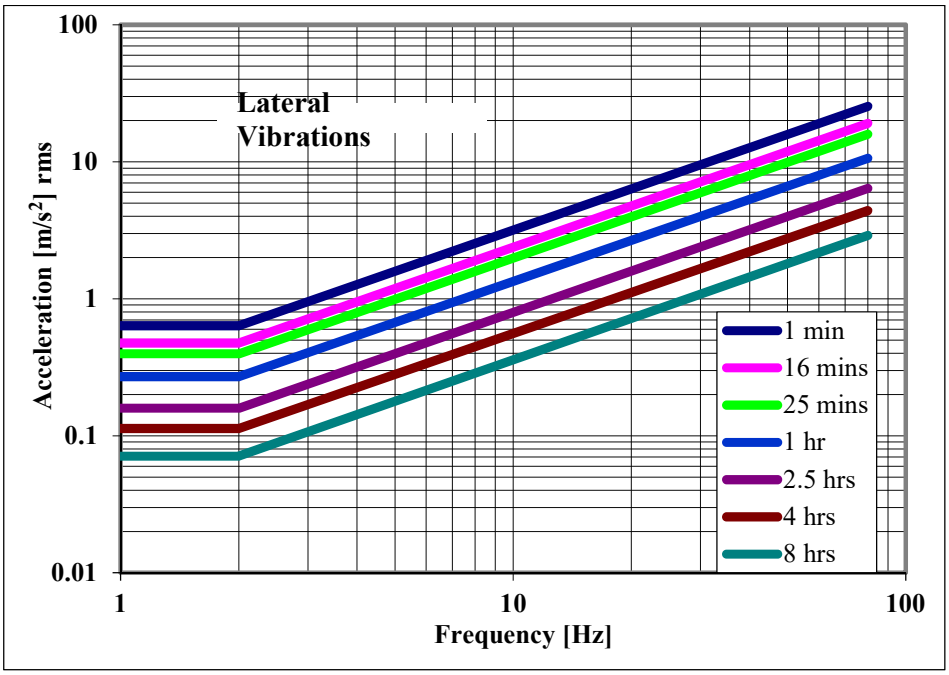


Figure VI-2 (b) ISO reduced comfort boundaries for lateral vibrations

Table VI-3 ISO reduced comfort boundaries for vertical and lateral vibrations

ISO-boundaries for Vertical Vibrations				
Frequency	a [m/s^2]		a [g]	
[Hz]	**1 hr**	**8 hrs**	**1 hr**	**8 hrs**
1	0.749	0.200	7.64E-02	2.04E-02
4	0.375	0.100	3.82E-02	1.02E-02
8	0.375	0.100	3.82E-02	1.02E-02
80	3.746	1.000	3.82E-01	1.02E-01

ISO-boundaries for Lateral Vibrations				
Frequency	a [m/s^2]		a [g]	
[Hz]	**1 hr**	**8 hrs**	**1 hr**	**8 hrs**
1	0.270	0.071	2.75E-02	7.24E-03
2	0.270	0.071	2.75E-02	7.24E-03
80	10.64	2.857	1.085	2.91E-01

The ISO reduced comfort boundaries may be superimposed on a plot of the acceleration of the vehicle body versus frequency, Fig. VI-3. Ride quality will be acceptable if the acceleration curve falls below the selected reduced comfort boundary throughout the frequency range of interest. If the acceleration rises above the selected reduced comfort boundary anywhere within the frequency range of interest, this will indicate inadequate ride quality.

VI-4. Body Bounce

Body bounce is the up and down (vertical) motion of the sprung mass on the suspension spring. The sprung mass is represented as an ideal point mass and the suspension system consists of a linear spring and a viscous damper in parallel as shown in Fig. VI-3. The unsprung mass and the tire elasticity are not considered. This model can be used to estimate the body bounce frequency of the vehicle when the sprung mass and suspension spring stiffness values are available.

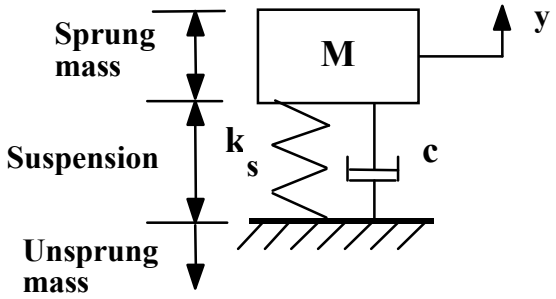


Figure VI-3. Body bounce model.

The bounce frequency of the body is given by the expression

$$\omega_n^{bb} = \sqrt{\frac{k_s}{M}} \qquad \text{(VI-1)}$$

It has been known for many years that the lower the frequency of vibration of the car body on its suspension springs, the greater the comfort. Improved ride has always appeared high on the list of priorities, and the selection of a proposed suspension frequency is the first step in suspension design. However, the selection of soft springs to improve ride comfort results in higher roll angles and degraded handling. Thus, a usual order of priorities is to determine the ride comfort first and then to control roll and tune the handling by the use of anti-roll bars. The introduction of anti-roll bars has removed the need to supply extra suspension stiffness to control roll angle by the main springs, and lower bounce frequencies are possible with vehicles equipped with anti-roll bars.

In modern medium size to large cars, the body bounce frequency has generally settled at about 70 c/min [≈1.2 Hz]. Further lowering is prevented by the need to limit the static deflection (wheel travel) that should be accommodated when the vehicle payload varies from minimum to maximum. The problem is worse in vehicles that have a large ratio of sprung laden weight/sprung unladen weight, i.e., in cars that are small for their payloads. For this reason, small cars seem to become limited at around 90 c/min [1.5 Hz] unladen. The cross country (off-road) vehicles have frequencies around 120 c/min [2.0 Hz] unladen.

Example VI-1

Determine the frequency and damping ratio of the bounce motion of a vehicle having a sprung mass of 1200 kg. The vehicle is equipped with all independent suspensions, each having springs of 16 kN/m stiffness and linear dampers each with a damping coefficient of 1000 N/m/s.

$$\omega_n^{bb} = \sqrt{\frac{k_T}{M}} = \sqrt{\frac{4k_s}{M}} = \sqrt{\frac{4*16000 \ \left[\frac{N}{m}\right]}{1200 \ [kg]}\left(\frac{kg\frac{m}{s^2}}{N}\right)} \cong 7.30 \ \left[\frac{rad}{s}\right] \ \left(\frac{cycle}{2\pi \ rad}\right)$$

$$\cong 1.2 \ \left[\frac{cyc}{s}\right] = 1.2 \ [Hz]$$

$$\zeta = \frac{c_T}{2\sqrt{k_T M}} = \frac{4c}{2M\omega_n^{bb}} = \frac{4*1000\left[\frac{Ns}{m}\right]}{2\sqrt{4*16000\left[\frac{N}{m}\right]1200[kg]\left(\frac{N}{kg\frac{m}{s^2}}\right)}}$$

$$\cong 0.228 \cong 23[\%]$$

Exercise VI-1

Estimate the undamped natural frequencies and damping ratios for the unladen and laden conditions of a compact car specified below.

Sprung mass (unladen/laden) : 820/ 1280 kg
Total spring stiffness : 62 kN/m
Total damping coefficient : 4.3 kN/m/s

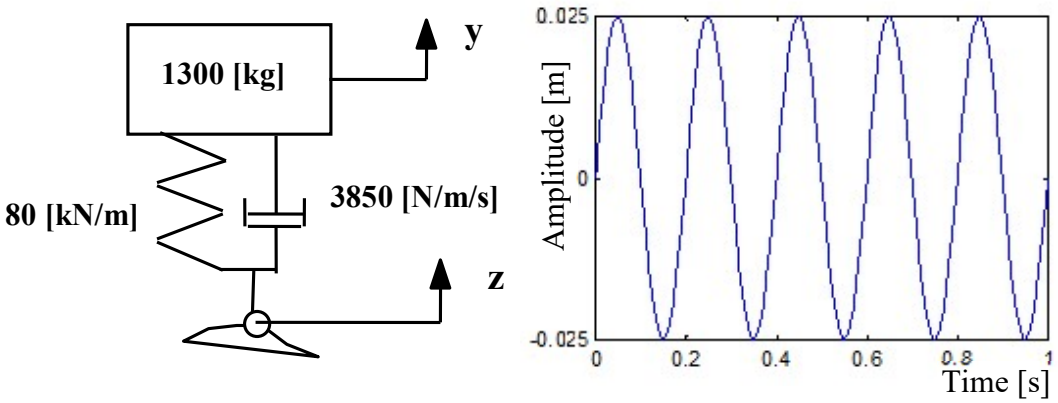
Ans. : 1.38 / 1.11 Hz, 30.2 / 24.1 %

Example VI-2

A car is driven on a specially profiled road surface which is characterized by a sinusoidal shape of 2.5 cm amplitude with 0.3 complete cycles for each meter.

a) What is the excitation frequency for a car travelling at 60 kph on this road?

b) Can the driver drive the vehicle on this road continuously at 60 kph for 1 hr according to the relevant ISO 2631 reduced comfort boundary? Use the single degree of freedom vehicle model shown in the figure.



a) The excitation frequency is calculated from the wave number n and the vehicle speed.

$$f = nV = 0.3\left[\frac{cyc}{m}\right]60\left[\frac{km}{h}\right]\left(\frac{1000m}{km}\right)\left(\frac{h}{3600s}\right) = 5\left[\frac{cyc}{s}\right] = 5[Hz]$$

Thus the road profile input is represented in the form $z = A\sin(\omega t)$ where A=0.025 [m] and $\omega=2\pi f=10\pi$ [rad/s].

b) The equation of motion for the vehicle model is given as

$$m\ddot{y} + c\dot{y} + ky = c\dot{z} + kz$$

Dividing all terms by m, and using the definitions of the undamped natural frequency (i.e. the body bounce frequency) and the damping ratio as

$$\omega_n^2 = \frac{k}{m} \qquad \zeta = \frac{c}{2m\omega_n}$$

the equation of motion can be written in the standard form

$$\ddot{y} + 2\zeta\omega_n \dot{y} + \omega_n^2 y = 2\zeta\omega_n \dot{z} + \omega_n^2 z$$

Since the forced motion of the body mass will be again according to a harmonic function with the same frequency as the excitation but with a different amplitude, assume a steady state solution in the form

$$y = Ye^{j\omega t}$$

$$\dot{y} = j\omega Ye^{j\omega t}$$

$$\ddot{y} = -\omega^2 Ye^{j\omega t}$$

Since $e^{j\omega t} = \cos\omega t + j\sin\omega t$, using the imaginary part of $Ze^{j\omega t}$ for $Z\sin\omega t$, the input displacement is given by

$$z = Ze^{j\omega t}$$

$$\dot{z} = j\omega Ze^{j\omega t}$$

Substituting the expressions for the input and response variables and their derivatives into the equation of motion, one obtains :

$$\left[\left(\omega_n^2 - \omega^2\right) + j\left(2\zeta\omega_n\omega\right)\right]Y = \left[\omega_n^2 + j\left(2\zeta\omega_n\omega\right)\right]Z$$

Dividing all terms by ω_n^2 and denoting the frequency ratio by $\Omega = \dfrac{\omega}{\omega_n}$,

$$\frac{Y}{Z} = \frac{1 + j\left(2\zeta\Omega\right)}{\left(1 - \Omega^2\right) + j\left(2\zeta\Omega\right)} = \frac{\sqrt{1 + \left(2\zeta\Omega\right)^2}\, e^{j\phi_1}}{\sqrt{\left(1 - \Omega^2\right)^2 + \left(2\zeta\Omega\right)^2}\, e^{j\phi_2}}$$

$$\frac{Y}{Z} = \frac{\sqrt{1 + \left(2\zeta\Omega\right)^2}}{\sqrt{\left(1 - \Omega^2\right)^2 + \left(2\zeta\Omega\right)^2}}\, e^{-j\phi}$$

where the magnitude of the amplitude ratio is given by

$$\left|\frac{Y}{Z}\right| = \frac{\sqrt{1+(2\zeta\Omega)^2}}{\sqrt{\left(1-\Omega^2\right)^2+(2\zeta\Omega)^2}}$$

and the phase is given by $\phi = \phi_2 - \phi_1$ with $\tan\phi_1 = 2\zeta\omega_n$ and $\tan\phi_2 = \dfrac{2\zeta\omega_n}{1-\Omega^2}$.

Using the given data

$$\omega_n = \sqrt{\frac{k}{m}} = \sqrt{\frac{80000\left[\frac{N}{m}\right]}{1300[kg]\left(\frac{N.s^2}{kg.m}\right)}} \cong 7.85\left[\frac{rad}{s}\right]$$

$$\zeta = \frac{c}{2m\omega_n} = \frac{c}{2m\sqrt{\frac{k}{m}}} = \frac{3850\left[\frac{Ns}{m}\right]}{2(1300)[kg]\sqrt{\frac{80000}{1300}}\left[\frac{rad}{s}\right]\left(\frac{N.s}{kg.m}\right)} = 0.189$$

The amplitude of the body displacement for a frequency ratio of $\Omega = \dfrac{\omega}{\omega_n} = \dfrac{10\pi}{7.85} = 4.00$ and an excitation amplitude of 0.025 [m] is:

$$|Y| = \frac{\sqrt{1+(2\zeta\Omega)^2}}{\sqrt{\left(1-\Omega^2\right)^2+(2\zeta\Omega)^2}}|Z| = \frac{\sqrt{1+2.286}}{\sqrt{227.3}}(0.025) = (0.12)(0.025) = 0.003[m]$$

It should be noted that the amplitude of vibrations of the vehicle body is considerably reduced when compared with the road profile amplitude. However, the ride comfort is based on acceleration rather than amplitude of vibration. Thus we are interested in the root mean square (rms) value of the body acceleration,

$$\ddot{y}_{rms} = (0.707)\ddot{y} = (0.707)\omega^2 Y = (0.707)(10\pi)^2(0.003) \cong 2.1\left[m/s^2\right]$$

If this value is compared with the 1 hour ISO reduced comfort boundary for vertical vibrations given on Table VI-3, it is clear that the acceleration level exceeds the allowed value.

VI-5. Wheel Hop (Wheel Bounce)

In this mode the wheel-hub assembly (unsprung mass) bounces on the tire and the suspension spring, and the motion is damped by the shock absorber. The wheel hop frequency is usually well separated from body bounce, pitch, and roll frequencies which are considerably lower. A model to obtain the approximate wheel hop frequency is shown in Fig. VI-4.

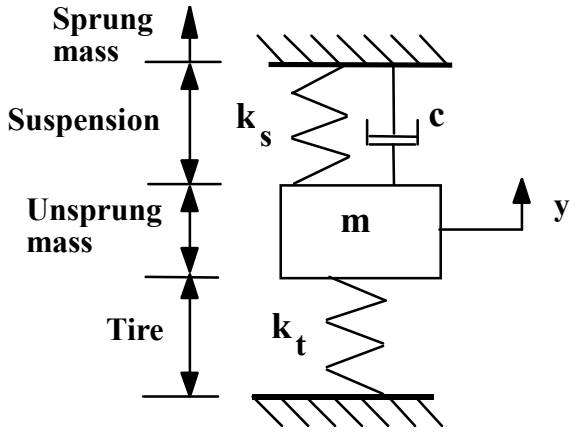


Figure VI-4. Wheel hop model

The wheel hop frequency can thus be approximated using the expression

$$\omega_n^{wh} = \sqrt{\frac{k_s + k_t}{m}} \qquad \text{(VI-2)}$$

It is noted that

$$\frac{M}{m} = \frac{k_t}{k_s} \approx 10$$

thus

$$\frac{\omega_n^{wh}}{\omega_n^{bb}} \approx 10$$

for vehicles with independent suspensions.

The conventional shock absorber has to damp the sprung mass on its springs and the unsprung mass on the tires. However with independent suspensions, by coincidence, the ratio (sprung mass/unsprung mass) is quite close to the ratio (wheelbounce frequency/suspension frequency) so that practically the same damping ratio can be obtained for both modes.

$$\xi_{bb} = \frac{c}{2M\,\omega_n^{bb}}, \qquad \xi_{wh} = \frac{c}{2m\,\omega_n^{wh}}$$

$$\frac{\xi_{bb}}{\xi_{wh}} = \frac{2M\,\omega_n^{bb}}{2m\,\omega_n^{wh}} = \left(\frac{M}{m}\right)\left(\frac{\omega_n^{bb}}{\omega_n^{wh}}\right) = \frac{\left(\frac{M}{m}\right)}{\left(\frac{\omega_n^{wh}}{\omega_n^{bb}}\right)} \approx 1.0$$

or

$$\xi_{bb} \approx \xi_{wh}$$

The ideal solution is, of course, to use the shock absorbers to damp the sprung mass on the suspension springs, and to utilize another means of damping such as the harmonic dampers used on Citroen 2 CV for wheel hop in the past.

Example VI-3

Determine the frequency and damping ratio of the wheel hop motion of the vehicle specified in the previous example. The unsprung mass for each suspension is 36 kg and the tire stiffness is 150 kN/m.

$$\omega_n^{wh} = \sqrt{\frac{k_s + k_t}{m}} = \sqrt{\frac{(16000+150000)\left[\frac{N}{m}\right]}{36[kg]}\left(\frac{kg\frac{m}{s^2}}{N}\right)} \cong 67.9\left[\frac{rad}{s}\right]\left(\frac{cycle}{2\pi\,rad}\right) \cong 10.8[Hz]$$

$$\zeta = \frac{c}{2\sqrt{(k_s+k_t)\,m}} = \frac{c}{2\,m\,\omega_n^{wh}} = \frac{1000\left[\frac{N\,s}{m}\right]}{2\sqrt{(16000+150000)\left[\frac{N}{m}\right]36[kg]\left(\frac{N}{kg\frac{m}{s^2}}\right)}}$$

$$\cong 0.205 = 20.5[\%]$$

VI-6. Quarter Car Model - Body Bounce and Wheel Hop

In many ride studies, a model involving both the body bounce and wheel hop modes is required. The so called 'Quarter car model' shown in Fig. VI-5 is the best known vehicle ride model with two degrees of freedom. It usually represents one suspension together with its share of the sprung mass. Despite its simplicity, it covers most of the fundamental features of real vehicle ride dynamics and leads to a basic understanding of the capabilities and limitations of suspension performance.

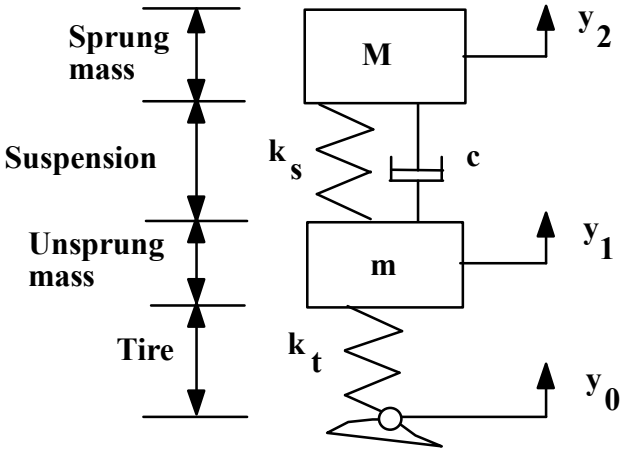


Figure VI-5. Quarter car model

It is possible to find the approximate body bounce and wheel hop frequencies using eqns. VI-1 and 2. As these frequencies are well separated, the results are normally quite close to exact values. The model can be used to study the motion of a vehicle on an irregular road surface which is represented by the input y_0.

The equations of motion for this system can be obtained by applying Newton's second law to the sprung and unsprung masses.

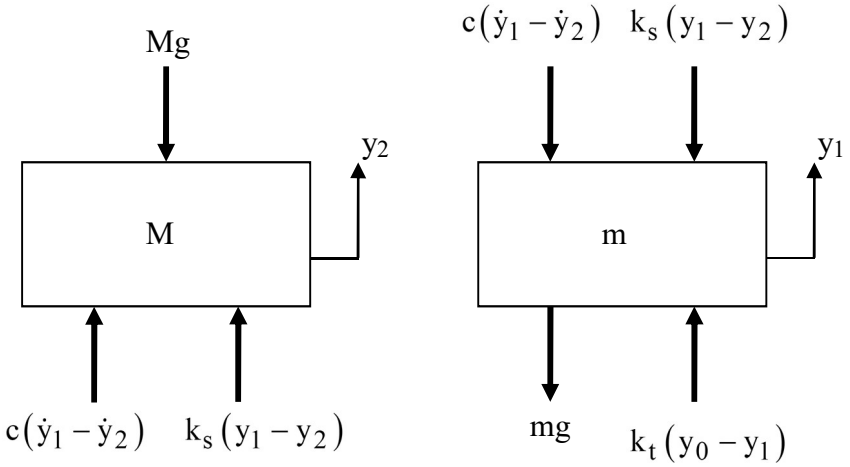


Figure VI-6. Forces acting on the sprung and unsprung masses

Here, the displacements of the masses are written with respect to the undeformed lengths of the suspension and tire springs. The equations of motion for this system are then obtained as:

$$M\ddot{y}_2 = c(\dot{y}_1 - \dot{y}_2) + k_s(y_1 - y_2) - Mg \tag{VI-3}$$

$$m\ddot{y}_1 = k_t(y_0 - y_1) - c(\dot{y}_1 - \dot{y}_2) - k_s(y_1 - y_2) - mg \tag{VI-4}$$

It is clear that the static deflections due to the sprung and unsprung masses are given by

$$y_2 = \frac{Mg}{k_s} + \frac{(M+m)g}{k_t}$$

$$y_1 = \frac{(M+m)g}{k_t}$$

The equations of motion can also be written with respect to the static deflection positions of the masses in matrix form

$$[M]\{\ddot{y}\} + [C]\{\dot{y}\} + [K]\{y\} = \{f\} \tag{VI-5}$$

where

$$\{y\} = \begin{Bmatrix} y_1 \\ y_2 \end{Bmatrix} \qquad \{f\} = \begin{Bmatrix} k_t \\ 0 \end{Bmatrix} y_0$$

$$[M] = \begin{bmatrix} m & 0 \\ 0 & M \end{bmatrix} \qquad [C] = \begin{bmatrix} c & -c \\ -c & c \end{bmatrix} \qquad [K] = \begin{bmatrix} k_s + k_t & -k_s \\ -k_s & k_s \end{bmatrix}$$

To determine the undamped natural frequencies of the system, consider the equations for undamped free motion.

$$[M]\{\ddot{y}\} + [K]\{y\} = \{0\} \tag{VI-6}$$

If a solution of the form

$$\{y\} = \{Y\}e^{i\omega t} \tag{VI-7}$$

is assumed, then

$$\left[-[M]\omega^2 + [K]\right]\{Y\} = \{0\} \tag{VI-8}$$

For a nontrivial solution to this equation, one must have:

$$\det\left|\left[K\right]-\left[M\right]\omega^{2}\right|=0 \tag{VI-9}$$

or

$$\begin{vmatrix} k_s+k_t-m\lambda & -k_s \\ -k_s & k_s-M\lambda \end{vmatrix}=0 \tag{VI-10}$$

The characteristic equation is then obtained as:

$$mM\lambda^{2}-\left[k_s m+\left(k_s+k_t\right)M\right]\lambda+k_s k_t=0$$

Dividing all terms by "mM", the roots of the resulting quadratic equation

$$\lambda^{2}-\left(\frac{k_s}{M}+\frac{k_s+k_t}{m}\right)\lambda+\frac{k_s k_t}{mM}=0 \tag{VI-11}$$

will give the exact undamped natural frequencies.

$$\lambda_{1,2}=\omega_{1,2}^{2}=\frac{1}{2}\left\{\frac{k_s}{M}+\frac{k_s+k_t}{m}\pm\sqrt{\left(\frac{k_s}{M}+\frac{k_s+k_t}{m}\right)^{2}-4\frac{k_s k_t}{mM}}\right\} \tag{VI-12}$$

One can write the characteristic equation in terms of the approximate (uncoupled) undamped natural frequencies given by eqns. (VI-1) and (VI-2).

$$\lambda^{2}-\left(\omega_{bb}^{2}+\omega_{wh}^{2}\right)\lambda+\omega_{bb}^{2}\left(\omega_{wh}^{2}-\frac{k_s}{m}\right)=0 \tag{VI-13}$$

It is clear that if

$$\frac{k_s}{m}<<\omega_{wh}^{2} \qquad \text{or} \qquad k_t>>k_s \tag{VI-14}$$

then

$$\lambda^{2}-\left(\omega_{bb}^{2}+\omega_{wh}^{2}\right)\lambda+\omega_{bb}^{2}\omega_{wh}^{2}=\left(\lambda-\omega_{bb}^{2}\right)\left(\lambda-\omega_{wh}^{2}\right)=0$$

and the body bounce and wheel hop motions are decoupled from each other. In such a case, the roots of the characteristic equation will be the same as the body bounce and wheel hop frequencies obtained from eqns. (VI-1) and (VI-2).

Transfer Functions of the Quarter Car Model

The transfer functions of sprung mass acceleration (indicates ride comfort), suspension travel (important for suspension packaging), and tire deflection (related to road holding) for road profile velocity input can be established as

$$H_{sma}(i\omega) = \frac{s^2 Y_2(s)}{s Y_0(s)} = \frac{s k_t A}{BC - A^2} \tag{VI-15}$$

$$H_{st}(i\omega) = \frac{Y_2(s) - Y_1(s)}{s Y_0(s)} = \frac{k_t (A - B)}{s\left(BC - A^2\right)} \tag{VI-16}$$

$$H_{td}(i\omega) = \frac{Y_1(s) - Y_0(s)}{s Y_0(s)} = \frac{(k_t - C)B + A^2}{s\left(BC - A^2\right)} \tag{VI-17}$$

where

$$s = - i\omega$$

$$A = c_s s + k_s \tag{VI-18}$$

$$B = Ms^2 + c_s s + k_s \tag{VI-19}$$

$$C = ms^2 + c_s s + k_s + k_t \tag{VI-20}$$

Logarithmic plot of the body (sprung mass) acceleration transfer function for the nominal vehicle parameters listed below are given in Figs. VI-7 (a). In Figures 7 (b) to (e), effects of changing these parameters on the sprung mass acceleration transfer function are illustrated. The logarithmic plots of the suspension travel and tire deflection transfer functions are presented in Figures 8 and 9, respectively.

M	:	sprung mass	=	320 kg
m	:	unsprung mass	=	46 kg
k_s	:	suspension spring stiffness	=	15 kN/m
c_S	:	damper damping coefficient	=	980 N/m/s
k_t	:	tyre stiffness	=	145 kN/m

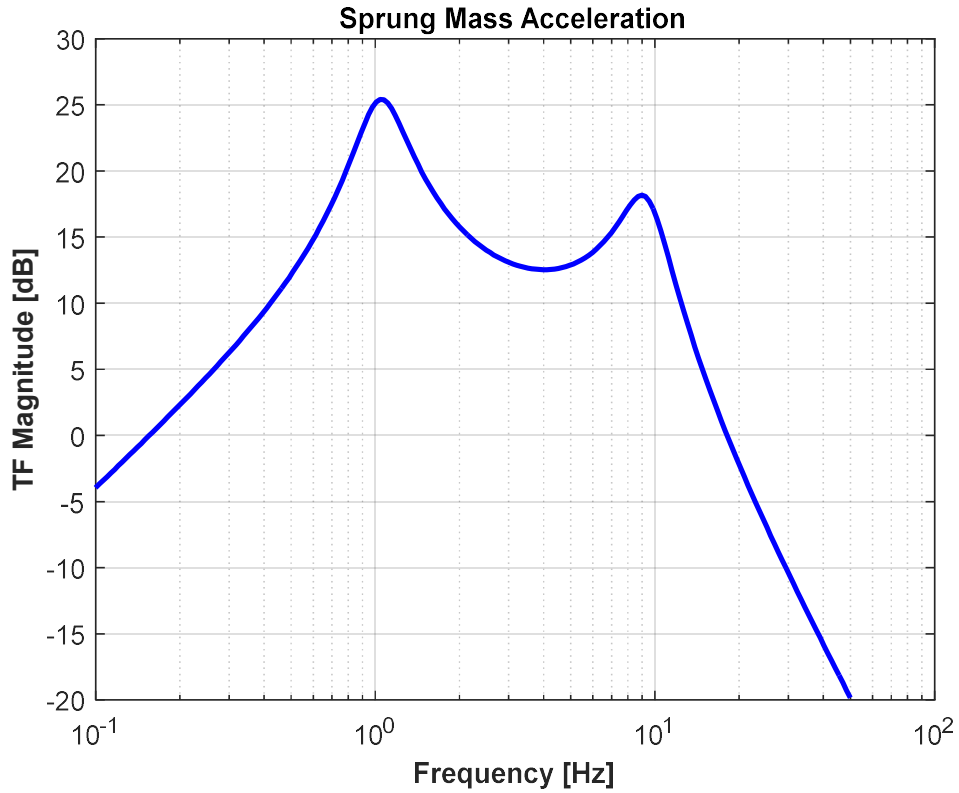


Figure VI-7. (a) Sprung mass acceleration transfer function – nominal parameter values

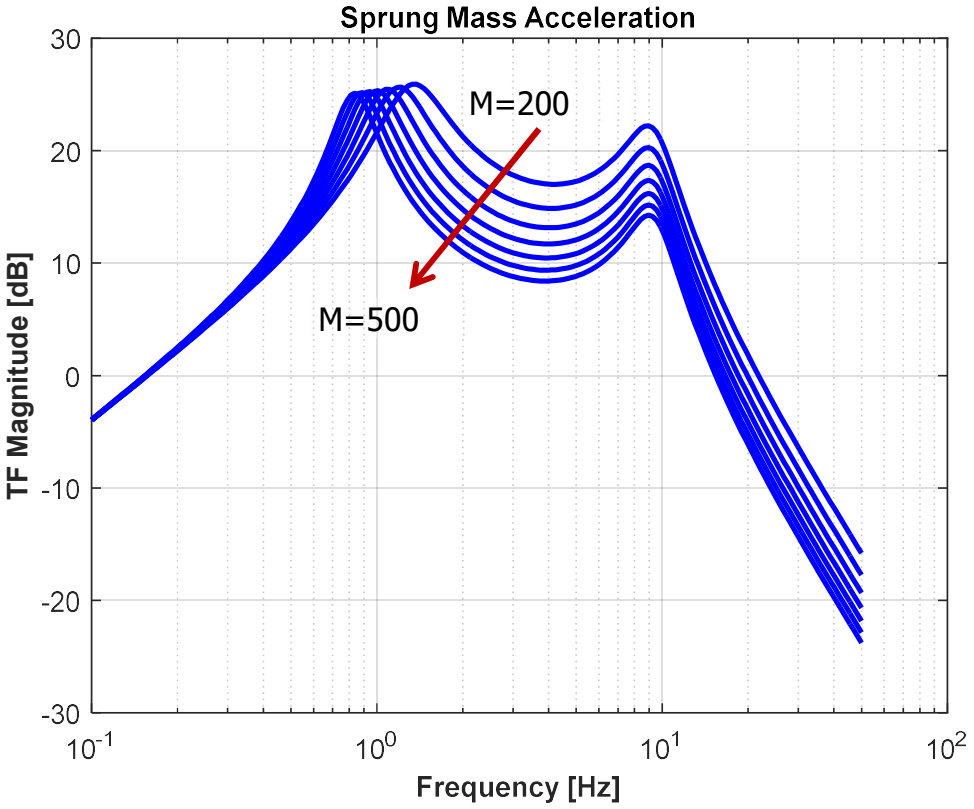


Figure VI-7. (b) Sprung mass acceleration transfer function – ΔM=50 [kg]

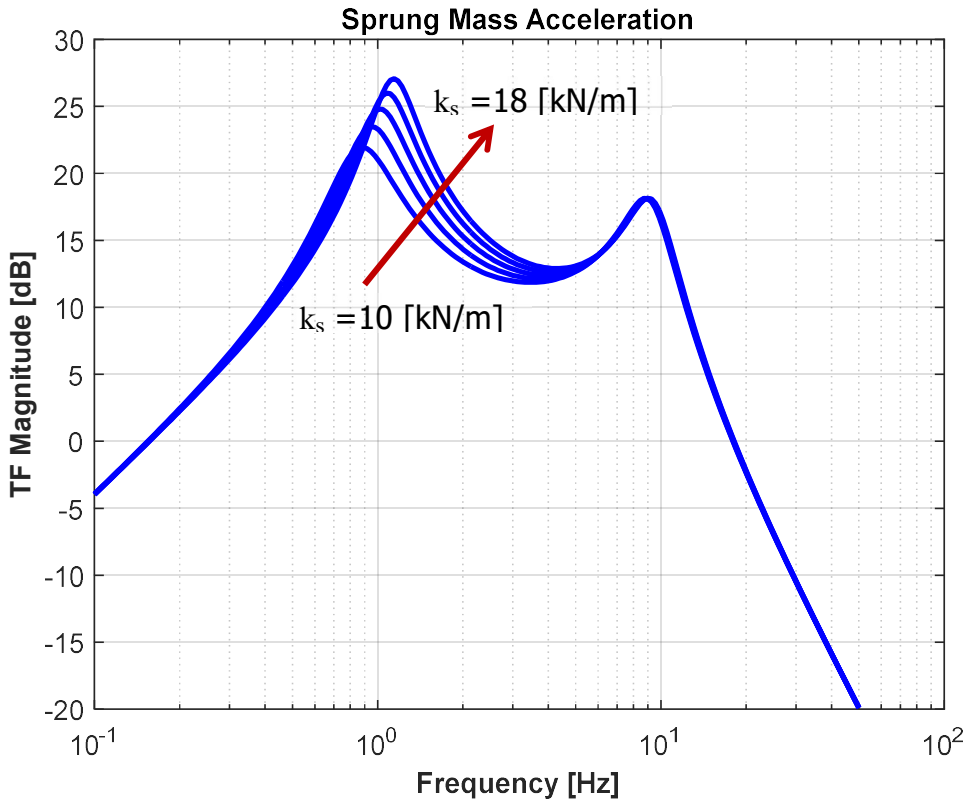


Figure VI-7. (c) Sprung mass acceleration transfer function – Δk_s=2 [kN/m]

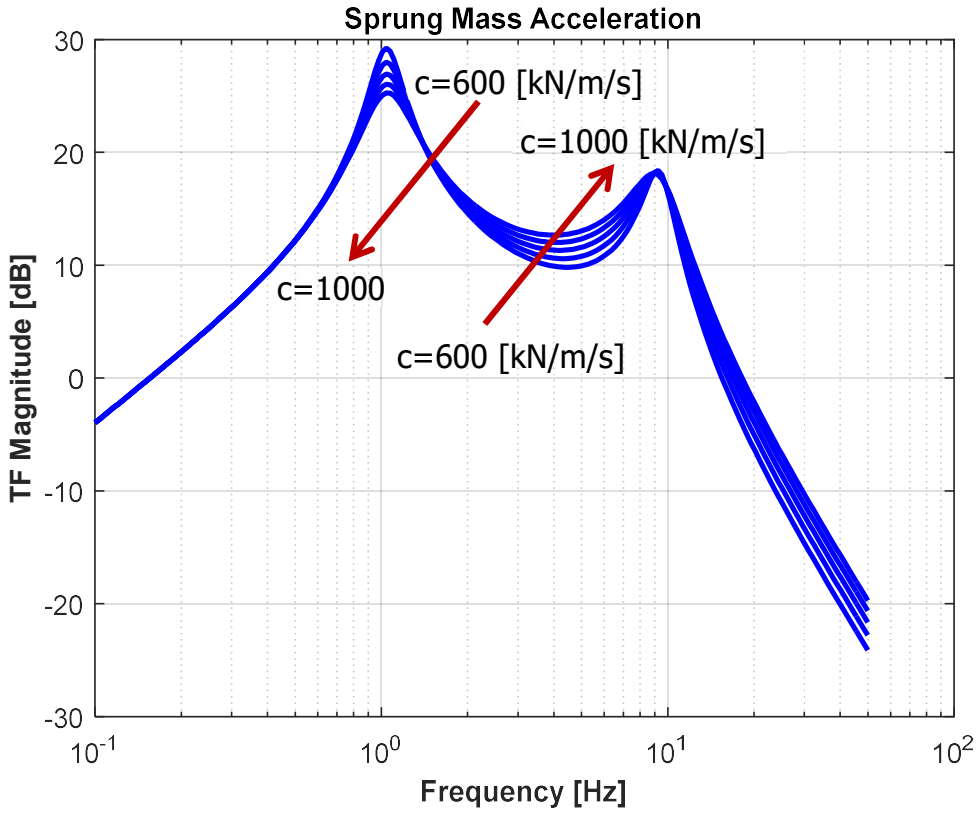


Figure VI-7. (d) Sprung mass acceleration transfer function – Δc=100 [N/m/s]

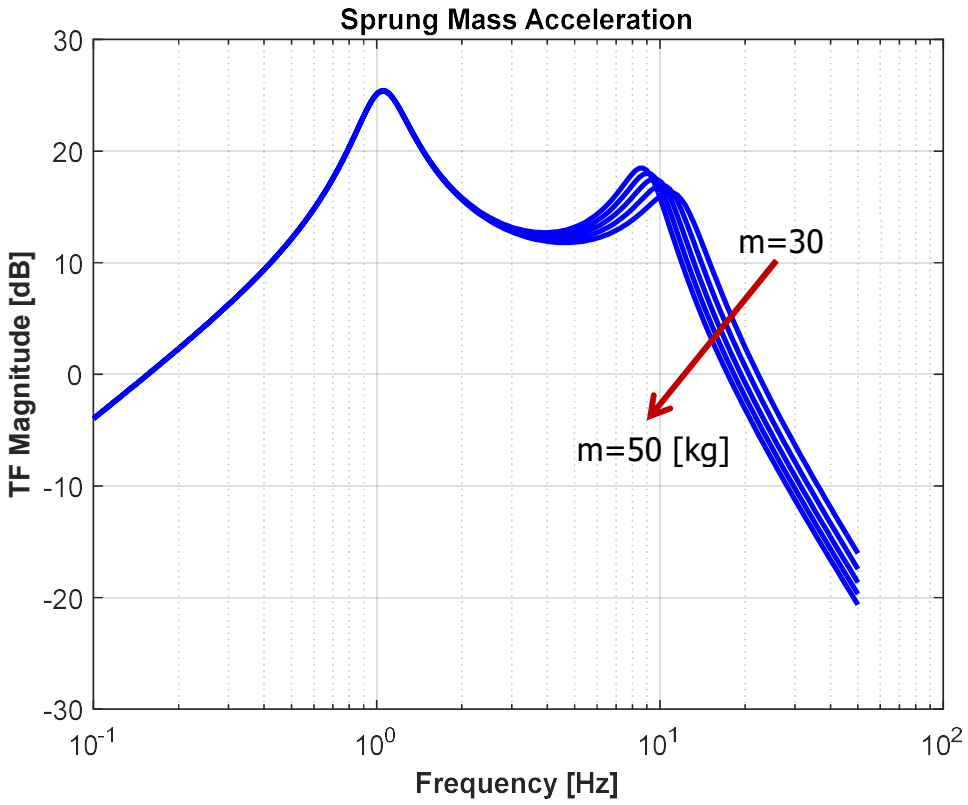


Figure VI-7. (e) Sprung mass acceleration transfer function – Δm=5 [kg]

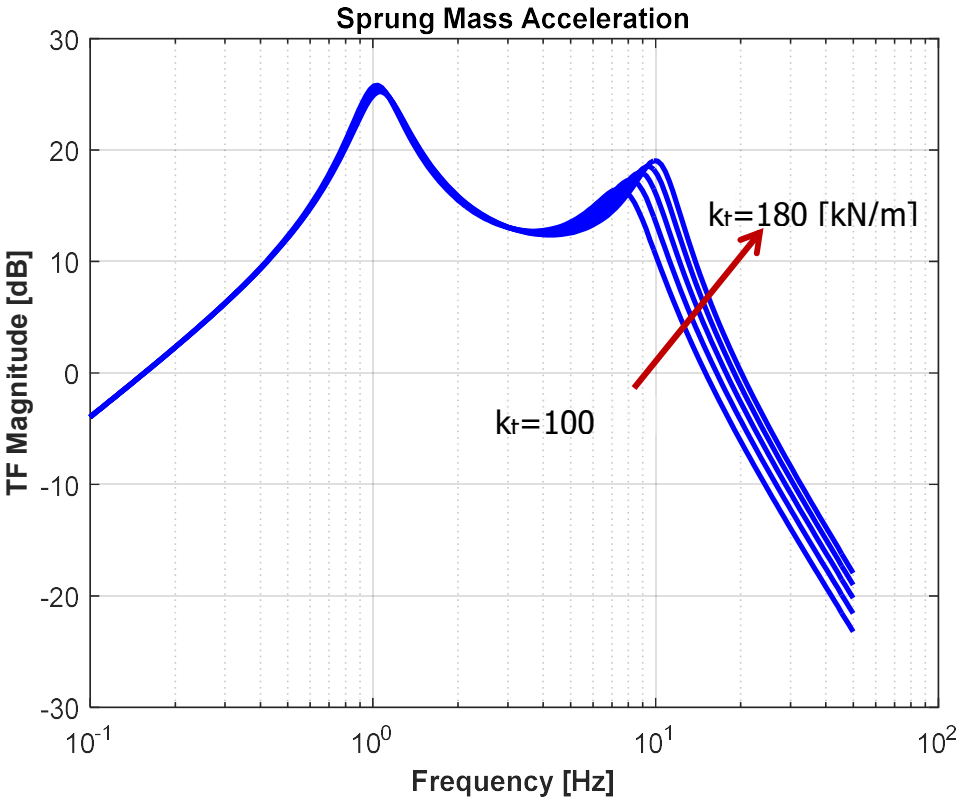


Figure VI-7. (f) Sprung mass acceleration transfer function – k_t=20 [kN/m]

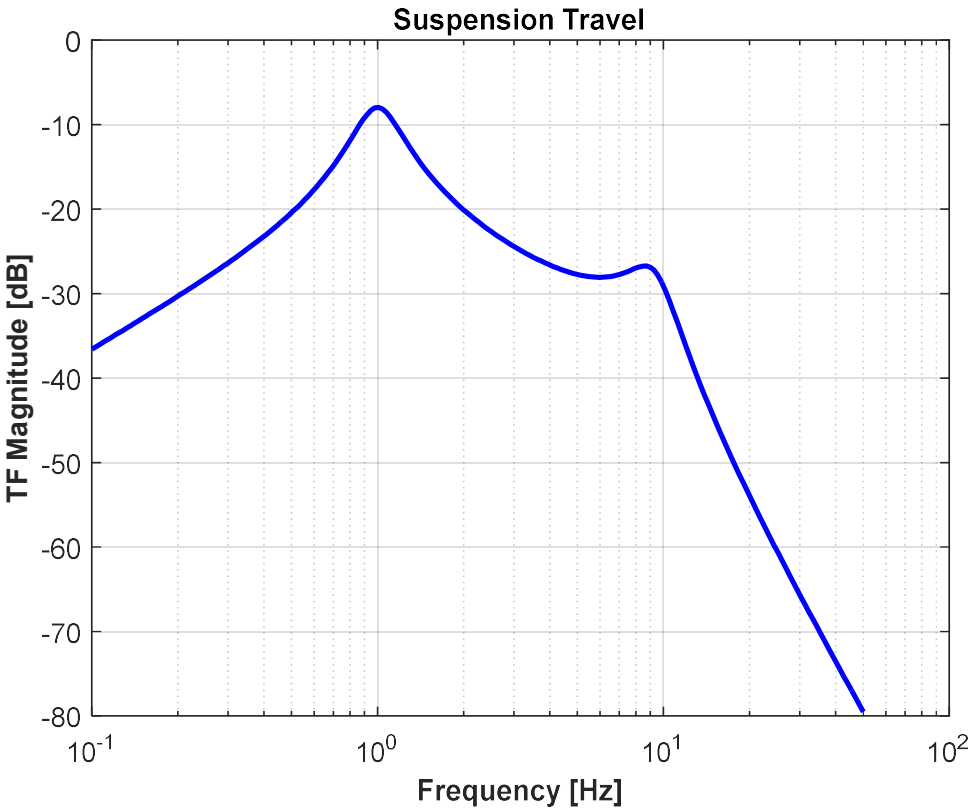


Figure VI-8. Suspension travel transfer function – nominal parameter values

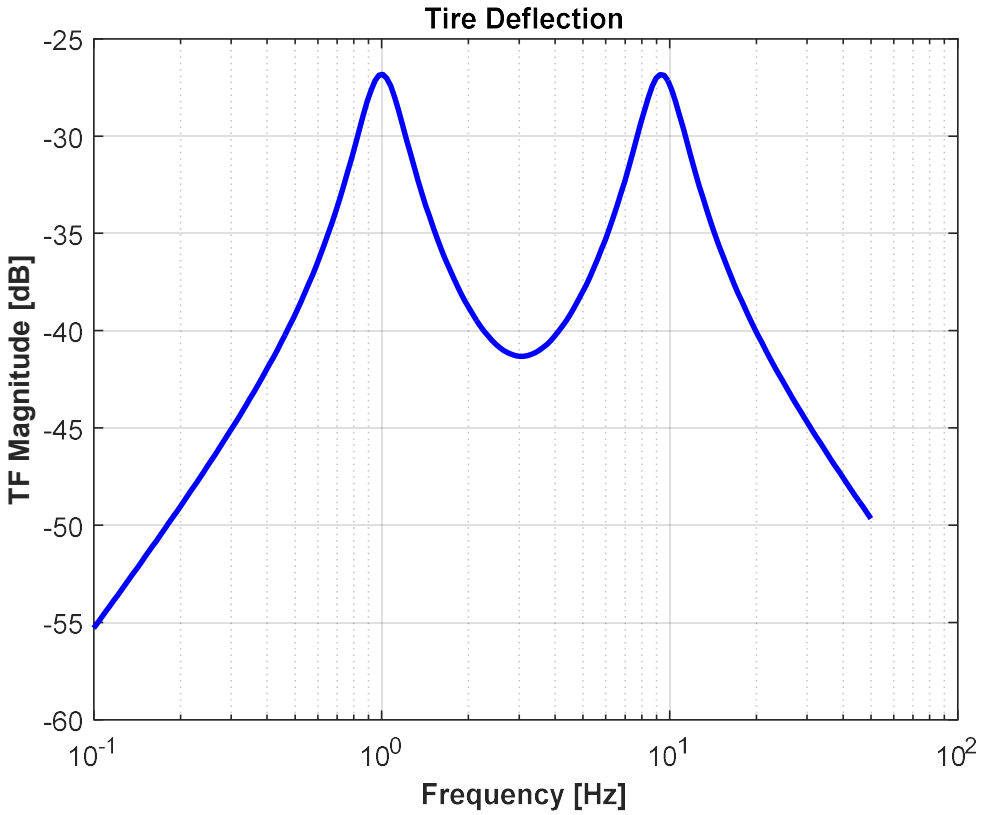


Figure VI-9. Tire deflection transfer function – nominal parameter values

VI-7. Half Car Model - Body Bounce and Pitch

Considering a vehicle with bounce and pitch freedom it is apparent that these two modes are close but the wheel resonance frequencies are well separated so that it is reasonable to consider pitch and bounce separately from wheel movements. A two degrees of freedom model is thus necessary to examine the pitch motion of the body in addition to the body bounce. Such a model is shown in Figure VI-10.

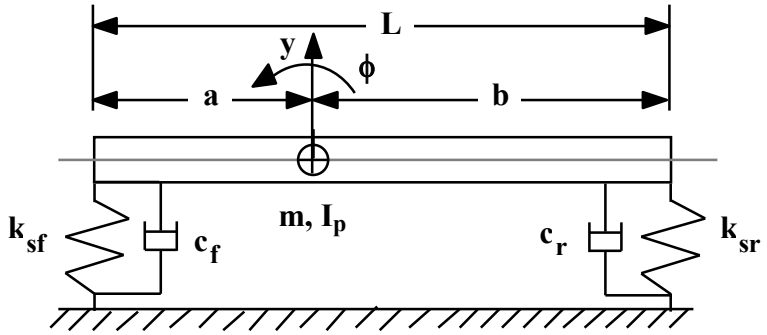


Figure VI-10. Body bounce and pitch model.

The vehicle has a mass m, and k_{sf} and k_{sr} are the total vertical stiffnesses of the front and rear suspensions. Denoting by c_f and c_r the effective damping constants of the front and rear dampers, the model represents the bounce, y, and pitch, ϕ, modes of the vehicle. Let I_p be the moment of inertia of the vehicle in pitch mode. The equations of motion are

$$m\ddot{y} = k_{sf}\left(a\phi - y\right) + k_{sr}\left(-b\phi - y\right) - c_f\left(a\dot{\phi} - \dot{y}\right) + c_r\left(-b\dot{\phi} - \dot{y}\right) \qquad \text{(VI-21)}$$

$$I_p\ddot{\phi} = -ak_{sf}\left(a\phi - y\right) + bk_{sr}\left(-b\phi - y\right) - ac_f\left(a\dot{\phi} - \dot{y}\right) + bc_r\left(-b\dot{\phi} - \dot{y}\right) \qquad \text{(VI-22)}$$

Neglecting damping, the characteristic equation is found as:

$$\left(ms^2 + k_{sf} + k_{sr}\right)\left(I_p s^2 + a^2k_{sf} + b^2k_{sr}\right) - \left(ak_{sf} + bk_{sr}\right) = 0$$

or

$$mI_p s^4 + \left\{I\left(k_{sf} + k_{sr}\right) + m\left(a^2k_{sf} + b^2k_{sr}\right)\right\}s^2 + L^2k_{sf}k_{sr} = 0 \qquad \text{(VI-23)}$$

Substitute

$$t = s^2$$

$$mI_p t^2 + \left\{I_p\left(k_{sf} + k_{sr}\right) + m\left(a^2k_{sf} + b^2k_{sr}\right)\right\}t + L^2k_{sf}k_{sr} = 0$$

$$t_{1,2} = \frac{-I_p\left(k_{sf}+k_{sr}\right)+m\left(a^2k_{sf}+b^2k_{sr}\right)}{2mI_p} \pm$$

$$\pm \frac{\sqrt{\left\{I_p\left(k_{sf}+k_{sr}\right)+m\left(a^2k_{sf}+b^2k_{sr}\right)\right\}^2-4mI_pL^2k_{sf}k_{sr}}}{2mI_p} \qquad \text{(VI-24)}$$

If one takes

$$ak_{sf} = bk_{sr} \qquad \text{(VI-25)}$$

then the bounce and pitch modes of the body are uncoupled (a moment applied at the center of gravity will result in a rotation about the center of gravity with no bounce and a force applied at the center of gravity in the vertical direction will result in only bounce with no rotation) and the natural frequencies are found from

$$\left(ms^2+k_{sf}+k_{sr}\right)\left(I_ps^2+a^2k_{sf}+b^2k_{sr}\right)=0$$

as

$$\omega_y = \sqrt{\frac{k_{sf}+k_{sr}}{m}} \qquad \text{(VI-26)}$$

for the bounce and

$$\omega_\phi = \sqrt{\frac{a^2k_{sf}+b^2k_{sr}}{I_p}} \qquad \text{(VI-27)}$$

for the pitch mode.

Front and Rear Suspension Frequencies

Let us now assume that the mass of the vehicle is replaced by two unequal parts, m_f and m_r, the former concentrated at the front axle vertical plane and latter concentrated at the rear axle vertical plane as illustrated in Fig. VI-11.

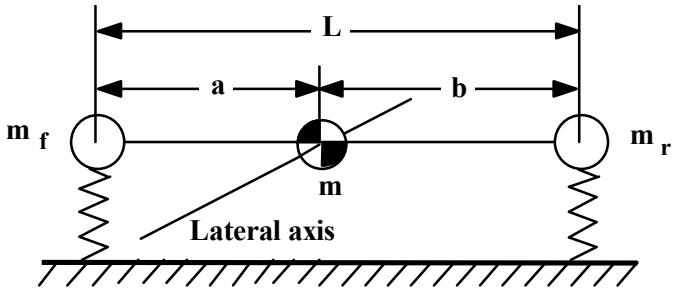


Figure VI-11. Concentrated masses at front and rear

In this case the sprung mass of the vehicle is shared between the front and rear suspensions according to the position of the sprung mass center of gravity. Thus

$$m_f = \frac{b}{L} m \qquad \text{and} \qquad m_r = \frac{a}{L} m$$

In this case, the front and rear suspension bounce frequencies will be given by:

$$\omega_{yf} = \sqrt{\frac{k_{sf}}{m_f}} \qquad \text{and} \qquad \omega_{yr} = \sqrt{\frac{k_{sr}}{m_r}} \tag{VI-28}$$

The pitch moment of inertia of the vehicle can be written as:

$$I_p = a^2 m_f + b^2 m_r = a^2 \left(\frac{b}{L} m \right) + b^2 \left(\frac{a}{L} m \right) = mab \tag{VI-29}$$

The pitch frequency from eqn. (6.27) then can be written in the form:

$$\omega_\phi = \sqrt{\frac{a^2 k_{sf} + b^2 k_{sr}}{I_p}} = \sqrt{\frac{a\left(a k_{sf}\right) + b\left(b k_{sr}\right)}{mab}}$$

If $ak_{sf}=bk_{sr}$:

$$\omega_\phi = \sqrt{\frac{(a+b) k_{sf}}{mb}} = \sqrt{\frac{L k_{sf}}{mb}} = \sqrt{\frac{k_{sf}}{m_f}} = \omega_{yf}$$
$$\omega_\phi = \sqrt{\frac{(a+b) k_{sr}}{ma}} = \sqrt{\frac{L k_{sr}}{mm}} = \sqrt{\frac{k_{sr}}{m_r}} = \omega_{yr} \tag{VI-30}$$

Thus, the front and rear suspension bounce frequencies, and the pitch frequency become all equal.

It is usual to write the moment of inertia in terms of the radius of gyration:

$$I_p = mk^2 \tag{VI-31}$$

Therefore an approximate relation between the radius of gyration and the center of gravity position is obtained.

$$k^2 = ab \tag{VI-31}$$

The ratio k^2/ab is an indication of how far an actual vehicle departs from equal pitch and bounce frequencies. A typical value of k^2/ab is 0.9 indicating pitch frequencies slightly higher than bounce frequencies. The almost pure pitch mode will have a higher frequency than the almost pure bounce mode. The smaller k^2/ab is, the higher will be the pitch frequency.

The effect of pitching vibrations is particularly undesirable since pitch introduces fore-and-aft (lateral) motion of the passengers to which they are more sensitive. As seen from Figures VI-2 (a) and (b), the sensitivity of driver and the passengers to lateral vibrations may be more critical than that for vertical vibrations, particularly in the frequency range from 1 to 2 Hz.

A practical way of to reduce pitching of the body quickly as the car goes over a bump on the road is to make the natural frequency of the rear suspension higher than the natural frequency of the front suspension. Then after a few cycles the two suspensions will move in phase resulting in bounce of the body only, as illustrated in Fig. VI-12.

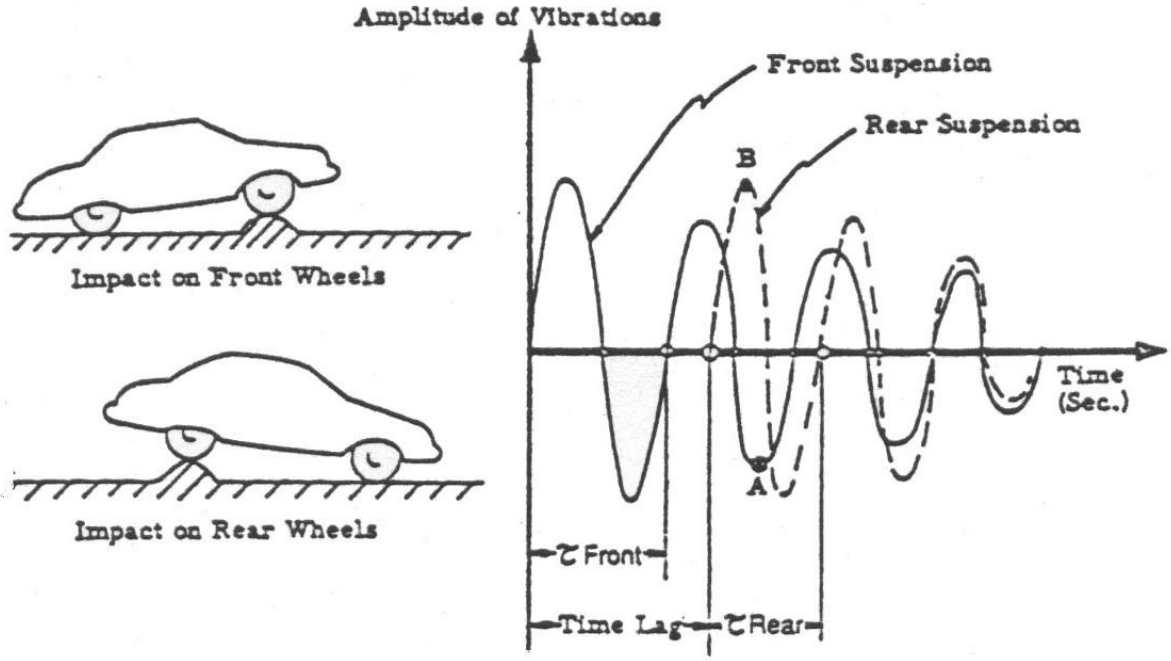


Figure VI-12. Control of pitching motion of the vehicle

Example VI-4

Consider the vehicle with specifications listed below.

a) Can you tell which of the body bounce and pitch frequencies will be higher?

b) Is the use of the uncoupled (pure) frequencies justified?

c) Determine the pure bounce and pitch frequencies.

M = 1240 kg, I_p = 1820 kg.m^2,
a = 1.37 m, b = 1.14 m,
k_{sf} = 35 kN/m, k_{sr} = 42 kN/m.

a) Check the value of k^2/ab.

$$\frac{k^2}{ab} = \frac{\frac{I_p}{M}}{ab} = \frac{\frac{1820}{1240}}{(1.37)(1.14)} = 0.94$$

Since $k^2/ab<1$, the pitch frequency is going to be higher than the body bounce frequency.

b) Check if $ak_{sf}=bk_{sr}$.

$$ak_{sf} = 1.37(35000) = 47950[\text{N}]$$
$$bk_{sr} = 1.14(42000) = 47880[\text{N}]$$
$$ak_{sf} \cong bk_{sr}$$

Since $ak_{sf} \cong bk_{sr}$, the pure body bounce and pitch frequencies are expected to be almost the same as the exact values (1.25 and 1.29 [Hz], respectively).

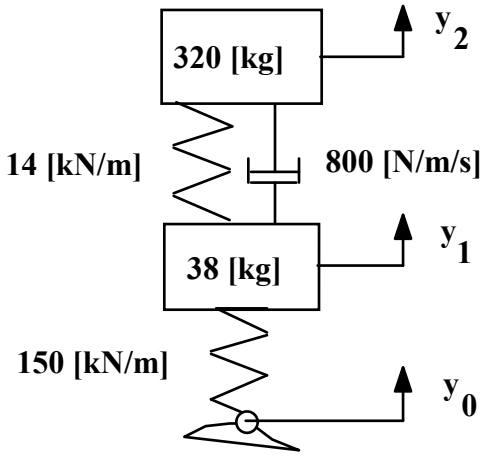
c) $$\omega_y = \sqrt{\frac{k_{sf}+k_{sr}}{m}} = \sqrt{\frac{(35000+42000)\left[\frac{\text{N}}{\text{m}}\right]}{1240[\text{kg}]}} \cong 7.9\left[\frac{\text{rad}}{\text{s}}\right] \cong 1.25[\text{Hz}]$$

$$\omega_\phi = \sqrt{\frac{a^2k_{sf}+b^2k_{sr}}{I_p}} = \sqrt{\frac{1.37^2(35000)+1.14^2(42000)\left[\frac{\text{N}}{\text{m}}\right]}{1820\left[\text{kg.m}^2\right]}\left(\frac{\text{kg.m}}{\text{N.s}^2}\right)}$$

$$\omega_\phi \cong 8.1\left[\frac{\text{rad}}{\text{s}}\right] \cong 1.3[\text{Hz}]$$

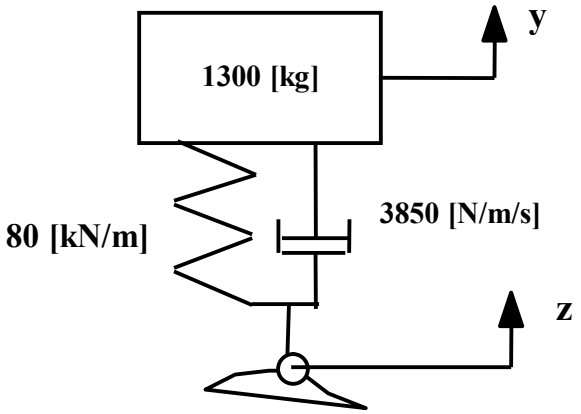
Exercises

VI-1) Estimate the body bounce and wheel hop frequencies (in [Hz]) for the vehicle represented by the quarter car model given in the figure. Would it be possible to use a suspension spring of 2 [kN/m] stiffness for the vehicle modelled in the previous question to improve ride comfort? If no, explain why not.



Ans.: 1.05 [Hz], 10.46 [Hz]

VI-2) A car is driven on a specially profiled road surface which is characterized by a sinusoidal shape with 0.3 complete cycles for each meter. If the driver is required to drive the vehicle on this road for at least one hour at a steady speed of 30 kph, what should be the maximum amplitude of the road surface profile?



Hint : Use the 1 hour reduced comfort boundary of ISO 2631 to determine the allowable rms acceleration of the body.

Ans.: 0.0053 [m]

VI-3) Estimate the body bounce and wheel hop frequencies, in Hz, and the damping ratios together with the static deflections of the sprung and unsprung masses for the vehicle with the following quarter car model parameters :

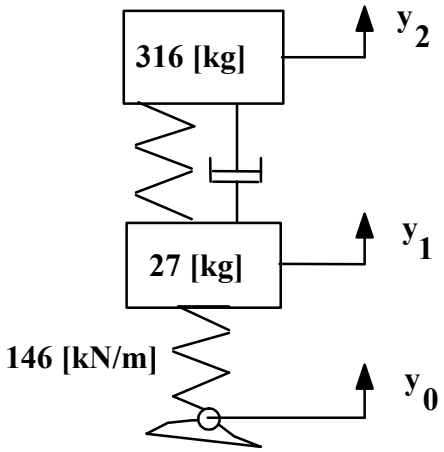
$$M = 286 \text{ kg}, m = 35 \text{ kg}, k_s = 15700 \text{ N/m}, c = 860 \text{ N/m}, k_t = 145000 \text{ N/m}$$

Ans.: 1.18 [Hz], 10.78 [Hz], 20.3 [%], 18.1 [%], 200 [mm], 22 [mm]

VI-4) The target parameters are determined for the front suspension of a medium size car as follows.

Body bounce frequency : 1.17 – 1.22 [Hz]
Wheel hop frequency : 12.2 – 12.4 [Hz]

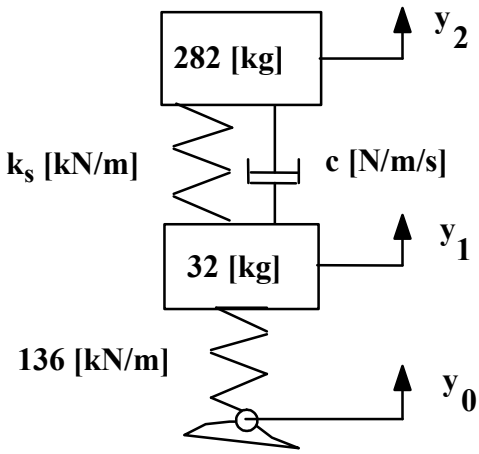
Propose a set of proper values for the suspension spring stiffness. Use the vehicle represented by the quarter car model given in the figure.



Ans.: $17077 \leq k_s \text{ [N/m]} \leq 17895$

VI-5) The target parameters are determined for the front suspension of a medium size car as follows.

Body bounce frequency : 1.10 – 1.20 [Hz]
Wheel hop frequency : 10.5 – 11.0 [Hz]
Damping ratio (Body bounce/wheel hop) : $(0.23<\xi<0.27)/(\xi>0.21)$



a) Propose a set proper values for the suspension spring stiffness.

b) Choose a spring stiffness of 15 kN/m and determine the range of damping coefficient to be provided by the damper.

Use the vehicle represented by the quarter car model given in the figure.

Ans. : $13471<k_s<16031$ [N/m],
$946<c<1111$ [N/m/s]

VI-6) Consider three vehicles with specified parameters as given below

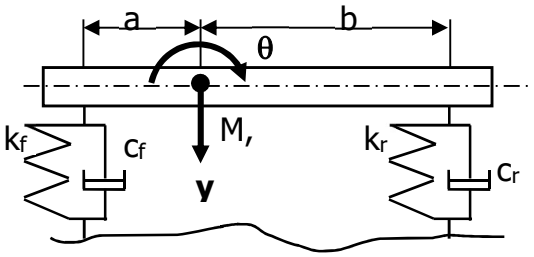
Vehicle	M [kg]	m [kg]	k_S [kN/m]	c_S [N/m/s]	k_t [kN/m]
I	1850	265	67.3	5600	526
II	1090	135	56.1	3800	552
III	1370	180	96.2	4800	590

For each one of the three vehicles :

a) Estimate the body bounce frequencies**.**
b) Estimate the wheel hop frequencies.
c) Calculate the damping ratios for the body bounce mode.
d) Calculate the damping ratios for the wheel hop mode.

Which one of the three vehicles would have the best ride confort ? Discuss.

VI-7) Consider the body bounce and pitch model of a vehicle.



M=1280 [kg], I_p=2340 [kgm^2], k_f=29 [kN/m], k_r=32 [kN/m], a=1.27 [m], b=1.31 [m], c_f=1820 [N/m/s], c_r=2150 [N/m/s].

a) Determine which one of the bounce and pitch frequencies will be higher than the other without actually calculating the frequencies.
b) Write the characteristic equation and solve for the roots to determine the bounce and pitch frequencies.
c) Consider only the bounce motion and try to calculate a rough estimate of the body bounce frequency.
d) Assume that $k^2/ab \approx 1$ and estimate the front and rear suspension frequencies.

CHAPTER VII

VEHICLE BODY CONSTRUCTION

VII-1. Introduction

Early vehicle body construction evolved from the modification of the existing horse carriage structures to carry the engine and the power train. The requirements introduced by the increased weight and shocks due to higher speed and engine power, however, resulted in entirely different body structures in time.

VII-2. Functions

The basic factors to be considered in the design of vehicle body structures can be listed as following :

i) Esthetic appearance : A vehicle has to look attractive to the potential customer, otherwise it will have limited chance of being sold in large quantities. Particularly, passenger cars are bought with primary emphasis on their appearance, sometimes even before the technical specifications.

ii) Adequate shelter from the environment : The body should protect the passengers and/or load from the environmental effects such as wind, rain, snow, cold, etc. It should also resist the same elements itself so that rusting and corrosion can be prevented.

iii) Aerodynamic shape : Aerodynamic shape will affect the performance and handling of the vehicle. However, a compromise has to be reached between the requirements of low drag coefficient and proper passenger space.

iv) Structural strength and rigidity : The body should be strong enough to handle forces such as the weights of the engine, passengers, and load carried as well as forces due to the motion of the vehicle. It should also protect the passengers from minor impacts during accidents. These all have to be achieved with a body structure that is not too heavy. If the body is not stiff enough, the it may collapse on the occupants and thus cannot protect them. However, making the body too rigid is not a solution to protect the passenger in a collision, as the body will absorb very little of the impact energy, transmitting more on the passengers. It seems that the best solution is to seat-belt the passengers inside a relatively rigid box, and to provide at each end of the box weaker extensions which will absorb energy by deforming progressively, Figure VII-1.

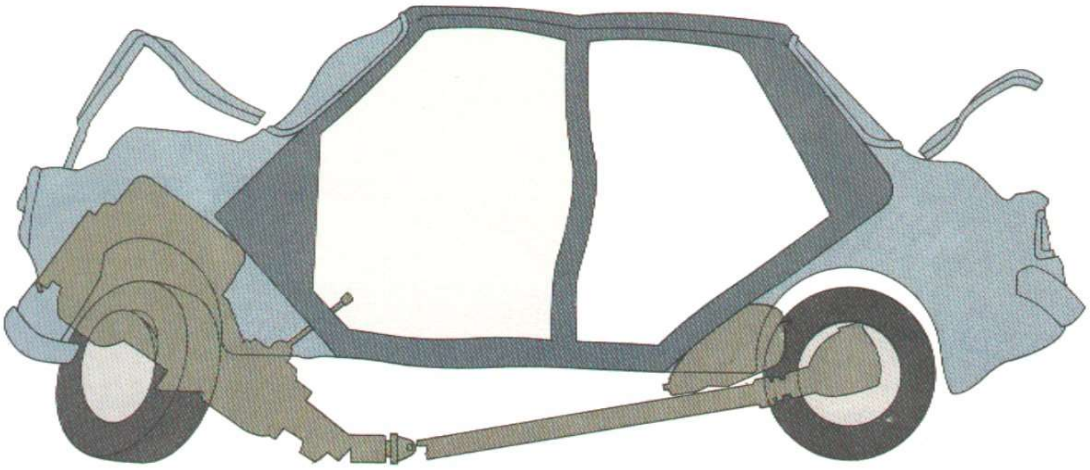
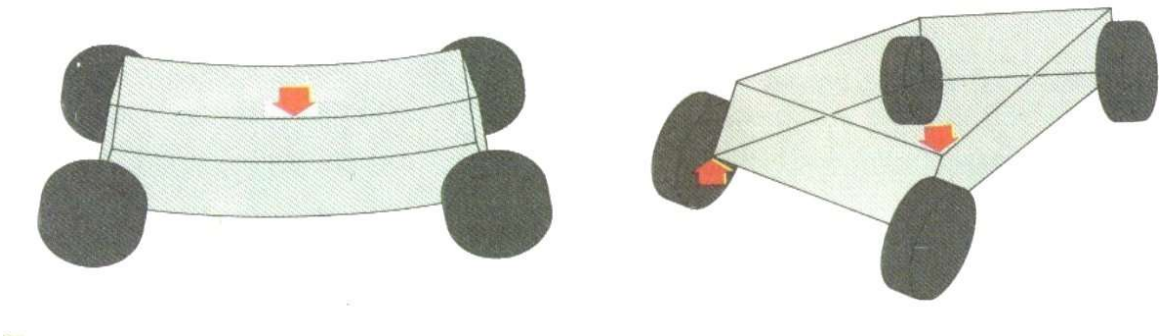


Figure VII-1. Safety boxes

It should be remembered that the body forms the base on which the suspension system is mounted. Therefore, a flexible body structure will adversely affect suspension performance particularly with respect to handling.

Beam stiffness : The body can be visualized as a beam supported at each end by the wheels. If it does not have sufficient bending rigidity, it will sag in the middle; thus doors will be difficult to close or they will jam when loaded, Figure VII-2. If a body structure does not have sufficient bending stiffness, it is not likely to have sufficient torsional stiffness either.

Torsional stiffness : The body must be sufficiently stiff with respect to torsional loads which tend to twist the body. Otherwise, the handling quality of the vehicle suffers and squeaks and rattles will develop.



(a) (b)

Figure VII-2. Body in (a) bending, and (b)torsion

VII-3. Basic Types

The first development in vehicle body structures was the development of separate chassis and body structures. This construction still dominates the heavy commercial vehicles. Four basic chassis types can be identified.

i) *Ladder Frame* is used in trucks because of the extremely small vertical space requirements, Figure VII-3. It is, however, not the best solution with respect to rigidity in bending and torsion.

ii) *Backbone* type of chassis structure is used for sports cars. It provides better torsional rigidity and compensates for the lack of rigidity of the body which is usually reinforced plastic, but is heavy and costly. Further it occupies too much space, Fig. VII-4.

iii) *X-form* chassis is a combination of the ladder and backbone types and provides a low cost compromise solution, Fig. VII-5. It provides a strong base, allowing ease of repair to body damage as well as body restyling without extensive redesigning.

iv) *Space frame* chassis is the best solution, Figure VII-6. It provides a very rigid and light structure and used commonly for buses and racing cars.

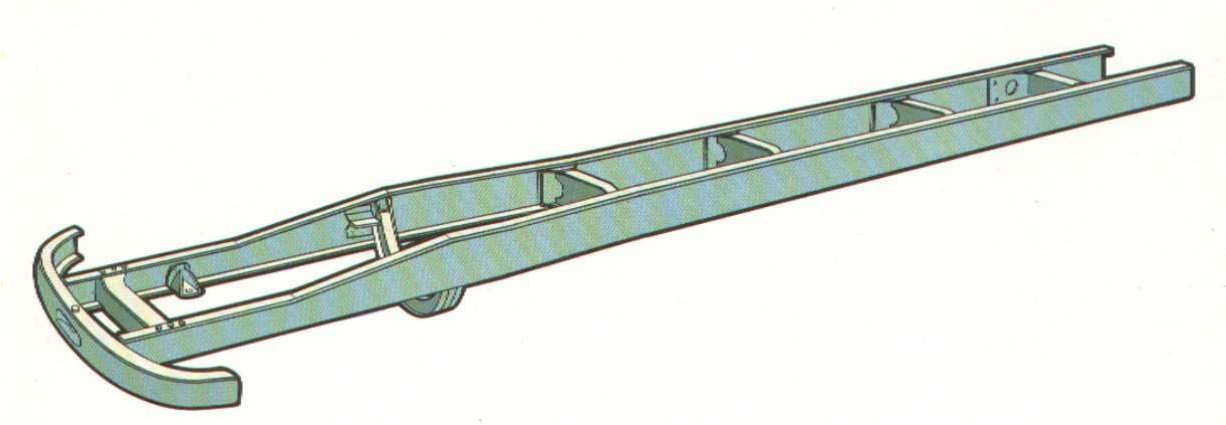


Figure VII-3. Ladder frame chassis

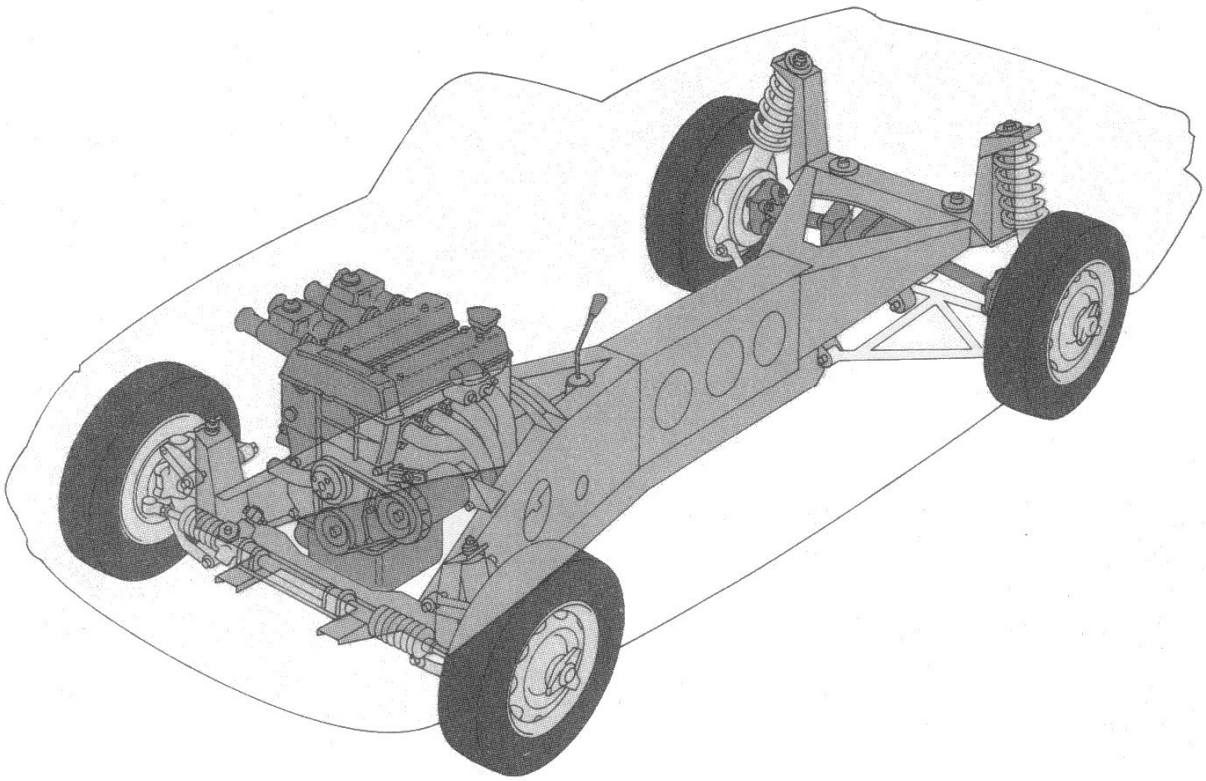


Figure VII-4. Backbone type of chassis structure

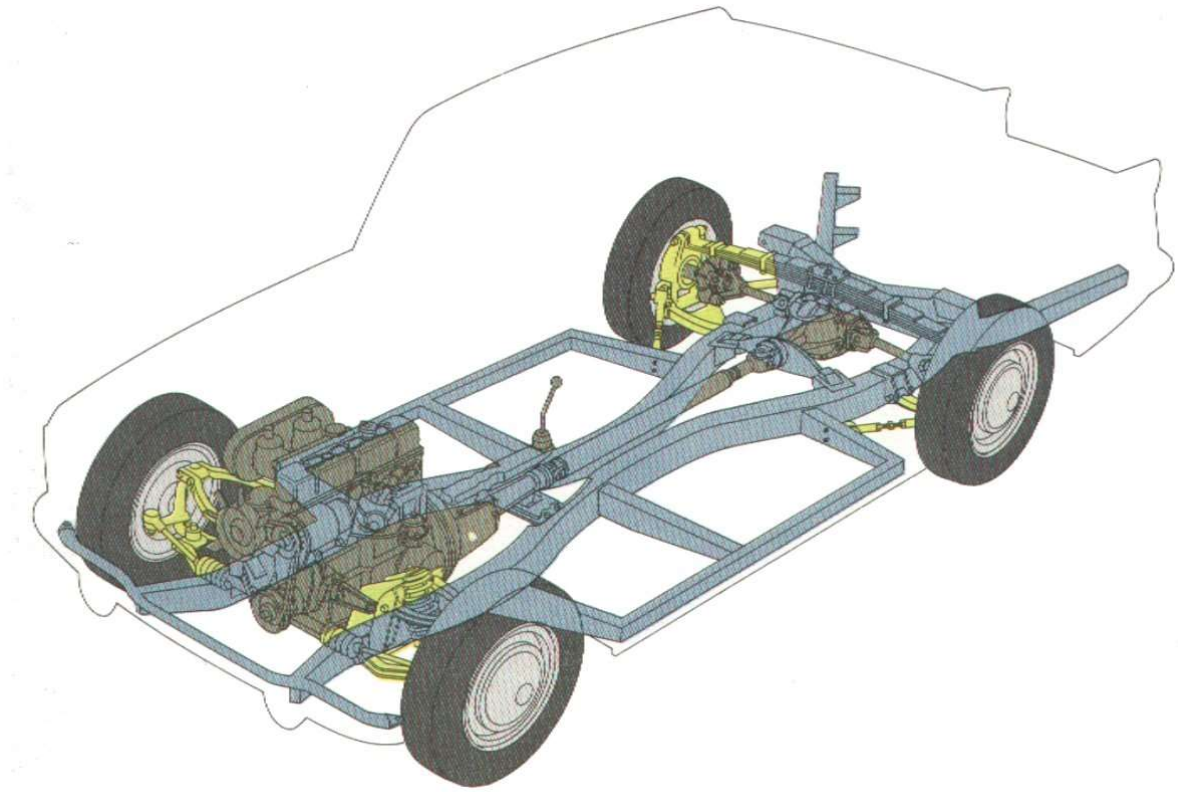


Figure VII-5. X-form chassis structure

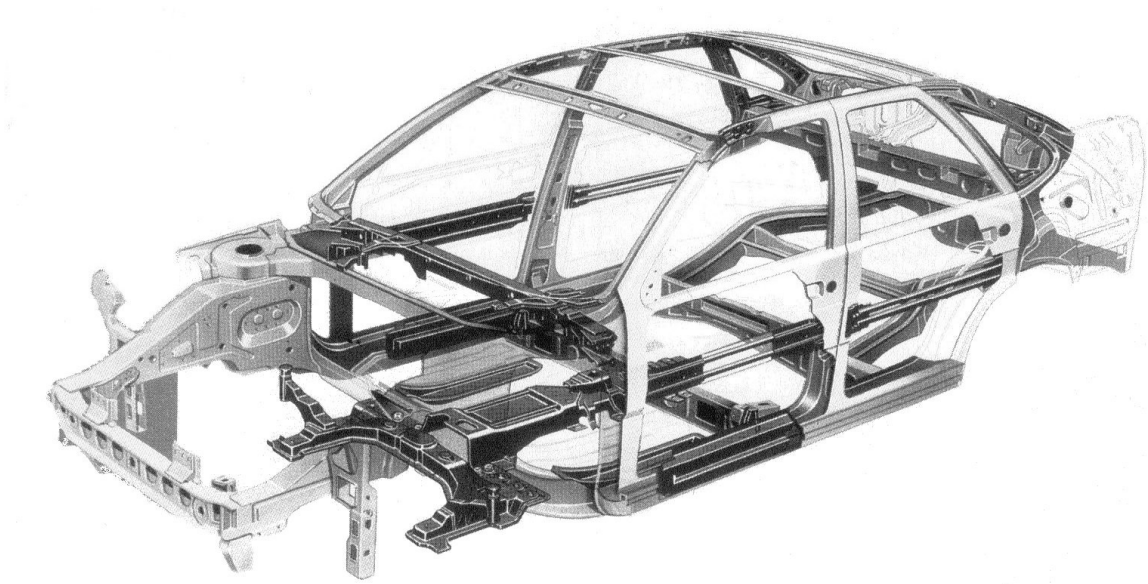


Figure VII-6. Space frame chassis

In the separate chassis and body structures, the chassis is designed to meet the stiffness and strength requirements and the contribution of the body is neglected. The developments in the reduction of weight through optimization of vehicle body structures led to a new design called the semi-integral body where the contribution of the body to the overall stiffness is substantial. Further development resulted in the integral (monocoque) body where there is no separate chassis and the load are carried by the members of the body structure, Figure VII-7.

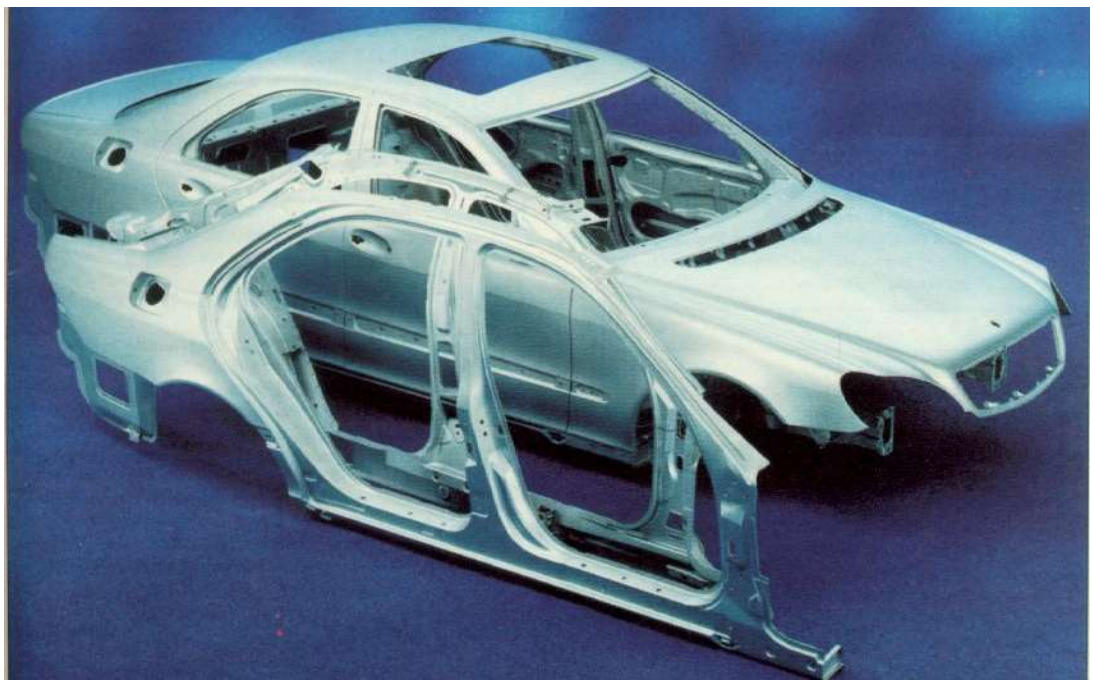


Figure VII-7. Fully integral body structure

VII-4. Vehicle Loads

Vehicle loads to be considered in the strength and deformation analysis of the structural design of a vehicle body are acquired through experience with earlier designs. If the designer/analyst does not have such data available, then tests and/or simulations may be used. It is important to determine the loads that will be applied to the vehicle body structure which may result in failure during service, or may cause fatigue failure with an inadequate life span.

It is usual to start the analyses with loads representing the worst cases that may be encountered. A body structure that can resist the worst load cases is assumed to have sufficient fatigue strength. Of course, as the design process develops, fatigue analyses of the critical components will have to be carried out. Further, it is to be remembered that a body structure designed for the worst case loadings are likely to be overdesigned.

The principal loads to be considered in the initial design stages are as follows:

- Bending Loads,

- Torsion Loads,

- Longitudinal Loads,

- Lateral Loads.

It is customary to apply these loads in various combinations representing load cases and account for the dynamic loading on the structure by applying a dynamic load factor, most often in terms of a gravitational acceleration ratio.

Dynamic Load = Static Load * Dynamic Load Factor

Commonly used Dynamic Load Factors are given in Table VII-1.

Table VII-1 Dynamic Load Factors for Load Cases

Load Case	Dynamic Load Factor [g]
Bending Loads	3
Torsion Loads	1.3
Longitudinal Loads	1
Lateral Loads	1

VII-5. Conventional Design Process

The conventional procedure followed in the design of a new car body starts with the determination of the main vehicle characteristics such as power, top speed, number of passengers, general shape (sedan, coupe, etc.), production rate, etc. by the general management.

The conventional design process basically consisted of the following steps.

1. Artistic 2D sketches capture the concept - styling.

2. Clay prototypes are built to interpret the sketches.

3. A 3D CAD representation is developed by digitizing the full size clay prototypes and transforming this information into extensive mathematical formulas.

4. Milling instructions are generated from the 3D CAD model.

VII-5.1 Styling and clay prototypes

A large number of drawings showing the views of the proposed body styles are then prepared by the stylists, Figures VII-8 to 13. The management selects a number, say 10, of these, Figure VII-14. Small scale (1/8 to 1/10) clay mockups are also prepared for management to choose.



Figure VII-8. Stylist at work



Figure VII-9. Stylist at work



Figure VII-10. Styling trials



Figure VII-11. Styling trials



Figure VII-12. Styling trials



Figure VII-13. Styling trials



Figure VII-14. Selection of body styles

Then, only the outside is drawn fullscale by measuring a few dimensions from the mockup, Figure VII-15. More details than mockup are then drawn subject to stylists approval.



Figure VII-15. Preliminary drawing

VII-5.2 Full size clay model

Full size clay models (exterior and interior) are made using plywood, flax and plaster, Figures VII-16 to 18. They are sculptured, scraped, and polished then judged by top management, sales, and stylists. They may not conform to preliminary drawings.



(a)



(b)

Figure VII-16. Full size model



Figure VII-17. Full size models



Figure VII-18. Complete front interior model

VII-5.3 Final drawing

Shape of clay model is translated into 3D CAD model with full inside and outside panels. Every piece of equipment such as hinges, locks, windscreen, seats, dashboard, etc. and surfaces on which gearbox, engine, suspension, etc. are to be mounted must be included.

VII-5.4 Production

Production starts with the instructions generated from the 3D CAD model developed and finalized.

VII-6 Recent Developments

The weakest point of the conventional method described is the amount of time that is required to start the production of a new model. Obviously reducing the delay would prove a great advantage in a highly competitive industry.

Recently, the stylists have turned to CAD tools for the styling work; hand sketches have practically disappeared. The abilities of these tools to allow examination of the design from all sides, to apply any color under different light sources at any angle and direction have facilitated the production of proposed body styles in a much shorter time and variety, Figure II-19 and 20.



Figure VII-19. Stylists at work



Figure VII-19. Computer Assisted Styling (CAS)

A major recent development has been the removal of the clay model from the design process. As a result of the developments in the CAD software, it is possible to decrease the design cycle span significantly with reduced costs. Furthermore, creativity could flourish in this environment, leading to a greater variety in designs. As a result, practically all automakers have adopted CAD design tools, which in turn have minimized the importance of the clay prototype. Most companies, however, still produce a clay model just for the final approval before production begins.

Elimination of the clay model necessitates tools to analyze the 3D CAD model. These tools are needed to simulate the methods applied to the clay model. One of such analysis tools is the use of reflection lines. Figures VII-20 and 21 illustrate the application of reflection lines. Many automakers employ reflection lines as a quality assurance tool, just before the car leaves the factory. Sets of parallel, long and thin light bulbs are set up in an otherwise dark room. The reflections of the light bulbs in the car are observed by technicians walking around the car. In a door panel, for example, the reflection lines should appear as smooth curves on the car. An unexpected ripple most likely means a dent in the door. This same technique was also applied to the clay model, which was painted in order to be reflective.



Figure VII-20. Use of reflection lines



Figure VII-21. Use of reflection lines

References

[1] Setright, L. J. K., Automobile Tires, Chapman and Hall, London, 1972.

[2] Jacobson, M. A. I., Know About Your Tires, Automobile Association, London, 1971.

[3] Shearer, G. R., The Rolling Wheel - The Development of the Pneumatic Tire, Proc. Instn. Mech. Engnrs., v191, 11/77, 1977.

[4] Wheels/rims for Pneumatic Tyres - Nomenclature, designation and marking, ISO/DIS 3911.

[5] Wolfe, W. A., "Analytical Design of an Ackermann Steering Linkage", Transactions of the ASME, Journal of Engineering for Industry, February, 1959, pp. 10-14.

[6] Zarak, C. E. and Towsend, M. A., "Optimal Design of Rack-and-Pinion Steering Linkages", ASME paper 82-DET-10.

[7] Miller, G., Reed, R., and Wheeler, "Optimum Ackerman for Improved Steering Axle Tire Wear on Trucks", ASME paper 912693.

[8] Nordeen, D. L. and Cortese, A. D., "Force and moment characteristics of rolling tyres", SAE Trans. v72 (1964), pp. 325-336.

[9] Hartley, J., "Suspension-waiting for a Revolution", Autocar, w/e 8 October, 1977, pp. 58-62.

[10] Lee, D. M. A., Pascoe, D. M., and ElMaraghy, W. H., “An Analysis of the multi-link independent suspension system”, Int. J. of Vehicle Design, v14 (1993), n1, pp.44-58.

[11] Horntrich, H., "Rear Suspension Design with FWD Vehicles", SAE Trans. v (1982), pp. 1595-1610, SAE paper 810421.

[12] Bastow, D., "Aspects of Car Rear Suspension", Proceedings Instn. Mech. Engnrs., v 190 (1976), pp. 611-626.

[13] Cronin, D. L., "MacPherson Strut Kinematics", Mechanism and Machine Theory, v16 (1981), n6, pp.631-644.

[14] M. L. Felzien and D. L. Cronin, “Comment on MacPherson Strut Kinematics”, Mechanism and Machine Theory, v18 (1983), n1, pp.91-93.

[15] M. L. Felzien and D. L. Cronin, “Steering Error Optimization of the MacPherson Strut Automotive Front Suspension”, Mechanism and Machine Theory, v20 (1985), n1, pp.17-26.

[16] Dizioğlu, B. and Eghtesad, M., "Ein Allgemeines Kinematisches Verfahren zur Ermittlung der Eigenfrequentz bei Radaufhangungen", Automobil-Industrie, v1 (1975), pp.23-29.

[17] Simanaitis, D., "Anti-roll Bars", Road and Track, August 1981, pp. 56-62.

[18] Gard, J. R., "Advanced Suspension Design and Chassis Tuning", The SAE-Australasia, Sept-Dec 1977, pp.170-185.

[19] Barak, P., "Magic Numbers in Design of Suspensions for Passenger Cars", SAE SP-878, Car Suspensions and Vehicle Dynamics, 1991, pp. 53-88.

[20] “An Introduction to Modern Vehicle Design”, Edited by J. H. Smith, Butterworth-Heinemann, 2002.

[21] Bastow, D., Car Suspension and Handling, 2nd edition, Pentech Press, London, 1988.

[22] Campbell, C., Automobile Suspensions, Chapman and Hall, London, 1981.

[23] Gillespie, T. D., Fundamentals of Vehicle Dynamics, Society of Automotive Engineers, Inc., 1992.

[24] Wong, J. Y., Theory of Ground Vehicles, John Wiley and Sons, New York, 2001.

[25] Ellis, J. R., Vehicle Dynamics, Business Books Limited, London, 1969.